

Assessing the bloom dynamics and the ecological role of the dinoflagellate *Noctiluca scintillans*

Dissertation

in fulfilment of the requirements for the degree of Doctor
of the Faculty of Mathematics and Natural Sciences at
the Christian-Albrechts-Universität of Kiel

submitted by

Katharina Kordubel

Kiel, 2025

Date of oral examination: 09.01.2025

First examiner: Prof. Dr. Burkard Baschek

Second examiner: Prof. Dr. Maarten Boersma

Third examiner: Prof. Dr. Rainer Kiko

Acknowledgements

First, I would like to thank my supervisor Klas Möller for his guidance, support, for the many meetings to discuss ideas and results, and for introducing me to the fascinating world of plankton imaging. I also thank my other supervisor Burkard Baschek for his consistent advice, and for his early preparation and encouragement that have been crucial in navigating the challenging yet rewarding journey of a PhD. I would also like to thank my two co-supervisors Yoana Voynova and Martin Hieronymi for their kindness, helpfulness, and for their specialized expertise that greatly enriched my work.

A very special thanks goes to Raúl Martínez-Rincón that has now provided help and support in two of my theses. His kindness, patience, and availability have been essential in fostering my interest in statistics and improving my skills in R. I also extend my gratitude to Maarten Boersma, Inga Kirstein, and David Johns for their valuable collaboration, data provision, and helpful advice, all of which significantly improved my work.

I would like to thank Daniel Blandfort, Saskia Rühl, Jana Hinners, and Ankita Vaswani for their friendship and advice, which made my time in Geesthacht so much more enjoyable. I thank Götz Flöser for his helpfulness, availability, and wonderful storytelling.

I would like to express my gratitude to Daniel Blandfort, Saskia Rühl, Jana Hinners, Götz Flöser, Klas Möller, Shun Bi, Eva Drenguis, Marie Flatow, Kilian Huss, Alina Zacharzewski and the crew of the RV Ludwig Prandtl for their indispensable help and support leading to three successful sampling campaigns in Helgoland. I thank Kerstin Heymann, Tanja Pieplow, and Luca Blüm for analysing the collected samples and I thank Daniel Behr for always keeping an eye on the North Sea and for providing the satellite images used in this thesis.

I extend my deepest gratitude to my family (Yvonne Kordubel, Tobias Famulok, Theresa Kordubel, Leonard Kordubel, and Arthur de Gourcuff) who has supported and encouraged me throughout my PhD. Without them, none of this would have been possible. And lastly, I thank Erick Diaz Delgado for being there in the good and in the most difficult moments. Thanks for always taking the time to discuss ideas, to check drafts, and to patiently listen to the many test-talks before important presentations. Thanks for always believing in me and constantly reminding me of it. I could not have made it without you.

Summary

The base of the marine ecosystem is built by planktonic organisms. Under climate change and anthropogenic pressures, changes within the plankton community including the increase of harmful algal bloom forming species, and spatiotemporal shifts have taken place. Over the last decades, blooms of the heterotrophic dinoflagellate *Noctiluca scintillans* have occurred more frequently and intensively in many regions. This harmful algal bloom forming species can alter food webs, reduce ecosystem productivity, and lead to economic losses while causing lower aquacultural yields and affecting tourism. Despite these recent trends and the significant ecological impact of *N. scintillans*, many knowledge gaps addressed in this thesis remain, including: (i) challenges in determining its spatiotemporal trends; (ii) limited knowledge about drivers triggering and ending blooms, and (iii) scarce information about feeding, reproduction, and interaction *in situ*.

With an extensive literature review (1857–2023), I described the potential global expansion of *N. scintillans* as well as the associated environmental factors. The analysis suggested that *N. scintillans* increased over time in several coastal regions and particularly in Australia, China, and Europe, including the North Sea. Eutrophication, ocean warming, and deoxygenation were proposed as possible key-drivers of these intensifications.

To validate these findings, I analysed two long-term, high-resolution time series. Therefore, data from the Helgoland Roads time series and Continuous Plankton Recorder survey were analysed to identify drivers and spatiotemporal hotspots of *N. scintillans* in the rapidly warming North Sea. New knowledge about *N. scintillans*' bloom dynamics was obtained through the identification of environmental drivers of the different bloom phases. Significant correlations were found between bloom initiation, nutrients and light availability since these factors lead to increased prey availability. Highest abundances of *N. scintillans* were associated with reduced wind speed causing dense surface accumulations. Elevated solar radiation was identified as a main driver for post-bloom conditions as it deteriorates the cells and leads to the decrease of *N. scintillans*. The analysis further revealed that after the 1990s, *N. scintillans* abundances significantly increased, and that a prolongation of the bloom window took place off the island of Helgoland, Germany. In the southern North Sea, *N. scintillans* occurrences intensified and spread since the 1980s with hotspots identified as the coastal waters adjacent to the estuaries of the Elbe and Rhine rivers.

After the identification of spatiotemporal hotspots of *N. scintillans* in the North Sea through the time series analysis, three sampling campaigns were carried out in summer 2022 around Helgoland to resolve an entire *N. scintillans* bloom. Traditional methods including nets and water samplers, as well as imaging devices such as the Continuous Plankton Imaging and Classification Sensor and the FlowCam, were deployed. Unusually high ammonium and phosphate concentrations were measured within dense *N. scintillans* surface patches, suggesting that this organism acts as an essential nutrient recycler. Images from the optical devices were analysed with applied machine learning techniques,

and allowed to resolve phytoplankton community composition, prey types, and intraspecific interactions. The frequently observed ingestion of diatoms by *N. scintillans* followed by an increase of phosphate- and/or ammonium-affine dinoflagellates, suggests a potentially important role of *N. scintillans* within plankton communities.

This thesis provides valuable new insights into the bloom dynamics, ecological role, and spatiotemporal distribution of *N. scintillans* in the North Sea. This was achieved with the combination of various data sources including literature, long-term time series and sampled data. The thorough literature review uncovered major knowledge gaps emerging from limitations in sampling methodologies. To fill these gaps, the analysis of two time series recognized for their unique resolution, quality, and duration was carried out. For the first time, two of the longest plankton time series were analysed to obtain novel information about spatial and temporal distribution of *N. scintillans* in the North Sea. This highlights the importance of long-term time series in identifying past, recent, and potential future trends of *N. scintillans* bloom dynamics in the North Sea and possibly in rapidly changing ecosystems at global level. The delineation of spatiotemporal hotspots enabled the targeted sampling of an *N. scintillans* bloom from initiation until decay. This unique dataset provided valuable novel information about drivers involved in different *N. scintillans* bloom phases and about the potential impact of *N. scintillans* on coastal phytoplankton communities.

Lastly, this thesis underscores the potential of innovative methodologies including underwater imaging devices, which allow the visualization of *in situ* behaviour of *N. scintillans* throughout the water column at unprecedented resolution, significantly advancing the current knowledge of this organism. This new information, together with the holistic methodological framework proposed here, will undoubtedly improve the predictability of this organism on the rise in many coastal regions worldwide. Given the significant economic and societal importance of coastal areas, this new knowledge could help mitigate future economic losses associated to *N. scintillans*, such as impacts on aquaculture, disruptions in food chains reducing fisheries, or adverse effects on tourism.

Zusammenfassung

Plankton bildet die Grundlage des marinen Ökosystems. Klimawandel und anthropogene Einflüsse haben zu Veränderungen innerhalb der Planktongemeinschaft geführt, darunter die Zunahme von schädlichen Algenarten, sowie räumliche und zeitliche Veränderungen. In den letzten Jahrzehnten sind Blüten des heterotrophen Dinoflagellaten *Noctiluca scintillans* in mehreren Regionen häufiger und intensiver aufgetreten. Diese schädliche Algenart kann Nahrungsnetze verändern, Ökosystemproduktivität verringern und zu wirtschaftlichen Verlusten führen, da sie Aquakultur und Tourismus negativ beeinflussen kann. Trotz dieser jüngsten Entwicklung und der signifikanten ökologischen Auswirkungen von *N. scintillans* gibt es noch viele Wissenslücken, welche in dieser Arbeit adressiert werden: (i) Herausforderungen bei der Bestimmung der räumlich-zeitlichen Entwicklung von *N. scintillans*; (ii) begrenztes Wissen über Umweltfaktoren, welche Blüten auslösen und beenden, und (iii) wenige Informationen über Ernährung, Fortpflanzung und Interaktion *in situ*. Mit einer umfassenden Literaturrecherche (von 1857 bis 2023), konnte ich die potenzielle globale Ausbreitung von *N. scintillans* und die damit verbundenen Umweltfaktoren beschreiben. Die Analyse zeigte, dass *N. scintillans*-Abundanzen im Laufe der Zeit in Küstenregionen Australiens, Chinas und Europas, anstiegen. Eutrophierung, Erwärmung und Sauerstoffmangel wurden als mögliche Ursachen erkannt.

Um diese Ergebnisse zu bestätigen, habe ich Daten aus den zwei hochaufgelösten Zeitserien Helgoland Roads und Continuous Plankton Recorder Survey analysiert, um Treiber und raumzeitliche Hotspots von *N. scintillans* in einer sich schnell erwärmenden Umgebung wie die Nordsee, zu identifizieren. Neue Erkenntnisse über die Blütendynamik von *N. scintillans* wurden durch die Identifizierung von Umweltfaktoren, welche die verschiedenen Blütenphasen antreiben, gewonnen. Signifikante Korrelationen wurden zwischen dem Blütenstart und Nährstoffen sowie der Lichtintensität festgestellt, da diese Faktoren die Nahrungsverfügbarkeit erhöhen. Die höchste *N. scintillans* Abundanz wurde mit reduzierter Windgeschwindigkeit assoziiert, was zu dichten Oberflächenansammlungen führte. Erhöhte Sonneneinstrahlung beschädigt *N. scintillans*-Zellen und wurde daher als Hauptursache des Blütenendes identifiziert. Die Analyse ergab zusätzlich, dass die *N. scintillans* Abundanzen vor Helgoland nach den 1990er Jahren deutlich zugenommen haben und dass sich das Blütenzeitfenster verlängert hat. In der südlichen Nordsee hat sich das *N. scintillans* Vorkommen seit den 1980er Jahren intensiviert und ausgebreitet. Die Küstengewässer in der Nähe der Mündungen von Elbe und Rhein wurden als Hotspots identifiziert.

Nach der Identifizierung der räumlich-zeitlichen Hotspots von *N. scintillans* in der Nordsee, wurden im Sommer 2022 drei Kampagnen um Helgoland durchgeführt, um eine gesamte *N. scintillans*-Blüte zu erfassen. Dabei wurden sowohl traditionelle Methoden wie Netze und Wasserprobennehmer als auch optische Geräte wie der Continuous Plankton Imaging and Classification Sensor und die FlowCam eingesetzt. In dichten *N. scintillans*-Oberflächenansammlungen, wurden ungewöhnlich

hohe Ammonium- und Phosphatkonzentrationen gemessen, was darauf hindeutet, dass *N. scintillans* als „Nährstoffrecycler“ fungiert. Die Bilder der optischen Geräte wurden mit Machine-Learning-Techniken analysiert und ermöglichten einzigartige Einsichten in die Zusammensetzung der Planktongemeinschaft, *N. scintillans*' Fressverhalten und intraspezifische Interaktionen. Die häufig beobachtete Aufnahme von Diatomeen durch *N. scintillans*, gefolgt von einer Blüte Phosphat- und/oder Ammoniumaffiner Dinoflagellaten, deutet auf eine potenziell wichtige Rolle von *N. scintillans* innerhalb der Planktongemeinschaft hin.

Diese Arbeit liefert wertvolle neue Erkenntnisse über die Blütendynamik, die ökologische Rolle und die räumlich-zeitliche Verteilung von *N. scintillans* in der Nordsee. Dies wurde durch die Kombination verschiedener Datenquellen erreicht, darunter Literatur, Zeitreihen und Probandaten. Die Literaturrecherche deckte bedeutende Wissenslücken auf, die sich aus den Einschränkungen der unterschiedlichen Beprobungsmethoden ergeben. Um diese Lücken zu schließen, wurden zwei Zeitreihen analysiert, die sich durch ihre einzigartige Auflösung, Qualität und Dauer auszeichnen. Zum ersten Mal wurden zwei der längsten Plankton-Zeitreihen analysiert, um neue Informationen über die räumliche und zeitliche Verteilung von *N. scintillans* in der Nordsee zu erhalten. Dies unterstreicht die Bedeutung langfristiger Zeitreihen für die Identifizierung vergangener, aktueller und potenzieller zukünftiger Trends der *N. scintillans*-Blütendynamik in der Nordsee und möglicherweise in sich schnell verändernden Ökosystemen auf globaler Ebene. Die Abgrenzung von raum-zeitlichen Hotspots ermöglichte die gezielte Beprobung einer *N. scintillans*-Blüte vom Blütenstart bis zum Absterben der Zellen. Dieser einzigartige Datensatz lieferte wertvolle neue Informationen über die Faktoren, die an den verschiedenen *N. scintillans*-Blütenphasen beteiligt sind, und über die potenziellen Auswirkungen von *N. scintillans* auf die Phytoplanktongemeinschaften in Küstengewässern. Schließlich unterstreicht diese Arbeit das Potenzial innovativer Methoden, einschließlich Unterwasserkameras, die die Visualisierung des *in situ*-Verhaltens von *N. scintillans* in der gesamten Wassersäule mit einer noch nie dagewesenen Auflösung ermöglichten, wodurch das derzeitige Wissen über diesen Organismus erheblich erweitert wurde. Diese neuen Informationen werden zweifellos die Vorhersagbarkeit dieses Organismus verbessern, der in vielen Küstenregionen weltweit zunimmt. In Anbetracht der großen wirtschaftlichen und gesellschaftlichen Bedeutung von Küstengebieten könnten diese neuen Erkenntnisse dazu beitragen, künftige wirtschaftliche Verluste im Zusammenhang mit *N. scintillans* zu mindern, z. B. Auswirkungen auf die Aquakultur, Unterbrechungen der Nahrungsketten, die die Fischerei einschränken, oder nachteilige Auswirkungen auf den Tourismus.

Contents

Acknowledgements	4
Summary	5
Zusammenfassung	7
Contents	9
List of figures	11
List of tables	16
1. General introduction	19
1.1. The importance of plankton in the marine environment	19
1.2. Harmful algal bloom forming species.....	21
1.3. Sampling strategies applied for plankton research.....	21
1.4. Rationale.....	25
1.5. General objectives	27
1.6. Thesis structure.....	28
2. Background of focus species <i>Noctiluca scintillans</i>	30
2.1. General description.....	30
2.2. Geographical distribution of <i>Noctiluca scintillans</i>	31
2.3. Ecological importance of <i>Noctiluca scintillans</i> in coastal ecosystems	38
2.3.1. Role in the food webs	38
2.3.2. Potential role in the carbon cycle.....	42
2.4. Economic and societal relevance	44
2.4.1. Aquaculture and fisheries.....	44
2.4.2. Tourism.....	45
2.5. Knowledge gaps	45
3. Material and Methods	46
3.1. Time series analysis of <i>Noctiluca scintillans</i> in the North Sea.....	46
3.1.1. Study area.....	46
3.1.2. Helgoland Roads time series	48
3.1.3. Continuous Plankton Recorder	54
3.2. High frequency <i>in situ</i> sampling of <i>Noctiluca scintillans</i> in the North Sea	56
3.2.1. Study area and sampling.....	56
3.2.2. Environmental data.....	56
3.2.3. Phytoplankton data.....	57
3.2.4. Statistical analyses.....	60

4. Results	62
4.1. Spatiotemporal long-term trends of <i>Noctiluca scintillans</i> in the North Sea	62
4.1.1. Main drivers of <i>Noctiluca scintillans</i> in the North Sea	62
4.1.2. Temporal trends of <i>Noctiluca scintillans</i> in the North Sea.....	65
4.1.3. Spatial trends of <i>Noctiluca scintillans</i> in the North Sea.....	69
4.2. The role of <i>Noctiluca scintillans</i> in the phytoplankton community composition in the southern North Sea.....	71
4.2.1. Phytoplankton community composition during different <i>Noctiluca scintillans</i> bloom phases	71
4.2.2. Drivers of <i>Noctiluca scintillans</i> abundances throughout a bloom.....	77
4.2.3. Changes in ambient nutrient concentrations.....	81
5. General discussion	84
5.1. Past, present and potential future spatiotemporal distribution of <i>Noctiluca scintillans</i> in the North Sea.....	84
5.2. Drivers throughout a <i>Noctiluca scintillans</i> bloom.....	90
5.2.1. Pre-bloom.....	90
5.2.2. Bloom peak.....	91
5.2.3. Post-bloom.....	93
5.3. <i>Noctiluca scintillans</i> ' influence on coastal ecosystems.....	96
5.4. Uncertainties of the methodological approach used for assessing <i>Noctiluca scintillans</i>	99
5.4.1. Traditional sampling methods	99
5.4.2. Methodologies with higher spatial coverage.....	102
5.4.3. <i>In situ</i> observations.....	105
6. Future directions	109
6.1. Proposed sampling scheme for field campaigns to resolve bloom dynamics and impacts of <i>Noctiluca scintillans</i>	109
6.2. Future expectations.....	113
7. Conclusions	116
References	118
Appendixes	148
Declaration	167
Erklärung des Eigenanteils an den erfolgten Publikationen	168

List of figures

- Figure 1.1:** Infographic summarizing the fundamental role of phytoplankton within marine ecosystems and specifically within the food webs and carbon export20
- Figure 1.2:** Infographic illustrating the variety of plankton size classes (adapted from Colombet *et al.*, 2020).....22
- Figure 1.3:** Example of several traditional plankton sampling methods including nets and water samplers.....23
- Figure 1.4:** Example of several optical and imaging methods for plankton including *in situ* cameras such as the Continuous Particle Imaging Classification system (CPICS), the Video Plankton Recorder (VPR), the *In Situ* Ichthyoplankton Imaging System (ISIIS), the Imaging Flow Cytobot (IFCB) and the Underwater Vision Profiler (UVP), as well as bench-top imaging systems such as the FlowCam and the ZooScan. Target ranges are indicated in italic. The light source is indicated by the yellow lines. The camera is represented by the black shape facing the light source.....25
- Figure 1.5:** Flowchart representing the general structure of the thesis.....29
- Figure 2.1:** Different aspects of *N. scintillans*. **(A.)** Multiple *N. scintillans* cells under the microscope, **(B.)** bioluminescence at night, **(C.)** two *N. scintillans* cells feeding on marine snow, image recorded with a CPICS, and **(D.)** a *N. scintillans* surface patch. All pictures were taken in June 2022 in Helgoland, Germany.....31
- Figure 2.2:** **(A.-D.)** Geographical distribution of documented occurrences (dots) of *N. scintillans* mentioned in literature between 1857 and 2023 and **(E.)** changes in documented occurrences of *N. scintillans* by decade by continent (see Appendix 1 for more details).....32
- Figure 2.3:** Overview of the influence of *N. scintillans* on coastal ecosystems: **(1)** rapidly proliferating through **(A.)** asexual and **(B.)** sexual reproduction. **(2)** Outcompeting and/or grazing down plankton populations and inhibiting their growth, leading to reduced food availability for zooplankton and fish. **(3)** Non-selective feeding occurring **(A.)** individually or **(B.)** agglomerated in feeding webs, intercepting prey of various size classes, **(C.)** including harmful species. **(4)** Increasing water viscosity and reducing food uptake of copepods, but increasing it for jellyfishes, **(5)** indirectly fuelling jellification. Altering water quality, while **(6)** depleting the oxygen in the water and **(7)** releasing ammonium, as well as **(8)** maintaining high prey availability through phosphate and nitrogen release. **(9)** Directly participating at carbon

export through bloom decay and indirectly through the fast-sinking faecal pellets of jellyfishes. **(10)** Asphyxiating benthic organisms by gill clogging or sinking of dense blooms. **(11)** Ingesting harmful algae and transfer of toxins to higher trophic levels. (See Appendix 4 for more details).....38

Figure 3.1: Study area in the North Sea. The sampling effort of the Helgoland Roads (HR) and Continuous Plankton Recorder (CPR) time series are indicated by dots. Main rivers estuaries are indicated in italic, RMSd corresponds to the Rhine-Meuse-Scheldt delta.....47

Figure 3.2: Flowchart representing the methodological approach used in this thesis.....48

Figure 3.3: Sketch illustrating the time-lag between dissolved inorganic nitrogen (DIN) and the abundance of *N. scintillans* (black line). The time-lag (black dashed lines) corresponds to the temporal window between peak concentration of DIN (purple line) and the start of the exponential increase of *N. scintillans*.....50

Figure 3.4: Sketch representing the different stages of a *N. scintillans* bloom in the North Sea. The cyan dashed line represents the selected threshold of 500 cellsL⁻¹, corresponding to the bloom condition for *N. scintillans*.....53

Figure 3.5: Map of the study area in the southeastern North Sea. Sampling stations are indicated by dots.....56

Figure 3.6: Example of segmented images with *N. scintillans* **(A.-E.)** feeding. Recorded with a CPICS in June 2022, Helgoland, Germany. The images represent: **(A.)** two *N. scintillans* cells feeding on marine snow and diatom chains. **(B.-E.)** Single cells ingesting different diatom chains.....60

Figure 4.1: Effect plots of the best-fitted GAM for the HR time series. Dashed lines represent two standard errors above and below the estimate of the smooth curve represented by the solid line. Y-axes are on the scale of the predictor variable, i.e. *N. scintillans* abundance (cellsL⁻¹). The rug plots at the bottom of the x-axes indicate observations of the predictor variable.....63

Figure 4.2: Effect plots of GAMs for the **(A.)** pre-bloom phase; **(B.)** post-bloom phase from the Helgoland Roads time series. All values are on the scale of the linear predictor. Dashed lines represent two standard errors above and below the estimate of the smooth curve. Y-axes are on the scale of the predictor variable, i.e. *N. scintillans* abundance (cellsL⁻¹). Rug plot (at the foot of each plot) shows observations of predictor variables.....63

Figure 4.3: Effect plots of the best-fitted GAM for the Continuous Plankton Recorder survey. Dashed lines represent two standard errors above and below the estimate of the smooth curve, represented by the solid line. Y-axes are on the scale of the predictor variable, i.e. <i>N. scintillans</i> abundance (cellsL ⁻¹). The rug plots at the bottom of the x-axes indicate observations of the predictor variable.....	65
Figure 4.4: Decadal variations in mean seasonal abundance of <i>N. scintillans</i> at Helgoland Roads for the period 1962-2020. Error bars represent the standard error from the mean.....	66
Figure 4.5: Variations of the <i>N. scintillans</i> bloom window length at Helgoland Roads shown as boxplots for the period 1962-2020. The bloom window corresponds to the yearly timeframe between the first and last measurement of <i>N. scintillans</i> abundances ≥ 500 cellsL ⁻¹ . The boxes extend from the 25th to the 75th percentile where the solid line indicates the median. Observations are indicated by dots.....	67
Figure 4.6: Seasonal variations of predicted <i>N. scintillans</i> abundance (cellsL ⁻¹) by decade (square root-transformed) shown as boxplots for the period 1985-2017 (Continuous Plankton Recorder). The boxes extend from the 25th to the 75th percentile where the solid line indicates the median. Observations are indicated by dots.....	69
Figure 4.7: Seasonal predictions of <i>N. scintillans</i> abundance (cellsL ⁻¹) by the best-fitted GAM for the Continuous Plankton Recorder survey in the North Sea (1985-2017).....	70
Figure 4.8: Temporal variation in abundances of <i>N. scintillans</i> and diatoms. (A.) corresponds to abundances measured in station 1, (B.) in station 2, and (C.) to abundances measured within dense <i>N. scintillans</i> surface slicks at stations 1 and 3. Error bars represent the standard error from the mean.....	72
Figure 4.9: Contour plots representing the vertical distribution and major axis length of the two main taxa observed during the sampling campaigns in summer 2022 with the CPICS. Highest occurrences are indicated by the darkest shade.....	73
Figure 4.10: Temporal variation in daily mean abundances of the main phytoplankton taxa recorded with the FlowCam. (A.) corresponds to abundances measured in station 1, and (B.) in station 2. Error bars represent the standard error from the mean.	74
Figure 4.11: Principal coordinates analysis (PCoA) of environmental parameters and main phytoplankton taxa identified during cruises #2 and #3 in the study area with the FlowCam. The axes labels indicate the percentage of variability explained by each axis. Samples (dots) and variables (lines) are plotted against the first two axes.....	76

Figure 4.12: Temporal variation of the pigment composition of the water samples collected in June and August 2022 in the study area. * indicates samples collected within dense *N. scintillans* surface occurrences.....77

Figure 4.13: Daily means of the environmental conditions at surface including **(A.)** SST and **(B.)** SSS during cruises #1-#3. The boxes extend from the 25th to the 75th percentile where the solid line indicates the median. Observations are indicated by dots.....77

Figure 4.14: Temporal variation in abundances of *N. scintillans* ingesting diatoms versus diatoms in the water column. Error bars represent the standard error from the mean.....78

Figure 4.15: Principal coordinates analysis (PCoA) of environmental parameters and main phytoplankton taxa identified during cruises #1, #2, and #3 in the study area with the CPICS. The axes labels indicate the percentage of variability explained by each axis. Samples (dots) and variables (lines) are plotted against the first two axes79

Figure 4.16: Effect plots of the best-fitted GAM for cruises **(A.)** #1, **(B.)** #2, and **(C.)** #3. Dashed lines represent two standard errors above and below the estimate of the smooth curve represented by the solid line. Y-axes are on the scale of the predictor variable, i.e. *N. scintillans* abundance (cellsL⁻¹).....81

Figure 4.17: Temporal variation of Si and NO₃ concentrations during cruises #1 - #3 at the different stations (1-3) in the study area. * indicates samples collected within dense *N. scintillans* surface occurrences.....82

Figure 4.18: Temporal variation of PO₄ and NH₄ concentrations during cruises #1 - #3 at the different stations (1-3) in the study area. * indicates samples collected within dense *N. scintillans* surface occurrences.....83

Figure 5.1: Yearly variations of mean seasonal abundance of *N. scintillans* at Helgoland Roads for the period 1962-2020.....87

Figure 5.2: Monthly means for all variables included in the GAMs for the Helgoland Roads time series represented as boxplots for the period 1962-2020. The boxes extend from the 25th to the 75th percentile where the solid line indicates the median. Observations are indicated by dots.....91

Figure 5.3: Schematic representation of the environmental preferences of *N. scintillans* during different bloom phases (including pre-bloom, bloom, and post-bloom). Suitable pre-bloom conditions for the growth of *N. scintillans* include high DIN and light availability, leading to phytoplankton growth and, thus, to high prey availability for *N. scintillans*. The bloom phase

with peak abundances occurs in June-July, once calm conditions (including low wind speed and stratification) prevail, leading to nutrient depleted surface waters, thus, low prey availability. With no prey encounter, *N. scintillans* cells accumulate at the surface. Post-bloom conditions correspond to high solar radiation, damaging the cells accumulated at the surface, hence, inducing the bloom collapse.....95

Figure 5.4: Schematic summary of the potential role of *N. scintillans* within the coastal phytoplankton community of the southern North Sea.....99

Figure 5.5: Number of field-based studies focusing on *N. scintillans* and use of methods for data collection between 1857 and 2023. Traditional methods include sampling performed with various types of zooplankton and phytoplankton nets, bottles, and buckets.....100

Figure 5.6: Overview of the information type obtained with the main sampling techniques applied in *N. scintillans*-focused research.....101

Figure 5.7: *N. scintillans* blooms at different scales. **(A. and B.)** Pictures taken from the research vessel Ludwig Prandtl in June 2022, Helgoland, Germany; and **(C.)** detail of a satellite image of an ~500 km long *N. scintillans* bloom along the Danish North Sea coast acquired by Sentinel-2MSI on 29 June 2022.....102

Figure 5.8: *N. scintillans* **(A.-D.)** feeding, and **(E. and F.)** asexually and **(G.)** sexually reproducing. Recorded with a CPICS in June 2022, Helgoland, Germany. The images represent: **(A.)** agglomerated *N. scintillans* cells feeding on marine snow. **(B.)** A single cell ingesting a diatom chain and marine snow. **(C.)** The phagotrophic ingestion of a diatom chain. **(D.)** The ingestion of *N. scintillans* by a Ctenophore. **(E.)** A single *N. scintillans* cell undergoing binary fission with cytoplasmic mass forming at the centre. **(F.)** The final stage of binary fission with the trophont dividing into two identical daughter cells. **(G.)** The final stage of the gametogenesis with progametes aggregating on one side of the parent cell.....108

Figure 6.1: Sketch of a *N. scintillans* bloom and environmental conditions in a coastal area of the northern hemisphere, and timeline of the proposed sampling scheme for field campaigns aiming to resolve *N. scintillans* bloom dynamics and associated impacts carried out over one year. Details regarding the sampling strategies are provided in Table 6.1.....110

List of tables

Table 2.1: Environmental conditions associated with <i>N. scintillans</i> occurrences in literature; included are drivers that are favourable for the development of <i>N. scintillans</i> in laboratory-based studies and in the field (see Appendix 2 for more details).....	36
Table 2.2: Prey of <i>N. scintillans</i> identified in laboratory-based studies, where listed prey was fed to <i>N. scintillans</i> and ensured high growth rates, and field-based studies, where the mentioned prey were found inside dissected <i>N. scintillans</i> food vacuoles or directly observed with underwater cameras, d: diameter, l: length (See Appendix 5 for details).....	40
Table 2.3: Possible predators of <i>N. scintillans</i> identified in literature.....	43
Table 3.1: Environmental data used in the GAMs for the Helgoland Roads and the Continuous Plankton Recorder time series.....	51
Table 3.2: Correlation matrices for the predictor variables for Helgoland Roads time series. On the lower diagonal are Pearson's correlation coefficients; on the upper diagonal are <i>p</i> -values. * indicates significant <i>p</i> -values (<0.05).....	52
Table 3.3: Correlation matrix for the predictor variables for the pre-bloom conditions of <i>N. scintillans</i> in Helgoland Roads. On the lower diagonal are Pearson's correlation coefficients; on the upper diagonal are <i>p</i> -values. * indicates significant <i>p</i> -values (< 0.05).....	52
Table 3.4: Correlation matrix for the predictor variables for the post-bloom conditions of <i>N. scintillans</i> in Helgoland Roads. On the lower diagonal are Pearson's correlation coefficients; on the upper diagonal are <i>p</i> -values. * indicates significant <i>p</i> -values (< 0.05).....	53
Table 3.5: Correlation matrices for the predictor variables for Continuous Plankton Recorder survey. On the lower diagonal are Pearson's correlation coefficients; on the upper diagonal are <i>p</i> -values. * indicates significant <i>p</i> -values (<0.05).....	55
Table 3.6: Environmental data collected during the cruises #1, #2, and #3. Nutrient data were vertically averaged.....	57
Table 4.1: Statistical summary of the best-fit GAMs for the Helgoland Roads and the Continuous Plankton Recorder time series.....	62
Table 4.2: Summary of drivers associated with different bloom phases of <i>N. scintillans</i> at HR (see Fig. 4.1, Fig. 4.2, and Appendix 6 for more details).....	64

Table 4.3:	Summary of the decadal sampling effort in Helgoland including number and percentage of analysed samples containing <i>N. scintillans</i> , as well as number and percentage of sampled <i>N. scintillans</i> blooms ($\geq 500 \text{ cellsL}^{-1}$).....	66
Table 4.4:	Summary table of decadal mean abundances of <i>N. scintillans</i> (cellsL^{-1}) in the summer for the Helgoland Roads time series, confidence limits (CL) at 95%, and GLM with Poisson distribution model outputs. * indicates p -values < 0.05	67
Table 4.5:	Summary table of <i>N. scintillans</i> bloom window duration (BWD) for the Helgoland Roads time series, confidence limits (CL) at 95%, and one-way ANOVA outputs. * indicates p -values < 0.05	68
Table 4.6:	Summary table of <i>N. scintillans</i> bloom window duration (BWD) for the Helgoland Roads time series without the unusual <i>N. scintillans</i> bloom event in 1989, confidence limits (CL) at 95%, and one-way ANOVA outputs. * indicates p -values < 0.05	68
Table 4.7:	Taxonomic composition of phytoplankton imaged throughout the cruises #1-#3 with the CPICS and the FlowCAM. Values are means per cruise of abundance (cellsL^{-1}) and size (μm) of the different taxa identified, “-” indicates unavailable data.....	71
Table 4.8:	Results for Bonferroni pairwise comparisons from the ANOVA testing differences in <i>N. scintillans</i> abundances among cruises, stations, and bloom condition (e.g. surface slick)....	72
Table 4.9:	Results for Bonferroni pairwise comparisons from the ANOVA testing differences in diatom abundances among cruises, stations, and bloom condition (e.g. surface slick).....	73
Table 4.10:	DistLM model output for FlowCam data during cruises #2 and #3.....	75
Table 4.11:	Output of stepwise selection of GAMs for the cruises #1-#3 carried out around Helgoland in summer 2022. * indicates the best-fitting model. AIC: Akaike’s Information Criterion. Variable in italic correspond to the most influential variable.....	80
Table 4.12:	Summary table of mean concentrations of the nutrients measured throughout the cruises #1, #2, and #3 (μmolL^{-1}) and standard error from the mean.....	82
Table 5.1:	Number of days with “strong wind events” within the yearly <i>N. scintillans</i> bloom windows (i.e. daily mean wind speed $> 10 \text{ m s}^{-1}$ (Siegismund and Schrum, 2001)) by decade.....	86
Table 6.1:	Steps of the high resolution and basic proposed sampling framework for the targeted assessment of <i>N. scintillans</i> bloom dynamics and associated impacts; the corresponding timeline is sketched in Fig. 6.1.....	112

1. General introduction

1.1. The importance of plankton in the marine environment

Accounting for approximately 50% of the global primary production and building the base of the aquatic food webs (Fig. 1.1), phytoplankton plays a fundamental role in both marine and freshwater ecosystems (Field *et al.*, 1998). These drifting, plant-like organisms encompass several thousands of species in the marine environment and exhibit a great diversity of sizes and shapes (Sournia, 1995; Righetti *et al.*, 2019; Dutkiewicz *et al.*, 2020). By harnessing nutrients and sunlight, phytoplankton performs photosynthesis and is therefore a major contributor to the oxygen on Earth, accounting for nearly half of the oxygen in the biosphere (Field *et al.*, 1998). Additionally, phytoplankton plays a pivotal role in major biogeochemical cycles including nitrogen, phosphate, and carbon cycles (Arrigo, 2005). Therefore, phytoplankton importantly contributes to the ocean's carbon sequestration and flux export via the biological carbon pump (Reid *et al.*, 2009; Siegel *et al.*, 2014).

The organic material produced by phytoplankton is consumed by zooplankton, serving as a crucial food source for higher trophic levels and influencing the occurrence and abundance of commercially important species, thereby affecting fishery yields (Chassot *et al.*, 2010). Copepods are often highlighted as main link between primary producers and higher trophic levels of the food webs (Turner, 2014). Nevertheless, several studies also identified microzooplankton like protists, ciliates and heterotrophic dinoflagellates as important grazers of phytoplankton, attributing their significance to their rapid and dense proliferations as well as their diverse feeding strategies (Lessard, 1991; Strom, 2001; Landry and Calbet, 2004).

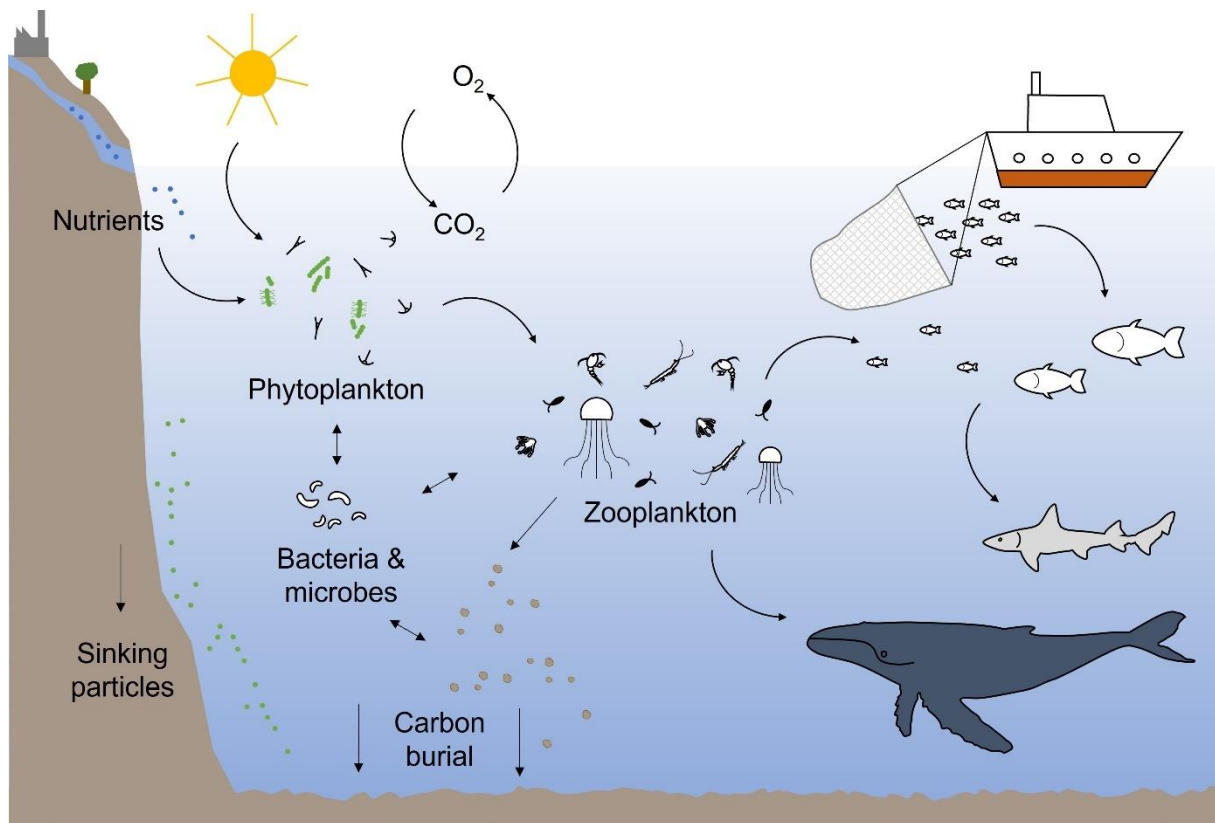


Figure 1.1: Infographic summarizing the fundamental role of phytoplankton within marine ecosystems and specifically within the food webs and carbon export.

Planktonic organisms react rapidly to changes in regional or global environmental conditions and act as ecosystem health indicators. Therefore, the gathering of knowledge about the assemblage composition, distribution patterns, and phenology of plankton, as well as the identification of main environmental drivers, are fundamentally important. In fact, plankton biomass and diversity are considered Essential Ocean Variables (EOVs) and Essential Climate Variables (ECVs) by the Global Ocean Observing System and the Global Climate Observing System, respectively (Miloslavich, Bax, *et al.*, 2018; Bax *et al.*, 2019).

Understanding the changes in phytoplankton biodiversity and spatiotemporal distribution is of utmost importance, particularly in the context of climate change. Changes in wind forcing and precipitation events, together with the global increase of water temperature influencing stratification as well as the metabolism of plankton (Lewandowska *et al.*, 2014), were linked to shifts in phytoplankton bloom dynamics. This includes major alterations of the plankton community, migration of species and shifts in bloom size, initiation and duration (Arrigo *et al.*, 2008; Moore *et al.*, 2008; Hallegraeff, 2010; González Taboada and Anadón, 2014; Friedland *et al.*, 2018; Ardyna and Arrigo, 2020). The increase of anthropogenic activities in the coastal areas such as industrialization and intensification of agriculture caused higher nutrient loadings over time, and also contributed to major alterations of phytoplankton productivity and community

composition (Anderson *et al.*, 2002; Davidson *et al.*, 2014; Van Meerssche and Pinckney, 2019).

1.2. Harmful algal bloom forming species

As some harmful algal bloom forming species (HABs) benefit from land runoff, the anthropogenic nutrient enrichment in coastal waters, and particularly of nitrogen and phosphate, was proposed as main factor leading to the regional increase in frequency and spatiotemporal extent of HABs (Hodgkiss and Ho, 1997; Imai *et al.*, 2006; Heisler *et al.*, 2008). Nevertheless, other factors such as temperature, stratification, light, ocean acidification, and grazing, were also identified as important drivers of HABs (Wells *et al.*, 2015). The alterations of these factors under climate change and particularly increased water stratification, decreased light availability, and expected temperature rise, may significantly influence the fate of HABs in the coming decades (Fraga *et al.*, 1989; Anderson *et al.*, 2005; Lewitus *et al.*, 2012; Hansson *et al.*, 2013). Especially their geographical occurrence and their bloom window length have been predicted to change (Wells *et al.*, 2015).

Harmful algal blooms have increased in many regions over the past decades (Hallegraeff, 1995; Berdalet *et al.*, 2016; Gobler *et al.*, 2017). This trend rises concern as HABs can cause mucilage formation (Smayda, 2006), disease and parasitism in animals including commercial species (Anderson *et al.*, 2019), and can cause significant oxygen depletion (Black, 2001), thus leading to economic losses in tourism and fisheries/aquaculture. Harmful algae can furthermore directly impact human health while producing a variety of potent biotoxins (Anderson *et al.*, 2002). The monitoring of HABs and the identification of environmental conditions initiating HABs need to be enhanced to increase predictive capabilities and to better seize the potential future impact of HABs. In that aspect, long-term time series recording plankton abundance combined with hydrological and meteorological conditions, are exceptionally valuable. In combination with species distribution models (SDM), predictions in time and space can be obtained (Araújo and Rahbek, 2006; Elith and Leathwick, 2009) and the role of environmental variables for the distribution and abundance of different plankton species can be assessed (Barton *et al.*, 2016; Jensen *et al.*, 2017; Matus-Hernández *et al.*, 2019).

1.3. Sampling strategies applied for plankton research

Over the past centuries, a great variety of sampling methodologies has been used to resolve plankton diversity, function, geographical distribution, and how these are linked to various

environmental factors (Wiebe and Benfield, 2003). This includes methods such as nets, bottle samplers, sediment traps, and more recently remote sensing and underwater imaging devices. Nevertheless, sampling plankton is challenging. First, due to the vast range of scales at which the information about the distribution of these organisms is obtained, ranging from a few centimetres to thousands of meters. Second, the immense diversity and size spectrum at which they occur (Fig. 1.2). Additionally, the temporal scale at which plankton develops, behaves, and blooms is also highly variable. This calls for methodologies that allow to resolve plankton dynamics at a great variety of spatiotemporal scales.

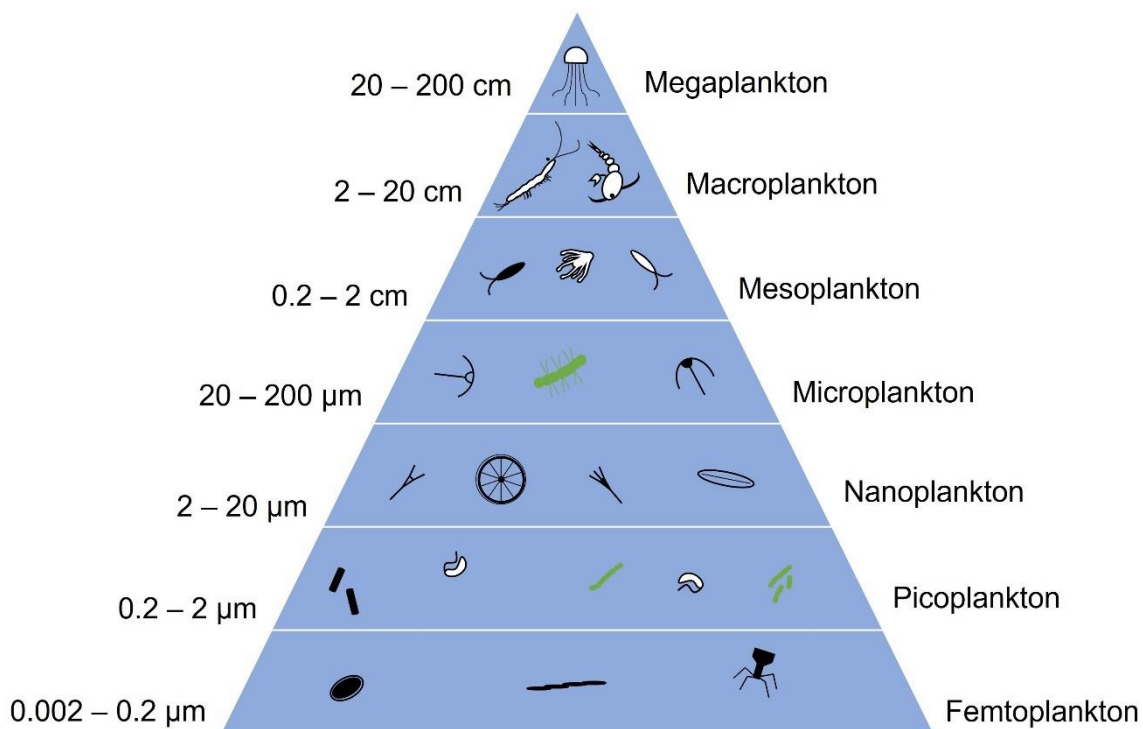


Figure 1.2: Infographic illustrating the variety of plankton size classes (adapted from Colombet *et al.*, 2020).

In 1828, plankton research started with the deployment of nets allowing the physical collection of samples (Fraser, 1968). Rapidly, a great variety of plankton nets and water samplers emerged (Fig. 1.3) and provided fundamental knowledge about plankton. These simple and unexpensive methods allowed the estimations of plankton abundances and community composition and are, until today, the most frequently used methods to sample plankton. Plankton nets of various mesh sizes (from $< 50 \mu\text{m}$ to $> 200 \mu\text{m}$) can be towed either vertically, horizontally, or obliquely through the water column, whereas buckets and bottles can be used for water sampling at the surface and at different depths. Traditional sampling methods allow the collection of plankton samples at high taxonomic resolution providing information about life stages, diversity, and

abundance. Nevertheless, these methods are spatiotemporally limited, since the sample taken in a water parcel is considered to be representative of the area around the station. This can lead to wrong estimates of abundance and hinder the resolution of fine-scale distribution patterns of plankton (Wiebe and Benfield, 2003). Indeed, many oceanic planktonic forms aggregate at various depths causing potential underestimations at distinct depths (Hardy, 1955). Limitations also exist when samples of fragile gelatinous or colony-forming organisms are collected by nets as they can easily be destroyed (Omori and Hamner, 1982; Albaina and Irigoien, 2007). Sampling with bottles preserves the structure of delicate organisms and allows insights into the plankton community composition at higher vertical resolution (Uhlir and Sahling, 1995; Dela-Cruz *et al.*, 2008). Nevertheless, since traditional sampling methods require time-consuming and expensive microscopic analysis, over the past decades, novel techniques such as underwater cameras and bench-top imaging devices have been developed to overcome many of these limitations including the reduced temporal, vertical and horizontal resolution, the preservation of organisms, and the time-consuming analysis.

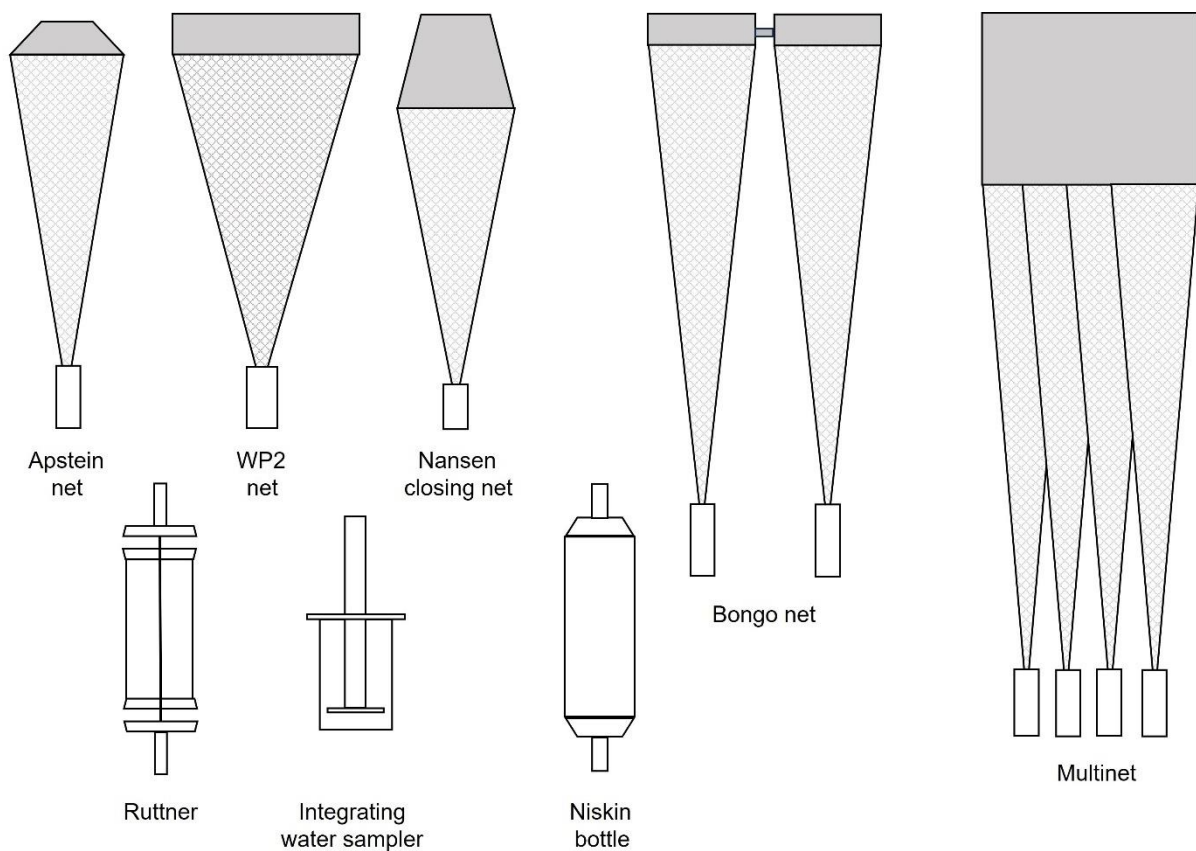


Figure 1.3: Example of several traditional plankton sampling methods including nets and water samplers.

While optical methods are generally considered a recent innovation in plankton research, the first attempts at optical plankton quantification date back to the 1950s (Wiebe and Benfield, 2003). Initially used in combination with plankton nets (Ortner *et al.*, 1981), optical methods have seen rapid development, particularly since the 1990s (Foote, 2000). Nowadays, a variety of camera system types are available (Fig. 1.4). Bench-top imaging devices such as the ZooScan (Grosjean *et al.*, 2004), the FlowCam (Sieracki *et al.*, 1998) or the PlanktoScope (Pollina *et al.*, 2022) digitalize plankton samples, which significantly reduces sample processing time through the utilization of specialized software with trained classifiers. *In situ* camera systems offer additional benefits by resolving vertical patterns and visualizing behaviour such as feeding, reproduction, and interaction of plankton in their natural environment thanks to non-intrusive and non-disruptive data collection. Moreover, data are of high spatiotemporal resolution. In combination with machine learning approaches and artificial intelligence (AI) these devices can deliver near real-time information about diversity, abundance, size, and distribution of planktonic organisms, while significantly reducing cost and need of taxonomic experts (Benfield *et al.*, 2007).

For example, the Video Plankton Recorder (VPR) (Davis *et al.*, 1992) or the *In Situ* Ichthyoplankton Imaging System (ISIIS) (Cowen and Guigand, 2008) can be towed through the water column to resolve mesoplankton diversity and abundance on scales ranging from millimetres to kilometres. Other *in situ* monitoring devices such as the Underwater Vision Profiler (UVP) (Picheral *et al.*, 2022), the Imaging Flow Cytobot (IFCB) (Olson and Sosik, 2007) or the Continuous Particle Imaging Classification system (CPICS) (Gallager, 2016) can be installed at autonomous cabled platforms, thereby providing continuous data of plankton throughout the water column (Fischer *et al.*, 2020). However, while underwater cameras offer numerous advantages, many devices are still costly. Moreover, taxonomic resolution is limited, as organisms can rarely be identified until species level. Nevertheless, this type of data can resolve plankton dynamics at unprecedented scale and facilitate the scalability of plankton observations from local to regional levels (Miloslavich, Pearlman, *et al.*, 2018). Therefore, an increased application of optical devices in the field of plankton research promises operational efficiency and potential global consistency, and might therefore facilitate the development of standardized outputs in the future (Lombard *et al.*, 2019).

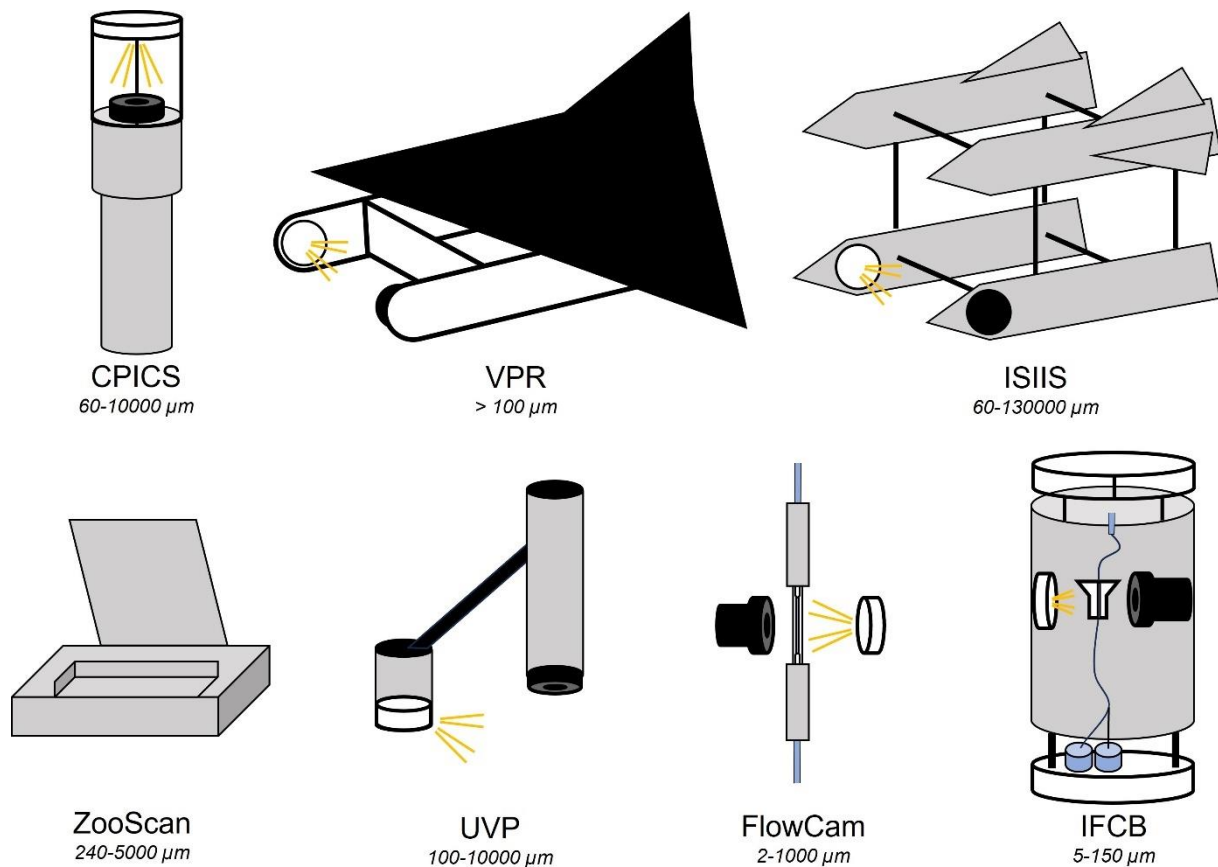


Figure 1.4: Example of several optical and imaging methods for plankton including *in situ* cameras such as the Continuous Particle Imaging Classification system (CPICS), the Video Plankton Recorder (VPR), the *In Situ* Ichthyoplankton Imaging System (ISIIS), the Imaging Flow Cytobot (IFCB) and the Underwater Vision Profiler (UVP), as well as bench-top imaging systems such as the FlowCam and the ZooScan. Target ranges are indicated in *italic*. The light source is indicated by the yellow lines. The camera is represented by the black shape facing the light source.

1.4. Rationale

Harmful algal blooms are intensifying, spreading, and occurring more frequently in many regions around the world and potentially at global level (Gobler *et al.*, 2017; Gobler, 2020). These recent changes have been linked to environmental alterations such as climate change induced temperature increases or rising nutrient inputs from anthropogenic sources (Imai *et al.*, 2006; Wells *et al.*, 2015). Harmful species often benefit from competitive advantages including fast proliferation, diverse feeding strategies, and tolerance towards rapidly changing environmental conditions, leading to plankton communities being increasingly dominated by HABs (Wells *et al.*, 2020). Among these species, the heterotrophic dinoflagellate *Noctiluca scintillans* was identified as one of the most common HAB forming organisms at global level (Wang *et al.*, 2023). The blooms of *N. scintillans* are regularly occurring in coastal waters of Australia, Europe, Asia, Africa, and America (Harrison *et al.*, 2011). In several of these regions, *N.*

scintillans blooms have recently occurred more frequently, intensively, and over wider areas (Hallegraeff *et al.*, 2019; Qi *et al.*, 2019; Ollevier *et al.*, 2021).

These recent trends are concerning as intense blooms of this dinoflagellate have been associated with various negative effects on coastal ecosystems including modified water quality, altered phytoplankton communities, and impacted zooplankton populations, with repercussions on higher trophic levels up to fish. *Noctiluca scintillans* is equipped with an array of competitive strategies ranging from various effective reproductive strategies (Sathish *et al.*, 2021) to non-selective phagotrophic feeding (Kiørboe and Titelman, 1998). This can lead to the outcompeting and replacement of less competitive species, and to plankton communities dominated by *N. scintillans* (Oguz and Velikova, 2010; Xiang *et al.*, 2019). Furthermore, the decay of dense *N. scintillans* blooms can alter water quality through the release of ammonium and phosphate (Ara *et al.*, 2013; Zhang *et al.*, 2021), as well as the decrease of oxygen (Zevenboom *et al.*, 1991), further influencing plankton community composition. Lastly, *N. scintillans* has a low nutritional value (Okaichi and Nishio, 1976; Kiørboe and Titelman, 1998) and is, therefore, rarely preyed upon. This has led to the denomination of this organism as “trophic dead end” or “food chain disruptor” (Uhlir and Sahling, 1990; Daro *et al.*, 2006).

Understanding the factors that have caused the recent increase of *N. scintillans* is crucial to predict the further development of these blooms at global level. However, sampling *N. scintillans* with traditional methods is challenging as these techniques cannot resolve the small-scale vertical and horizontal distribution patterns of plankton (Picheral *et al.*, 2022). This is especially problematic for a gelatinous organism like *N. scintillans* that can form “feeding-webs” (Omori and Hamner, 1982) and vertically migrate through the water column while accumulating at the surface in thin patches of only a few meters width (Astoreca *et al.*, 2005). Moreover, due to the rapidity of the proliferations and the sampling often occurring too late (e.g. once visible blooms appear at surface), the drivers leading to the different bloom phases of *N. scintillans* are still not fully understood, which represents a significant limitation for predicting the occurrences of this harmful organism. To improve the understanding about the bloom dynamics, reproduction, feeding, interactions, and ultimately the impact of this dinoflagellate, a sampling approach including *in situ* imaging devices that allow to visualize and quantify these processes is needed.

The North Sea is a particularly compelling study area to investigate, since the water temperature in this coastal shelf sea has increased significantly faster than at global level (Wiltshire *et al.*, 2008). Since 1962, global ocean temperatures have risen by $\sim 0.7^{\circ}\text{C}$ in 57 years, while average temperatures in the North Sea have increased by $\sim 1.3^{\circ}\text{C}$ over the same period (Amorim *et al.*, 2023). Available climate projections imply that the region will be subject to a variety of climate

change impacts in the future, including further warming, sea level rise, and altered precipitation. River discharge of large rivers such as the Elbe or Rhine, and the nutrient loads they carry to the coast, contribute to anthropogenic eutrophication, which is another factor that influences the coastal ecosystems of the southern North Sea and is affected by climate change (Quante and Colijn, 2016; Voynova *et al.*, 2017). As important nutrient inputs enhance plankton growth (Groß *et al.*, 2022), it can be expected that the plankton communities of the North Sea will exhibit substantial alterations over the coming decades. These changes have already led to major shifts in plankton diversity and abundance (Hinder *et al.*, 2012), and more precisely to the decrease of mixotrophic and autotrophic dinoflagellates in the North Sea (Di Pane *et al.*, 2022). In contrast, the heterotrophic *N. scintillans* has recently followed an increasing trend in abundance in parts of the North Sea (Ollevier *et al.*, 2021). Since the North Sea is of high importance for anthropogenic activities including fisheries, wind farms, oil platforms, shipping, and tourism (Quante and Colijn, 2016), there is a critical need to improve the understanding of past, present, and future bloom dynamics of a potentially important organism such as *N. scintillans*. With several unique datasets monitoring plankton diversity and abundance over several decades including the Helgoland Roads time series (HR) (Wiltshire and Manly, 2004) and the Continuous Plankton Recorder survey (CPR) (Richardson *et al.*, 2006), long-term and recent trends of *N. scintillans* in the North Sea can be investigated at appropriate scales.

In consideration of current and projected climate change scenarios for the North Sea, it can be expected that *N. scintillans*' bloom frequency, duration, and intensity may further increase in the future. Given the significant impact of *N. scintillans* on coastal ecosystems across multiple trophic levels, a potential increase in abundance may considerably influence the composition of local plankton communities in the North Sea and as a result, alter the associated food webs. Better understanding *N. scintillans*' bloom dynamics, and its long-term and recent changes, is required to improve the predictive capacities for this species within the North Sea and potentially in changing coastal ecosystems on a global scale.

1.5. General objectives

Improving the understanding of an organism such as *N. scintillans*, which affects the ecosystem at various levels and that is on the rise in many coastal regions around the globe, is of great importance. Therefore, the main objective of this thesis is to increase the knowledge regarding the bloom dynamics and the ecological role of *N. scintillans* within the plankton communities of the North Sea, a rapidly warming water body. Specifically, this thesis aims to: (i) identify long-

term trends and spatiotemporal hotspots of *N. scintillans* in the North Sea, (ii) to assess the impact of a *N. scintillans* bloom on the coastal ecosystem of the North Sea, and finally (iii) to propose a methodological framework providing novel insights into behaviour, spatiotemporal distribution, and impact of *N. scintillans*. These different objectives are addressed in three main sections outlined below.

1.6. Thesis structure

The structure of this thesis is visually represented in Fig. 1.5.

The first section of this thesis is based on the analysis of literature focusing on *N. scintillans* aiming to identify the main gaps in the knowledge regarding *N. scintillans*, as well as the spatiotemporal distribution and involved drivers of *N. scintillans* at global level.

The second part represents the analysis of two long-term time series (Helgoland Roads time series and Continuous Plankton Recorder survey). The main objectives here were to identify long-term trends of *N. scintillans*, to determine environmental factors driving distinct bloom phases of *N. scintillans*, and finally to delineate spatiotemporal hotspots of this organism in the North Sea.

In the third part of this thesis, data from three sampling campaigns carried out around Helgoland were analysed. The spatiotemporal hotspots identified in the time series analysis enabled the targeted sampling of an entire bloom of *N. scintillans* from initiation until decay and the collection of a unique dataset revealing *in situ* feeding behaviour, prey selection, and interaction of *N. scintillans* at unprecedented resolution. These data provided new insights in how *N. scintillans* shapes coastal ecosystems and more specifically phytoplankton community composition and water quality.

Lastly, the results of the previous section highlighted the potential of combining traditional sampling techniques and optical methods for improving the understanding of *N. scintillans*' ecological role. Nevertheless, as some limitations were still experienced, a holistic methodological framework was proposed to overcome methodological limitations and to ultimately close the remaining knowledge gaps.

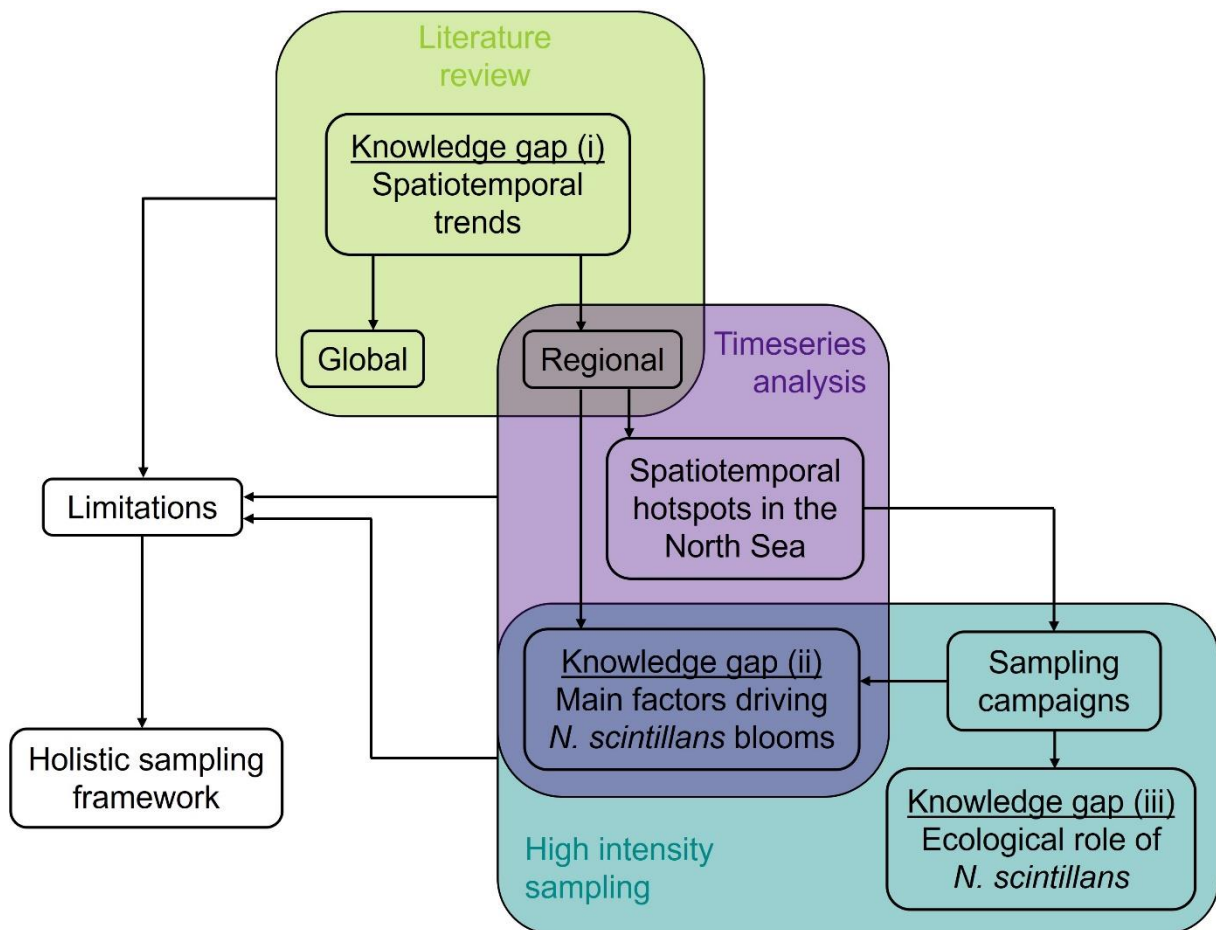


Figure 1.5: Flowchart representing the general structure of the thesis.

2. Background of focus species *Noctiluca scintillans*

2.1. General description

Noctiluca scintillans (Macartney) is a large cosmopolitan dinoflagellate, with a cell diameter between 100 and 1000 μm , reaching up to 2000 μm (Elbrächter and Qi, 1998) (Fig. 2.1A, C). Commonly known as “sea-sparkle”, *N. scintillans* is a bioluminescent organism (Fig. 2.1B) using this ability to visually repel potential predators (Buskey, 1995). At daylight, and particularly during the final bloom stages, proliferations of *N. scintillans* are visible as red surface patches (Fig. 2.1D). This discoloration is a result of the carotenoids contained in the cells of *N. scintillans* (Balch and Haxo, 1984; Astoreca *et al.*, 2005).

Various temperature ecotypes of *N. scintillans* exist, allowing this organism to proliferate at temperatures ranging from 0°C (Elbrächter and Qi, 1998) to over 30°C (Qi *et al.*, 2004). *Noctiluca scintillans* also tolerates wide ranges of salinities (Kang, 2010; Hallegraeff *et al.*, 2019). This tolerance explains the cosmopolitan occurrence of *N. scintillans*. In fact, there is a consensus that it is an important species of the global coastal ecosystems, being the most prominent red-tide forming species in China (Huang and Qi, 1997; Qi *et al.*, 2004; Song *et al.*, 2020) and Australia (Hallegraeff *et al.*, 2019), and seasonally dominating the plankton community in the North Sea (Astoreca *et al.*, 2005), the Black Sea (Aytan and Şentürk, 2018) or the southern Bay of Biscay (Cabal *et al.*, 2008).

Although *N. scintillans* is classified as dinoflagellate, several of its characteristics challenge its classification within phytoplankton. Consequently, *N. scintillans* is commonly listed as component of the zooplankton community in literature. It is mainly its size, feeding behaviour, and reproductive strategies that complicate its definite classification. In fact, *N. scintillans*' large diameter, its non-discriminate phagotrophic feeding, diploid vegetative cells and the vast amount of gametes produced during sexual reproduction (Elbrächter and Qi, 1998; Fukuda and Endoh, 2006) are atypical characteristics for dinoflagellates and hence position *N. scintillans* at the intersection between phytoplankton and zooplankton.

Two forms of *N. scintillans* exist, namely the mixotrophic green and the exclusively heterotrophic red form. The green form harbours a photosynthetic symbiont (e.g. *Pedinomonas noctilucae*) ensuring survival with or without external food supply. Its occurrence is restricted to the tropical waters around the Asian continent. The red form occurs globally in all temperate, subtropical and tropical waters (Harrison *et al.*, 2011). Both forms spread and intensified over the past decades. A drastic increase of the green form was observed in the Arabian Sea (Gomes *et al.*, 2014), whereas blooms of the red form have intensified, expanded and increased in

frequency and duration in many regions around the globe (Dela-Cruz *et al.*, 2003; McLeod *et al.*, 2012; Hallegraeff *et al.*, 2019; Qi *et al.*, 2019; Ollevier *et al.*, 2021; Wang *et al.*, 2023). In the study area of this thesis, the North Sea, only the red form of *N. scintillans* is present. Moreover, the global dimension at which recently increasing trends of red *N. scintillans* took place, makes this form particularly noteworthy. Consequently, this thesis focusses exclusively on the red form of *N. scintillans*.

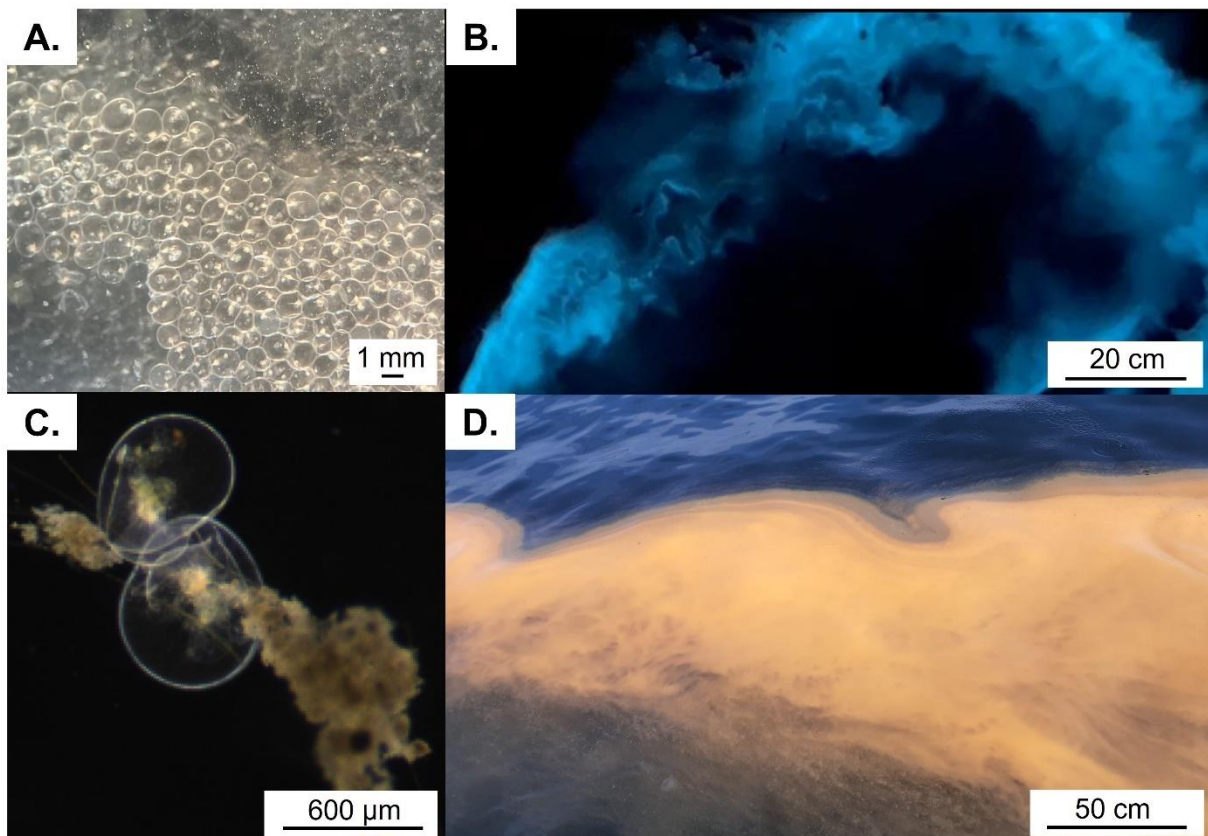


Figure 2.1: Different aspects of *N. scintillans*. **(A.)** Multiple *N. scintillans* cells under the microscope, **(B.)** bioluminescence at night, **(C.)** two *N. scintillans* cells feeding on marine snow, image recorded with a CPICS, and **(D.)** a *N. scintillans* surface patch. All pictures were taken in June 2022 in Helgoland, Germany.

2.2. Geographical distribution of *Noctiluca scintillans*

Noctiluca scintillans blooms have increased over time in frequency and intensity in several regions worldwide (Dela-Cruz *et al.*, 2003; Hallegraeff *et al.*, 2019; Qi *et al.*, 2019; Ollevier *et al.*, 2021; Wang *et al.*, 2023). To describe its spatiotemporal distribution, global records of *N. scintillans* occurrences documented in the literature between 1857 and 2020, were compiled (Appendix 1), as well as the environmental conditions associated with these occurrences (Appendix 2). To reduce observational biases as much as possible, the focus was put on regions

where extensive sampling of plankton has been carried out over several years or decades, thereby enhancing the robustness of the conclusions.

Before 1900, only three reports observing *N. scintillans* were found, namely in eastern Australia, Russia, and Japan (Fig. 2.2A). From 1900 to 1950, *N. scintillans* occurrences recorded in literature increased, with 29 records mostly observed in eastern China and southern India (Fig. 2.2B). Within the following 50 years, over 750 occurrences were documented globally, with *N. scintillans* being witnessed along large parts of the Chinese, eastern Australian, north-eastern, and south-western American coasts, as well as in the Red Sea, the Arabian Sea and in all European Seas except the Baltic Sea (Fig. 2.2C). A strong increase in number of reported *N. scintillans* proliferations can be noticed especially between the 1970s and 1990s (Fig. 2.2E). Since 2000, over 400 occurrences were documented around the globe (Fig. 2.2D), particularly in Asian countries, where 75% of the total observations were made (Fig. 2.2E).

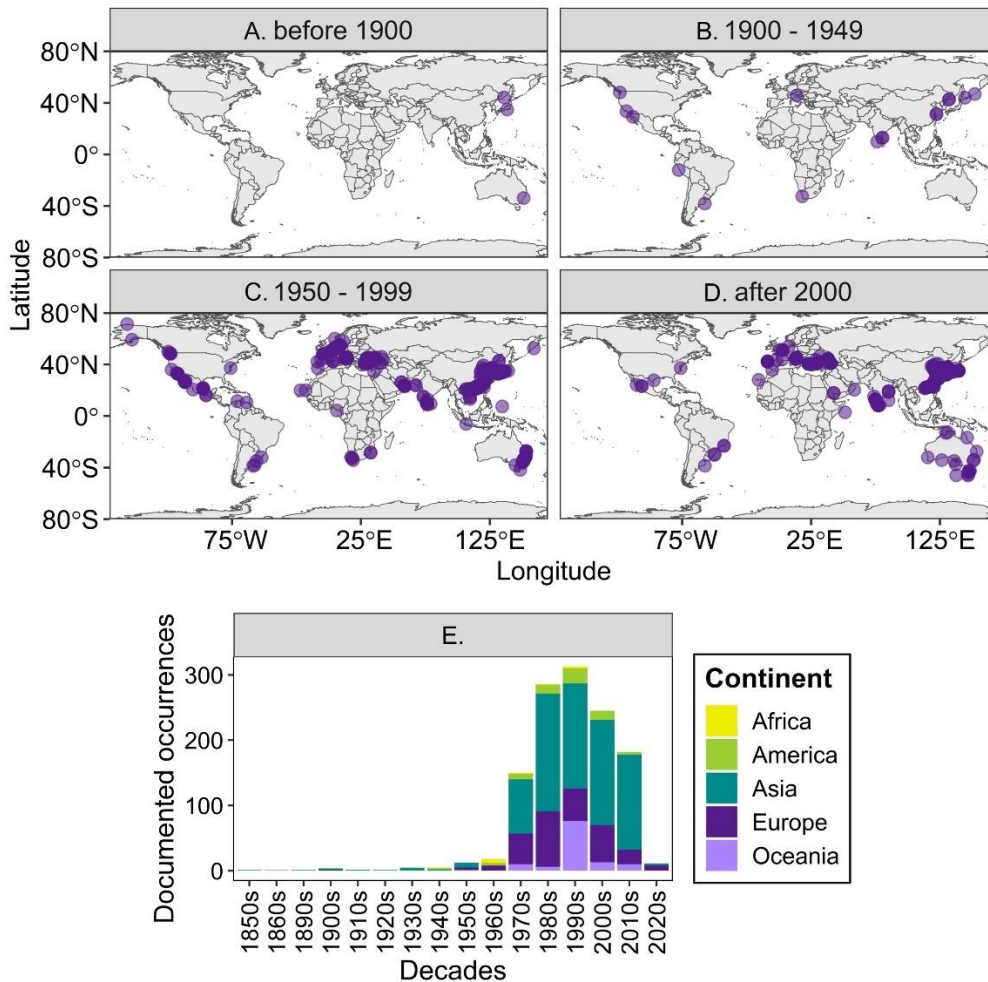


Figure 2.2: (A-D.) Geographical distribution of documented occurrences (dots) of *N. scintillans* mentioned in literature between 1857 and 2023 and (E.) changes in documented occurrences of *N. scintillans* by decade by continent (see Appendix 1 for more details).

Many publications lack information regarding initiation and frequency of reported monitoring programs, rendering statistical analysis unfeasible and preventing definitive conclusions. It is therefore difficult to assess if *N. scintillans* appeared in an area or if it was already present and simply sampled for the first time. To reduce this observational bias and verify potential trends, the focus was brought to areas where regular sampling has taken place.

In Australian waters, for example, reports covering 16 decades indicate a significant increase in biomass and spatial expansion of *N. scintillans* (Davies *et al.*, 2016). Since 1800, sampling was carried out irregularly by several independent ships exploring Australia (Dakin and Colefax, 1940). After the establishment of the Australian museum in 1827 and the foundation of the University of Sydney in 1850, samples were occasionally but regularly collected around Sydney. *Noctiluca scintillans* was first sampled in the Sydney Harbor in 1860 (Bennett, 1860). Between 1929 and 1938, samples were collected every 14 days at Port Jackson, Sydney, where *N. scintillans* was regularly recorded in samples, but at low abundances. Hence, *N. scintillans* was considered as a minor component of the local phytoplankton community (Dakin and Colefax, 1940). Between 1950 and 1989, extensive sampling was carried out around Australia (P. Ajani *et al.*, 2001; Davies *et al.*, 2016). In this timeframe, *N. scintillans* was detected in two more locations, but it was still considered as a rare and ephemeral species until the late 1980s (Hallegraeff *et al.*, 2020). The first visible bloom occurred in 1982 in New South Wales (Hallegraeff, 1995). Since 2008, first occurrences were also recorded in Northern and Western Australia (Hallegraeff *et al.*, 2008). Nowadays, *N. scintillans* is found at all IMOS National Reference Stations (Hallegraeff *et al.*, 2020), where monthly samples are collected around Australia since 2009 (Davies, 2023), and it is considered to be the most prominent red tide-causing organism in many areas (Hallegraeff *et al.*, 2019).

In Tasmania, samples are collected since 1944, with sampling frequencies varying from weekly to quarterly collections (Thompson *et al.*, 2008). Nevertheless, it was only in the 1990s that *N. scintillans* expanded southward and was observed for the first time in 1994 off Tasmania (Hallegraeff *et al.*, 2008), becoming a dominant species in the area since the 2000s (Thompson *et al.*, 2008). Moreover, the seasonal bloom window of *N. scintillans* blooms increased in duration. For example, highest abundances in Tasmania were previously recorded in summer (Thompson *et al.*, 2008), while lately, populations thriving in winter can be witnessed as well (Hallegraeff *et al.*, 2019). Similarly, in southeastern Australia where *N. scintillans* used to only bloom in the spring, proliferations were detected during all seasons since the late 1990s (Dela-Cruz *et al.*, 2002).

Along the Chinese coasts, *N. scintillans* was documented for the first time in 1933 in the East China Sea (Fei, 1952). Defining how *N. scintillans* developed over the following 20 years is challenging, since plankton studies in China started in the 1950s and were carried out on regular basis only since the 1980s (Song *et al.*, 2016). Ecological investigations around China related to or focusing on *N. scintillans* between 1959 and 2019 varied from monthly to seasonal sampling and revealed a gradual increase in density and frequency of *N. scintillans* occurrences (Xiaodong *et al.*, 2023). Within this period, *N. scintillans* established itself as a major component of the plankton community, causing over 30% of all red tides recorded along China's coasts (Tian, 2017). From 1981 to 1988, *N. scintillans* was even responsible for 80% of the red tides reported in the Yangtze estuary (Tian, 2017). Wang *et al.*, 2023 showed that, between 1981 and 2020, *N. scintillans* blooms were observed to become more frequent during spring and summer, to increase in duration and to spread northwards along the eastern Chinese coast.

In Hong Kong, plankton studies were initiated in the 1970s after frequent HABs affected the area (Lee and Chen, 2001). Before 1970, plankton research around Hong Kong was uncommon, as the only documented plankton monitoring in the area was carried out between 1954 and 1959 by the University of Hong Kong and on yearly basis between 1968 and 1969 by Chiu and Tse (Chiu and Tse, 1978). Weekly sampling was carried out between 1969 and 1971 in Tolo Harbor, Hong Kong (Fung and Trott, 1973), yet the *N. scintillans* bloom documented in 1971 was considered as an “uncommon event” (Morton and Twentyman, 1971). In the 1980s, several monitoring programs, such as the Red tide Reporting Network, documenting visible discolorations around Hong Kong (Agriculture Fisheries and Conservation department, 2023) or the monitoring program from the Environmental Protection Department collecting monthly samples around Hong Kong (Environmental Protection Department, 2022) were established. Several cruises of varying sampling frequencies were carried out over the last decades around Hong Kong (Appendix 3), establishing *N. scintillans* as most common HAB species in the area (Zhang, Harrison, *et al.*, 2017).

In Europe, the Adriatic Sea is another example where *N. scintillans* blooms intensified and expanded geographically over time. *Noctiluca scintillans* was first sighted in the northern Adriatic in 1902 (Steuer, 1903). Between 1972 and 2003, biweekly to monthly samples collected in the Gulf of Trieste (45°40.06'N, 13°42.60'E) indicated that *N. scintillans* became a bloom forming species in 1977 (Fonda Umani *et al.*, 1983) and is regularly blooming in the area since. *Noctiluca scintillans* seems to have spread throughout the Adriatic Sea, being detected for the first time in the southern parts in 2009 (Batistić *et al.*, 2018). An intensification of *N. scintillans* blooms was also observed in recent years in the Belgian part of the North Sea where data,

collected on a monthly basis between 2014 and 2018, showed that abundances nearly tripled over a period of 5 years (Ollevier *et al.*, 2021).

The reviewed literature suggested that *N. scintillans* underwent significant changes in several coastal regions around the globe over the last decades. More specifically, a regional increase of *N. scintillans* was observed, indicating a local range expansion and potential intensification. This suggests that this organism is becoming more important at regional level. Since changes in regional or global environmental conditions importantly influence the distribution and abundance of plankton, the recent trends of *N. scintillans* are likely driven by climatic or anthropogenic alterations. Indeed, many environmental factors have been described as potential drivers of *N. scintillans* blooms (Table 2.1).

The northwards spread of *N. scintillans* observed along the eastern Chinese coast for example, was linked to changes in the water temperature (Wang *et al.*, 2023). Temperature is often mentioned in literature as one of the main drivers of *N. scintillans*, with highest growth rates measured for temperatures between 19 and 25°C (Uhlig *et al.*, 1995; Harrison *et al.*, 2011). As dinoflagellates are generally associated with warmer conditions, climate-induced warming of surface water temperatures could explain the local increase of dinoflagellate occurrences (Baretta-Bekker *et al.*, 2009) and can, thus, potentially fuel the increase of *N. scintillans*. For instance, with the strengthening of the East Australian current increasing the transport of warm-core eddies southward, *N. scintillans* has undergone a pole-ward shift since 2010 (McLeod *et al.*, 2012), further expanding southward since 2013 (Hallegraeff *et al.*, 2020). Under climate change conditions, temperatures have been predicted to increase even faster at high latitudes (IPCC, 2021). This suggests that the pole-ward shift of *N. scintillans* might have been driven by increasing temperatures, providing favourable conditions for the development of this species. Similarly, the bloom window elongation observed in several regions may be connected to suitable environmental conditions for *N. scintillans* which are maintained over longer periods. Nevertheless, as *N. scintillans* benefits from numerous temperature ecotypes, it is especially its tolerance towards rapidly changing temperatures that is often mentioned as real competitive advantage. In fact, wide ranges of both temperature and salinity (Table 2.1) have been associated with *N. scintillans* (Huang and Qi, 1997; Hallegraeff *et al.*, 2019) suggesting that this organism is able to thrive in various environments.

However, *N. scintillans* blooms cannot solely be driven by favourable temperatures since the literature-based analysis indicates that warm conditions do not automatically lead to high cell concentrations (Appendix 2). High abundances of *N. scintillans* ($> 100\,000\ \text{cellsL}^{-1}$) were also

recorded at temperatures around 10°C (Turkoglu, 2013). This implies that other factors might contribute to the described changes in *N. scintillans* bloom dynamics.

Table 2.1: Environmental conditions associated with *N. scintillans* occurrences in literature; included are drivers that are favourable for the development of *N. scintillans* in laboratory-based studies and in the field (see Appendix 2 for more details).

Main drivers	Continents			
	America	Asia	Europe	Oceania
SST (°C)	12-23	10.2-30.6	5-25	10-25
Salinity	23-35.4	17-40	10-38.8	20-36.5
pH	-	6.87-8.42	8.2	-
Nutrient concentration	-	High	High	High
Calm/present MLD	Yes	Yes	Yes	Yes
Wind	Low	Low	Low	-
Light intensity	Low/High	High	Moderate/High	-
Precipitation	High	Low	Low	High
Prey availability	High	High	High	High

The geographical spread of *N. scintillans* blooms was associated to local nutrient enrichment of the water masses in the Adriatic Sea (Batistić *et al.*, 2018) and along the southeastern Australian coast (Hallegraeff *et al.*, 2020), suggesting that *N. scintillans* might benefit from high nutrient concentrations. This is supported by the geographical occurrence of *N. scintillans* generally restricted to coasts, where this dinoflagellate is often associated with nutrient-rich waters and even acts as an indicator of eutrophication in many areas (Daskalov, 2002; Batistić *et al.*, 2018). For instance, the most widespread *N. scintillans* blooms documented in the Adriatic Sea correlated with the highest river discharge of phosphorus in the early 1980s (Fonda Umani *et al.*, 2004). Commonly, phosphorus is positively correlated with *N. scintillans*. Like other dinoflagellates, *N. scintillans* has a high DNA-content with high phosphorus requirements (Rizzo, 2003). Accordingly, reducing phosphorus input has been effective in limiting *N. scintillans* proliferations in several areas (Fonda Umani *et al.*, 2004; Oguz and Velikova, 2010). Nutrients, however, cannot directly be assimilated by heterotrophic *N. scintillans* and play an important but indirect role for the proliferation of this organism while increasing prey availability.

Prey availability is a significant driver for *N. scintillans*, and intense blooms can only develop with abundant prey. Therefore, abundances generally peak in temperate seas from late spring until summer, following the diatom spring bloom (Dela-Cruz *et al.*, 2002; Kiørboe, 2003). Altered environmental conditions have induced changes in plankton diversity such as in the Atlantic Ocean and North Sea, where abundances of diatoms recently increased (Hinder *et al.*,

2012). Since diatoms are the preferred prey type of *N. scintillans*, such changes could also have contributed to the potential spread on this organism.

Another factor which is influencing nutrient concentrations and thereby prey availability is stratification. Some dinoflagellates including *N. scintillans* are able to vertically migrate through the water column and benefit from these conditions (Fraga *et al.*, 1989). In the Huon estuary in Tasmania, increased stratification was previously identified as a possible factor initiating dinoflagellate blooms (Thompson *et al.*, 2008). Particularly the phagotrophy of *N. scintillans* is a real asset in warm-stratified and nutrient-poor environments. Since stratification is increasing around the globe and is predicted to follow this trend under future climate change scenarios (Sallée *et al.*, 2021), it can be inferred that this factor could have further contributed to the expansion of *N. scintillans*.

Being a heterotrophic organism, dense surface agglomerations of *N. scintillans* have been associated with low oxygen concentrations (Zevenboom *et al.*, 1991; Hallegraeff *et al.*, 2019). Hypoxia is commonly associated with *N. scintillans* and specifically with the decay of high cell densities, but it is unclear if it also contributes to the bloom formation of *N. scintillans*. Nevertheless, in some regions which have experienced a decrease in oxygen, the Black Sea, for example (Reid *et al.*, 2009), *N. scintillans* dominates the plankton community (Oguz and Velikova, 2010). It can be speculated that, under low oxygen concentrations, which is normally detrimental for other plankton species (Wong *et al.*, 2023), more adapted organisms such as *N. scintillans* might thrive.

It was shown here that *N. scintillans*' tolerance to rapidly changing conditions, increasing temperatures, high nutrient concentrations and prey availability, as well as low oxygen levels, can potentially provide favourable conditions for the spatiotemporal changes of *N. scintillans* identified above. Alterations in coastal phytoplankton community composition have further contributed to these changes. Other factors such as ship ballast water might have accelerated the spread of *N. scintillans* (Hallegraeff *et al.*, 2020). It was postulated that with uncontrolled nutrient input, and the foreseen climate change conditions, *N. scintillans* might potentially widen its geographical spread in the next decades, which could have a strong impact on coastal ecosystems at global level. This, however, still requires a deeper investigation into the factors, which have led to the geographical expansion of this dinoflagellate. Since many of the reviewed field-based studies of *N. scintillans* were carried out once blooms were already visible, i.e. during bloom peak or towards the end of a bloom, crucial information about bloom initiation and associated drivers is still missing. To address these limitations, the analysis of the two long-term

time series, namely the Helgoland Roads time series and the Continuous Plankton Recorder survey, was carried out. These results are discussed in the following sections.

2.3. Ecological importance of *Noctiluca scintillans* in coastal ecosystems

2.3.1. Role in the food webs

Defining the role of *N. scintillans* in coastal ecosystems is complex, since this organism can simultaneously influence food webs, nutrients, and water consistency, both positively and negatively (Fig. 2.3). This dinoflagellate can affect food webs at several trophic levels from phytoplankton to zooplankton and even up to fish in various ways. *Noctiluca scintillans* can outcompete organisms through fast development, effective feeding strategies and through the ability to thrive and effectively reproduce in various environments.

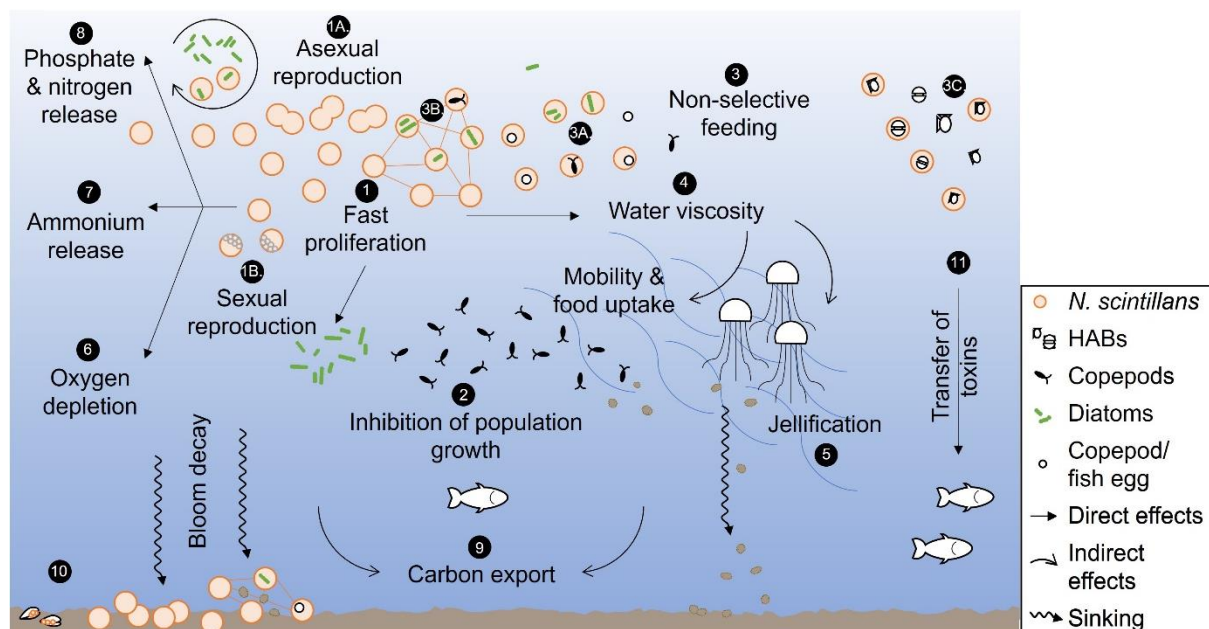


Figure 2.3: Overview of the influence of *N. scintillans* on coastal ecosystems: **(1)** rapidly proliferating through **(A.)** asexual and **(B.)** sexual reproduction. **(2)** Outcompeting and/or grazing down plankton populations and inhibiting their growth, leading to reduced food availability for zooplankton and fish. **(3)** Non-selective feeding occurring **(A.)** individually or **(B.)** agglomerated in feeding webs, intercepting prey of various size classes, **(C.)** including harmful species. **(4)** Increasing water viscosity and reducing food uptake of copepods, but increasing it for jellyfishes, **(5)** indirectly fuelling jellyfification. Altering water quality, while **(6)** depleting the oxygen in the water and **(7)** releasing ammonium, as well as **(8)** maintaining high prey availability through phosphate and nitrogen release. **(9)** Directly participating at carbon export through bloom decay and indirectly through the fast-sinking faecal pellets of jellyfishes. **(10)** Asphyxiating benthic organisms by gill clogging or sinking of dense blooms. **(11)** Ingesting harmful algae and transfer of toxins to higher trophic levels. (See Appendix 4 for more details.)

Noctiluca scintillans benefits from two distinct reproductive strategies (Fig. 2.3, 1). It reproduces asexually (Fig. 2.3A), through longitudinal binary fission (Uhlig and Sahling, 1990) and sexually

(Fig. 2.3B) through formation of flagellate zoospores (Fukuda and Endoh, 2006). While the asexual reproduction has been observed mainly during initial and exponential growth phases (Sathish *et al.*, 2021), sexual reproduction occurs mainly during bloom peaks (Zingmark, 1970). Flagellate zoospores or “swarmer cells” are key triggers for bloom formation (Miyaguchi *et al.*, 2008) and can maintain binary fission when encountering stimulate vegetative cells, leading to exponential growth in areas of high cell density (Miyaguchi *et al.*, 2006). Moreover, zoospores allow *N. scintillans* to bloom year-round once suitable environmental conditions are reached (Miyaguchi *et al.*, 2008). In conjunction with its fast growth and dense accumulations of cells with various effective feeding strategies, *N. scintillans* is able to graze down or inhibit the growth of entire plankton populations (Fig. 2.3, 2) (S. Kitatsuji *et al.*, 2019).

Noctiluca scintillans-specific feeding has been shown to occur in numerous ways. An essential component for feeding is buoyancy. *Noctiluca scintillans* is positively buoyant through active regulation of the ion composition of its cell sap (Uhlig and Sahling, 1985), with intracellular accumulation of NH_4 (Okaichi and Nishio, 1976; Montani *et al.*, 1998), or with increased cell size (Kiørboe and Titelman, 1998). While ascending, starved cells passively intercept prey. The food vacuoles of ascending cells that did not intercept prey remain empty and prevent cells from sinking again, leading to surface accumulations (Uhlig and Sahling, 1990), if not resuspended in the water column by turbulent mixing. The feeding behaviour varies from solitary cells secreting viscous substances (Fig. 2.3, 3A) (Fukuda and Endoh, 2006) to aggregate feeding, where several cells produce mucus strings forming “feeding webs” (Fig. 2.3, 3B) (Omori and Hamner, 1982). This latter has the advantage of increasing both the ascent rate and probability of interception (Uhlig and Sahling, 1990), enabling *N. scintillans* to effectively clear the water from suspended matter or organisms (Kiørboe and Titelman, 1998). Through phagotrophy, *N. scintillans* is able to feed on prey of various size classes ranging from 0.2 μm to several mm (Table 2.2), but the optimal prey size has been previously defined as $> 10 \mu\text{m}$ (Nakamura, 1998b). This might explain its wide spectrum of prey, including phytoplankton (Prasad, 1958; Stauffer *et al.*, 2017), bacteria (Lucas, 1982; Dharani *et al.*, 2004), faecal pellets, detritus (Kiørboe, 2003; Nikishina *et al.*, 2011), fish eggs (Enomoto, 1956; Changjiang *et al.*, 1997) and zooplankton (Dodgson, 1922; Zhang, Harrison, *et al.*, 2017).

Table 2.2: Prey of *N. scintillans* identified in laboratory-based studies, where listed prey was fed to *N. scintillans* and ensured high growth rates; and field-based studies, where the mentioned prey were found inside dissected *N. scintillans* food vacuoles or directly observed with underwater cameras, d: diameter, l: length (See Appendix 5 for details).

	Prey	Size range
Laboratory	Bacteria	0.5 μm (d); 1.25 μm (l)
	Chlorophytes	0.2 – 20 μm (l)
	Coccolithophores	2 – 75 μm (d)
	Copepod eggs	150 – 300 μm (l)
	Diatoms	20 – 500 μm (d)
	Dinoflagellates	10 – 70 μm (l)
	Marine Snow/Detritus	> 2000 μm (l)
	Prymnesiophytes	3 – 9 μm (d)
	Rapidophytes	10 – 80 μm (d)
	Zooplankton	700 – 1800 μm (l)
	Zooplankton larvae	110 – 300 μm (l)
Field	Chaetognathes	> 2000 μm (l)
	Coccolithophores	2 – 75 μm (d)
	Copepod eggs	70 – 200 μm (d)
	Copepods (adults, larvae)	700 – 1800 μm (l)
	Crustacean eggs	160 μm (d)
	Diatoms	20 – 500 μm (d)
	Dinoflagellates	10 – 70 μm (l)
	Fish eggs	500 – 1300 μm (d)
	Marine Snow/Detritus	> 2000 μm (l)
	Prymnesiophytes	3 – 9 μm (d)
	Zooplankton larvae	110 – 300 μm (l)

Among *N. scintillans*' many prey types, zooplankton can be considered as the most impacted, since it is affected both directly through consumption of eggs (Quevedo *et al.*, 1999; Daro *et al.*, 2006) and larvae (Dodgson, 1922; Prasad, 1958; Yilmaz *et al.*, 2005) and indirectly through competition for food (Fonda Umani *et al.*, 2004; Yilmaz *et al.*, 2005). *Noctiluca scintillans* has been observed to ingest up to 60% of daily copepod egg production, ending the growth of copepod populations (Daan, 1987). Furthermore, zooplankton and *N. scintillans* both feed on nano- and picoplankton (Fonda Umani *et al.*, 2004). This type of prey is effectively ingested by dense *N. scintillans* populations; hence, prey availability for zooplankton significantly decreases. Zooplankton is also regularly outcompeted by *N. scintillans* through its dense and rapidly proliferating blooms (Buskey, 1995). On the other hand, *N. scintillans* is too big for most mesozooplankton to be grazed (Gomes *et al.*, 2014). Lastly, with the secretion of viscous substances, dense *N. scintillans* blooms can locally increase water viscosity (Fig. 2.3, 4). This affects mobile zooplankton such as copepods, impeding their movements and food uptake

(Schaumann *et al.*, 1988), while enhancing jellyfish proliferations due to an increased probability of prey encounter (Fig. 2.3, 5) (Fraser, 1969).

Noctiluca scintillans' most common prey type, phytoplankton, is also impacted significantly when *N. scintillans* blooms intensively. Especially less mobile centric diatoms, that are easily entangled in its mucus threads (Suzuki *et al.*, 2014), are heavily grazed (Dela-Cruz *et al.*, 2002; S. Kitatsuji *et al.*, 2019). Diatoms cannot escape the mucus threads due to their reduced mobility, whereas flagellates have been observed to do so (Kiørboe and Titelman, 1998). Other diatoms secrete mucus, increasing their "stickiness" (Decho, 1990) and leading to the formation of aggregates that can effectively be colonized by *N. scintillans* (Tiselius and Kiørboe, 1998). Since *N. scintillans* is an indiscriminate predator, it can outcompete other nutrient-limited organisms such as diatoms that strongly rely on silicate availability (Xiang *et al.*, 2019). The high density and feeding speed of *N. scintillans* cells can lead to down-grazed diatom populations (Fig. 2.3, 2) (Prasad, 1958) and, hence, disrupt diatom-sustained food webs (Harrison *et al.*, 2017).

Moreover, *N. scintillans* blooms indirectly affect marine organisms through changing the local nutrient and oxygen concentrations. It has been shown that the decay of dense proliferations of the heterotrophic *N. scintillans* reduces oxygen availability (Fig. 2.3, 6) and leads to increased ammonium concentration or even toxicity (Fig. 2.3, 7). This negatively influences pelagic and benthic communities (Hallegraeff *et al.*, 2019). On the other hand, *N. scintillans* is considered to be an efficient nitrogen and phosphate recycler (Mohanty *et al.*, 2007; Zhang *et al.*, 2021). Through active feeding, the cells accumulate PO_4 and NH_4 (Montani *et al.*, 1998). These nutrients are subsequently excreted at high rates (Zhang, Liu, Glibert, *et al.*, 2017) through direct catabolic release, food vacuole egestion or mucus production (Schaumann *et al.*, 1988) and are then mineralized in the water column (Vasas *et al.*, 2007). This local nutrient increase has been observed to enhance the development of phytoplankton (Fig. 2.3, 8) (Drits *et al.*, 2013; Genitsaris *et al.*, 2019). The enhanced phytoplankton availability supports the development of higher trophic levels, including zooplankton and fish (Vasas *et al.*, 2007), and represents a direct benefit for *N. scintillans* as it increases bloom duration (Schaumann *et al.*, 1988).

With its non-selective feeding, effective reproduction, its euryhaline and eurythermal properties, *N. scintillans* can develop fast, while maintaining its populations in a great variety of environments. The combination of these properties might give *N. scintillans* significant competitive advantages over the plankton community. These advantages have certainly contributed to the expansion and intensification of this organism described above. Nevertheless, with most of the analyzed literature based on laboratory studies, it is probable that essential

information about behavior, including reproduction, feeding, as well as intra- and interspecific interaction in the natural environment, is missing.

2.3.2. Potential role in the carbon cycle

Noctiluca scintillans might substantially contribute to the biological carbon pump, i.e. the flux of organic carbon throughout the water column. *Noctiluca scintillans* mainly contributes indirectly to the export of carbon, as the main carbon export occurs through jellyfishes or salps feeding on *N. scintillans* (Table 2.3) and releasing large and rapidly sinking faecal pellets (Henschke *et al.*, 2013; Smith *et al.*, 2014). In a different way, *N. scintillans* might contribute to the export of carbon through the important ingestion of marine snow and copepod faecal pellets (Kjørboe, 2003), which are effectively transported to the seafloor upon ingestion and sinking of cells (Fig. 2.3, 9). Similarly, the feeding webs that *N. scintillans* builds entrap detritus, plankton and debris, increasing their weight and pulling them downward (Omori and Hamner, 1982). Gelatinous zooplankton can effectively act as vectors for particulate organic matter and contribute to the carbon export, causing so-called “jelly-falls” (Lebrato *et al.*, 2012). When considering the gelatinous constitution of *N. scintillans* and the density of its blooms, jelly-falls are expected upon bloom decay. Moreover, as *N. scintillans* blooms can collapse within a few hours, this might lead to “pulses” of exported carbon. Therefore, *N. scintillans* could significantly contribute to the export of carbon. Nevertheless, the contribution of *N. scintillans* to carbon export might be limited, particularly when compared to other species, such as coccolithophores, accounting for > 80% of the organic carbon flux (Zondervan *et al.*, 2001),.

Table 2.3: Possible predators of *N. scintillans* identified in literature.

Phylum	Species	References
Arthropoda	<i>Calanus sp.</i>	(Murray and Suthers, 1999)
	<i>Cancer sp.</i>	(Sulkin <i>et al.</i> , 1998)
Chaetognatha	<i>Sagitta sp.</i>	(Oguz and Velikova, 2010)
Chordata	<i>Ammodytidae sp.</i>	(Nakamura, 1998a)
	<i>Unspecified</i>	(Batistić <i>et al.</i> , 2018)
Ciliophora	<i>Strombidium sp.</i>	(Zhang, Chan, <i>et al.</i> , 2016)
	<i>Unspecified</i>	(Baliarsingh <i>et al.</i> , 2016)
Cnidaria	<i>Aurelia sp.</i>	(Kirchner <i>et al.</i> , 1996; Piontkovski <i>et al.</i> , 2021)
	<i>Cyanea sp.</i>	(Nakamura, 1998a)
	<i>Catostylus sp.</i>	(Pitt <i>et al.</i> , 2007)
	<i>Lizzia sp.</i>	(Fock and Greve, 2002)
	<i>Obelia sp.</i>	(Johnson and Shanks, 2003)
	<i>Pelagia sp.</i>	(Malej, 1982)
	<i>Phialidium sp.</i>	(Piontkovski <i>et al.</i> , 2021)
Ctenophora	<i>Mnemiopsis sp.</i>	(Kamburska <i>et al.</i> , 2003)

Only few studies focused on the impact of *N. scintillans* blooms on the carbon cycle and oppositely measured high (Tada *et al.*, 2000) and low (Menden-Deuer and Lessard, 2000) ratios of carbon per cell volume. Nakamura (1998a) found that the production of *N. scintillans* is comparable to that of calanoid copepods and plays an important role in the carbon cycle of Japan. In the Yellow Sea, carbon biomass of *N. scintillans* was found to even exceed that of phytoplankton and copepods (Wang *et al.*, 2018). Nevertheless, the carbon content of cultured cells was found to be nearly two orders of magnitude lower when compared to other dinoflagellates (Kjørboe and Titelman, 1998). Those different results might be linked to the type of ingested prey, influencing the concentration of intracellular carbon. Large diatom species such as *Coscinodiscus wailesii*, for example, enhanced the carbon content of *N. scintillans*, whereas starved cells contained low carbon (Tada *et al.*, 2000).

With climate change, plankton communities are expected to be increasingly dominated by smaller picoplankton with lower export efficiency (Buesseler *et al.*, 2007). Hence, the delivery of particulate organic carbon reaching the seafloor is foreseen to decrease in the future (Smith *et al.*, 2008). Reduced export implies low food availability for the benthos and inhibited carbon sequestration of the oceans (Smith *et al.*, 2008). Therefore, the biomass of gelatinous zooplankton, generally benefitting from climate warming, will become increasingly important and might alleviate some of the planktonic carbon losses (Lebrato *et al.*, 2012). In consideration of the previously described regional intensification of *N. scintillans* and its potentially important role within the coastal carbon cycle, completing the knowledge about the carbon export by this

gelatinous plankton species is critical.

2.4. Economic and societal relevance

2.4.1. Aquaculture and fisheries

As described above, the decay of dense *N. scintillans* proliferations reduces oxygen availability and can cause ammonium toxicity. Intense blooms can modify water consistency and have occasionally been associated with reduced fishing and aquacultural yields. Fish avoid the blooms mainly because of competition for resources (Ogawa and Nakahara, 1979b) since *N. scintillans* feeds on the same prey as planktivorous fish (Vasas *et al.*, 2007). *Noctiluca scintillans* can also directly impact fish populations through the occasional consumption of their eggs (Enomoto, 1956). Benthic communities can suffer from asphyxiation (Fig. 2.3, 10) by abrupt bloom collapses and rapid sinking of large amounts of dead cells forming mucus-like layers (Genitsaris *et al.*, 2019). Due to non-selective feeding, toxic bacteria (Xia *et al.*, 2020), or paralytic shellfish toxin and diarrhetic shellfish toxin-producing microalgae (Escalera *et al.*, 2007) might be ingested (Fig. 2.3, 3C) and transferred to fish when toxins are released in the water after cell lysis (Fig. 2.3, 11). Moreover, the shortening of food webs or jellification (i.e. the significant increase in biomass of gelatinous organisms) can significantly reduce the productivity of an area and hence the food availability for fishes (Fig. 2.3, 2). In the Black Sea, lower fish catches were linked to the reduced zooplankton biomass following a regime shift in which *N. scintillans* and jellyfishes became dominant and led to lower ecosystem productivity (Oguz and Velikova, 2010). Due to its suitable size, *N. scintillans* is a potential prey for planktivorous fish. It is, however, considered as a poor food source due to its low carbon (Kjørboe and Titelman, 1998) and high NH₄ (Okaichi and Nishio, 1976) content, and is not commonly preyed upon. Salps and jellyfishes are the most common of its rare predators (Table 2.3).

For aquaculture and fish farms, the impacts on water quality represent a far greater problem than for the commercial open-water fisheries, as the animals cannot avoid the affected areas. Farmed fishes suffer not only from direct but also from indirect ammonium intoxication, since harmful algal species such as *Gymnodinium catenatum* have a high affinity for ammonium (Yamamoto *et al.*, 2004). Acting as a vector for the harmful *Dinophysis sp.*, *N. scintillans* induced high cultured shellfish mortality in Greece (Escalera *et al.*, 2007). In eastern China, abalone, scallop and mussel farms suffered from high mortality rates when *N. scintillans* proliferated nearby (Yan *et al.*, 2002). Due to the persistence of some blooms, vast aquacultural areas suffered important economic losses, such as in the Yellow Sea in 2008 or in the East China Sea in 2009, leading to economic losses of \$32.6 thousand and \$1.14 million, respectively (Guo *et al.*,

2014). Between 1933 and 2019, the cumulative financial losses associated with *N. scintillans* blooms along Chinese coasts exceeded \$6.9 million (Xiaodong *et al.*, 2023).

2.4.2. Tourism

Several observations of *N. scintillans* blooms negatively affecting tourism can be found in non-scientific reports or local newspapers. Frequently mentioned are the red discoloration and the modified water consistency as reported in the Andaman Sea (Dharani *et al.*, 2004) or in southeast India, where the colour and “soup-like” consistency of the water kept tourists away (Nayar *et al.*, 2001; Padmakumar, Cicily, *et al.*, 2016). A review about the global diversity of HABs reported that *N. scintillans* blooms led to mucilage problems and repellent odours (Zingone and Enevoldsen, 2000). The indirect influence of *N. scintillans* on jellification caused a demographic explosion of jellyfishes in the Adriatic Sea, affecting tourism and requiring the installation of protective nets along the beaches (Salamanca, 2001). In other parts of the Mediterranean, the main impact on tourism is caused by mucilage problems, as in Greece (Genitsaris *et al.*, 2019) and the Dardanelles (Turkoglu, 2013). The main positive effect that *N. scintillans* blooms have on tourism is the bioluminescence, attracting tourists for nocturnal water-based activities (Finlay *et al.*, 2015; Gershwin *et al.*, 2015; Su *et al.*, 2021; Ramyani, 2023).

2.5. Knowledge gaps

Despite the ecological importance and recently increasing trends of *N. scintillans*, the reviewed literature revealed major knowledge gaps. These include: (i) the determination of *N. scintillans*' spatiotemporal trends, particularly at global level; (ii) limited knowledge about drivers triggering and ending blooms; (iii) scarce information about feeding, reproduction, and interaction *in situ*, and (iv) uncertainty regarding its contribution to carbon export. These gaps are partly due to the rapidity at which *N. scintillans* blooms develop and collapse. Point sampling with traditional methods often miss blooms or sample them too late, once surface slicks are visible. This hampers the precise identification of spatiotemporal bloom patterns and drivers inducing bloom initiation, peak, and decay. Since most literature focusing on the behaviour of *N. scintillans* is restricted to laboratory-based investigations, studies aiming to assess feeding, reproduction, and interaction of *N. scintillans* *in situ* are scarce. This significantly limits the available information regarding *N. scintillans*' *in situ* behaviour. This thesis aims to close some of these major knowledge gaps. The focus here has been brought to knowledge gaps (i), (ii), and (iii).

3. Material and Methods

3.1. Time series analysis of *Noctiluca scintillans* in the North Sea

3.1.1. Study area

The North Sea is a semi-enclosed shallow shelf sea reaching a maximum water depth of 750 m in the Skagerrak (De Haas *et al.*, 1997), but most of the North Sea has depths shallower than 100 m. The deeper north is subject to North Atlantic water inflow and is stratified during the warmer months (Artioli *et al.*, 2012), whereas water masses in the shallow south are generally well-mixed by winds and tides, with occasional stratified periods (van Leeuwen *et al.*, 2015) and are significantly influenced by continental runoff (Bozec *et al.*, 2005). Water masses are transported by an anticlockwise residual current system induced by the tidal motion and the dominantly westerly winds and influenced by the shape of the North Sea basin (De Haas *et al.*, 1997). The North Sea is highly productive and intensively used for fishing, wind farms, oil platforms, and shipping (Quante and Colijn, 2016).

Helgoland is a North Sea Island located in the German Bight about 60 km off the German coast. The waters surrounding the island are influenced by the Elbe River, as nutrient loads from the estuary plume can extend in the coastal region as far as Helgoland (Voynova *et al.*, 2017). The maximum water depth around the island is 60 m (Michaelis *et al.*, 2019). Since 1962, the Helgoland Roads (HR) time series has monitored physicochemical and biological parameters including plankton on a daily basis (work-days) at Helgoland (54°11.3'N, 7°54.0'E) (Wiltshire *et al.*, 2008) and is one of the longest marine datasets worldwide. In the North Sea and North Atlantic, the Continuous Plankton Recorder (CPR), a mechanical plankton sampler, has been deployed to collect plankton samples since 1931 (Colebrook, 1960) (Fig. 3.1). The CPR survey is the most extended multi-decadal plankton monitoring program in the world.

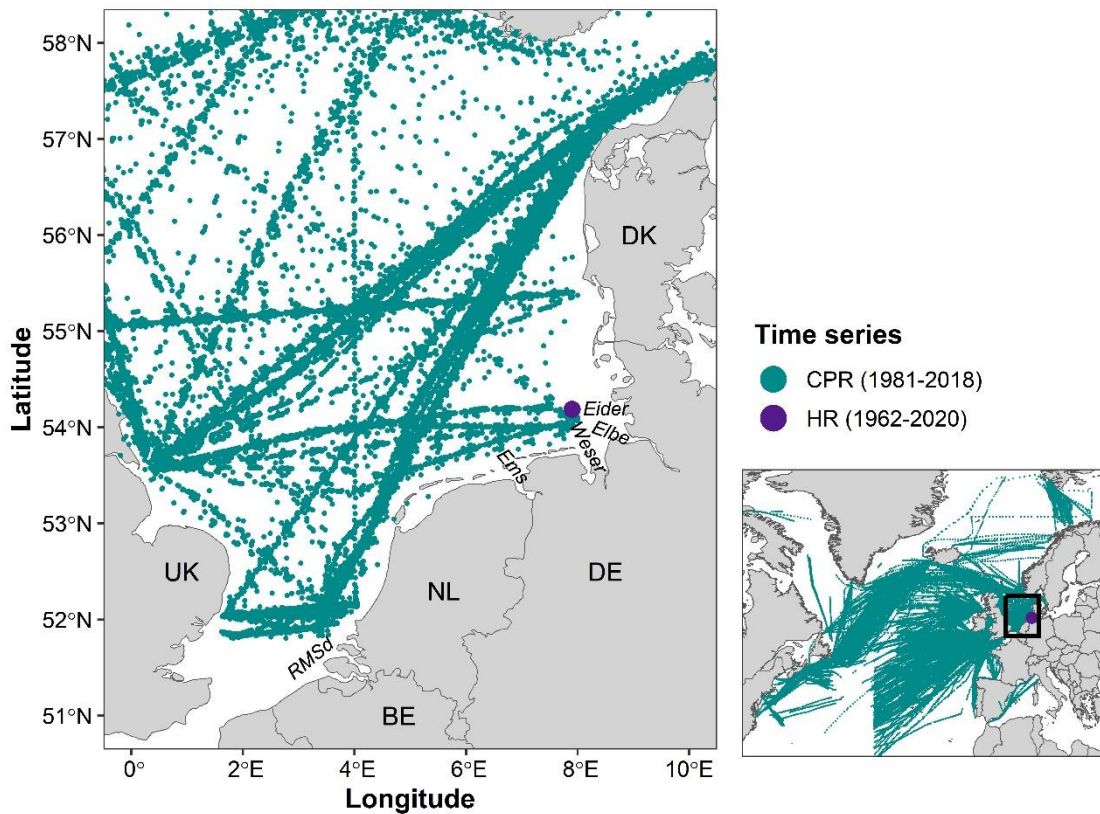


Figure 3.1: Study area in the North Sea. The sampling effort of the Helgolandsriffs (HR) and Continuous Plankton Recorder (CPR) time series are indicated by dots. Main rivers estuaries are indicated in italic, RMSd corresponds to the Rhine-Meuse-Scheldt delta.

Since *N. scintillans* blooms exhibit exponential growth and sudden collapse (Dela-Cruz *et al.*, 2002; Sathish *et al.*, 2021), continuous monitoring at high temporal resolution is needed to accurately elucidate the bloom dynamics of this organism. The HR time series has a uniquely high temporal resolution (work-daily sampling) but is restricted to one specific location (Wiltshire *et al.*, 2008), and hence lacks a reliable spatial coverage. To adequately determine *N. scintillans*' geographical hotspots and a potential spatial spread of this organism, additional data with good horizontal coverage are required. The CPR survey has a lower temporal resolution (monthly sampling), but covers vast areas (Richardson *et al.*, 2006) and therefore complements data from HR. The different spatiotemporal resolution as well as the distinct sampling and plankton quantification methods that were applied for the HR and CPR time series, result in great differences particularly in terms of absolute abundances. Generally, abundance estimates from the CPR data are semi-quantitative and are most useful for assessing interannual or seasonal patterns rather than changes in absolute abundances (Richardson *et al.*, 2006). Therefore, the two datasets were analysed separately to study distinct spatial and temporal patterns. This was done to assess the potential temporal increase of *N. scintillans* by using the

HR data and its spatial increase with the CPR data. A summary of the different methodological approaches applied in this study can be found in Fig. 3.2.

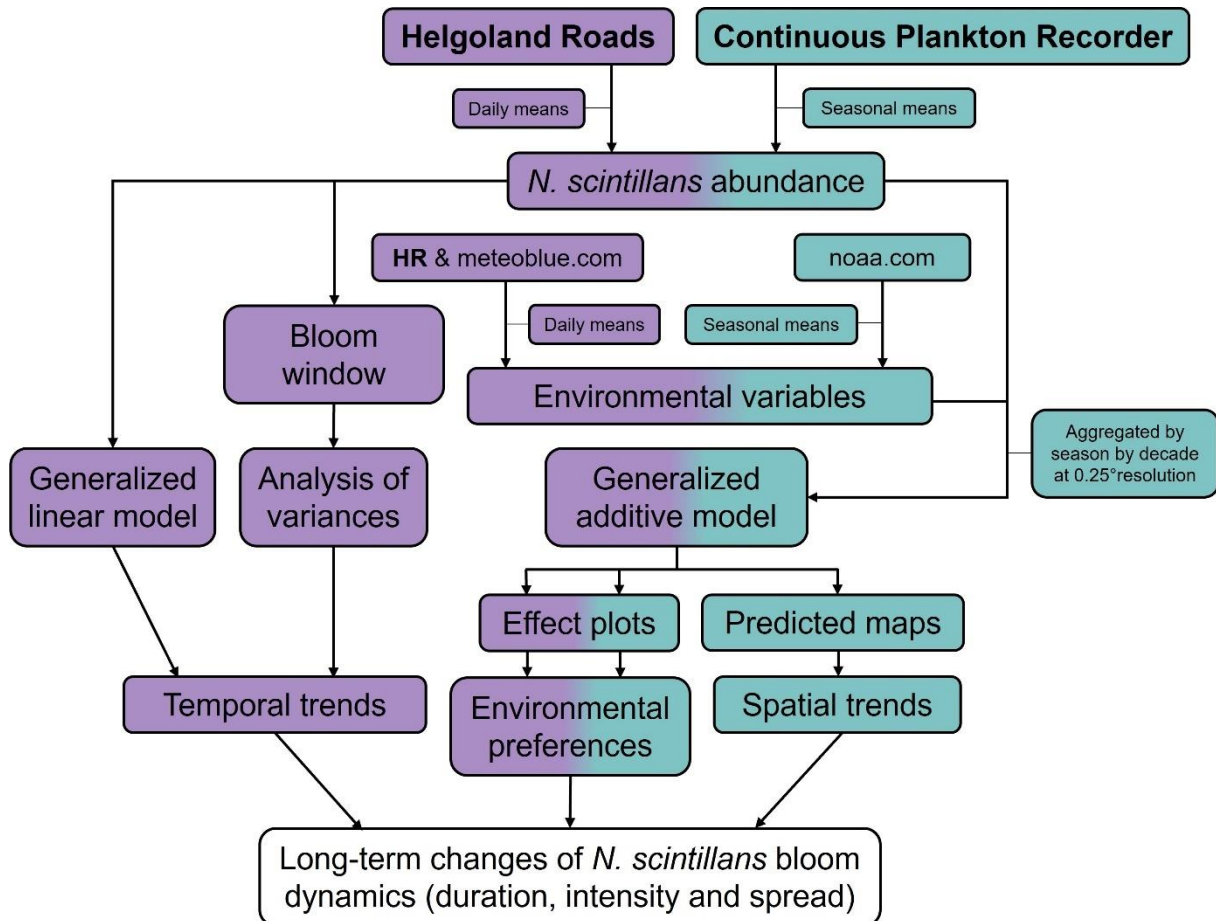


Figure 3.2: Flowchart representing the methodological approach used in this thesis.

3.1.2. Helgoland Roads time series

3.1.2.1. *Noctiluca scintillans* abundance data

For HR, surface water samples were collected on a work-daily basis from 1962 to 2020 with buckets lowered from a research vessel. Subsamples were obtained and preserved with Lugol's solution (final concentration 0.1% Lugol) for plankton analysis (Dummermuth *et al.*, 2023). Enumeration and identification to species level when possible, were carried out in the laboratory with the Utermöhl method and an inverted microscope (Schlüter *et al.*, 2008; Wiltshire *et al.*, 2008).

3.1.2.2. Environmental data

Simultaneously, chemical, and physical parameters were also recorded work-daily along with the plankton samples since 1962. Surface water temperature was measured *in situ*, whereas for salinity and nutrient measurements, surface water samples were collected and analysed in the laboratory. For nutrients, subsamples were analysed by standard colorimetric methods (Grasshoff, 1976), whereas salinity was measured using a salinometer (Wiltshire *et al.*, 2010). The data underlying this study are available in the Data Publisher for Earth & Environmental Science PANGAEA or will be made available on request. Daily means of wind speed and precipitation, as well as solar radiation averaged over 24 hours were downloaded from the meteoblue website for the period 1962-2020 near Helgoland (54°25'N, 8°0'E). The selection of variables was based on their mention in the literature as potentially important drivers influencing the dynamics of *N. scintillans* blooms (See section 1.4.2.). Specifically, sea surface temperature (SST), sea surface salinity (SSS), dissolved inorganic nitrogen (DIN), solar radiation, wind speed, and precipitation were used. Dissolved inorganic nitrogen plays a major role in promoting the growth of a variety of phytoplankton species (Zhang *et al.*, 2024), so this parameter was used rather than including the biomass of specific organisms due to the uncertainty of their importance for *N. scintillans*. A time lag of 30 days was used for DIN based on the temporal shift between the peak of DIN and the start of the exponential growth of *N. scintillans* from May to June (Fig. 3.3), to account for *N. scintillans*' indirect response to changes in chemical variables because of its heterotrophy.

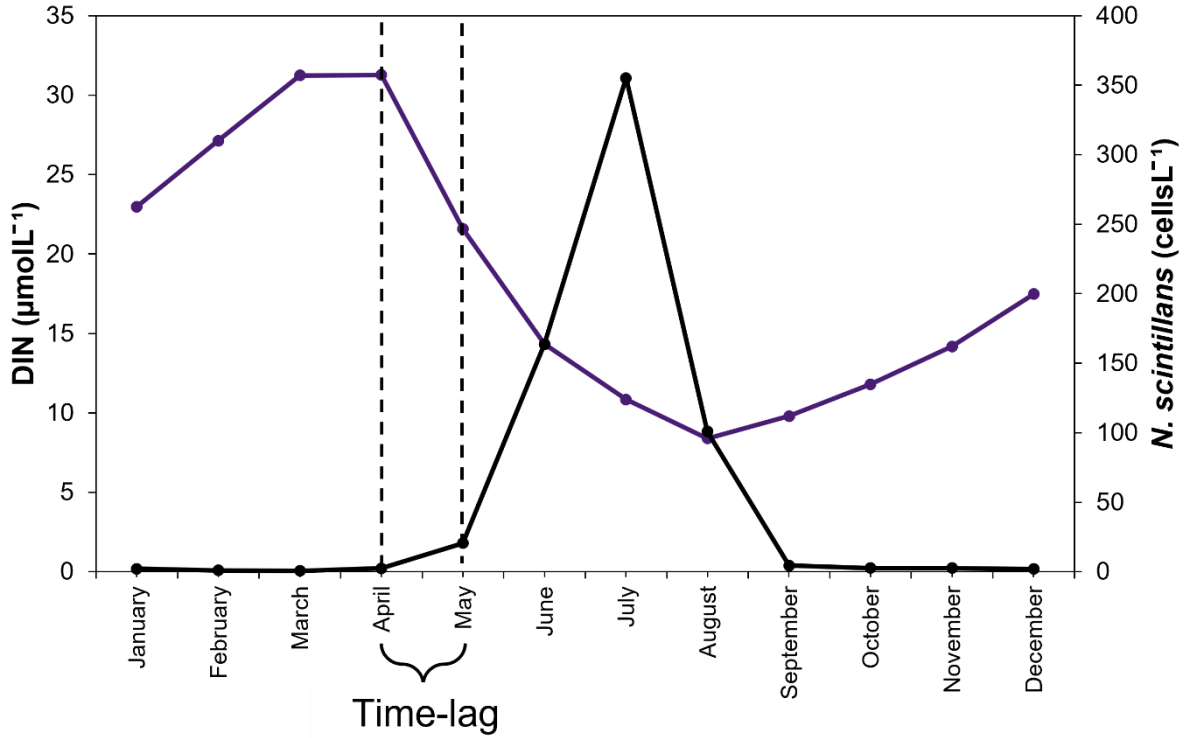


Figure 3.3: Sketch illustrating the time-lag between dissolved inorganic nitrogen (DIN) and the abundance of *N. scintillans* (black line). The time-lag (black dashed lines) corresponds to the temporal window between peak concentration of DIN (purple line) and the start of the exponential increase of *N. scintillans*.

3.1.2.3. Statistical analyses

To assess the potential changes in *N. scintillans* densities over time, differences in *N. scintillans* abundances between different decades were assessed by using a generalized linear model (GLM) (Nelder *et al.*, 1972). Since *N. scintillans* is most abundant from June to August, only abundances during these months were included in the GLM. The model was fitted with a Poisson distribution, given the integer nature of the data. This expresses the abundance of *N. scintillans* x as:

$$(1) x \sim \text{Poisson}(\mu)$$

where μ represents the daily mean. The relationship between $\log(\mu)$ and the predictor is modelled as a linear function. Here,

$$(2) \log(\mu) = \beta_0 + \beta_1 D$$

where β_0 represents the intercept term, and β_1 the coefficients for the factor Decade D .

To assess differences in the length of the *N. scintillans* bloom window over time, a one-way analysis of variances (ANOVA) was used. This method was chosen for its statistical power,

robustness and group mean estimations when compared with non-parametric tests which are based on ranks and, thus, limit interpretations. This expresses the length of the bloom window y as:

$$(3) y \sim \text{Gaussian}(\mu, \sigma^2)$$

where μ represents the mean and σ^2 the variance. The relationship between μ and the predictor is modelled as a linear function. Here,

$$(4) \mu = \beta_0 + \beta_1 D$$

where β_0 represents the intercept term, and β_1 the coefficients for the factor Decade D . A bloom was defined as a day or several consecutive days with abundances ≥ 500 cellsL⁻¹. This abundance was suggested as warning threshold for *N. scintillans* blooms in the Yellow Sea (Xue *et al.*, 2020). Additionally, surface patches were observed at concentrations around 500 cellsL⁻¹ during the cruises, as described in the following sections (see section 4.2.1.). The bloom window corresponds to the entire period during which *N. scintillans* blooms, i.e. all the days from the first until the last measurements of abundance ≥ 500 cellsL⁻¹. Therefore, daily data was inspected, and the length of the bloom window was calculated for each year.

To describe the effect of environmental variables on the abundance of *N. scintillans*, generalized additive models (GAMs) were built using the “mgcv” package in R (Wood, 2017). Generalized additive models are semiparametric extensions of GLMs describing complex relationships and allowing non-linear regressions to be fitted to the data (Wood, 2008). Here, the response variable was the daily abundance of *N. scintillans* (cellsL⁻¹) and the predictor variables are the environmental factors listed in Table 3.1.

Table 3.1: Environmental data used in the GAMs for the Helgoland Roads and the Continuous Plankton Recorder time series.

	Variable	Units	Range (min. – max.)	Average	Source/method	Temporal resolution	Temporal range
HR	SST	°C	-1.6 – 20.5	10.5	<i>In situ</i>	Work-daily	1962-2020
	SSS	-	22.8 – 36.1	32.2	Laboratory		
	DIN	µmolL ⁻¹	0.0 – 143.9	18.2			
	Solar radiation	Wm ⁻²	2.4 – 335.8	128.7	meteoblue.com	Daily	
	Wind speed	m s ⁻¹	1.2 – 18.1	7.7			
	Precipitation	mm	0.0 – 43.5	2.2			
CPR	SST	°C	4.1 – 18.5	10.5	noaa.com	Seasonal	1985-1994
	SSS	-	29.6 – 35.3	34.1			1995-2004
							2005-2017
	MLD	m	5.2 – 81.4	23.8			1981-2010
						2011-2017	

To identify highly correlated predictor variables which can lead to collinearity issues, Pearson's correlation coefficients (Pearson, 1920) were estimated for all predictors (Table 3.2, Table 3.3, and Table 3.4). Variables with coefficients higher than 0.6 or lower than -0.6 were considered collinear (Dormann *et al.*, 2013). Here, no collinearity was found, thus, all variables were included in the model. Since the response variable is integer and positive, the Poisson family of error distribution and logarithm as link function was used for the GAMs. The general model can be expressed as follows:

$$(5) \log(z) = a + f_1(SST) + f_2(SSS) + f_3(DIN) + f_4(Year) + f_5(Month) + f_6(Precipitation) + f_7(Wind\ speed) + f_8(Solar\ radiation)$$

where z is the daily abundance of *N. scintillans*, a is the intercept and f_n are the smooth functions (thin plate regression splines). A backward stepwise procedure was used to select the minimal adequate model (best-fit model). This consisted of building a full model (with all predictor variables), then removing a single variable, and evaluating the significance of its removal for the new model with Akaike's Information Criterion (AIC) (Sakamoto *et al.*, 1986). If the AIC of a model was lower by at least by 2 units, than the previous model, then this model was retained as the best-fit one (Sakamoto *et al.*, 1986). The best-fit GAM was used to describe the effects of the environmental variables on the estimated abundance of *N. scintillans* by the effect plots.

Table 3.2: Correlation matrices for the predictor variables for Helgoland Roads time series. On the lower diagonal are Pearson's correlation coefficients; on the upper diagonal are p -values. * indicates significant p -values (<0.05).

	SST	SSS	DIN	Precipitation	Wind speed	Solar radiation
SST	-	*	*	*	*	*
SSS	-0.12	-	*	*	*	*
DIN	-0.41	-0.23	-	*	*	*
Precipitation	0.09	0.07	-0.09	-	*	*
Wind speed	-0.15	0.16	-0.06	0.31	-	*
Solar radiation	0.40	-0.32	0.11	-0.23	-0.36	-

Table 3.3: Correlation matrix for the predictor variables for the pre-bloom conditions of *N. scintillans* in Helgoland Roads. On the lower diagonal are Pearson's correlation coefficients; on the upper diagonal are p -values. * indicates significant p -values (< 0.05).

	SST	SSS	DIN	Precipitation	Wind speed	Solar radiation
SST	-	0.49	*	*	*	0.12
SSS	0.03	-	*	0.17	*	0.13
DIN	-0.5	-0.31	-	*	*	0.09
Precipitation	0.12	0.06	-0.10	-	*	*
Wind speed	-0.09	0.21	-0.12	0.21	-	*
Solar radiation	0.07	-0.07	-0.07	-0.41	-0.26	-

Table 3.4: Correlation matrix for the predictor variables for the post-bloom conditions of *N. scintillans* in Helgoland Roads. On the lower diagonal are Pearson's correlation coefficients; on the upper diagonal are *p*-values. * indicates significant *p*-values (< 0.05).

	SST	SSS	DIN	Precipitation	Wind speed	Solar radiation
SST	-	*	*	0.27	*	*
SSS	0.09	-	*	*	*	0.18
DIN	-0.54	-0.25	-	*	0.28	*
Precipitation	0.05	0.08	-0.15	-	*	*
Wind speed	-0.17	0.12	-0.04	0.29	-	*
Solar radiation	0.11	-0.05	-0.12	-0.34	-0.29	-

The high temporal resolution of the HR data allowed not only the identification of suitable drivers leading to abundance peaks of *N. scintillans* (i.e. bloom conditions), but also the drivers of different *N. scintillans* bloom phases. Therefore, the daily HR data were additionally subdivided into pre-bloom and post-bloom phases (Fig. 3.4). Considering the fast development and break-down of *N. scintillans* blooms, the pre-bloom phase represents the two weeks before an abundance of ≥ 500 cellsL⁻¹ was measured, and the post-bloom phase represents the two weeks after an abundance of ≥ 500 cellsL⁻¹ was measured. These phases can occur several times per year. These time frames were chosen following Sathish *et al.* (2021), who observed distinct reproductive strategies in those specific time frames and established these guidelines as indicators for the different *N. scintillans* bloom phases. Generalized additive models were built for both pre- and post-bloom phases (Appendix 6).

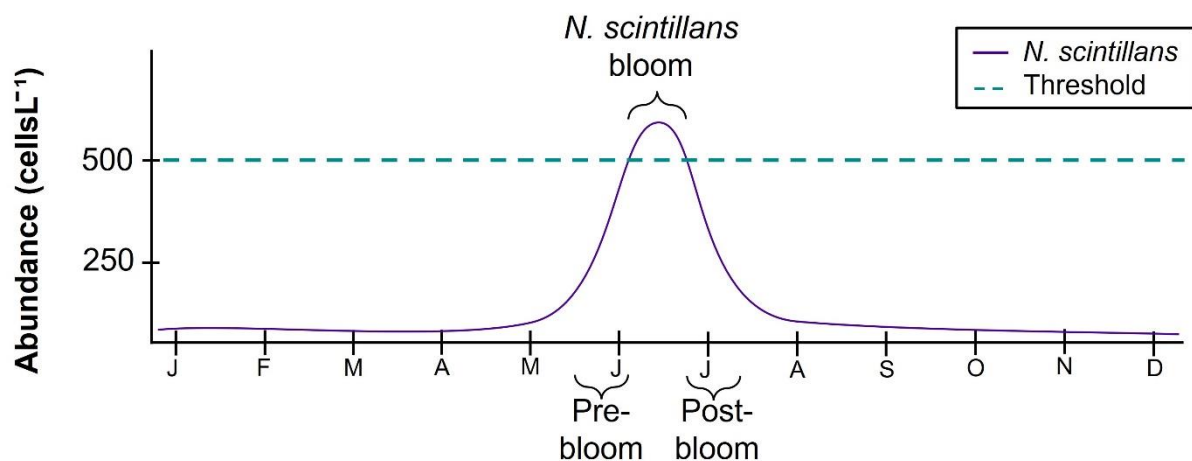


Figure 3.4: Sketch representing the different stages of a *N. scintillans* bloom in the North Sea. The cyan dashed line represents the selected threshold of 500 cellsL⁻¹, corresponding to the bloom condition for *N. scintillans*.

3.1.3. Continuous Plankton Recorder

3.1.3.1. *Noctiluca scintillans* abundance data

Samples were collected continuously by using the CPR, a filtering mechanism housed in an external body, towed repeatedly in the year by ships-of-opportunity on regular routes (Fig. 3.1) at an average speed of 8.7 knots and at a fixed depth of 7-10 m (Warner and Hays, 1994). Planktonic organisms were continuously filtered upon a silk band moving in the housing at a rate of approximately 10 cm per 10 nautical miles, and preserved in 4% formaldehyde (Warner and Hays, 1994). One sample represents approximately 3 m³ of seawater taken over 10 nautical miles. After each tow, samples were analysed in the laboratory, for identification and counting of organisms (counts 3 m⁻³) following the methodology described in Batten *et al.* (2003). *Noctiluca scintillans* is usually identified by its striated ventral tentacle in the CPR samples (Richardson *et al.*, 2006; Kraberg *et al.*, 2010). In this study, *N. scintillans* abundances that were collected with the CPR for nearly four decades (1981-2018) in the North Sea (51°0'-58°0'N, 0°0'-10°0'E) were used (Johns, 2020).

3.1.3.2. Environmental data

For the CPR data, environmental variables were downloaded from the World Ocean Atlas 2018. Seasonal means (winter = January-March, spring = April-June, summer = July-September, autumn = October-December) of SST, SSS, and mixed layer depth (MLD) were obtained (Table 3.1). For modelling, environmental variables and abundance data were aggregated by season and decade over an area of 0.25°.

3.1.3.3. Statistical analyses

For the CPR data, collinearity was checked (Table 3.5) before building GAMs to describe the effects of the environmental (SST, MLD, and SSS), spatial (longitude and latitude as interaction term), and temporal (season and decade) variables (predictor variables) on the abundance of *N. scintillans* (response variable). Because the response variable was continuous, positive, and had large overdispersion, the negative binomial family of distribution and logarithm as a link function was used in the GAMs. The general equation can be written as follows:

$$(6) \log(z) = a + f_1(SST) + f_2(SSS) + f_3(MLD) + f_4(Longitude, Latitude) + f_5(Season) + f_6(Decade)$$

with z as the abundance of *N. scintillans*, a as the intercept and f_n as the smooth functions.

The minimal adequate model was selected as described above. The best-fit GAM was used to describe the effects of the environmental variables on the estimated abundance of *N. scintillans* using the effect plots, whereas the spatiotemporal variability of *N. scintillans* was described with the predicted maps by decade and by season. All data analyses were realized using the R programming software version 4.2.1 (R Core Team, 2023).

Table 3.5: Correlation matrices for the predictor variables for Continuous Plankton Recorder survey. On the lower diagonal are Pearson’s correlation coefficients; on the upper diagonal are *p*-values. * indicates significant *p*-values (<0.05).

	SST	SSS	MLD
SST	-	*	*
SSS	-0.04	-	*
MLD	-0.16	-0.54	-

3.2. High frequency *in situ* sampling of *Noctiluca scintillans* in the North Sea

3.2.1. Study area and sampling

Samples were collected around the North Sea Island Helgoland during three cruises carried out with research vessel Ludwig Prandtl (Fig. 3.5). To capture the entire bloom period of study species *N. scintillans* from onset until decay, the cruises took place in June 2022 (cruise #1: 08.06.2022-12.06.2022 and cruise #2: 21.06.2022-28.06.2022) and August 2022 (cruise #3: 01.08.2022-12.08.2022). Daily samples were collected at two stations: one in the deep trough (maximum depth 60 m) in the south of the island (station 1, 54°14'N-7°9'E), and one in the shallower (maximum depth 20 m) north of the island (station 2, 54°20'N-7°86'E). In the event of visible *N. scintillans* surface accumulations, additional sampling was carried out (station 3, 54°14'N-7°85'E).

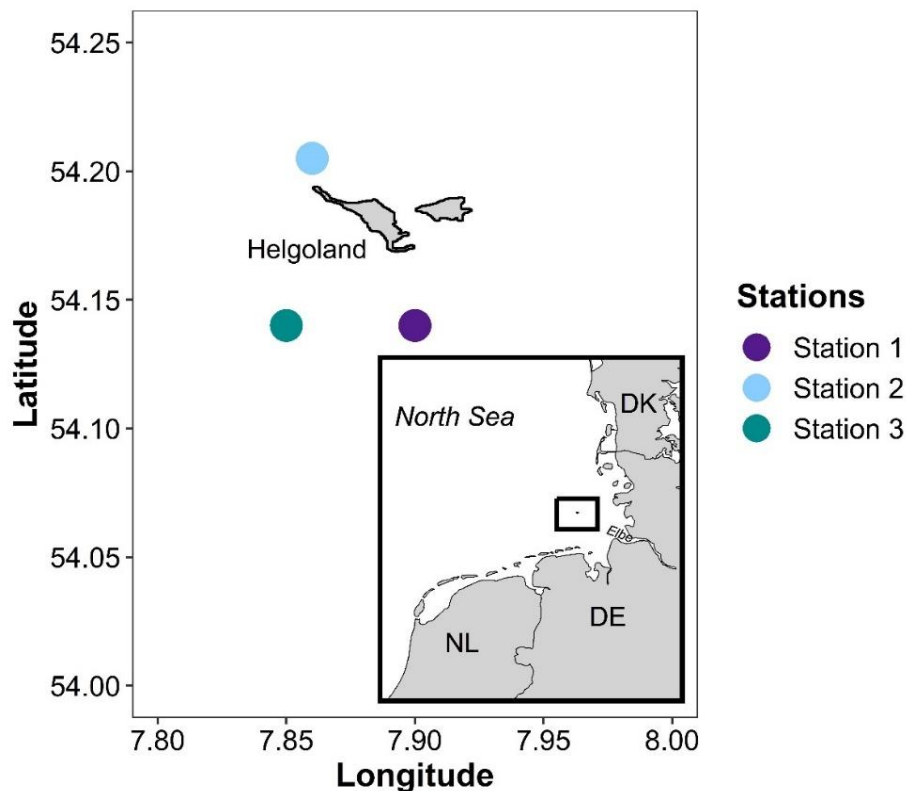


Figure 3.5: Map of the study area in the southeastern North Sea. Sampling stations are indicated by dots.

3.2.2. Environmental data

At each sampling station, vertical profiles of SST and SSS were measured using a calibrated conductivity, temperature, and depth profiler CTD (CTD313, Sea & Sun Technology). Surface

conditions were continuously measured with an on-board flow-through membrane pump or FerryBox with a resolution of one data point per minute (Petersen *et al.*, 2011). At each station, 6 L of seawater per depth were collected below and above the thermocline, and within the chlorophyll-*a* (Chl*a*) maximum, resulting in three reference depths per station.

For nutrients, seawater from each reference depth was immediately filtered through pre-combusted (450°C for 1 h) 47 mm Whatman GF/F filters. Of the filtered water aliquots, 50 mL were transferred in plastic jars and preserved at -20°C until analysis. The water samples were analysed for phosphate (PO₄), silicate (Si), nitrate (NO₃), and ammonium (NH₄) concentrations using an automated continuous flow system (AA500 auto analyser, Seal Analytical) and standard colorimetric techniques (Hansen and Koroleff, 1999). All variables are listed in Table 3.6.

Table 3.6: Environmental data collected during the cruises #1, #2, and #3. Nutrient data were vertically averaged.

	Variable	Units	Range (min.-max.)	Mean	Source/method	Temporal range
Cruise #1	SST	°C	12.1 - 16.8	13.0	CTD	08.06.2022
	SSS	-	30.0 - 32.3	32.0		
	NO ₃	µmolL ⁻¹	2.0 - 5.1	3.7	Water samples	12.06.2022
	NH ₄		1.0 - 4.4	2.6		
	Si		0.0 - 5.5	2.0		
	PO ₄		0.0 - 0.2	0.1		
Cruise #2	SST	°C	13.4 - 18.7	15.4	CTD	21.06.2022
	SSS	-	30.9 - 32.7	32.0		
	NO ₃	µmolL ⁻¹	0.0 - 2.3	1.0	Water samples	28.06.2022
	NH ₄		0.5 - 42.1	2.5		
	Si		0.0 - 7.4	1.5		
	PO ₄		0.0 - 6.3	0.3		
Cruise #3	SST	°C	16.3 - 20.4	17.3	CTD	01.08.2022
	SSS	-	30.4 - 32.7	32.1		
	NO ₃	µmolL ⁻¹	0.0 - 1.3	0.4	Water samples	12.08.2022
	NH ₄		0.1 - 2.2	1.0		
	Si		2.9 - 10.0	7.0		
	PO ₄		0.1 - 0.5	0.2		

3.2.3. Phytoplankton data

3.2.3.1. Pigment data

For pigments, the method applied is a modified version described in Garrido *et al.* (2003). Seawater from each reference depth was immediately filtered through pre-combusted (450°C for 1 h) 47 mm Whatman GF/F filters. The filtered volume of seawater varied between 200 mL and 3000 mL, depending on plankton and particulate matter density. The filters were then placed in 2 mL vials, immediately frozen, and stored at -20°C until analysis. For analysis, the pigments were extracted with 2 mL of 100% acetone for 24 h at -20°C using 6 mL plastic

scintillation vials. The extract was cleared by filtration through a 0.2 µm syringe filter (Spartan 13). Measurement of the pigment concentration in the extract was done using a HPLC system (Shimadzu Prominence-i) and the concentration of the pigment (in µgL⁻¹) was calculated while taking the filtration, extraction, and injecting volume into account. For the HPLC system calibration, pigment standards from DHI and Sigma-Aldrich were used. The true concentrations of the standards were determined by spectrophotometric measurement using the specific extinction coefficient for each pigment as provided in Roy *et al.* (2011).

3.2.3.2. Bench-top imaging

To analyse organisms and particles ranging from 20 µm to 150 µm (Giering *et al.*, 2020), water samples were analysed using a Flow Cytometer and Microscope FlowCAM series VS4 (Fluid Imaging, USA). During cruises #2 and #3, 200 mL of water from each reference depth was sieved through a 150 µm mesh to avoid obstructions of the flow cell and transferred into a pre-rinsed glass bottle. After gentle stirring, 20 mL of the water aliquots were immediately processed with the FlowCAM set up with a 4× objective and a corresponding flow cell. Images were later analysed using the VisualSpreadsheet software of FlowCAM (Version 3.4). Based on prior scanning of the image data, common taxa were identified and libraries for each taxon were established. Cell concentrations (cellsL⁻¹) and sizes (µm) were determined for each dataset.

3.2.3.3. *In situ* imaging

For high-resolution *in situ* imaging of particles and planktonic organisms between 60 µm and 10000 µm (Lombard *et al.*, 2019), the automated underwater camera system CPICS (Coastal Vision Inc., USA) was deployed at each station at the reference depths for 30 minutes per depth. During cruise #3, the CPICS was additionally deployed stationary for 24h with the vertical profiler WireWalker at station 2 (DMO Inc, USA) (Rainville and Pinkel, 2001). The CPICS is an *in situ* particle and plankton imaging microscope with an open flow design thereby providing images of fragile organisms in their natural environment (Lombard *et al.*, 2019). The 6 MP CPICS is equipped with a Point Grey Grasshopper3 camera, bi-telecentric lens 0.9x magnification, and synchronized strobe light in a waterproof housing. Fullframe volume and sampling rate were calculated as:

$$(7) V(fullframe) = W * H * DoF$$

Where V is the volume, W the width, H the height and DoF the depth of field of a fullframe. Sampling rate (volume sampled by the setup per unit time) was calculated as:

$$(8) \text{ Sampling rate} = V(\text{fullframe}) * Fps$$

where Fps is the number of frames per second acquired.

With these settings, the CPICS images 0.83 mL of water per full frame at an average of 13 frames per second, hence sampling at a rate of $\sim 10.75 \text{ mLs}^{-1}$. The CPICS is equipped with a RBR concerto CTD (RBR Ltd) to simultaneously collect environmental data. Each CPICS full frame (2736 x 2192 pixels) was analysed in real-time to detect and save 'Regions of Interest (ROIs)' exceeding an area threshold of 200 adjacent pixels. Size estimations of the main taxa imaged with the CPICS were performed on ROIs and calculated with the number of pixels forming the organism/particle in the ROI (μm).

The images were analysed with semi-supervised machine learning techniques (Vaswani and Möller, 2022). For the unsupervised step improving the classification accuracy, a convolutional neural network (CNN) with a ResNet50 feature extractor (Schanz *et al.*, 2023) was used for pre-training on ~ 700000 unlabelled ROIs. For the supervised fine-tuning step, a random subset (~ 3000 ROIs) was manually annotated for type, class, or species. These labelled images were used to train the CNN in the supervised training step. The accuracy of the CNN on withheld labels was evaluated and predictions on the full dataset were inferred. To each ROI, the CNN assigned probabilities for each of the annotated classes. The class with the maximum probability (max_p) resulted in the predicted label. These predictions were used to extract classes with high conditional accuracy ($max_p > 0.75$) including images of *N. scintillans*, which were labelled to generate trait annotations capturing information about morphological and behavioural characteristics of the imaged organisms. This allowed the identification and quantification of the most frequently consumed prey types (Fig. 3.6), therefore providing valuable additional information that was not available in the previously analysed time series for instance (see section 3.1.). A flowchart with the different steps of the analysis is provided in Appendix 7.

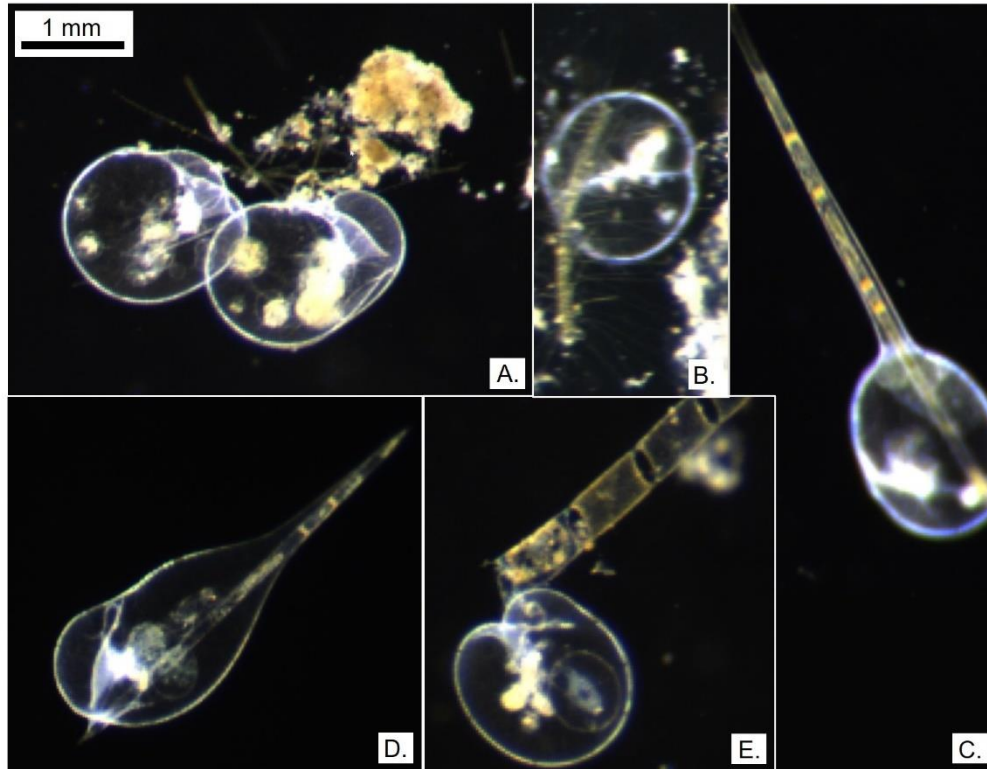


Figure 3.6: Example of segmented images with *N. scintillans* (A.-E.) feeding. Recorded with a CPICS in June 2022, Helgoland, Germany. The images represent: (A.) two *N. scintillans* cells feeding on marine snow and diatom chains. (B.-E.) single cells ingesting different diatom chains.

3.2.4. Statistical analyses

Differences in *N. scintillans* and diatoms abundances were assessed among cruises, stations, and bloom conditions (e.g. surface slick) using an ANOVA. Pairwise comparisons were performed using the Bonferroni adjustment. To determine if physical variables (temperature and salinity) or biological factors (abundance of diatoms) influenced the abundance of *N. scintillans*, GAMs were built for each cruise. The model was limited to three smoothing knots, thereby increasing the comparability and reliability of the model outputs. In the models, the abundance of *N. scintillans* was the response variable, whereas physical and biological factors were predictor variables. The general formula of the model can be expressed as followed:

$$(9) \log(b) = a + f_1(SST) + f_2(SSS) + f_3(Diatom\ abundance)$$

With b as the abundance of *N. scintillans*, a the intercept and f_n are the smooth functions (thin plate regression splines). Analyses including GAMs and ANOVA were performed with the R software (R Core Team, 2023).

The phytoplankton community structure was analysed with non-parametric multivariate methods using the software PRIMER (7.0.23). The data were forth-root transformed to even out the contribution of rare and/or abundant taxa prior to the analysis. A Bray-Curtis similarity

matrix reflecting changes in abundance and taxonomic composition was used and visualized with a principal coordinates analysis (PCoA). To assess the differences among cruises, a Permutational multivariate analysis of variance (PERMANOVA) with 9 999 permutations was applied (Anderson, 2001). A stepwise distance-based linear model (DistLM) was applied to investigate relationships between the abundance of phytoplankton taxa and the environmental variables among cruises. The stepwise selection was based on AIC. A DistLM was chosen here as it offers several advantages in ecological and environmental research. This model effectively handles multivariate response data and, while using permutation tests for significance assessment, it is robust against non-normal data. Complex relationships can be modelled with DistLM as its flexibility allows the inclusion of various predictor types.

4. Results

4.1. Spatiotemporal long-term trends of *Noctiluca scintillans* in the North Sea

4.1.1. Main drivers of *Noctiluca scintillans* in the North Sea

The best-fit model obtaining the highest explained deviance (55.54%) and lowest AIC for the HR time series included all the predictor variables (Table 4.1). The results of the GAMs revealed that SST and wind speed are most influential for peak abundances of *N. scintillans* (Appendix 6). Variables contributing least were precipitation, DIN concentrations, and SSS.

Table 4.1: Statistical summary of the best-fit GAMs for the Helgoland Roads and the Continuous Plankton Recorder time series.

Time series	Model	Explained Deviance	Adjusted R ²
HR	$y = a + f_1(\text{SST}) + f_2(\text{SSS}) + f_3(\text{DIN}) + f_4(\text{Year}) + f_5(\text{Month}) + f_6(\text{Precipitation}) + f_7(\text{Wind speed}) + f_8(\text{Solar radiation})$	55.54%	0.16
CPR	$y = a + f_1(\text{SST}) + f_2(\text{SSS}) + f_3(\text{MLD}) + f_4(\text{Longitude, Latitude}) + f_5(\text{Season})$	29.45%	0.05

The model results for the HR time series (Fig. 4.1), showed that maximum abundances of *N. scintillans* are most likely to occur at water temperatures between 15 and 20°C (Fig. 4.1A) and at salinities around 30 (Fig. 4.1B). Moreover, highest densities are expected in waters with DIN concentrations around 30 μmolL^{-1} (Fig. 4.1C). Favourable conditions for abundant *N. scintillans* also include daily solar radiation below 75 Wm^{-2} (Fig. 4.1D), local precipitation around 7.5 mm (Fig. 4.1E), and wind speed below 6 m s^{-1} (Fig. 4.1F). Years in which conditions for *N. scintillans* were most suitable were between 1980-1990, and after 2010 (Fig. 4.1G). The months in with highest cell densities are expected to be June and July (Fig. 4.1H). The results of the GAMs showed that the most influential drivers for the pre-bloom phase were SST, SSS, and DIN (Fig. 4.2A, Appendix 6), whereas during the post-bloom phase SST, solar radiation and DIN are most relevant factors for *N. scintillans* (Fig. 4.2B, Appendix 6). The environmental factors at which the different bloom phases of *N. scintillans* are most likely to occur are summarized in Table 4.2.

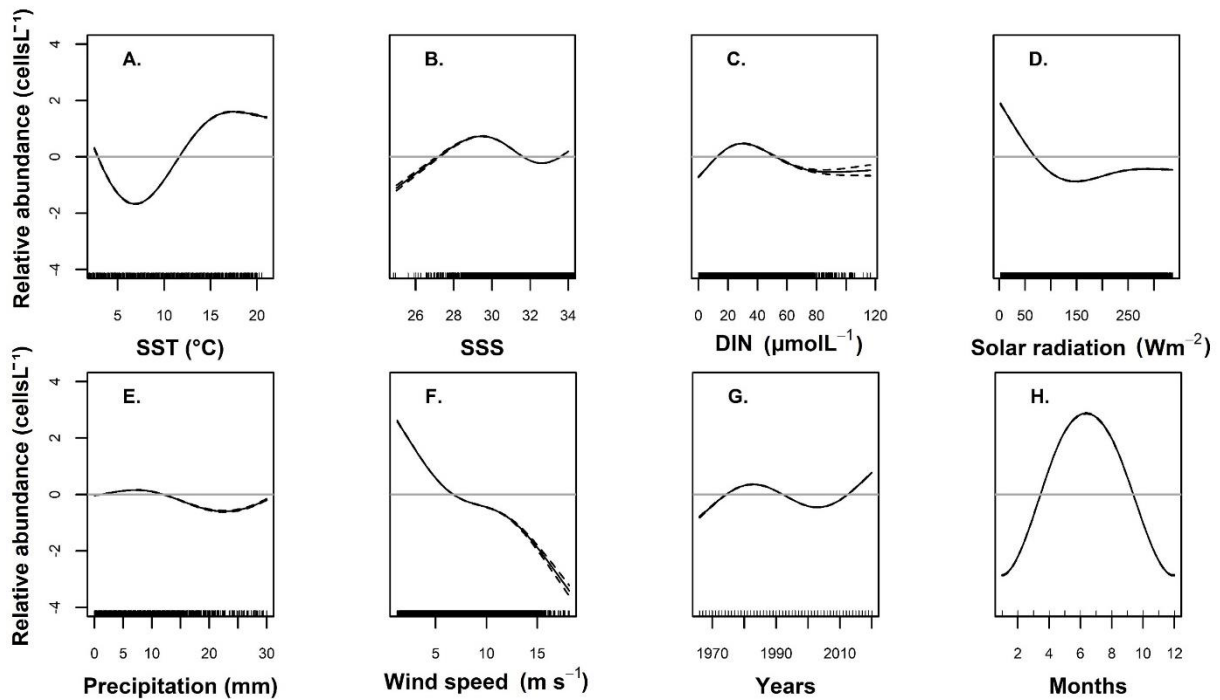


Figure 4.1: Effect plots of the best-fitted GAM for the Helgoland Roads time series. Dashed lines represent two standard errors above and below the estimate of the smooth curve represented by the solid line. Y-axes are on the scale of the predictor variable, i.e. *N. scintillans* abundance (cells L^{-1}). The rug plots at the bottom of the x-axes indicate observations of the predictor variable.

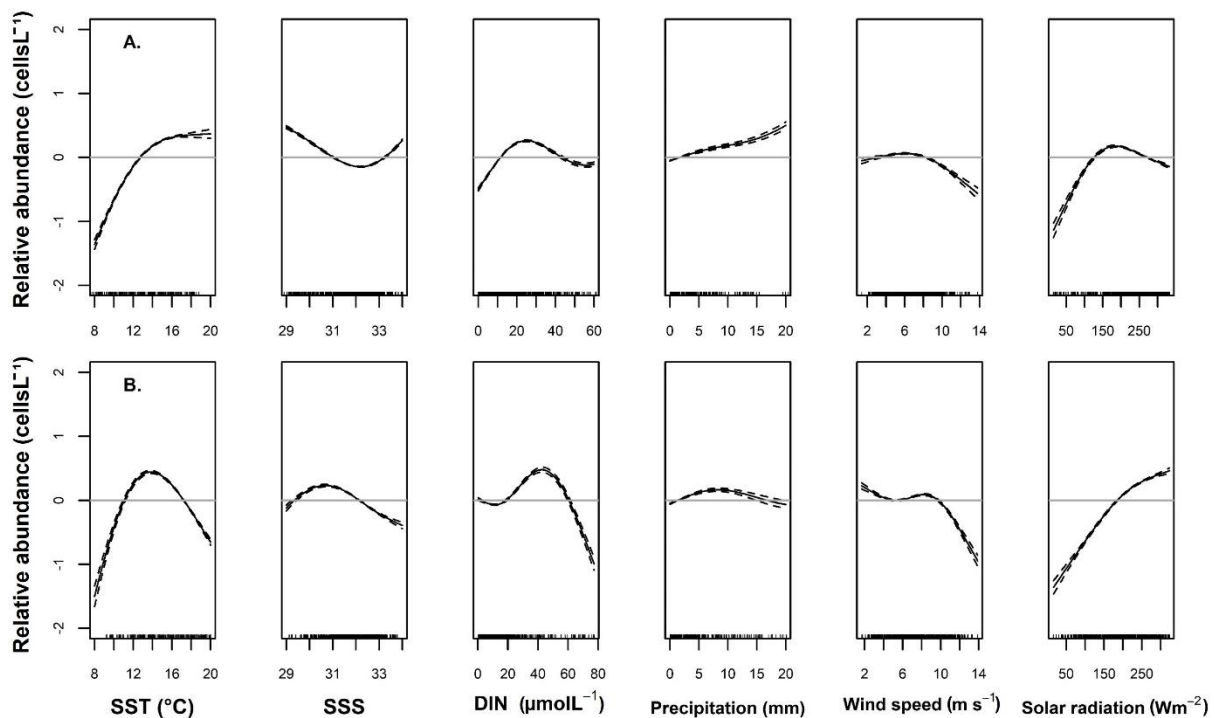


Figure 4.2: Effect plots of GAMs for (A.) pre-bloom phase; (B.) post-bloom phase from the Helgoland Roads time series. All values are on the scale of the linear predictor. Dashed lines represent two standard errors above and below the estimate of the smooth curve. Y-axes are on the scale of the predictor variable, i.e. *N. scintillans* abundance (cells L^{-1}). Rug plot (at the foot of each plot) shows observations of predictor variables.

Table 4.2: Summary of drivers associated with different bloom phases of *N. scintillans* at Helgoland Roads (see Fig. 4.1, Fig. 4.2, and Appendix 6 for more details).

	Pre-bloom	Bloom	Post-bloom
SST °C	> 12	15-20	12-16
SSS	> 34	29-31	~ 30.5
DIN μmolL^{-1}	20-30	~ 30	~ 45
SR Wm^{-2}	~ 175	< 75	> 200
Prec mm	> 5	~ 7.5	~ 7.5
WS m s^{-1}	~ 6	< 6	< 10

For the CPR data, the highest deviance explained (29.45%) and lowest AIC was obtained for the model including all factors except decade (Table 4.1). The results of the GAMs applied to the CPR time series, indicated that position (longitude and latitude), MLD, and Season were most important for *N. scintillans* in the North Sea. Variables contributing least were SSS and SST (Appendix 8). Highest densities of *N. scintillans* in the North Sea can be expected to occur in waters with a MLD of < 20 m (Fig. 4.3A), salinity > 34 (Fig. 4.3B) and temperature above 11°C (Fig. 4.3C). High abundances of *N. scintillans* are more likely to occur in coastal environments and particularly near river outflows such as the Elbe Estuary. Densities of *N. scintillans* are expected to decrease with distance from the coast and lowest abundances are expected to occur in the open sea (Fig. 4.3D). Highest abundances are more likely to occur in summer (Fig. 4.3E).

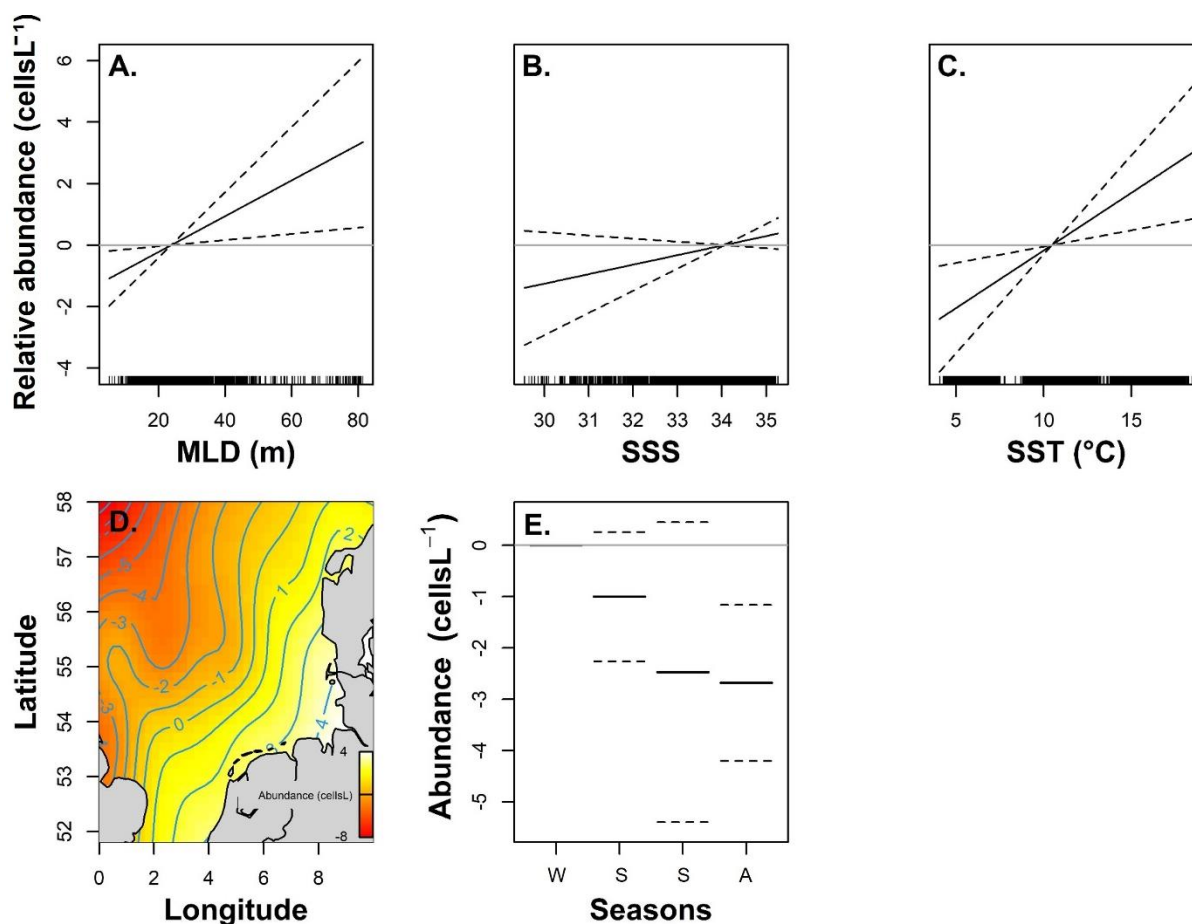


Figure 4.3: Effect plots of the best-fitted GAM for the Continuous Plankton Recorder survey. Dashed lines represent two standard errors above and below the estimate of the smooth curve, represented by the solid line. Y-axes are on the scale of the predictor variable, i.e. *N. scintillans* abundance (cellsL⁻¹). The rug plots at the bottom of the x-axes indicate observations of the predictor variable.

4.1.2. Temporal trends of *Noctiluca scintillans* in the North Sea

The analysis of the HR time series revealed that *N. scintillans* was present in over 2600 from nearly 13000 samples collected between 1962 and 2020, with yearly maximum abundances ranging from 80 to 22500 cellsL⁻¹ (in 1965 and 1984, respectively). Over time, occurrences, and blooms of *N. scintillans* have been increasing, particularly after the 1990s (Table 4.3). In comparison with the 1990s, the organism was encountered more often in the samples in the 2020s (14% and 34%, respectively). Similarly, the number of blooms sampled in this period showed a positive trend between the 1990s and the 2020s (1.5% and 2.0%, respectively).

Table 4.3: Summary of the decadal sampling effort in Helgoland including number and percentage of analysed samples containing *N. scintillans*, as well as number and percentage of sampled *N. scintillans* blooms (≥ 500 cellsL⁻¹).

Decades	Total samples	Samples with <i>N. scintillans</i>	<i>N. scintillans</i> occurrence (%)	Sampled <i>N. scintillans</i> blooms	<i>N. scintillans</i> blooms (%)
1960s	1111	178	16.0	24	2.2
1970s	1914	340	17.7	48	2.5
1980s	2445	464	19.0	60	2.5
1990s	2393	331	13.8	37	1.5
2000s	2442	566	23.2	42	1.7
2010s	2373	670	28.2	43	1.8
2020s	250	84	33.6	5	2.0

Abundances of *N. scintillans* displayed a strong seasonal pattern in Helgoland with lowest abundances measured in winter, increasing in spring, reaching a peak in summer, and decreasing again in autumn (Fig. 4.4). Since the 2010s, an increase in *N. scintillans* abundances in spring and autumn was found. Highest seasonal mean of *N. scintillans* was recorded in the 1970s in summer with 280.8 cellsL⁻¹. Results from the GLM indicated that *N. scintillans*' summer mean abundances decreased significantly between the 1970s and the 1990s by nearly a factor of 2 ($p < 0.05$). Whereas, after the 1990s, a significant 1.65-fold increase in *N. scintillans* abundance occurred ($p < 0.05$) (Table 4.4).

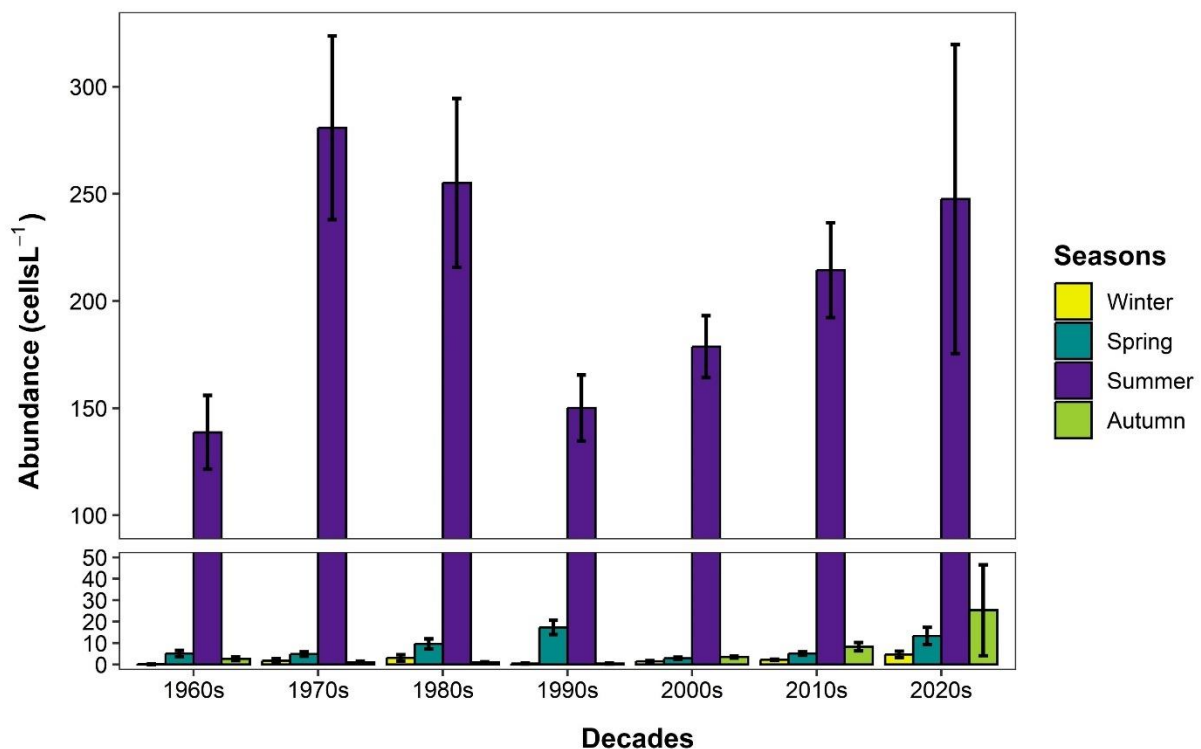


Figure 4.4: Decadal variations in mean seasonal abundance of *N. scintillans* at Helgoland Roads for the period 1962-2020. Error bars represent the standard error from the mean.

Table 4.4: Summary table of decadal mean abundances of *N. scintillans* (cellsL⁻¹) in the summer for the Helgoland Roads time series, confidence limits (CL) at 95%, and GLM with Poisson distribution model outputs. * indicates *p*-values < 0.05.

Decades	<i>N. scintillans</i> (cellsL ⁻¹)	Std. error	Lower-upper CL	<i>p</i> -value
1960s	138.69	38.94	113.38-140.02	< 2e ⁻¹⁶ *
1970s	280.80	48.68	277.76-283.84	< 2e ⁻¹⁶ *
1980s	255.08	47.34	252.08-257.82	< 2e ⁻¹⁶ *
1990s	150.06	47.30	150.06-151.78	< 2e ⁻¹⁶ *
2000s	178.70	47.30	178.70-180.70	< 2e ⁻¹⁶ *
2010s	214.39	47.37	214.39-216.74	< 2e ⁻¹⁶ *
2020s	247.58	92.45	247.58-252.08	< 2e ⁻¹⁶ *

After the 1990s, a positive trend was found for the length of the *N. scintillans* bloom window at HR, increasing 3.6-fold between the 1990s and 2020s (Fig. 4.5). The shortest bloom window occurred in the 1960s with 19.7 days, whereas the longest bloom window was recorded in the 2020s with 98 days (Fig. 4.5, Table 4.5). The analysis of variances showed a significant elongation of the *N. scintillans* bloom window between the 1970s and 1980s, and between the 2010s and 2020s (*p* < 0.05). Nevertheless, the difference in the bloom window length between the 1970s and 1980s became insignificant after the removal of an extreme value (i.e. *N. scintillans* bloom recorded January 1989) (Table 4.6).

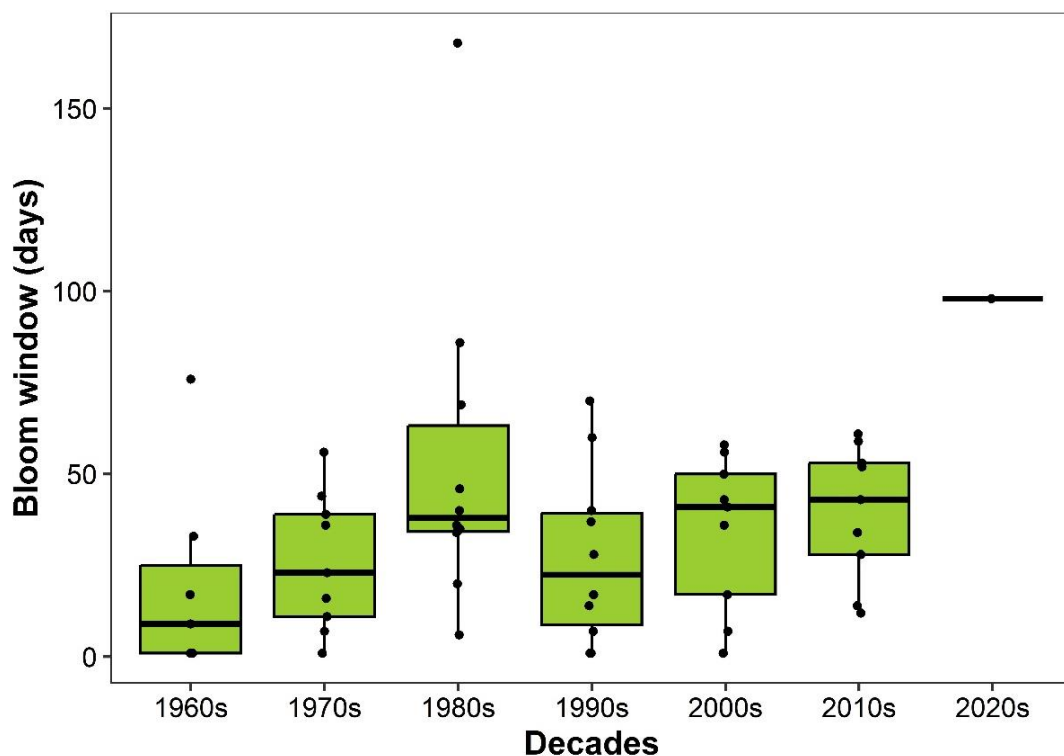


Figure 4.5: Variations of the *N. scintillans* bloom window length at Helgoland Roads shown as boxplots for the period 1962-2020. The bloom window corresponds to the yearly timeframe between the first and last measurement of *N. scintillans* abundances ≥ 500 cellsL⁻¹. The boxes extend from the 25th to the 75th percentile where the solid line indicates the median. Observations are indicated by dots.

Table 4.5: Summary table of *N. scintillans* bloom window duration (BWD) for the Helgoland Roads time series, confidence limits (CL) at 95%, and one-way ANOVA outputs. * indicates p -values < 0.05.

Decades	BWD (days)	Std. error	Lower-upper CL	p -value
1960s	19.7	10.6	-1.7 – 41.1	0.07
1970s	25.9	9.4	7.1 – 44.7	0.66
1980s	54	8.9	36.1 – 71.9	0.02*
1990s	27.5	8.9	9.6 – 45.4	0.58
2000s	34.3	9.4	15.5 – 53.2	0.31
2010s	39.6	9.4	20.7 – 58.4	0.17
2020s	98	28.1	41.5 – 154.5	0.01*

Table 4.6: Summary table of *N. scintillans* bloom window duration (BWD) for the Helgoland Roads time series without the unusual *N. scintillans* bloom event in 1989, confidence limits (CL) at 95%, and one-way ANOVA outputs. * indicates p -values < 0.05.

Decades	BWD (days)	Std. error	Lower-upper CL	p -value
1960s	19.7	8.4	3.3 – 36.2	0.02*
1970s	25.9	11.2	4 – 28.1	0.58
1980s	40.5	10.9	5.6 – 42.2	0.06
1990s	27.5	10.9	27 – 29.2	0.48
2000s	34.3	11.2	0.5 – 36.5	0.20
2010s	39.6	11.2	12.6 – 41.8	0.08
2020s	98	23.7	71.4 – 144.5	0.00*

Abundances of *N. scintillans* also displayed a strong seasonal pattern in the entire North Sea with lowest abundance in autumn and winter, increasing in spring, and peaking in summer (Fig. 4.6). Highest abundances were observed in summer between 2005 and 2017. Over time, an increasing trend in *N. scintillans* abundance was observed mainly for summer, but a positive trend was also present during winter and spring. Densities in autumn remained rather constant over time.

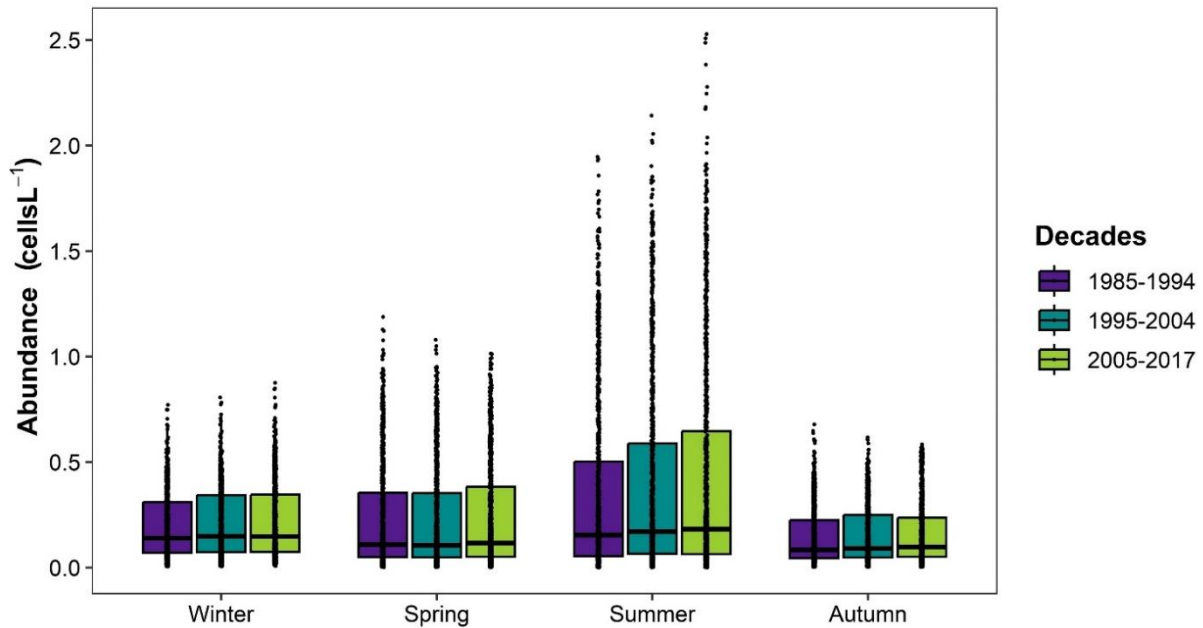


Figure 4.6: Seasonal variations of predicted *N. scintillans* abundance (cellsL⁻¹) by decade (square root-transformed) shown as boxplots for the period 1985-2017 (Continuous Plankton Recorder). The boxes extend from the 25th to the 75th percentile where the solid line indicates the median. Observations are indicated by dots.

4.1.3. Spatial trends of *Noctiluca scintillans* in the North Sea

The spatiotemporal predictions of *N. scintillans* in the North Sea are represented in Fig. 4.7. In general, the distribution of this dinoflagellate is more common in the coastal regions of the southern North Sea and highest values are predicted to occur during summer. Over time, the distribution of *N. scintillans* underwent a geographical spread and an intensification especially in areas near outflows from major estuaries. Between 1985 and 1994, abundances were very low in winter (Fig. 4.7A) and in autumn (Fig. 4.7D), with highest densities (0.6-0.7 cellsL⁻¹) predicted to occur off the coast of Zeeland, Netherlands. Abundances in spring (Fig. 4.7B) were highest in the Rhine-Meuse-Scheldt delta (1-2 cellsL⁻¹). In summer, highest concentrations of *N. scintillans* (2-5 cellsL⁻¹) are expected to occur near the main river plumes (Meuse, Rhine, Ems, Weser, Elbe) (Fig. 4.7C). Between 1995 and 2004, the distribution of *N. scintillans* followed a similar pattern during winter (Fig. 4.7E), spring (Fig. 4.7F) and autumn (Fig. 4.7H) compared to previous decades. During summer, the region with higher *N. scintillans* concentrations (2-5 cellsL⁻¹) spread from the Elbe Estuary to the East Frisian Islands and northwards along the Danish coast (Fig. 4.7G). From 2005 to 2017, the predicted maps suggested a slight widening of the area of occurrence of low densities (0.2-0.3 cellsL⁻¹) of *N. scintillans* in winter when compared to previous decades (Fig. 4.7I). The distribution of *N. scintillans* in spring follows a similar pattern than in previous decades, with a slight intensification at regional level such as the southern

Danish coast (Fig. 4.7J). In summer, abundances are predicted to increase in the Rhine-Meuse-Scheldt delta, reaching maximum abundances of 5-10 cellsL⁻¹, corresponding to more than double the abundances measured in the previous periods (2-5 cellsL⁻¹ between 1995-2004) (Fig. 4.7K). The area in which low abundances (0.2-0.3 cellsL⁻¹) of *N. scintillans* are expected to occur in autumn widened when compared to the previous decade, extending from the Ems to the Elbe estuary and up to the Danish coast (Fig. 4.7L).

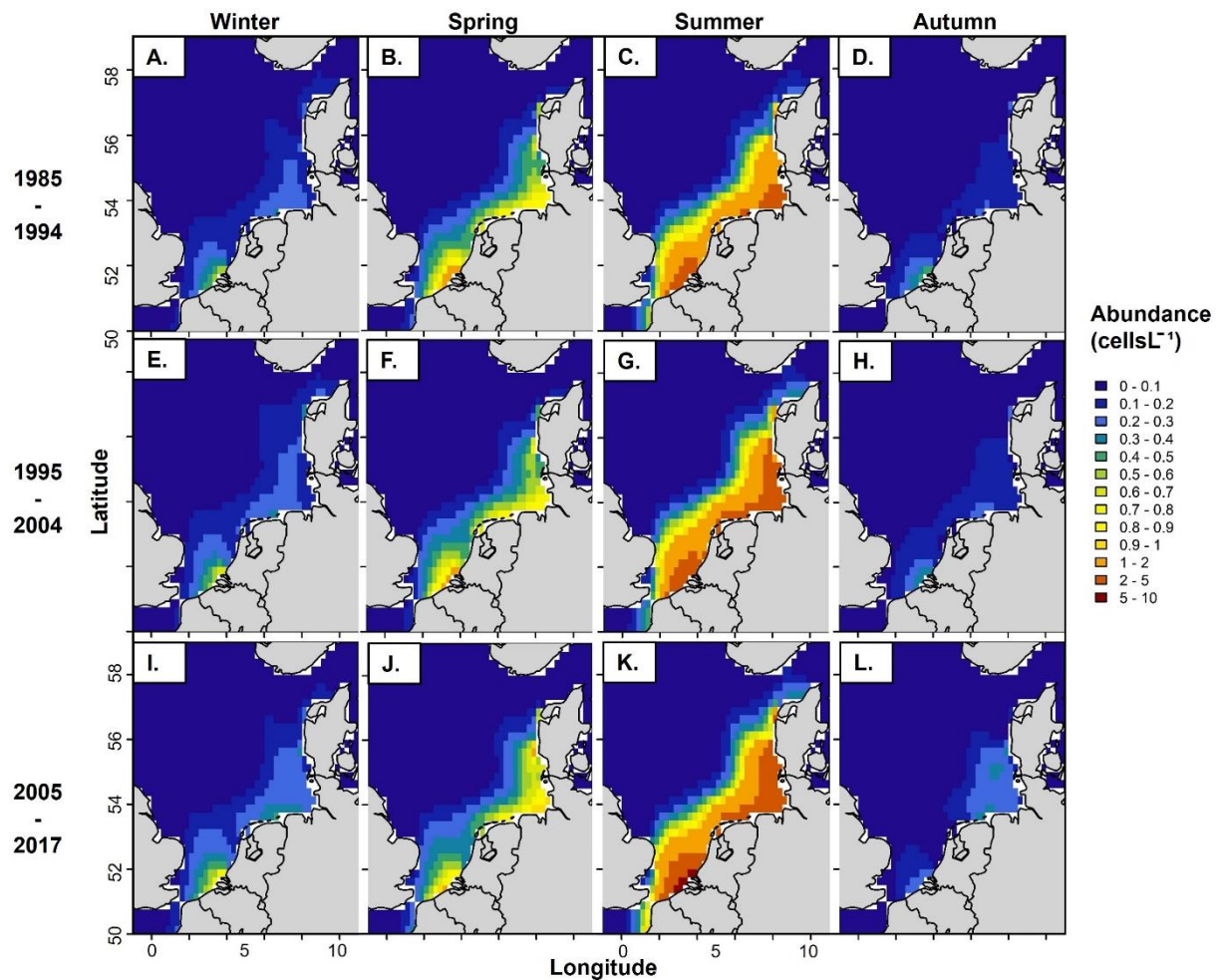


Figure 4.7: Seasonal predictions of *N. scintillans* abundance (cellsL⁻¹) by the best-fitted GAM for the Continuous Plankton Recorder survey in the North Sea (1985-2017).

4.2. The role of *Noctiluca scintillans* in the phytoplankton community composition of the southern North Sea

4.2.1. Phytoplankton community composition during different *Noctiluca scintillans* bloom phases

Throughout the cruises carried out near Helgoland, *N. scintillans* abundances varied. Abundances peaked during the second cruise (Fig. 4.8), with highest mean abundances of 877 cellsL⁻¹, followed by 268.8 cellsL⁻¹ during cruise #3 and 176.5 cellsL⁻¹ during cruise #1 (Table 4.7). Maximum *N. scintillans* abundances of 9673 cellsL⁻¹ were sampled during cruise #2 within *N. scintillans* surface slicks. Diatoms on the other hand, were significantly more abundant during cruise #1 (highest mean abundance reaching 418 cellsL⁻¹) and drastically decreased by a factor 35 during cruise #2 with a mean abundance of 11.8 cellsL⁻¹ (Table. 4.7).

Table 4.7: Taxonomic composition of phytoplankton imaged throughout the cruises #1-#3 with the CPICS and the FlowCAM. Values are means per cruise of abundance (cellsL⁻¹) and size (µm) of the different taxa identified, “-“ indicates unavailable data.

Taxa	CPICS		FlowCam		
	Mean abundance (std. error)	Mean major axis length (std. error)	Mean abundance (std. error)	Mean equivalent spherical diameter (std. error)	
Cruise #1	Diatoms	418 (88.3)	1538.4 (6.1)	-	-
	<i>N. scintillans</i>	176.5 (29.5)	849.4 (7.4)	-	-
	Ceratium	-	-	-	-
	Ciliates	-	-	-	-
	Prorocentrum	-	-	-	-
Cruise #2	Diatoms	11.8 (2.1)	1235.7 (30.6)	242.7 (22.2)	45.6 (1.4)
	<i>N. scintillans</i>	877 (189.3)	667.0 (1.1)	-	-
	Ceratium	-	-	0.4 (0.1)	39.7 (0.5)
	Ciliates	-	-	3.4 (0.8)	38.4 (0.8)
	Prorocentrum	-	-	0.3 (0.0)	32.7 (0.6)
Cruise #3	Diatoms	59 (38.8)	660.6 (6.6)	14.1 (2.3)	31.3 (1.3)
	<i>N. scintillans</i>	268.8 (158)	650.9 (3.2)	-	-
	Ceratium	-	-	38.9 (18.1)	44.3 (1.6)
	Ciliates	-	-	3.4 (0.5)	37.7 (1.0)
	Prorocentrum	-	-	6.7 (0.7)	29.3 (0.2)

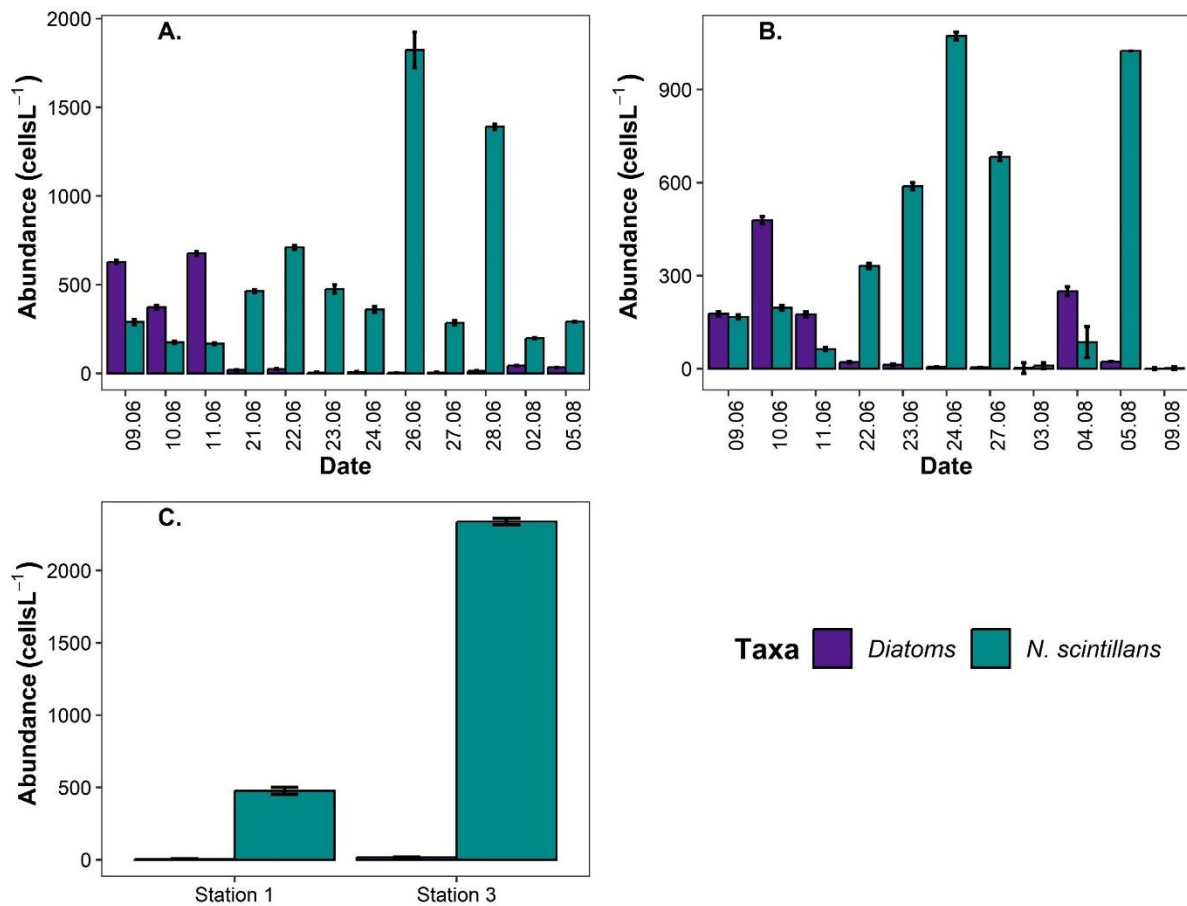


Figure 4.8: Temporal variation in abundances of *N. scintillans* and diatoms. **(A.)** corresponds to abundances measured in station 1, **(B.)** in station 2, and **(C.)** to abundances measured within dense *N. scintillans* surface slicks at stations 1 and 3. Error bars represent the standard error from the mean.

The analysis of the cruise data revealed significant changes of *N. scintillans* abundances between June and August. Moreover, the GLM showed a significant difference in abundances of *N. scintillans* between the stations and bloom conditions ($p < 0.05$) (Table 4.8). Similarly, diatom abundances also varied significantly among the cruise, station, and bloom conditions ($p < 0.05$) (Table 4.9 and Fig. 4.8).

Table 4.8: Results for Bonferroni pairwise comparisons from the ANOVA testing differences in *N. scintillans* abundances among cruises, stations, and bloom condition (e.g. surface slick).

Comparison	t-ratio	p-value
Cruises		
Cruise #1 – Cruise #2	268.4	< 0.05
Cruise #1 – Cruise #3	-17.0	< 0.05
Cruise #2 – Cruise #3	-412.7	< 0.05
Stations		
Station 1 – Station 2	-264.9	< 0.05
Station 1 – Station 3	113.9	< 0.05
Station 3 – Station 2	183.3	< 0.05
Surface slick		
Yes - No	248.4	< 0.05

Table 4.9: Results for Bonferroni pairwise comparisons from the ANOVA testing differences in diatom abundances among cruises, stations, and bloom condition (e.g. surface slick).

Comparison	t-ratio	p-value
Cruise #1 – Cruise #2	-355.0	< 0.05
Cruise #1 – Cruise #3	-356.9	< 0.05
Cruise #2 – Cruise #3	11.2	< 0.05
Stations		
Station 1 – Station 2	-124.2	< 0.05
Station 1 – Station 3	-39.3	< 0.05
Station 3 – Station 2	-7.5	< 0.05
Surface slick		
Yes - No	-37.4	< 0.05

The mean major axis length of *N. scintillans* was highest over the course of the first cruise with 849.4 μm . During the second and last cruise, *N. scintillans* cells were smaller with a mean major axis length of 667.0 μm and 650.9 μm , respectively. The size of the potential prey of *N. scintillans* (e.g. diatoms, dinoflagellates, and ciliates) recorded with the FlowCam ranged from 29.3 to 45.6 μm , whereas the major axis length of the diatoms recorded with the CPICS ranged from 660.9 to 1538.4 μm (Table 4.7). Throughout the sampling campaigns, large *N. scintillans* cells with a major axis length up to 1500 μm were exclusively observed in the first 10 m. With depth, the size of the *N. scintillans* cells decreased. Generally, the highest amount of *N. scintillans* was recorded in surface waters. Diatoms were mostly observed at a water depth of 20 m, where the major axis length of most cells ranged from 500 to 2000 μm . In surface waters, mostly small-sized diatoms were recorded (Fig. 4.9).

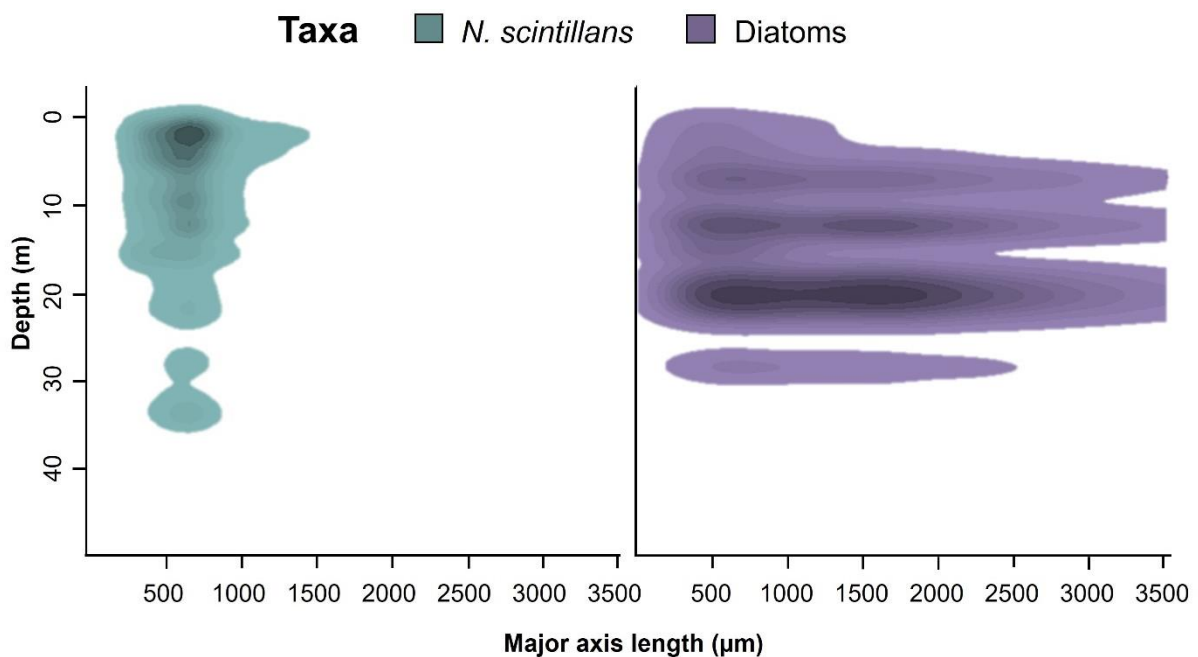


Figure 4.9: Contour plots representing the vertical distribution and major axis length of the two main taxa observed during the sampling campaigns in summer 2022 with the CPICS. Highest occurrences are indicated by the darkest shade.

Results from the FlowCam showed that the mean abundance of diatoms massively declined between cruise #2 and #3, from 242.7 cellsL⁻¹ to 14.1 cellsL⁻¹ (Fig. 4.10, Table 4.7). On the other hand, the densities of dinoflagellates such as *Prorocentrum sp.* and particularly of *Ceratium sp.* increased between cruise #2 and #3. Abundances of *Ceratium sp.* increased by a factor 100 between June and August (0.4 cellsL⁻¹ to 38.9 cellsL⁻¹), while *Prorocentrum sp.* densities increased from 0.3 cellsL⁻¹ to 6.7 cellsL⁻¹ (Fig. 4.10, Table 4.7).

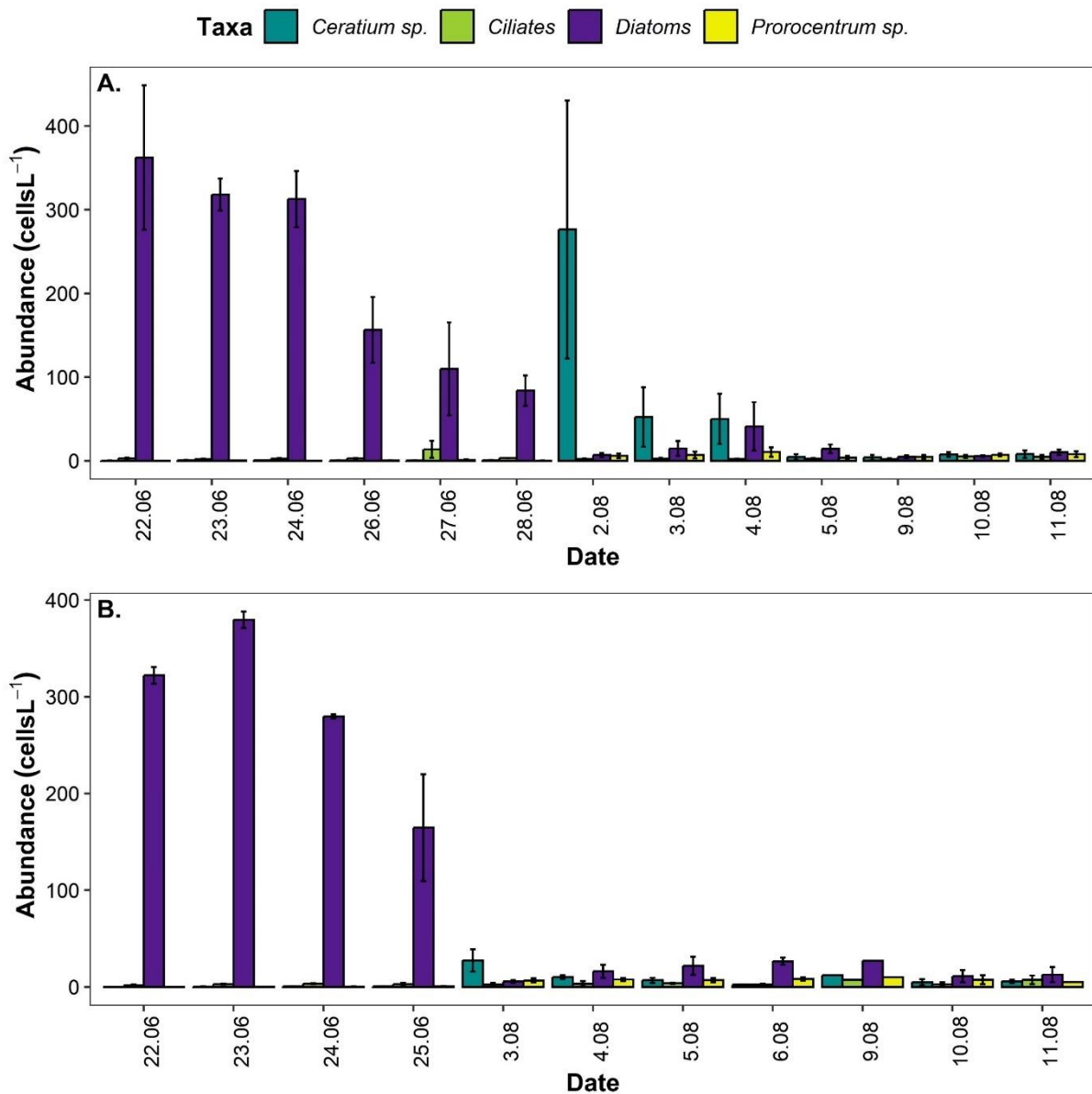


Figure 4.10: Temporal variation in daily mean abundances of the main phytoplankton taxa recorded with the FlowCam. **(A.)** corresponds to abundances measured in station 1, and **(B.)** in station 2. Error bars represent the standard error from the mean.

Results from the PERMANOVA indicated significant differences in the abundance of phytoplanktonic taxa among the cruises #2 and #3 (Pseudo-F = 128.84, $p < 0.05$). The best-fitted

model obtained from the stepwise procedure included temperature, salinity, fluorescence, DO, Si, and turbidity. The model explained 79% of the variation (AIC = 285.02, $R^2 = 0.788$). Temperature alone explained 54% of the total variation in the DistLM ($p < 0.05$) (Table 4.10).

Table 4.10: DistLM model output for FlowCam data during cruises #2 and #3.

Variable	AIC	<i>p</i>-value	Proportion	Residual degrees of freedom
SST	321.7	< 0.05	0.54	58
SSS	305.5	< 0.05	0.12	57
Fluorescence	293.9	< 0.05	0.07	56
DO	290.4	< 0.05	0.02	55
Si	287.7	< 0.05	0.02	54
Turbidity	285.0	< 0.05	0.02	53

The PCoA explained 74.4% of the total variation. The PCoA showed a clear separation between diatoms and dinoflagellates abundances (*Ceratium sp.* and *Prorocentrum sp.*) among cruises #2 and #3. Diatoms were negatively correlated with temperature and silicate, and positively correlated with NO_3 . Dinoflagellates were negatively correlated with NO_3 , PO_4 and NH_4 (Fig. 4.11).

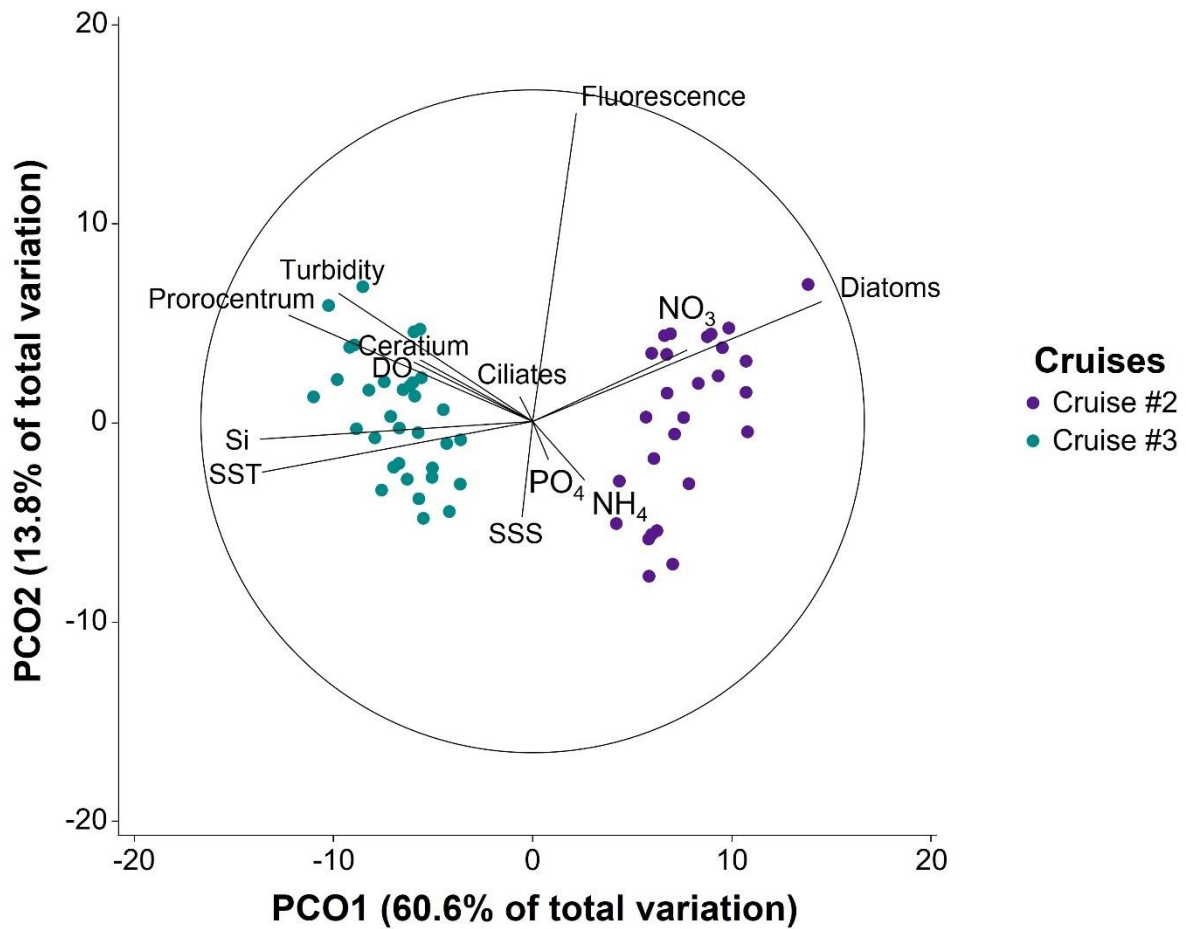


Figure 4.11: Principal coordinates analysis (PCoA) of environmental parameters and main phytoplankton taxa identified during cruises #2 and #3 in the study area with the FlowCam. The axes labels indicate the percentage of variability explained by each axis. Samples (dots) and variables (lines) are plotted against the first two axes.

Results from the pigment analysis showed similar trends. Higher concentrations of fucoxanthin were measured during the two first cruises (cruise #1 0.37 ± 0.06 and #2 $0.55 \pm 0.3 \mu\text{gL}^{-1}$) in comparison to cruise #3 ($0.2 \pm 0.07 \mu\text{gL}^{-1}$). Concentrations of peridinin were significantly higher during cruise #3 ($0.32 \pm 0.15 \mu\text{gL}^{-1}$) when compared with the two first cruises ($0.01 \pm 0.01 \mu\text{gL}^{-1}$ during cruise #1 and $0.05 \pm 0.05 \mu\text{gL}^{-1}$ during cruise #2) (Fig. 4.12).

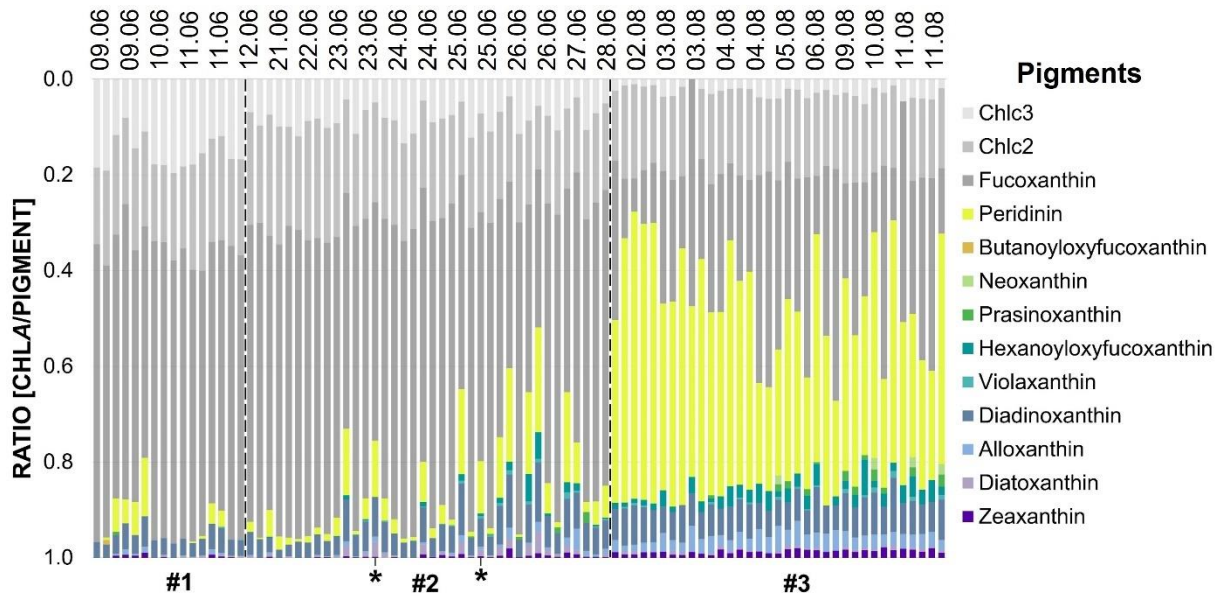


Figure 4.12: Temporal variation of the pigment composition of the water samples collected in June and August 2022 in the study area. * indicates samples collected within dense *N. scintillans* surface occurrences.

4.2.2. Drivers of *Noctiluca scintillans* abundances throughout a bloom

Throughout the three cruises carried out around Helgoland in summer 2022, temperatures followed an increasing trend. The lowest mean SST was measured during cruise #1 in early June (13.0°C). In August, the mean SST was highest (17.3°C) (Fig. 4.13A). Salinity varied between 30 and 33 over the course of the cruises, with lowest salinities recorded during cruise #1, and highest values during cruise #2 (Fig. 4.13B).

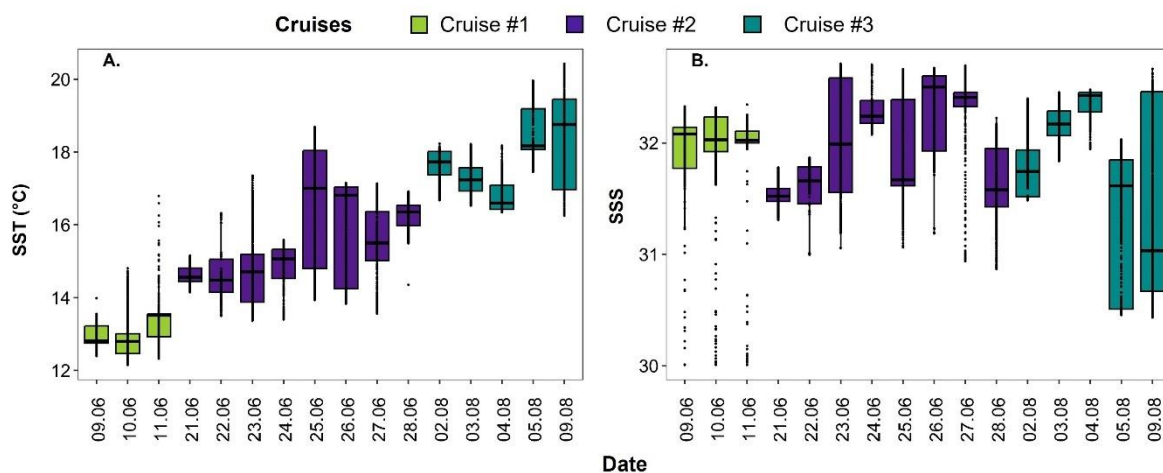


Figure 4.13: Daily means of the environmental conditions at surface including (A.) SST and (B.) SSS during cruises #1-#3. The boxes extend from the 25th to the 75th percentile where the solid line indicates the median. Observations are indicated by dots.

The images recorded with the CPICS revealed numerous *N. scintillans* feeding on diatom chains (Fig. 3.6). The highest number of *N. scintillans* cells ingesting diatoms was observed during cruises #1 and #2, with mean abundances of 361 and 356 cellsL⁻¹, respectively. In August, the amount of *N. scintillans* feeding on diatoms was significantly lower than during the previous cruises (204 cellsL⁻¹, $p < 0.05$). On June 25th and 26th, highest predation of *N. scintillans* on diatoms was observed with abundances of *N. scintillans* ingesting diatoms reaching 583 and 569 cellsL⁻¹, respectively. The mean abundances of *N. scintillans* phagocytizing diatoms significantly exceeded those of diatoms in the water column on these days (Fig. 4.14).

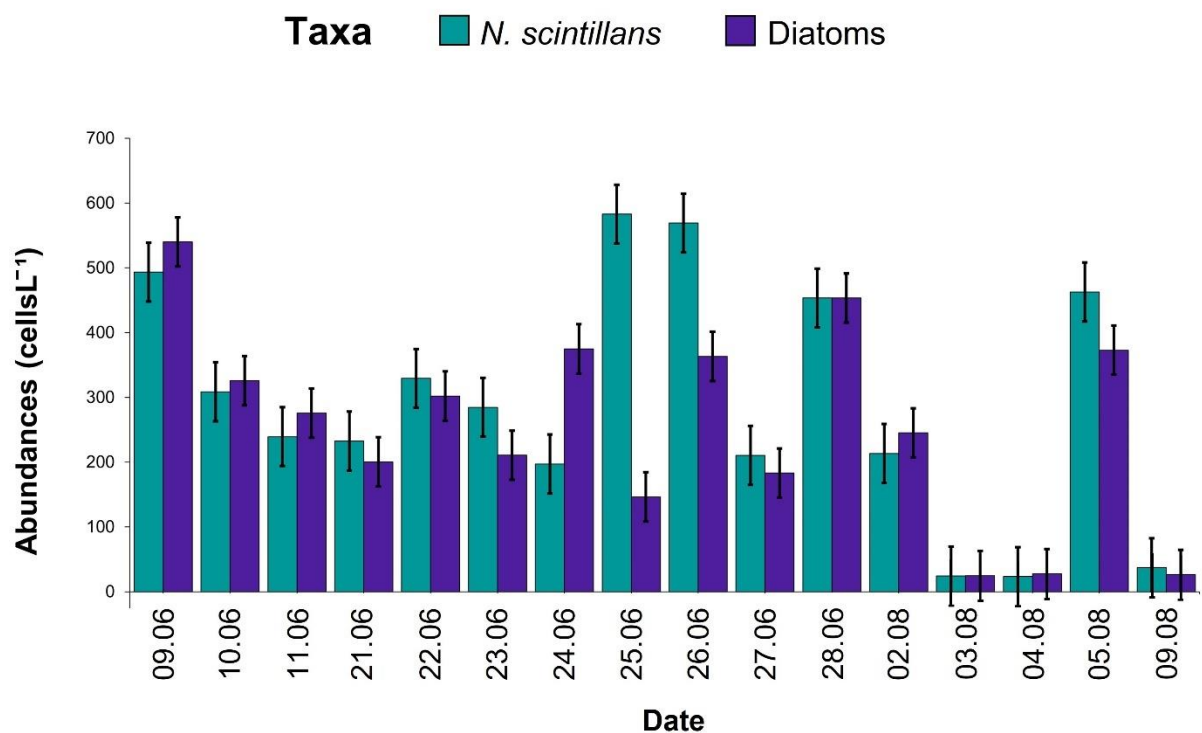


Figure 4.14: Temporal variation in abundances of *N. scintillans* ingesting diatoms versus diatoms in the water column. Error bars represent the standard error from the mean.

With a total explained variation of 83.4%, the PCoA for the CPICS data showed a clear separation between diatoms and *N. scintillans* among cruises #1 and #2. Diatoms were negatively correlated with SST, fluorescence, and SSS, and positively correlated with NO₃ and depth. *Noctiluca scintillans* was positively correlated with PO₄ and NH₄, and negatively correlated with depth (Fig. 4.15).

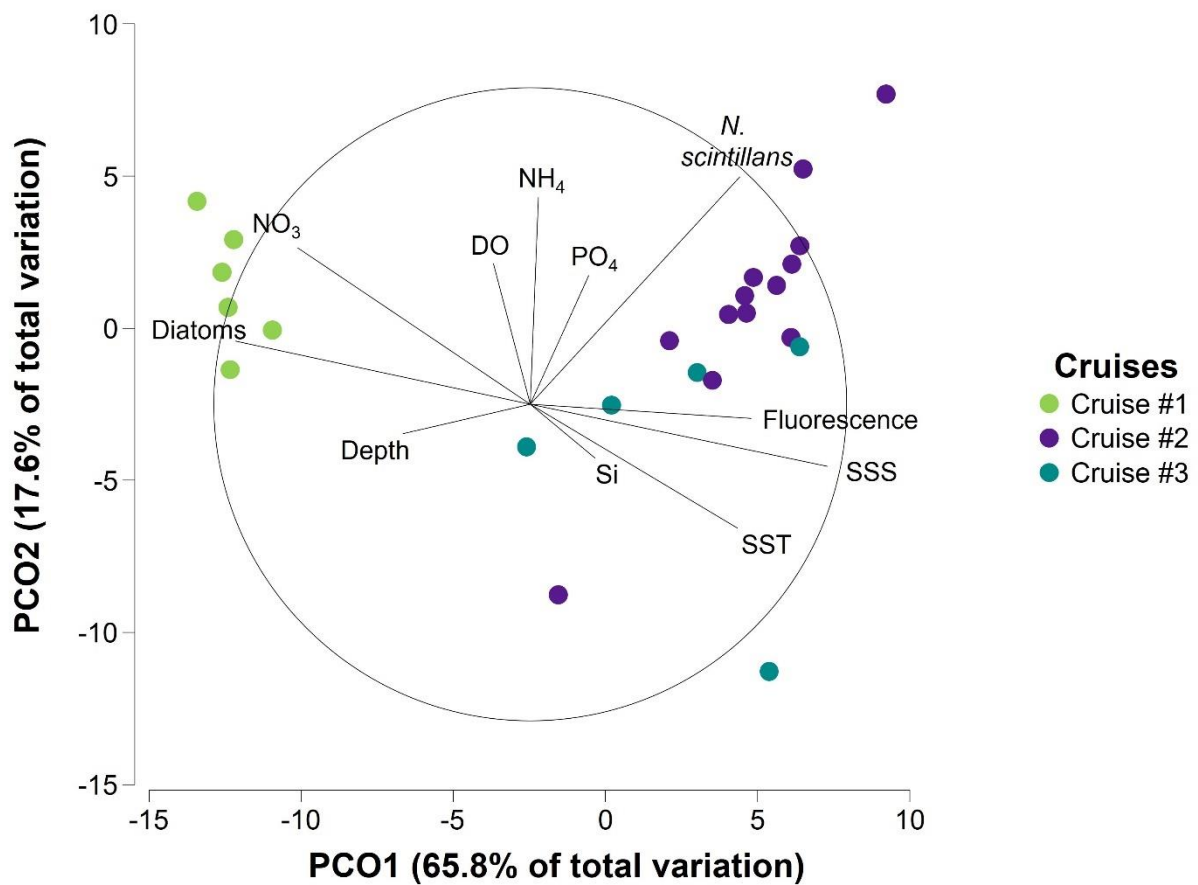


Figure 4.15: Principal coordinates analysis (PCoA) of environmental parameters and main phytoplankton taxa identified during cruises #1, #2, and #3 in the study area with the CPICS. The axes labels indicate the percentage of variability explained by each axis. Samples (dots) and variables (lines) are plotted against the first two axes.

The best-fitted GAMs showing the drivers of *N. scintillans* abundances are listed in Table 4.11. All predictor variables used had a significant effect on the abundances of *N. scintillans* ($p < 0.05$). During cruise #1, the abundance of diatoms was the most significant predictor. The most significant variable in the model for cruise #2 and #3 was SST (Table 4.11).

Table 4.11: Output of stepwise selection of GAMs for the cruises #1-#3 carried out around Helgoland in summer 2022. * indicates the best-fitting model. AIC: Akaike's Information Criterion. Variable in italic correspond to the most influential variable.

Family	Variable	Deviance explained (%)	Adjusted R ²	AIC
Cruise #1				
Gaussian	Full	4.41	0.04	98611.59
Poisson	Full	8.13	0.05	53153975
Non-binomial*	Full	8.67	0.04	76455.65
	-SSS	8.41	0.04	76568.79
	-SST	8.07	0.04	77329.41
	- <i>Diatoms</i>	0	0	80859.6
Cruise #2				
Gaussian*	Full	24.22	0.24	417590.8
	- <i>Diatoms</i>	21.82	0.22	422723.3
	-SST	20.79	0.05	454062.2
	-SSS	0	0	540614.5
Poisson	Full	21.18	0.25	351133.8
Non-binomial	Full	21.18	0.25	380492.4
Cruise #3				
Gaussian	Full	11.59	0.12	251023
Poisson	Full	22.34	0.12	144909.5
Non-binomial	Full	24.28	0.11	163380.2
	- <i>Diatoms</i>	23.93	0.11	163773.1
	-SSS	23.19	0.12	164591.8
	-SST	0	0	219844.6

During the first cruise, highest abundances of *N. scintillans* were associated with high abundances of diatoms, temperatures between 12 and 14°C and salinities below 32 (Fig. 4.16A). During cruise #2, the results of the GAM revealed that highest abundance of *N. scintillans* occurred at temperatures above 16°C, salinities above 32 and very low diatom abundances (Fig. 4.16B). In August, *N. scintillans* was most abundant at temperatures between 18 and 20°C, at salinities around 31.5 and with low diatom densities (Fig. 4.16C).

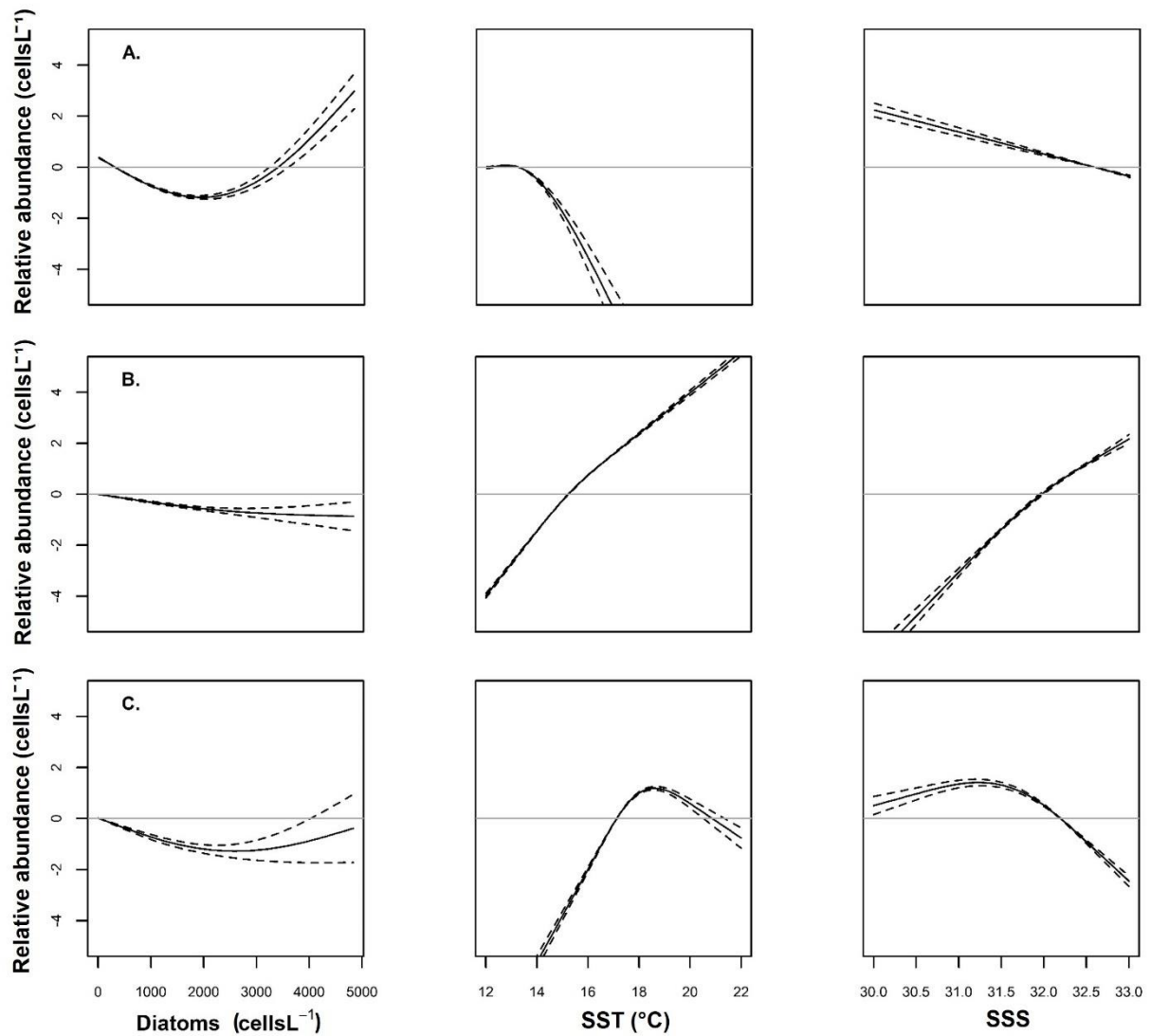


Figure 4.16: Effect plots of the best-fitted GAM for cruises **(A.)** #1, **(B.)** #2, and **(C.)** #3. Dashed lines represent two standard errors above and below the estimate of the smooth curve represented by the solid line. Y-axes are on the scale of the predictor variable, i.e. *N. scintillans* abundance (cellsL^{-1}).

4.2.3. Changes in ambient nutrient concentrations

The concentrations of the various nutrients measured throughout the sampling campaigns are summarized in Table 4.12. For silicates, concentrations were low during the two first cruises and increased during cruise #3 (Fig. 4.17). During cruises #1 and #2, respectively, mean concentrations of $2.0 \mu\text{molL}^{-1}$ and $1.5 \mu\text{molL}^{-1}$ were measured. During the third cruise, mean concentrations of $7.0 \mu\text{molL}^{-1}$ were measured. Highest concentrations of silicates were measured during the cruise #2 within the dense *N. scintillans* surface patches at stations 1 and 3, with concentrations reaching 7.4 and $12.3 \mu\text{molL}^{-1}$, respectively.

Table 4.12: Summary table of mean concentrations of the nutrients measured throughout the cruises #1, #2, and #3 (μmolL^{-1}) and standard error from the mean.

Cruises	NO_3		Si		PO_4		NH_4	
	Mean	Std. error	Mean	Std. error	Mean	Std. error	Mean	Std. error
Cruise #1	3.7	0.2	2.0	0.4	0.1	0.0	2.6	0.3
Cruise #2	1.0	0.1	1.5	0.3	0.3	0.2	2.5	1.3
Cruise #3	0.4	0.1	7.0	0.3	0.2	0.0	1.0	0.1

In contrast, highest nitrate concentrations were measured during cruise #1, whereas the lowest concentration was measured during cruise #3 (Table 4.12, Fig. 4.17). During the first cruise, nitrate reached a mean concentration of $3.7 \mu\text{molL}^{-1}$. Mean nitrate concentrations dropped during cruise #2 to $1.0 \mu\text{molL}^{-1}$ and even further to $0.4 \mu\text{molL}^{-1}$ in august at both stations.

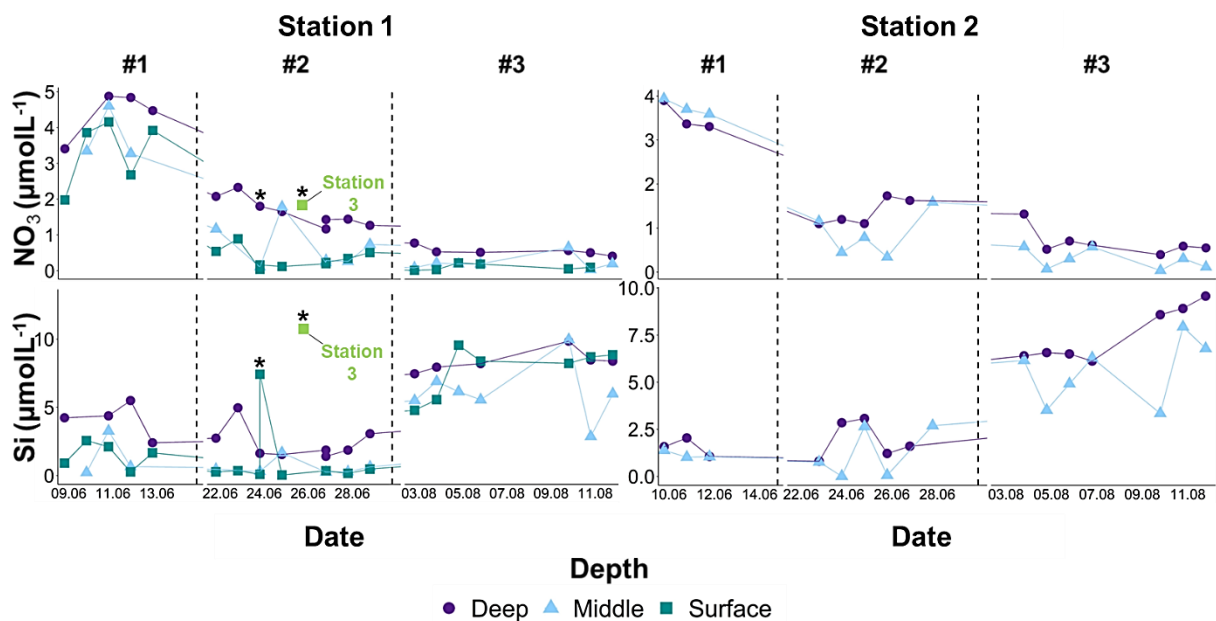


Figure 4.17: Temporal variation of Si and NO_3 concentrations during cruises #1 - #3 at the different stations (1-3) in the study area. * indicates samples collected within dense *N. scintillans* surface occurrences.

Concentrations of ammonium and phosphate remained constant over the sampling period with mean concentrations of $1.9 \mu\text{molL}^{-1}$ and $0.2 \mu\text{molL}^{-1}$, respectively (Table 4.12, Fig. 4.18). Within *N. scintillans* surface patches the highest concentrations reached $42.9 \mu\text{molL}^{-1}$ for ammonium and $6.28 \mu\text{molL}^{-1}$ for phosphate. When compared to the mean concentrations, this represents a 30-fold increase for ammonium, and a 48-fold increase for phosphate.

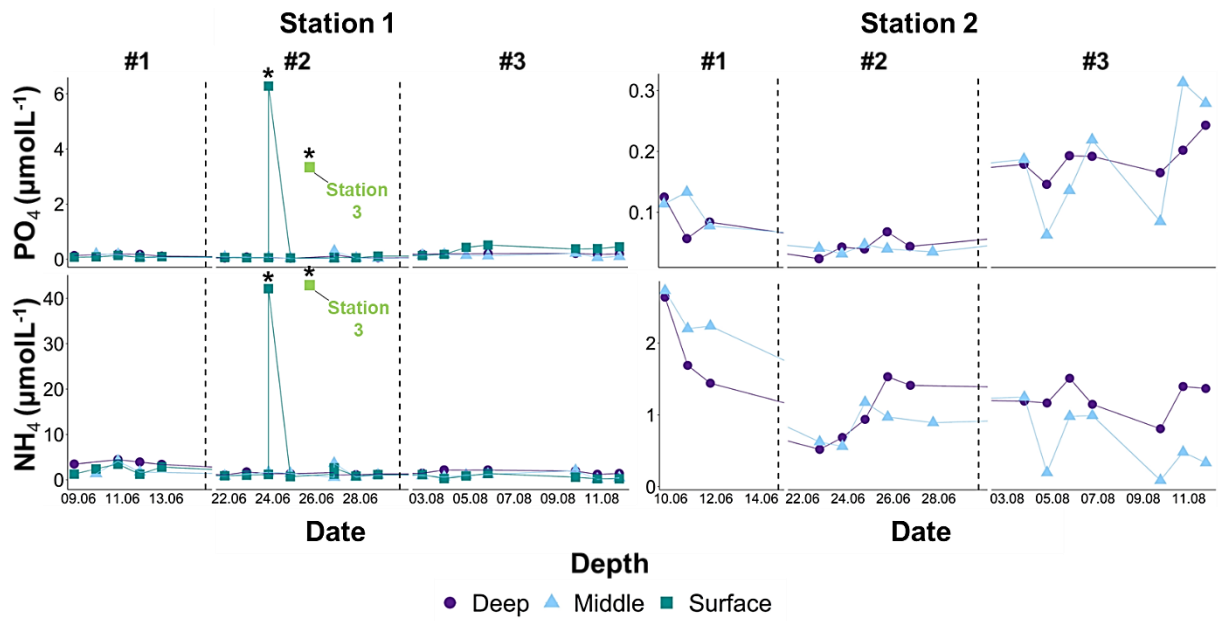


Figure 4.18: Temporal variation of PO_4 and NH_4 concentrations during cruises #1 - #3 at the different stations (1-3) in the study area. * indicates samples collected within dense *N. scintillans* surface occurrences.

5. General discussion

5.1. Past, present and potential future spatiotemporal distribution of *Noctiluca scintillans* in the North Sea

5.1.1. Temporal increase of *Noctiluca scintillans* in the North Sea

The literature review on documented global occurrences of *N. scintillans* indicated a potential geographical expansion and increase of *N. scintillans* since the 1970s. To validate these apparent trends, attention was focused on regions with consistent and long-term sampling records. This compilation revealed a significant increase in the abundance, a spatial spread, and an elongation of the bloom window of *N. scintillans* in several coastal regions including Australia, China, and Europe (see section 2.2.). The analysis of two distinct long-term time series showed that *N. scintillans* followed similar increasing trends in the North Sea over the last decades. Abundances of this organism continuously increased after the 1990s. Furthermore, a significant elongation of the bloom window in Helgoland was observed, with a 3.6-fold increase between the 1990s and 2020s.

While the literature review suggested that temperature cannot be the only environmental factor driving *N. scintillans* (see section 2.2.), the results of the GAMs applied to the long-term time series data suggested that SST is one of the most important factors for *N. scintillans* in the North Sea. Temperature is being widely acknowledged as important environmental factor shaping marine ecosystems, and particularly the abundance and community composition of phytoplankton (Richardson, 2008). In fact, ocean warming affects plankton indirectly through increased stratification limiting the nutrient supply and directly through increased plankton metabolic rates (Lewandowska *et al.*, 2014). In the North Sea, temperatures increased significantly faster than the global average ($\sim 1.3^{\circ}\text{C}/57$ years versus $\sim 0.7^{\circ}\text{C}/57$ years). The waters around Helgoland are experiencing an even more accelerated warming, evidenced by an increase of $1.86^{\circ}\text{C}/57$ years (Amorim *et al.*, 2023). Considering that *N. scintillans* reaches highest densities in warm waters, it can be deduced that the warming trend observed in the North Sea results in more frequent conditions that are favourable for population growth and for longer bloom periods. In Helgoland, the occurrence of warm months with water temperatures between $17\text{-}18^{\circ}\text{C}$ shifted from 2.3% to 12.4% since 1991, whereas the cold months with temperatures below $2\text{-}3^{\circ}\text{C}$ have significantly decreased (Amorim *et al.*, 2023). Since *N. scintillans* can engage cell division at low water temperature (Uhlig and Sahling, 1990), it can be speculated that the temperatures around Helgoland fall within the suitable range for *N. scintillans* nearly year-round. In fact, small populations are maintained throughout the year as evidenced by the increase of *N. scintillans* abundance in spring and autumn in Helgoland since the 2010s (see

section 1.4.2.). Additionally, the regional occurrences of *N. scintillans* in the southern North Sea in winter and autumn also suggest that suitable temperatures occur even during the colder months. A significant correlation between *N. scintillans* abundance and winter SST has been previously established for waters around Helgoland, indicating that when higher SST occurs in winter, higher abundances of *N. scintillans* can be expected in the following summer (Heyen *et al.*, 1999). This not only partially explains the increasing trend in *N. scintillans* abundances, but also accounts for the elongation of the bloom window. Climate change has also caused a significant increase of marine heatwaves (Oliver *et al.*, 2018). As observed during the heatwave in the German Bight in 2018, rapid changes in temperatures can significantly increase water column stratification and reduce nutrient loads to coastal waters (Kaiser *et al.*, 2023). This might affect the timing of blooms as well as the phytoplankton community composition, shifting from less resilient species towards more tolerant and rapidly developing species (Remy *et al.*, 2017), such as *N. scintillans*.

The alterations in the bloom timing of different phytoplankton groups were previously associated with the warming of the North Sea. Diatoms reached their peak abundance 22 days earlier in the early 2000s than in the late 1950s, whereas dinoflagellates peaked 23 days earlier (Richardson, 2008). *Noctiluca scintillans* is known to effectively feed on a variety of prey types, including diatoms and dinoflagellates (Fonda Umani *et al.*, 2004; Zhang *et al.*, 2015). Since heterotrophic *N. scintillans* requires high prey availability to bloom, the earlier blooms of its most common prey types have certainly contributed to the earlier start of *N. scintillans* blooms evidenced here.

The analysis in this thesis suggests that *N. scintillans* did not follow a constant increase between the 1960s and 2020s in Helgoland. The abundances rather fluctuated with a significant decrease of *N. scintillans*' summer mean abundance between the 1970s and the 1990s and an intensification after the 1990s. The southern North Sea is affected by eutrophication, driven by anthropogenic nutrient inputs from the outflow of several major rivers. For Helgoland, the Elbe River Estuary plays an important role, since nutrients from the river are carried until the island (Voynova *et al.*, 2017). First measures to reduce nutrient inputs in the North Sea were implemented in the second half of the 20th century, achieving a reduction of 50% in nutrient loads by the late 2000s (Howarth and Paerl, 2008; Rewrie *et al.*, 2023). This trend was confirmed by the analysis of abiotic factors between 1962 and 2001 in the waters around Helgoland, observing a major decrease in phosphorus since the mid-1970s (Wiltshire *et al.*, 2008). The high DNA-content of dinoflagellates implies a high demand for phosphorus (Rizzo, 2003). This link has been established in earlier investigations observing dense *N. scintillans* blooms when phosphorus concentrations were high (Ollevier *et al.*, 2021; Zhang *et al.*, 2021).

Since reductions of phosphorus inputs have been proven effective in limiting *N. scintillans* proliferations (Fonda Umani *et al.*, 2004; Oguz and Velikova, 2010), it can be hypothesized that the steep decline in abundance that was observed between the 1970s and 1990s may be linked to the decreasing concentrations of phosphorus during this period. Additionally, diatoms seem to have followed a decreasing trend between the 1960s and 1990s in the North Sea (Leterme *et al.*, 2006). Since diatoms are a common prey of *N. scintillans* (Dela-Cruz *et al.*, 2002), this could provide another explanation for the observed decrease in *N. scintillans* abundances after the 1970s. Similar results were obtained in mesocosm experiments, where the abundance of *N. scintillans* significantly decreased with lower proportions of diatoms within the phytoplankton community (Moreno *et al.*, 2022).

The decrease in abundance between the 1970s and 1990s coincided with a significant increase in the bloom window length. This can be attributed to the unusual occurrence of a *N. scintillans* bloom in January 1989, which substantially elongated the bloom window for that year and influenced the bloom window length for the 1980s. Another possible explanation is the increase in “strong wind events” in the North Sea during the 1980s (Siegismund and Schrum, 2001). Findings revealed that the daily mean wind speed during the 1980s more frequently surpassed 10 m s^{-1} during the *N. scintillans* bloom windows compared to other decades (Table 5.1). This could have affected abundances, as cells could be more easily resuspended in the water and were less likely to accumulate densely at the surface. Additionally, as well-mixed conditions benefit the development of *N. scintillans*, more windy days might cause favourable bloom conditions over longer periods, thereby increasing the bloom window length.

Table 5.1: Number of days with “strong wind events” within the yearly *N. scintillans* bloom windows (i.e. daily mean wind speed $> 10 \text{ ms}^{-1}$ (Siegismund and Schrum, 2001)) by decade.

Decade	Number of days with “strong wind events”
1960s	57
1970s	158
1980s	359
1990s	340
2000s	330
2010s	279
2020s	33

The intensification of *N. scintillans* after the 1990s could partly be related to the increase in oceanic water inflow into the North Sea during the late 1980s (Drinkwater *et al.*, 2003), leading to warmer water temperatures. Moreover, diatom abundances have been increasing in the North Sea since the 1990s, due to increased wind speed in summer, stimulating vertical mixing

(Hinder *et al.*, 2012). The increased prey availability, and particularly of diatoms, might have positively influenced *N. scintillans* in the North Sea and contributed to the observed increase.

The trends identified here, differ from the 3-year interval oscillations in *N. scintillans* abundance observed by Uhlig and Sahling (1990) in the German Bight. Maximum abundances every third year could not be clearly identified, as abundances remained high over several consecutive years (Fig. 5.1). Similarly, results from a time series analysis carried out between 2014 and 2018 in the Belgian Part of the North Sea, revealed an increase of *N. scintillans* over time rather than 3-year oscillations (Ollevier *et al.*, 2021).

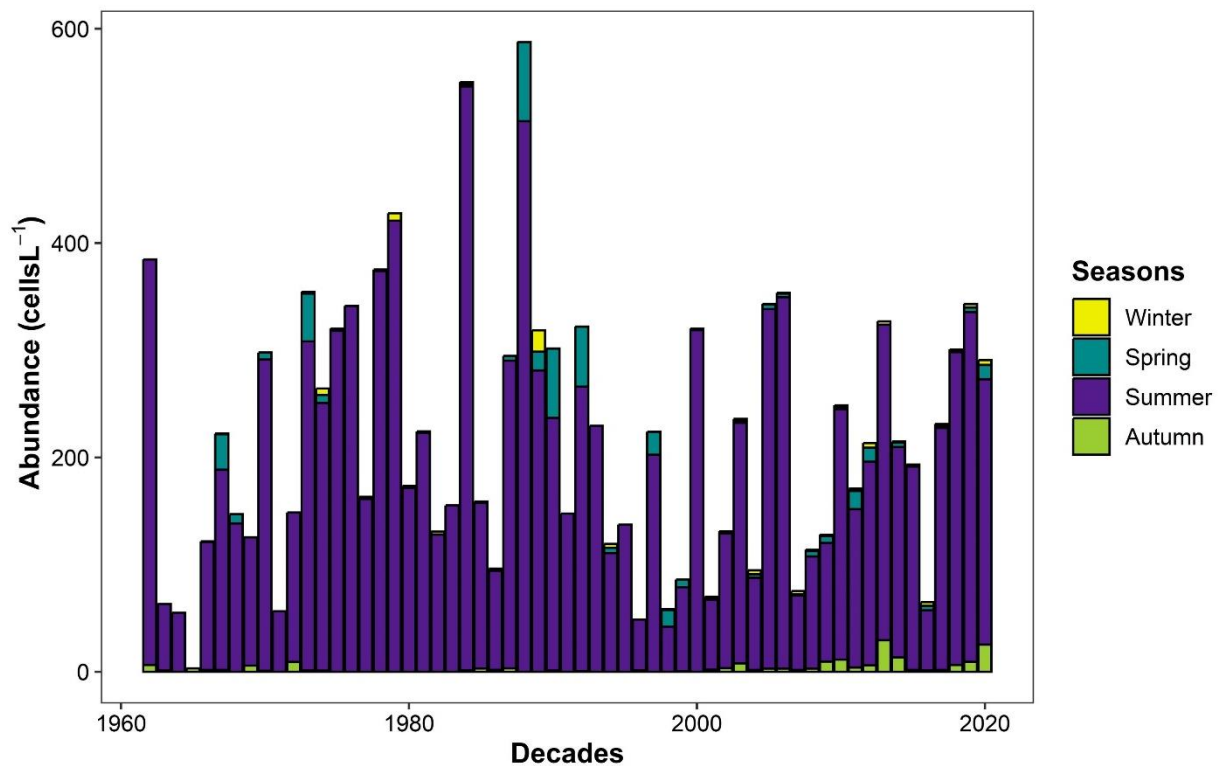


Figure 5.1: Yearly variations of mean seasonal abundance of *N. scintillans* at Helgoland Roads for the period 1962-2020. See Appendix 9 for more details.

It is important to note that while the data for the 2020s exhibited comparable patterns to the increasing trends observed in the preceding decades, this decade is represented solely by data from the year 2020. This was reflected by the standard error from the mean abundance and from the mean bloom window duration in the 2020s, which were considerably higher for the 2020s than for precedent decades (see section 4.1.2.). In fact, with fewer samples, the confidence in the average decreases, leading to a higher standard error. Therefore, these results might solely be considered as indicators of potential recent trends.

5.1.2. Spatial spread of *Noctiluca scintillans* in the North Sea

Results from the models applied in this thesis, suggested that the highest abundances of *N. scintillans* can be expected during summer in coastal waters and especially close to the outflow of rivers mouths and estuaries. Similarly, Tasmanian coastal waters showed elevated concentrations of *N. scintillans*, whereas lower concentrations were observed offshore (Hallegraeff *et al.*, 2019). Interestingly, in autumn and winter *N. scintillans* exclusively occurred in estuaries in the North Sea. Overwintering populations of *N. scintillans* were also found in estuaries near Sydney, where conditions for stable but low standing stocks of the dinoflagellate (e.g. warm waters and high nutrients) are maintained throughout the colder season (Dela-Cruz *et al.*, 2003). The ability of *N. scintillans* to survive in estuarine environments can undoubtedly be attributed to its euryhaline characteristics. Hallegraeff *et al.* (2019) found that the tolerance of *N. scintillans* to a wide range of salinities is a fundamental asset during transport and range extension. Additionally, *N. scintillans* benefits from several temperature ecotypes, allowing it to grow at temperatures from near 0°C (Elbrächter and Qi, 1998) up to 30°C (Qi *et al.*, 2004), another asset in the coastal environment where conditions can rapidly change.

Over time, the geographical distribution of *N. scintillans* expanded, initially concentrating near the main estuaries in the late 1980s and spreading along the coasts of the southern North Sea until 2017 (See section 4.1.3.). The main bloom intensification of this dinoflagellate was observed in summer between 2005 and 2017 within the river plume of the Rhine, where abundances increased from 2-5 cellsL⁻¹ in the late 1990s/early 2000s to 5-10 cellsL⁻¹ in the late 2000s/2010s. Supporting these results, geographical hotspots for *N. scintillans* were identified at the East Frisian islands in the late 1980s (Uhlig and Sahling, 1990). Together with estuaries, these shallow, well-mixed and nutrient-rich areas offer ideal conditions for the initiation of *N. scintillans* population growth and were identified as main reproduction areas for this organism in the southern North Sea (Uhlig and Sahling, 1995). Since the mid-1990s, the area in which *N. scintillans* occurred at abundances between 2-5 cellsL⁻¹ spread northwards up to the central Danish coast, and westwards up to the West Frisian Islands in summer. Within the North Sea, the German Bight showed the highest warming trend in recent decades and particularly since the 1980s (Wiltshire *et al.*, 2008). The high nutrient input through the main rivers and the rising SST have certainly played an important role in the observed spatial spread of *N. scintillans* over time. Additionally, throughout the 21st century, occurrences of westerly winds increased in the North Sea (Gaslikova *et al.*, 2013). Given that *N. scintillans* hotspots are located around the West and East Frisian Islands, and that populations commonly drift from coastal to more offshore

environments (Uhlig and Sahling, 1990), these changes in wind direction could have further contributed to the spread of this dinoflagellate along the coasts of the southern North Sea.

Overall, *N. scintillans* has bloomed more intensively, frequently and longer in various regions worldwide over the last decades (see section 2.2.). The geographical expansion, the rising abundance and elongation of the bloom duration identified here show that *N. scintillans* underwent similar changes within the North Sea. When considering the many competitive advantages of *N. scintillans* including its tolerance to changing environmental conditions, and the foreseen climate change scenarios predicting further increasing SST, decreasing salinities, increased stratification, and potentially increasing river nutrient loads caused by increased runoff in the North Sea (Quante and Colijn, 2016), it can be expected that the identified trends might follow similar patterns in the future. Dense *N. scintillans* blooms are associated with many negative impacts on coastal ecosystems and food webs (see section 2.3). Further increases and broader areas of occurrence of *N. scintillans* could have major repercussions on ecosystem productivity and can lead to substantial economic losses. Therefore, the monitoring of this species needs to be further improved to minimize ecological and economic damage.

5.2. Drivers throughout a *Noctiluca scintillans* bloom

Based on the abundances of *N. scintillans* measured throughout the three cruises, the main bloom phases were identified including the pre-bloom phase during cruise #1, the bloom peak with a nearly 5-fold increase in mean abundances, several consecutive days with abundances above 500 cellsL⁻¹, and apparent surface slicks in cruise #2, followed by the post-bloom phase during cruise #3. In line with these findings, Uhlig and Sahling (1990) observed that between March and mid-June in Helgoland, *N. scintillans* populations started growing and generally collapsed at the end of July or beginning of August. Results from the time series analysis agreed as well and showed that *N. scintillans* blooms develop from April to May, whereas highest abundances can be expected in June and/or July and the bloom decay in late summer.

5.2.1. Pre-bloom

The results from the Helgoland Roads time series analysis showed that pre-bloom conditions, leading to the initiation of *N. scintillans* blooms, included DIN concentrations and solar radiation above average (20-30 μmolL^{-1} and $\sim 175 \text{ Wm}^{-2}$, respectively). As phytoplankton relies on nutrients and light to grow, it can be expected that *N. scintillans* can start developing when light and nutrients are available, and, hence, prey is abundant. These findings align with earlier investigations, identifying prey availability as the main requirement for the growth of *N. scintillans* (Kiørboe and Titelman, 1998; Kopuz *et al.*, 2014; W. Zhang *et al.*, 2020). Pre-bloom conditions were associated with temperatures above 12°C. Together with DIN concentration (Fig. 5.2D) and solar radiation (Fig. 5.2I), the SST associated with the pre-bloom phase corresponds to the environmental conditions between April and May (Fig. 5.2A), during the temporal range of the annual spring bloom. *Noctiluca scintillans* usually follows the diatom spring bloom (Dela-Cruz *et al.*, 2002; Kiørboe, 2003). The analysis of the cruise data validated these findings while revealing that during the initial bloom phase, *N. scintillans* abundances were mainly influenced by increased prey availability (i.e. diatom abundance). Accordingly, highest abundances of diatoms have been measured during the first cruise. Diatoms have been previously identified as main factors driving the initiation of *N. scintillans* blooms, with several studies observing highest growth rates of *N. scintillans* when fed with non-motile diatoms including *Thalassiosira sp.* or *Chaetoceros sp.* (Zhang, Liu, *et al.*, 2016; Hallegraeff *et al.*, 2019). Nevertheless, Uhlig and Sahling (1990) observed first *N. scintillans* cells already dividing in March at SST between 5 and 6°C. This observation suggests that *N. scintillans* initiates its

development in early spring but attains pre-bloom conditions only in April-May due to insufficient prey.

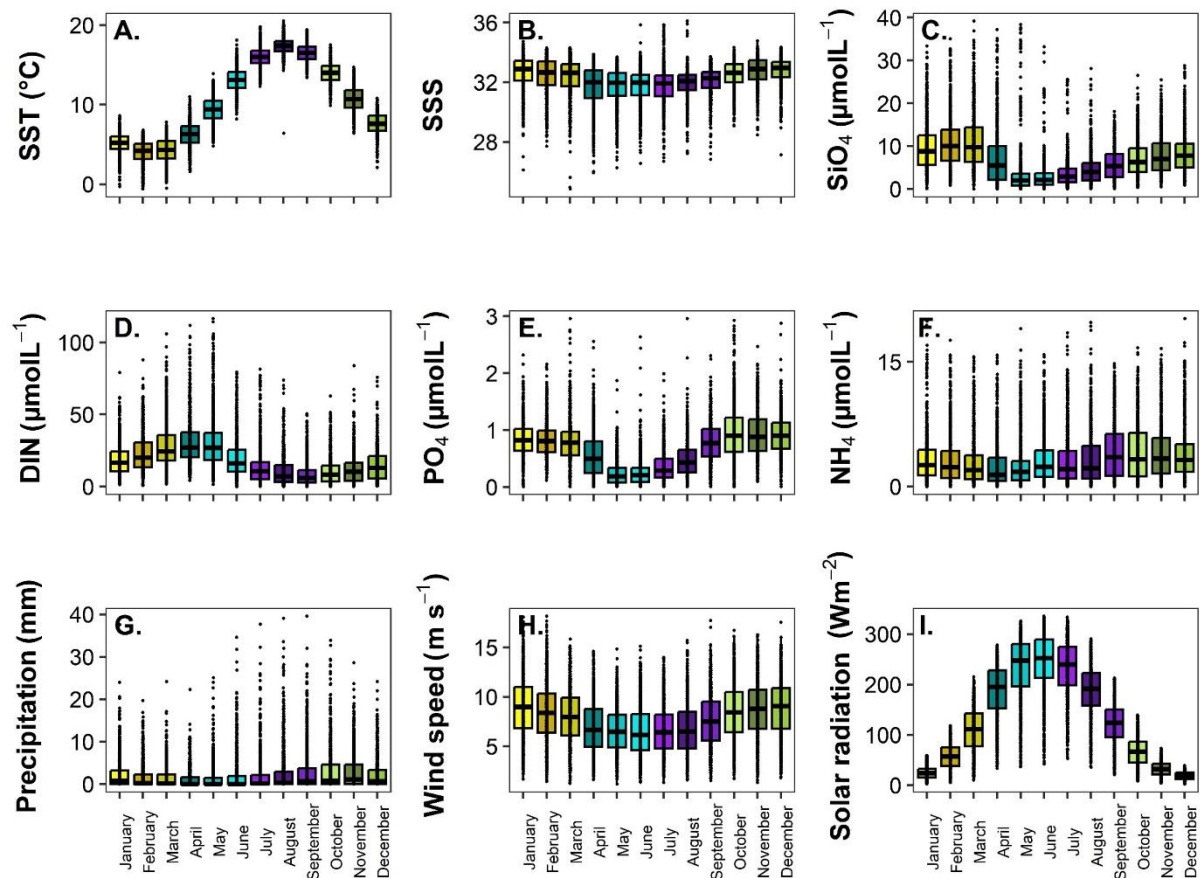


Figure 5.2: Monthly means for all variables included in the GAMs for the Helgoland Roads time series represented as boxplots for the period 1962-2020. The boxes extend from the 25th to the 75th percentile where the solid line indicates the median. Observations are indicated by dots.

5.2.2. Bloom peak

From the time series analysis, it was determined that dense *N. scintillans* occurrences are influenced by several factors combined, including warm waters and low wind speed, as well as average light intensity below 75 Wm⁻². The cruise data additionally revealed the influence of prey abundance for peak densities of *N. scintillans*. The best-fit models for both analysed time series and cruise data included multiple predictor variables and exhibited suitable predictive capabilities, underscoring the effectiveness of GAMs in evaluating the impact of diverse variables, including chemical and physical factors, on *N. scintillans* abundance.

Temperature was identified as main factors driving *N. scintillans* abundances around Helgoland as evidenced by the results of the GAMs for both time series and cruise data. The results of the time series analysis predicted peak densities of *N. scintillans* for waters between 15 and 20°C.

This corresponds to the highest range of temperatures measured around Helgoland (Fig. 5.2A) and coincides with results obtained with cultured *N. scintillans*, reporting highest growth rates at water temperatures between 19 and 25°C (Uhlig *et al.*, 1995; Harrison *et al.*, 2011). During the cruises, highest abundances of *N. scintillans* were expected to occur at temperatures above 16°C, thereby aligning with the findings of the time series analysis. It was demonstrated that cell division activity of *N. scintillans* increased together with increasing temperatures between spring and summer in the southern North Sea (Uhlig and Sahling, 1990). *Noctiluca scintillans* densities have indeed significantly increased between the two first cruises. This abrupt increase between initial bloom phase and bloom peak might be explained by the reproductive strategies of *N. scintillans*, since this dinoflagellate can maintain binary fission in areas of high cell density, which leads to exponential growth (Miyaguchi *et al.*, 2006).

Calm wind conditions (wind speed < 6 m s⁻¹) have been identified as another significant factor contributing to high concentrations of *N. scintillans* around Helgoland, as reported in various studies (Uhlig and Sahling, 1990; Nakamura, 1998a; Zhang *et al.*, 2021). This is consistent with the buoyant nature of *N. scintillans*, leading to the formation of dense surface patches when wind or tidal mixing fails to resuspend the cells in the water column. Enhanced stratification often results in nutrient-depleted environments, and, hence, to lower phytoplankton biomass (Lewandowska *et al.*, 2014). Accordingly, results of the GAMs revealed that peak abundances of *N. scintillans* are expected at low diatom abundances. Between cruises #1 and #2, the abundance of diatoms drastically decreased. This could be a result of the increased feeding pressure of *N. scintillans* on diatoms (Saho Kitatsuji *et al.*, 2019), evidenced by the high abundances of *N. scintillans* phagotrophically ingesting diatoms during cruise #2 (see section 4.2.2.). As cells feed while rising in the water column, limited food availability prevents the cells from intercepting prey and leads to dense accumulations at the surface (Uhlig and Sahling, 1990). This was corroborated by the vertical distribution data from the campaigns, which showed highest abundances of *N. scintillans* near the surface. The peak densities observed in the surface slicks during cruise #2 likely contributed to this result (see section 4.2.1.). Nevertheless, changing environmental conditions such as reduced silicate availability or higher temperatures, conditions that are usually detrimental for diatoms (Xiao *et al.*, 2018), could have further contributed to the observed decline in diatoms.

Peak abundances of *N. scintillans* have been predicted to occur at SSS between 27 and 30 at HR and above 32 during cruise #2, encompassing nearly the entire range of salinities recorded within the study area (Fig. 5.2B). This underscores the tolerance of *N. scintillans* to a wide range of salinities, as evidenced by earlier investigations (Hallegraeff *et al.*, 2019; Wang *et al.*, 2023). Furthermore, the results showed that high abundances of this organism are expected at low

solar radiation. High light intensity has the potential to damage *N. scintillans* cells, and with peak abundances often associated with surface accumulation, high light intensity would be detrimental and could lead to a bloom collapse (Uhlir and Sahling, 1990).

Results from the CPR analysis showed that highest *N. scintillans* abundance in the North Sea were associated with water temperatures above 11°C, significantly different from the results obtained near Helgoland. This difference could imply either that the optimal temperature range for *N. scintillans* varies with the study area, indicating potential adaptability of this dinoflagellate to its local environment, or that SST only partially drives *N. scintillans*.

The CPR analysis additionally showed that a deep mixed-layer depth (< 20 m) positively influenced *N. scintillans*, contradicting the findings in Helgoland, where calm conditions and low prey availability promoted peak densities. As the sampling depth of the CPR is usually between 7 and 10 m, dense surface patches are likely to be missed. If surface accumulations are not accounted for, it is logical that a deep MLD corresponding to well-mixed waters, was found to favour high *N. scintillans* abundance. In fact, highest *N. scintillans* abundances within the water column have been associated with well-mixed, nutrient-rich waters, benefitting the growth of phytoplankton (Dela-Cruz *et al.*, 2008). In the eastern Atlantic, stronger spring blooms occurred when a deep MLD and strong winds occurred (Martinez *et al.*, 2011). Furthermore, a deep MLD may limit light availability which has been previously associated with shifts from autotrophic to heterotrophic organisms (Monier *et al.*, 2015), thereby potentially benefitting *N. scintillans*.

5.2.3. Post-bloom

Results from the time series analysis showed that post-bloom conditions were characterized by SST between 12 and 16°C, DIN concentration around 45 μmolL^{-1} , as well as solar radiation above average and peak values up to 800 Wm^{-2} . The temperatures associated with the post-bloom phase fall within the suitable temperature range for *N. scintillans* and the DIN concentration is above average. Therefore, it can be deduced that the bloom termination is most likely attributed to the limited prey availability and intense solar radiation. Accordingly, the GAMs applied to the cruise data revealed that in the post-bloom phase, *N. scintillans* is correlated to low diatom abundances. During dense *N. scintillans* blooms, cells heavily graze on diatoms and can cause a bloom collapse (Saho Kitatsuji *et al.*, 2019). It can therefore be expected that after the bloom peak of *N. scintillans*, prey availability drastically drops due to intense predation, which would in turn contribute to the accumulation of cells at the surface. Since *N. scintillans* cells in surface waters which are exposed to elevated light suffer from irreversible deterioration, elevated solar

radiation could accelerate the bloom decay. Moreover, the elevated DIN concentrations associated with the post-bloom phase might be partially influenced by the excretion of NH_4 by *N. scintillans* upon cell lysis (Ara *et al.*, 2013; Zhang *et al.*, 2021). Highest concentrations of NH_4 were measured in late summer in Helgoland (Fig. 5.2F), following the decline of *N. scintillans* abundances.

Interestingly, the temperature range associated with post-bloom conditions was higher in the cruise data (18-20°C). This could be caused by the anomalously high temperatures recorded in summer 2022 and particularly in August in the North Sea (Ibebuchi and Abu, 2023). The rapid warming induced by the heatwaves in 2022 could have contributed to the diatom bloom termination and fuelled the development of dinoflagellates such as *Ceratium sp.* and *Prorocentrum sp.*, usually thriving under higher temperatures (Xiao *et al.*, 2018). This aligns with results from the DistLM (section 4.2.1.) suggesting that temperature was the main driver of the changes between cruises #2 and #3. Furthermore, this might explain why abundances of *N. scintillans* declined between the two last cruises, since the availability of its main prey rapidly decreased and got replaced by prey that can be consumed by *N. scintillans* but leads to lower growth rates. Nevertheless, dinoflagellates can support the “revival” of *N. scintillans* populations but at lower scale than diatoms (Zhang *et al.*, 2021). This aligns with the findings regarding the cell size of *N. scintillans*, being lowest in August. Smaller cells generally imply a good health status, with cells capable of population growth (Dela-Cruz *et al.*, 2003). Therefore, a second but less intense *N. scintillans* peak can be expected after cruise #3, fuelled by the availability of dinoflagellates.

In accordance with observations from the literature review, the findings emerging from the analyses of the time series and the cruise data demonstrated that the abundance of *N. scintillans* is not solely driven by individual variables but rather by several factors acting together (Fig. 5.3). In fact, the models indicated that at HR, the temporal variable “month” was particularly important for *N. scintillans* blooms, accounting for a combination of environmental conditions. High temperatures, low wind speed, low prey availability, and moderate light intensity collectively contributed to favourable conditions for dense *N. scintillans* blooms during June and July.

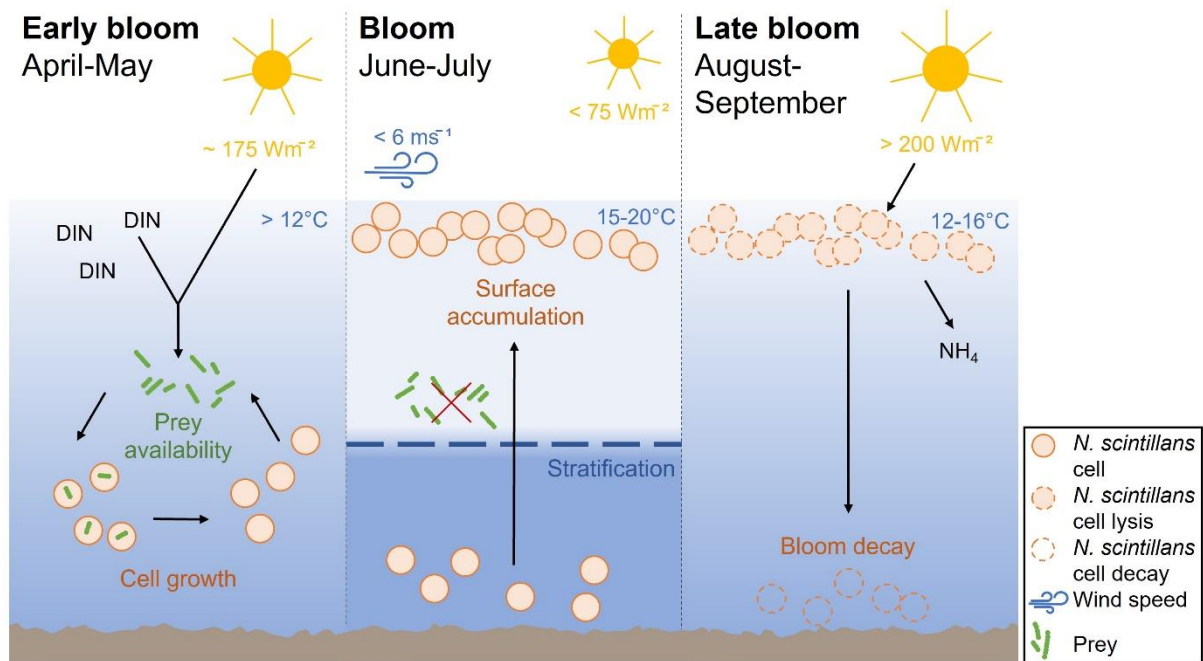


Figure 5.3: Schematic representation of the environmental preferences of *N. scintillans* during different bloom phases (including pre-bloom, bloom, and post-bloom). Suitable pre-bloom conditions for the growth of *N. scintillans* include high DIN and light availability, leading to phytoplankton growth and, thus, to high prey availability for *N. scintillans*. The bloom phase with peak abundances occurs in June-July, once calm conditions (including low wind speed and stratification) prevail, leading to nutrient depleted surface waters, thus, low prey availability. With no prey encounter, *N. scintillans* cells accumulate at the surface. Post-bloom conditions correspond to high solar radiation, damaging the cells accumulated at the surface, hence, inducing the bloom collapse.

5.3. *Noctiluca scintillans*' influence on coastal ecosystems

During the three cruises carried out off Helgoland in summer 2022, the phytoplankton community composition significantly varied, being dominated by diatoms during cruise #1, by *N. scintillans* during cruise #2 and finally by dinoflagellates including *Ceratium sp.* and *Prorocentrum sp.* during cruise #3. This bloom succession was also reflected in the results of the pigment analysis. With fucoxanthin and peridinin being recognized as the diagnostic pigments of diatoms and dinoflagellates, respectively (Canuti, 2023), the results suggested a shift from diatom-dominated waters in June towards dinoflagellate-dominated waters in August. Temperature was identified as one of the most important drivers of these changes. In fact, diatoms were negatively correlated to temperature, which was reflected in the observations, as diatoms were more abundant in June when temperatures were lowest (see section 4.2.2.). Furthermore, a negative correlation was found between diatoms and silicate, reflecting their high demand for this nutrient to build their siliceous frustules (Spillane, 2016). Diatoms are generally associated with colder, nutrient-rich waters (Lewandowska *et al.*, 2014), benefitting from several competitive advantages over dinoflagellates under these conditions, including rapid nitrogen uptake and storage (Xiao *et al.*, 2018).

In August, under warm, nutrient-depleted surface waters, dinoflagellates (*Ceratium sp.*, *Prorocentrum sp.*) replaced the diatoms. While higher temperatures can inhibit the growth of diatoms, particularly under nutrient-depleted conditions, they can be outcompeted by dinoflagellates, benefitting from several growth strategies, vertical migration capabilities, and mixotrophy (Smayda and Reynolds, 2003; Xiao *et al.*, 2018). Accordingly, the highest *Ceratium sp.* abundance (582 cellsL⁻¹) was measured on the 2nd of August at 40 m depth. This was also reflected by the high standard error for this species on that day (see section 4.2.1.), as extreme values can significantly increase the variability in the data, leading to inflated standard errors when calculating mean abundances. On the 2nd of August, the water temperature in depth was particularly high (17.3°C) and the water column was stratified with depleted nutrients in surface, increasing with depth. These factors might have contributed to the high abundances of *Ceratium sp.* measured in depth. Moreover, dinoflagellates are not limited by silicates, giving them an additional competitive advantage over diatoms, which were limited by the low silicate concentration. The negative correlation between dinoflagellates and PO₄, reflects their high demand in phosphorus due to their high DNA cell-content (Spector, 1984; Rizzo, 2003; Berdalet *et al.*, 2016).

Throughout the three cruises, the ambient nutrient concentration significantly varied, with higher concentrations of NO₃ at the beginning of June, decreasing and reaching a minimum in

August. Silicates followed the opposite trend, with lower concentrations in June, increasing in August. This could also reflect changes in the phytoplankton community composition with silicates utilized by diatoms in June, and nitrates by dinoflagellates in August. Moreover, Si concentrations were particularly high within dense *N. scintillans* surface patches. This could reflect the important diatom consumption by *N. scintillans*, as the cells decaying and lysing at the surface release considerable amounts of digested prey (i.e. diatoms), thus, silicates. Accordingly, the smallest diatoms were generally observed at the surface during the sampling campaigns.

Concentrations of NH_4 and PO_4 followed an interesting trend, remaining constant over the sampling period and drastically increasing within dense *N. scintillans* surface slicks. This was also reflected in the elevated standard errors for NH_4 and PO_4 during cruise #2 when compared with the other cruises (see section 4.2.3.). The high variability introduced by these extreme values of NH_4 and PO_4 , significantly increased the standard error, indicating greater uncertainty in the average nutrient concentrations within *N. scintillans* surface slicks. In contrast, the concentrations during the other cruises remained consistently lower and more uniform, resulting in lower variability and narrower standard errors.

Abrupt increases in ammonium and phosphate in *N. scintillans* patches have previously been observed (Okaichi and Nishio, 1976; Montani *et al.*, 1998). As efficient nitrogen and phosphate recycler (Mohanty *et al.*, 2007; Zhang *et al.*, 2021), *N. scintillans* is able to excrete high amounts of intracellularly accumulated NH_4 and PO_4 during cell lysis (Ara *et al.*, 2013; Zhang *et al.*, 2021). Therefore, the positive correlation between *N. scintillans*, NH_4 and PO_4 , is likely a result of the dinoflagellate's regenerative capabilities. In fact, because of its high ammonium content, *N. scintillans* acts as one of the most important contributors to nitrogen cycles in temperate coastal waters (Okaichi and Nishio, 1976; Montani *et al.*, 1998; Tada *et al.*, 2000). These nutrient pulses, originating from decaying *N. scintillans* blooms might considerably contribute to the nutrient availability, especially in warm, stratified and nutrient-depleted waters of the southern North Sea in late summer. Under these conditions, plankton biomass is primarily driven by nutrient supply to the photic zone (Lewandowska *et al.*, 2014), which *N. scintillans* provides. Through the increased nutrient availability, *N. scintillans* can fuel bottom-up processes and significantly contribute to phytoplankton production. This was observed in different areas including the Black Sea (Drits *et al.*, 2013), the North Sea (Schoemann *et al.*, 1998), and the Mediterranean Sea (Genitsaris *et al.*, 2019). In Japan, the excretion of PO_4 and NH_4 by *N. scintillans* even supplied up to 135% of the phosphorus and 85% of the nitrogen needed for primary production (Ara *et al.*, 2013). This process can be considered as “self-help” since it provides *N. scintillans* with food allowing it to thrive longer in an otherwise inhospitable environment (Schaumann *et al.*, 1988).

The bloom succession of diatoms followed by *N. scintillans* and ultimately by dinoflagellates such as *Prorocentrum sp.* and *Ceratium sp.*, hints a potential contribution of *N. scintillans* because of its central position. Diatoms are *N. scintillans*' most common prey type (Kiørboe, 2003). Particularly, large, non-motile or chain-forming diatoms resulted in higher ingestion (Kiørboe and Titelman, 1998) and growth rates (Zhang *et al.*, 2016). *Noctiluca scintillans* has been previously identified as active grazer of diatoms (Dela-Cruz *et al.*, 2002). Along the Belgian coast in summer, *N. scintillans* grazed 15% of diatoms, suggesting a strong impact on the diatoms occurring in the late spring and summer (Daro *et al.*, 2006). In Japan, *N. scintillans* was even responsible for a diatom bloom collapse (Saho Kitatsuji *et al.*, 2019). The many *N. scintillans* cells ingesting diatom chains during cruise #2, followed by a drastic decrease in diatom abundances, support the possibility that *N. scintillans* contributed to the end of the diatom bloom. After the *N. scintillans* bloom, an increase of dinoflagellates occurred. In consideration of the high affinity that dinoflagellates have for phosphate (Huang *et al.*, 2005), the anomalously high concentrations of PO₄ released by decaying *N. scintillans* blooms, might have contributed to the development of the dinoflagellate bloom in August. Additionally, dinoflagellates including *Prorocentrum sp.* are able to use various nitrogen sources (Ou *et al.*, 2014) but favour ammonium (Fan *et al.*, 2003). This could have further contributed to the increase of dinoflagellates after the *N. scintillans* bloom (Glibert, 2017). Dinoflagellates were not identified as superior prey type for *N. scintillans* (Zhang *et al.*, 2015) as they can escape the mucus threads of *N. scintillans*. Nevertheless, they can support the "revival" of *N. scintillans* under conditions where diatoms are not available (Zhang *et al.*, 2021). Cultured *N. scintillans* exhibited comparable growth rates when fed with the small motile flagellates than when fed with diatoms (Hallegraeff *et al.*, 2019).

In summary, the findings indicate that *N. scintillans* can importantly influence the phytoplankton community composition in the southern North Sea. Under suitable conditions including temperatures around 13°C and prey availability, *N. scintillans* rapidly develops. The high feeding pressure of *N. scintillans* on diatoms, nutrient depletion and warm waters are likely to induce the end of the diatom bloom, causing *N. scintillans* to accumulate at the surface. Upon cell lysis, nutrients are released, which might contribute to the development of a dinoflagellate bloom. This specific bloom succession was previously observed in the Seto Inland Sea (Nakamura, 1998a) or the South China Sea (Elbrächter and Qi, 1998) (Fig.5.4).

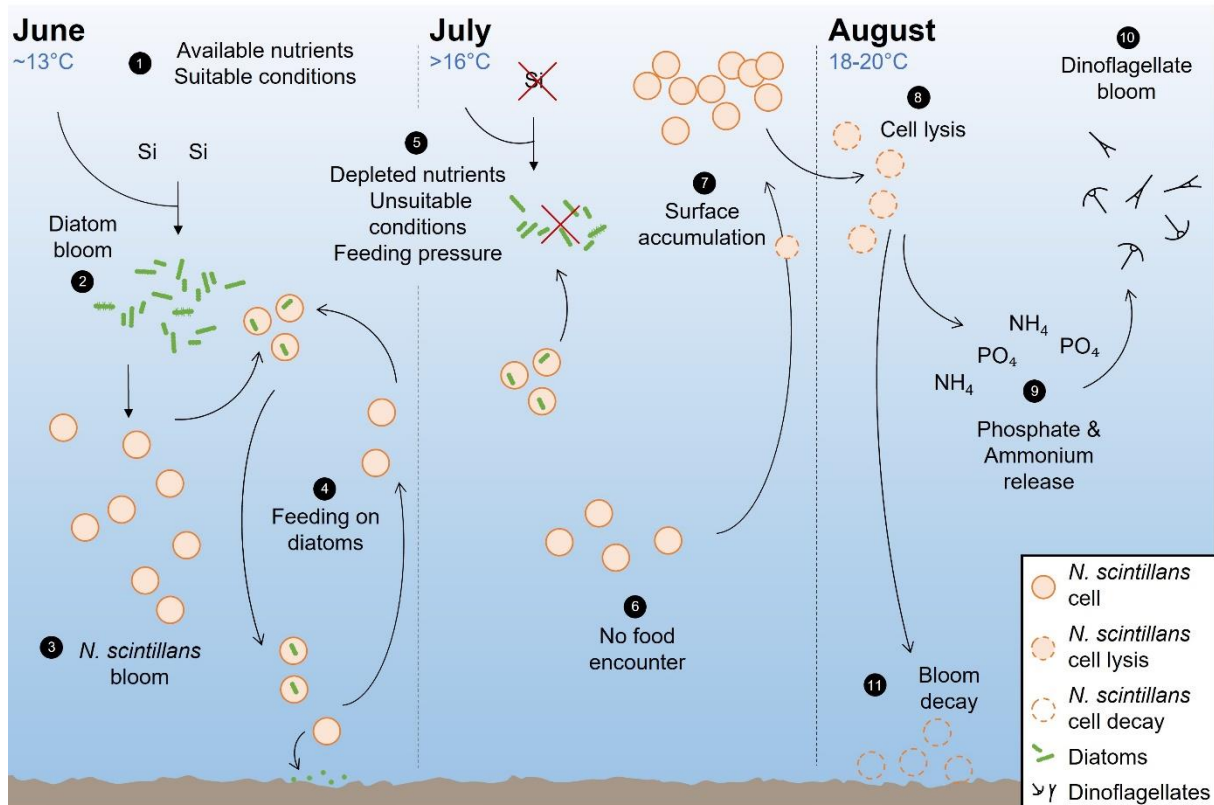


Figure 5.4: Schematic summary of the potential role of *N. scintillans* within the coastal phytoplankton community of the southern North Sea.

5.4. Uncertainties of the methodological approach used for assessing *Noctiluca scintillans*

5.4.1. Traditional sampling methods

The findings presented in the previous sections provided valuable new insights into the long-term trends, bloom dynamics, and the ecological role of *N. scintillans*. Particularly the combined use of traditional methods as well as bench-top and *in situ* imaging devices provided novel information about the ecological role of *N. scintillans* at unprecedented resolution. Nevertheless, several uncertainties were identified throughout the literature review, and the analyses of time series and sampled data. Most of these uncertainties emerged from traditional sampling techniques commonly utilized for the assessment of *N. scintillans*. For instance, no definite conclusions could be made regarding the potential global spread of *N. scintillans*. This was partly due to unavailable information about sampling frequency, duration, and location in the various studies. Another factor contributing to this inconclusiveness, is that nearly 90% of all field-based studies focusing on *N. scintillans* used traditional sampling methods, including bottles, nets, and buckets (Fig. 5.5).

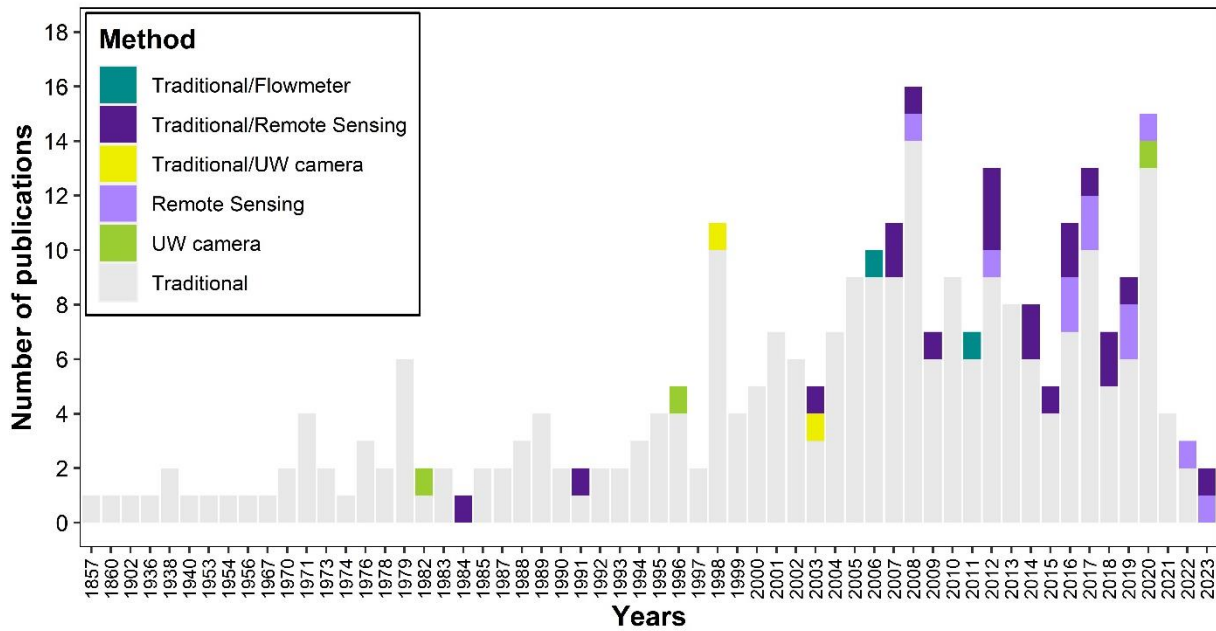


Figure 5.5: Number of field-based studies focusing on *N. scintillans* and use of methods for data collection between 1857 and 2023. Traditional methods include sampling performed with various types of zooplankton and phytoplankton nets, bottles, and buckets.

Net samples can provide valuable information about *N. scintillans* abundances, food vacuole content, size, and status of individual cells (Fig. 5.6). Nevertheless, the highly variable size of *N. scintillans* cells (Elbrächter and Qi, 1998) implies that the chosen mesh size of sampling nets can importantly influence detection rates. Additionally, the gelatinous constitution of *N. scintillans* and fragility of its agglomerations can lead to deteriorated cells and disrupted colonies when sampled with traditional methods such as nets (Omori and Hamner, 1982). This can lead to significant underestimations of abundance.

Water samples with bottles or buckets are generally better suited for sampling delicate organisms (Uhlig and Sahling, 1995; Dela-Cruz *et al.*, 2008). Microscopic analyses of these samples permit the identification and quantification of individual and agglomerated fragile plankton taxa at high resolution as well as food vacuole content analysis, cell status, abundance, and size estimations of single *N. scintillans* cells and agglomerates. Bottle samples can additionally provide an insight into the vertical distribution of *N. scintillans* since the samples can be collected at different depths (Fig. 5.6). Nevertheless, the vertical distribution of *N. scintillans* varies greatly among bloom stages and feeding conditions. Abundance peaks were recorded at the surface (Changjiang *et al.*, 1996; Turkoglu, 2013), sub-surface (Furuya *et al.*, 2006; Isinibilir *et al.*, 2011) and near the lower limit of the photic layer (Nikishina *et al.*, 2011). Other studies observed a homogenous distribution of cells throughout the upper mixed layer of the water column (Fonda Umani *et al.*, 2004). This can lead to under- or overestimations of *N. scintillans* populations. At HR, this is not an issue, since the sampling occurs in shallow and

generally well-mixed waters, where surface samples are representative of the entire water column (Wiltshire and Manly, 2004). Nevertheless, in regions with greater depths and/or that are subject to stratification, resolving the vertical distribution of *N. scintillans* with traditional methods is limited and requires other methodologies such as continuous *in situ* observations.

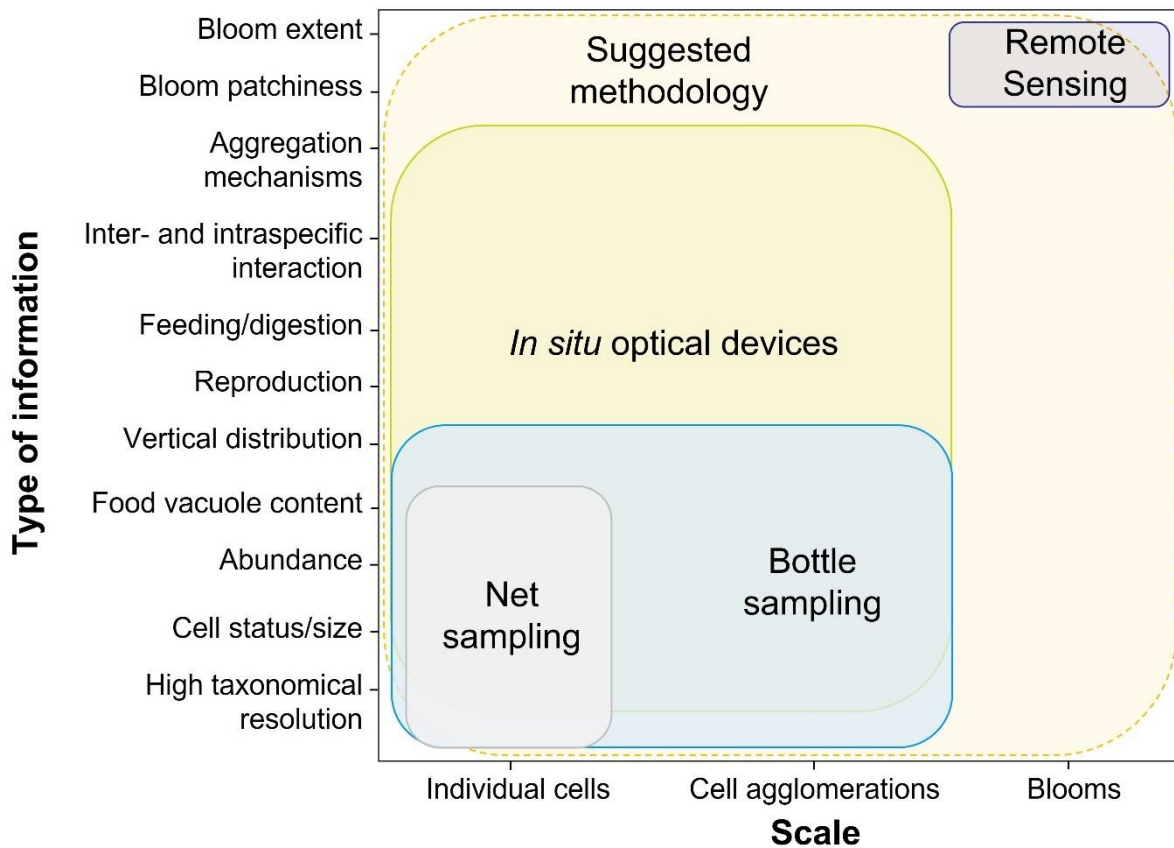


Figure 5.6: Overview of the information type obtained with the main sampling techniques applied in *N. scintillans*-focused research.

Noctiluca scintillans grows exponentially (Sathish *et al.*, 2021) and forms structurally complex blooms. These occur in filamentous surface patches of variable size, extending over several meters (Astoreca *et al.*, 2005) (Fig. 5.7A and B) up to hundreds of kilometres (Fig. 5.7C), and can rapidly break down (Dela-Cruz *et al.*, 2002). Assessing *N. scintillans* is therefore challenging, particularly when using sporadic discrete sampling techniques, as the probability to miss a bloom is high. This highlights the necessity of data at high temporal resolution to effectively monitor and understand these blooms. In fact, a local range expansion and potential intensification of *N. scintillans*, could be defined while focusing on regularly sampled regions (see section 2.2). However, there is still a lack of information needed to fully understand the past and recent dynamics of this organism at large geographical scale. Therefore, to verify these

findings and hypotheses, there is a highlighted need for methods that allow continuous monitoring of *N. scintillans* at high spatial resolution.

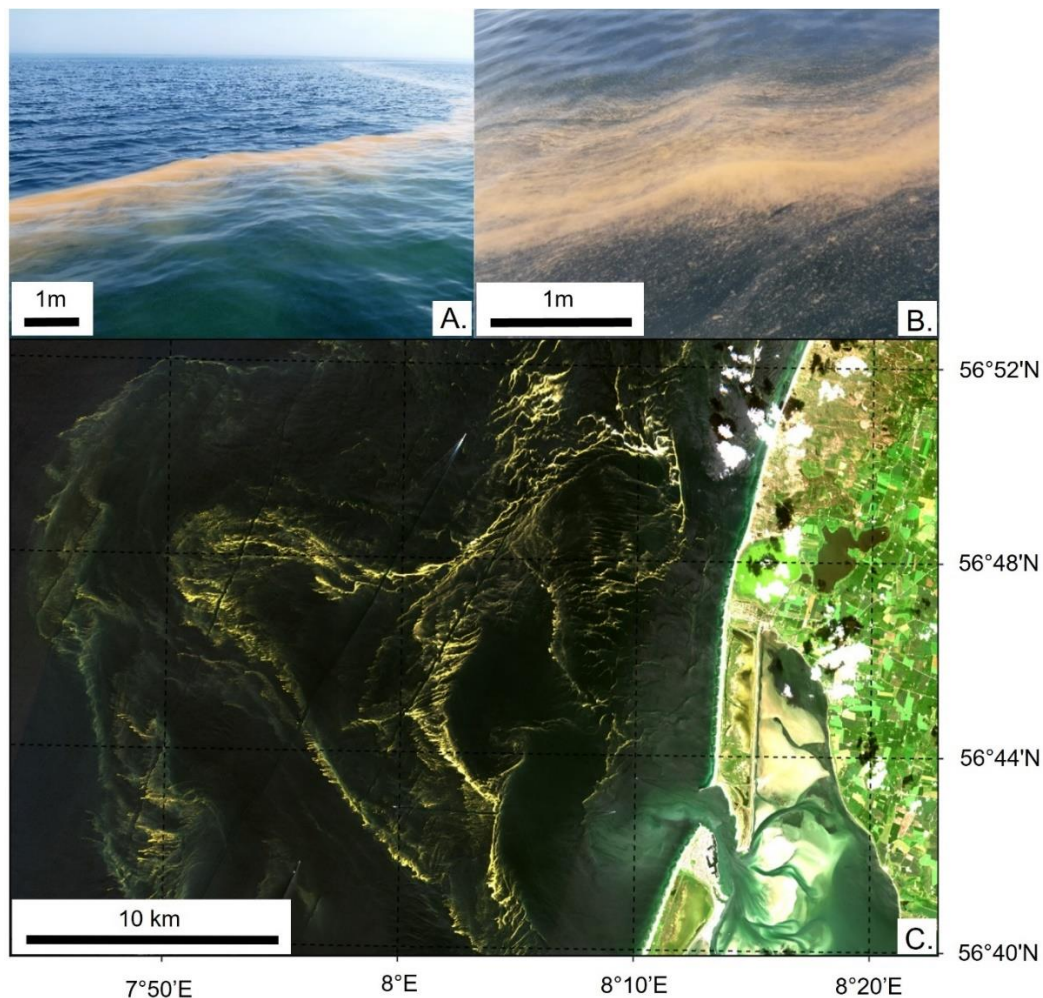


Figure 5.7: *N. scintillans* blooms at different scales. **(A. and B.)** pictures taken from the research vessel Ludwig Prandtl in June 2022, Helgoland, Germany; and **(C.)** detail of a satellite image of an ~500 km long *N. scintillans* bloom along the Danish North Sea coast acquired by Sentinel-2MSI on 29 June 2022.

5.4.2. Methodologies with higher spatial coverage

Time series such as the CPR survey, provide information about plankton diversity at high spatial resolution. It was shown here that for *N. scintillans*, reliable estimates of long-term trends over large spatial scales can be made when using time series such as the CPR survey. Despite the numerous modifications applied to the original sampling mechanism over time (Batten *et al.*, 2003), data from the CPR are robust, providing multi-decadal information of marine plankton dynamics at high horizontal resolution (Richardson *et al.*, 2006). The main constraint associated with the CPR survey, particularly for coastal species like *N. scintillans*, is that sampling typically

begins approximately 10 km offshore. This limits the accurate identification of hotspots near the immediate coastline. When comparing the densities of *N. scintillans* between the two time series, abundances measured with the CPR were substantially lower. Similarly, a comparison between the CPR and the Longhurst-Hardy Plankton Recorder revealed that the CPR underestimated abundances by a factor of 40 (Richardson *et al.*, 2004). This underestimation has been linked to the clogging of the CPR mesh by *N. scintillans*, reducing the filtering efficiency of the CPR (McLeod *et al.*, 2012). Physical damage to the organisms leading to the deterioration of morphological key features (e.g. *N. scintillans*' striated flagellum), can further impact counts. Additionally, the sampling depth of 7-10 m, may contribute to inaccurate abundance estimates, as the vertical distribution of *N. scintillans* is highly variable and blooms can be missed (Omori and Hamner, 1982).

Despite the high horizontal resolution of the CPR, the patchiness of *N. scintillans* proliferations also increases the likelihood of missing blooms. Moreover, the CPR data used in this thesis were averaged over wide spatial (i.e. 0.25°) and temporal scales (seasonal means), resulting in lower abundances when compared to the HR data collected at daily resolution. In consequence, the abundance threshold for blooms at HR, defined as $\geq 500 \text{ cellsL}^{-1}$, did not apply to the CPR data. This does not imply that no *N. scintillans* blooms were sampled. Instead, blooms may be represented by significantly lower values (5-10 cellsL^{-1}), which could be visually confirmed using satellite imagery for example. These abundance underestimations limit the precise determination of spatial distribution patterns when using CPR survey data. Therefore, data with higher spatial resolution, such as remote sensing, are needed. This was also reflected by the difference in the spread of the upper and lower standard errors in the effect plots for HR (Fig. 4.1 and 4.2) and CPR (Fig. 4.3). The HR time series, exhibits lower variability due to the consistency in sampling frequency and sampling location. This consistency reduces the overall variance and, consequently, results in narrower confidence intervals around the model predictions. In contrast, the CPR survey encompasses greater variability due to the lower spatiotemporal resolution of the data. The less frequent sampling, coupled with the diverse environmental conditions across different locations, introduces higher variability into the model. This increased variability is reflected in the wider spread of the standard errors in the effect plot, indicating greater uncertainty in the model's predictions (deviances explained of 55.54% for HR versus 29.45% for the CPR survey).

Optical remote sensing of phytoplankton blooms is a useful tool to obtain near real-time information about the horizontal aspect of proliferations and more specifically about the spatial extent, drift, timing, and duration of blooms (Fig. 5.6). Remote sensing of ocean colour can provide information about water constituents and phytoplankton communities, since the

accumulated pigments in the cells determine the spectral absorption and in turn the remote sensing reflectance (R_{rs}). Based on ocean colour information with sufficient spectral resolution, some phytoplankton groups can be differentiated during algal blooms when algal organisms are dominating (H. Xi *et al.*, 2015; Xi *et al.*, 2017). Due to their rapid growth and heavy predation rate, visible *N. scintillans* blooms at the surface are often monospecific (Detoni *et al.*, 2023; Gernez *et al.*, 2023), facilitating their remote detection.

The cells of *N. scintillans* are almost completely deprived of chl-*a* but contain carotenoids, originating from *de novo* synthetization, that cause the red discoloration of cells (Balch and Haxo, 1984). In accordance, a peak of carotenoid absorption at 488 nm was recorded in pure *N. scintillans* cultures (Astoreca *et al.*, 2005). A high and flat R_{rs} spectrum was also measured within *N. scintillans* surface blooms in the field, indicating elevated pixel brightness, and that chl-*a* and the associated absorption are less significant for *N. scintillans* than for other phytoplankton species (Gernez *et al.*, 2023). This unique spectral shape enables the identification of blooms or at least the discrimination of *N. scintillans* from other species with remote sensing. Similar spectral properties were measured along the Spanish coast (Detoni *et al.*, 2023) and in the southeastern Arabian Sea (Shaju *et al.*, 2018). In temperate waters, *N. scintillans* blooms typically appear in red-orange slicks at the surface (Fig. 5.7A and B) and in golden bright structures in true and false-colour composites (Fig. 5.7C). This means that standard red-edge algorithms are not suited for the detection of *N. scintillans* blooms (Gernez *et al.*, 2023). Instead, the development of specific chl-*a*-independent algorithms is needed (Qi *et al.*, 2019). Also, further research regarding bio-optical properties of *N. scintillans* is necessary. The nature of the carotenoid causing the absorption peak at 488 nm is still unclear (Detoni *et al.*, 2023) and the inherent optical properties of *N. scintillans* can vary with the type of ingested prey, which can impede the optical detection of this dinoflagellate (Van Mol *et al.*, 2007). Lastly, the detection of *N. scintillans* is challenging for atmospheric correction algorithms since dense surface blooms increase the signal in the near infrared R_{rs} , which can lead to great uncertainties and incorrect estimates of chl-*a* concentration or aerosol properties (Ruddick *et al.*, 2000; Hieronymi *et al.*, 2023).

Currents, Langmuir circulation or frontal structures can cause high concentrations of buoyant *N. scintillans* cells to accumulate in thin surface slicks (Fig. 5.7C) (Schaumann *et al.*, 1988) of ~10 m width (Astoreca *et al.*, 2005). Therefore, the detection and assessment of *N. scintillans* blooms with remote sensing is possible not only through optical properties but also with the unique spatial properties of *N. scintillans* blooms. The high resolution of satellites such as Landsat (30 m) or Sentinel-2 (10, 20 and 60 m, depending on the spectral bands), allows the detection of thin *N. scintillans* bloom structures. Even with Sentinel-3 OLCI (300 m resolution), which is

operationally used to estimate chl-*a*, such blooms are visible. Nevertheless, the fine structures cause high subpixel variability, which weakens the overall signal, limiting the detection of spatial *N. scintillans* features. Methodologies combining both spatial and optical signatures might effectively improve detection of this dinoflagellate from space.

Remote sensing presents many advantages for the large-scale detection of *N. scintillans* and can be considered as the key tool to gain knowledge about the global distribution of this organism. Nevertheless, ocean colour represents an integrated signal over the upper water layer with a depth depending on water turbidity. For example, the depth of penetration for scum forming blooms corresponds to only a few tens of centimetres (Kutser, 2004), thereby solely detecting proliferations near the surface. This is problematic for *N. scintillans*, since cell agglomerations can occur in depth (Drits *et al.*, 2013; Xue *et al.*, 2020). Furthermore, to overcome issues related to cloud coverage, sun glint or satellite overpass, and to obtain continuous data allowing the monitoring of brief *N. scintillans* blooms, the remote detection resorts to combining data from different satellites. The low spatial resolution of satellites such as MODIS-Aqua (250, 500 and 1000 m depending on the spectral band) is, however, not adapted for *N. scintillans*, since they are likely to miss fine structures and blooms in turbid nearshore waters. Algorithms able to detect even low concentrations of *N. scintillans* are needed to overcome this (Qi *et al.*, 2022). Other possibilities for the remote monitoring of *N. scintillans* are drones or airplanes. Depending on flight altitude, airplanes can deliver data at high resolution up to 1 m (Vander Woude *et al.*, 2019), while still covering vast areas. They do, however, represent a higher financial impact than drones. Drones are indeed less expensive, and the data are of very high resolution, but the geographical coverage is limited to a radius of 500 m (Ruiz-Villarreal *et al.*, 2022). Nevertheless, the high resolution of the data can help to rapidly detect small visible surface patches, which are undetectable via satellite. Moreover, as these instruments can fly in nearshore regions and under clouds, they can help fill the spatial gaps in satellite data (Vander Woude *et al.*, 2019).

5.4.3. *In situ* observations

The analysis of two technically different time series has been proven effective in defining the main drivers, as well as identifying long-term temporal and spatial dynamics of *N. scintillans* in the North Sea. Nevertheless, it must be mentioned that due to the heterotrophic nature of *N. scintillans*, the models for HR might have performed better, if prey abundances would have been included as potential drivers. In fact, the GAMs applied to the cruise data demonstrated that diatom abundance is an important driver of *N. scintillans*. Therefore, technical set-ups allowing

continuous *in situ* observations of the phytoplankton community composition, and, thus, of *N. scintillans*' potential prey, such as cabled underwater observatories (Fischer *et al.*, 2020), are crucial for improving predictions of the bloom dynamics of this species. In fact, underwater imaging can provide valuable insights of *N. scintillans*' behaviour in its natural environment (Fig. 5.6). The size and transparency of the cells allow for a direct identification and quantification of prey within its food vacuoles (Drits *et al.*, 2013; Mikaelyan *et al.*, 2014) and can hence provide essential *in situ* information on the ingestion, digestion and egestion habits of *N. scintillans* (Fig. 5.8A–C). Observations with *in situ* imagery are non-intrusive and non-destructive, thus, intraspecific interactions such as aggregation mechanisms and the formation of feeding webs can be visualized and quantified (Fig. 5.8A). Moreover, the vertical distribution of *N. scintillans* cells can be resolved (Fig. 4.9), providing valuable new insights into the vertical migration throughout different bloom phases and behaviour of *N. scintillans* at various depths, as well as the impact of *N. scintillans* on the biological carbon pump. A certain autonomy of the different devices (Fischer *et al.*, 2020; Giering *et al.*, 2020) presents a great advantage for continuous observations, crucial for ephemeral *N. scintillans* blooms. Through long-term monitoring strategies, blooms can be sampled from initiation until decay, enhancing the knowledge about environmental factors driving the different *N. scintillans* bloom phases. The deployment of autonomous devices ensures continuous data collection, necessary for the monitoring of blooms in areas where conditions are harsh and prevent ship-based sampling (Fischer *et al.*, 2020). In combination with machine learning algorithms for image analysis, time-consuming procedures such as enumeration, identification, and cell size measurements can be significantly accelerated, thereby continuously providing near-real time *in situ* data. Artificial intelligence also enables large-scale analyses of aquatic *in situ* data, which would be inconceivable with human annotators (Bochinski *et al.*, 2019). Stationary underwater observatories are, however, also subject to undersampling. While at the cost of temporal resolution at one location, towed camera systems, such as the VPR, have greater geographical coverage, which can enhance the chance to encounter *N. scintillans* blooms. This calls for the use of different *in situ* imaging devices in combination with remote sensing for the sampling of this dinoflagellate, as it would increase the temporal, spatial, and vertical coverage.

Lastly, one main goal of this thesis was to identify the environmental factors driving the different bloom phases of *N. scintillans* in the southern North Sea. Three possibilities to identify bloom phases exist and include abundances, cell diameter or reproductive stages. Here, for the analysis of both time series and cruise data, the determination was based on *N. scintillans* abundance. For the time series analysis, the threshold was set based on previously reported abundances

associated with bloom conditions (i.e. $\geq 500 \text{ cellsL}^{-1}$) (Xue *et al.*, 2020). For the cruise data *N. scintillans* abundances varied throughout the cruises, suggesting an increase between cruises #1 and #2, several days with mean abundances above 500 cellsL^{-1} during cruise #2, followed by a decline of abundances in cruise #3. Nevertheless, due to the structural complexity and rapidity of *N. scintillans* bloom formation and decay, this approach is limited since under-, or overestimations of abundances can easily occur.

It is also possible to define bloom phases based on cell diameter. Thresholds were defined with cells below $525 \mu\text{m}$ capable of population growth, hence corresponding to bloom initiation and peak, and cells above $600 \mu\text{m}$ associated to senescent cells, therefore corresponding to the bloom decay (Dela-Cruz *et al.*, 2002). Cell size can effectively and continuously be measured with *in situ* imaging devices, thereby providing essential information about the cell's condition and health status (Uhlig and Sahling, 1990; Dela-Cruz *et al.*, 2003). It also supplies indirect information about the ambient nutrient availability, as small-sized cells are generally found in nutrient-rich environments (Murray and Suthers, 1999). Lastly, small cells are spatiotemporal indicators of recent proliferations (Dela-Cruz *et al.*, 2002) and can help determining the cell drift during a bloom (Huang and Qi, 1997). For the cruise data, the smallest *N. scintillans* cells were recorded in August, suggesting that cells were still capable of growth. Nevertheless, this was not reflected in the measured abundances, clearly showing a decline in August. This was most likely due to the lower prey quality and availability.

The most promising approach to precisely determine bloom phases is based on the observation and quantification of cells undergoing distinct reproductive stages. *Noctiluca scintillans* cells undergo binary fission mainly during bloom initiation and peak, and rely mostly on sexual reproduction during bloom peak and decay (Sathish *et al.*, 2021). This also requires *in situ* data at high temporal resolution covering at least an entire year and thereby an entire *N. scintillans* bloom window. Underwater cameras are highly adapted for the *in situ* observations of reproductive behaviour since both the sexual and asexual reproduction of *N. scintillans* can be visualized (Fig. 5.8E–G).

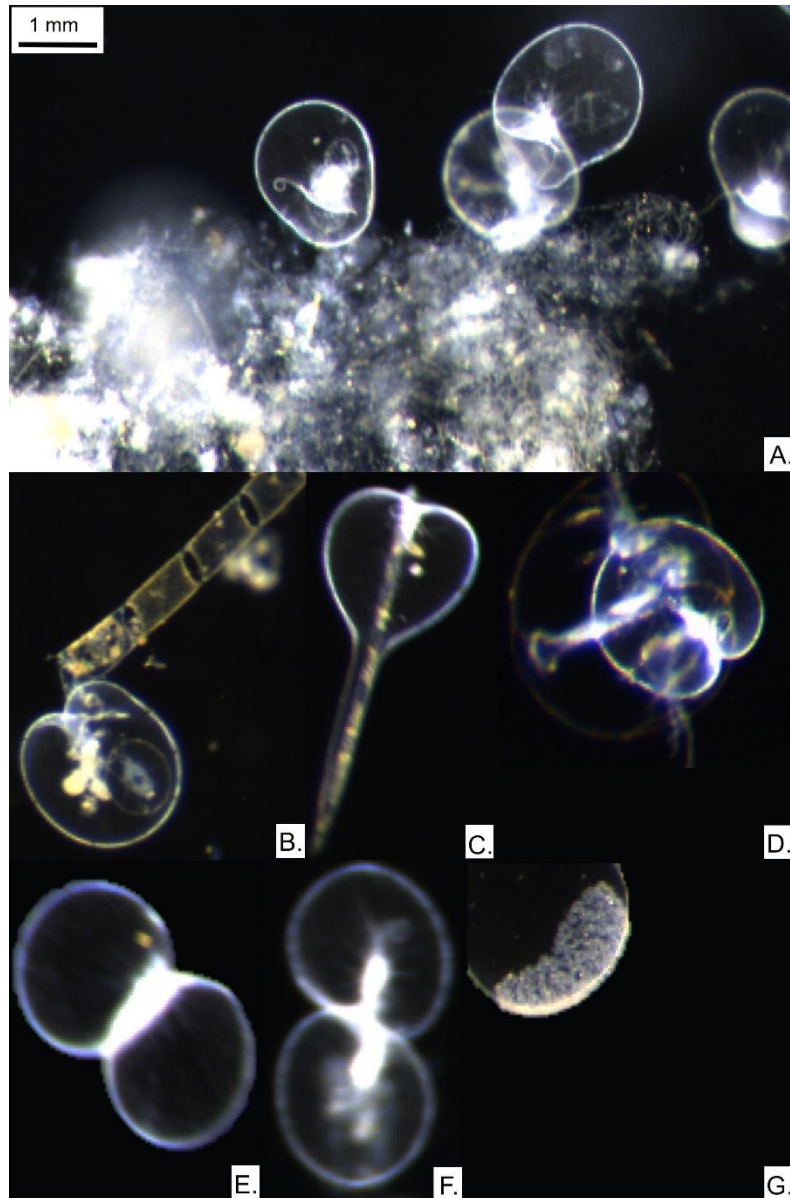


Figure 5.8: *N. scintillans* (A.-D.) feeding, and (E. and F.) asexually and (G.) sexually reproducing. Recorded with a CPICS in June 2022, Helgoland, Germany. The images represent: (A.) agglomerated *N. scintillans* cells feeding on marine snow. (B.) a single cell ingesting a diatom chain and marine snow. (C.) the phagotrophic ingestion of a diatom chain. (D.) the ingestion of *N. scintillans* by a Ctenophore. (E.) a single *N. scintillans* cell undergoing binary fission with cytoplasmic mass forming at the centre. (F.) the final stage of binary fission with the trophont dividing into two identical daughter cells. (G.) the final stage of the gametogenesis with progametes aggregating on one side of the parent cell.

6. Future directions

6.1. Proposed sampling scheme for field campaigns to resolve bloom dynamics and impacts of *Noctiluca scintillans*

Thus far, traditional sampling strategies used in the assessment of *N. scintillans* delivered important information about this species' distribution and ecological role. However, several major knowledge gaps regarding *N. scintillans* remain and emerge from limitations in these methods. Consequently, a critical need exists to refine the current methodological sampling protocols to address the remaining knowledge gaps, and to provide a holistic understanding of the bloom dynamics of this and other plankton species. The different methodologies applied to sample *N. scintillans* supply distinct information: from individual cells to blooms, and of either high taxonomic resolution or high spatiotemporal resolution (Fig. 5.6). For example, since net samples provide detailed information about the plankton community composition during a bloom, they can be used to assess the influence of *N. scintillans* on plankton diversity locally and at a precise moment in time. To quantify the influence of the bloom on the ecosystem, further knowledge about the bloom's horizontal and vertical extent and its duration is required, which cannot be obtained solely from point sampling but requires aerial measurements, as well as *in situ* data from underwater cameras. Additionally, to ensure a holistic understanding of *N. scintillans* bloom dynamics and associated impacts, methodologies covering the following aspects are required: the temporal aspect of the blooms, including the identification of drivers initiating and terminating a bloom; the biological aspect, including cell size and reproduction; and the spatial aspect resolving bloom extent, surface slick formation and the vertical distribution of cells. Therefore, there is a need for an integrative approach combining traditional measurements and novel technologies (Fig. 5.6).

In a first step, an *a priori* analysis of time series based on remote sensing data for example is required to identify the regional hotspots and time frames in which the likelihood to encounter *N. scintillans* is highest. Remote sensing is a cost-effective method available at a global level with year-round data and can, thus, inform about the inter-annual variations and help to regionally narrow down the sites of *N. scintillans* occurrences as well as their typical temporal trends and spatial extent (Qi *et al.*, 2019, 2022). This is necessary to determine the position of the sampling station(s) for the *in situ* long-term monitoring and the high-frequency sampling during the bloom period (Fig. 6.9).

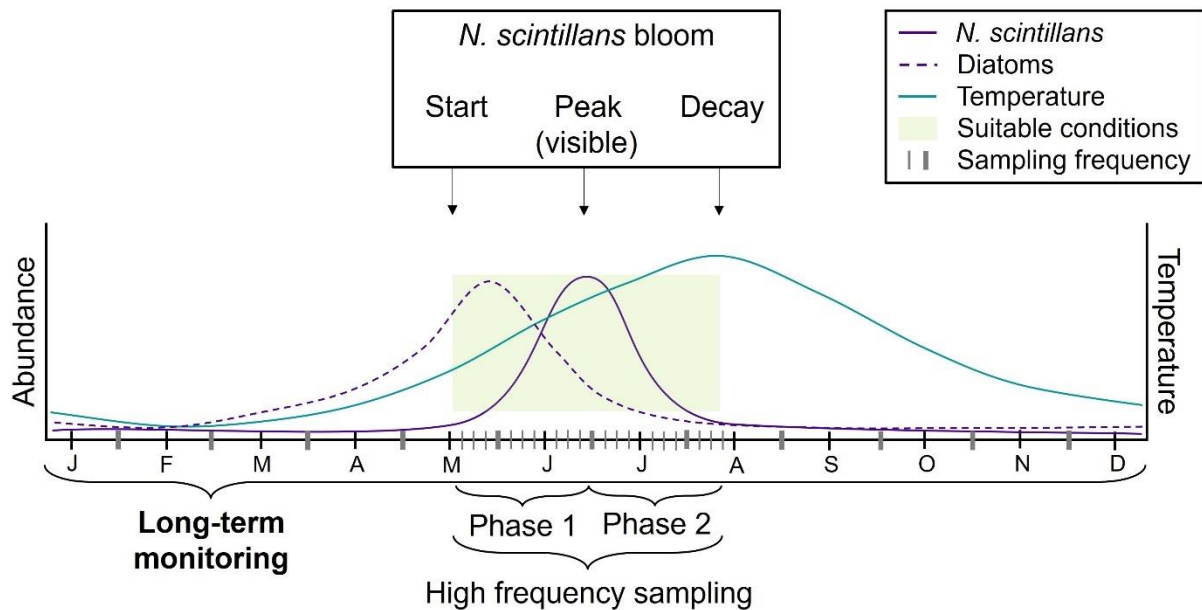


Figure 6.1: Sketch of a *N. scintillans* bloom and environmental conditions in a coastal area of the northern hemisphere, and timeline of the proposed sampling scheme for field campaigns aiming to resolve *N. scintillans* bloom dynamics and associated impacts carried out over one year. Details regarding the sampling strategies are provided in Table 6.1.

For the long-term assessment of *N. scintillans*, the regular monitoring of environmental drivers, such as temperature, salinity, and nutrients, abundance of plankton, including *N. scintillans*, and the behaviour of *N. scintillans*, particularly its reproduction, is needed. Temperature and salinity can be measured automatically via a conductivity temperature and depth (CTD) profiler attached to the vertically profiling underwater camera system, or via an autonomous surface water quality monitoring system such as the FerryBox. Nutrients can be measured either through the collection of water samples at the station(s) analysed in the laboratory or through nutrient analysers integrated in a FerryBox (Petersen *et al.*, 2018). The regular monitoring of environmental drivers is crucial for identifying suitable conditions that lead to the initiation and decay of *N. scintillans* blooms. The monitoring of plankton abundance and *N. scintillans* behaviour by means of stationary cabled (to overcome high power demands) underwater camera(s) with real-time data transfer, continuously collecting data throughout the photic layer, is required. The use of optical *in situ* instruments with different target ranges is useful to obtain a complete size spectrum of the plankton community occurring before, during and after *N. scintillans* blooms (Giering *et al.*, 2020). In combination with AI, data from the stationary observatories provide near real-time information about the bloom onset through the identification of intense reproduction and specifically of binary fission, bloom peak and decay. The monitoring of plankton diversity and abundance is critical to identify suitable conditions for *N. scintillans*, as blooms can develop only if prey availability (e.g. diatoms) is high (Fig. 5.9).

With the long-term monitoring, the precise moment of bloom initiation can be identified; however, the equipment for the high-frequency sampling must be prepared in advance (early spring) so that data can immediately be collected upon bloom onset. The high-frequency sampling should be split into two phases during which different equipment can be used: Phase 1 corresponds to the bloom start, when cells are distributed throughout the photic layer, and Phase 2 corresponds to the bloom peak and end, when bloom structures are visible at the surface (Fig. 6.1). At the bloom start, *in situ* shipboard sampling needs to be carried out at weekly to daily sampling frequency at and between the defined station(s) by means of stationary and towed underwater camera(s) to achieve a good horizontal resolution. The towed camera system(s) must be lowered stepwise (1–10 m, depending on the photic depth) throughout the photic layer to resolve the entire water mass in which *N. scintillans* is expected to occur. Moreover, at each station, temperature and salinity should be measured simultaneously and water samples must be collected for the analysis of nutrient concentrations. A FerryBox on board of the vessel can also be used to provide continuous information about the surface water conditions.

During the *N. scintillans* bloom peak and end phase, blooms are visible at the surface. Hence, drones or airplanes can be added to the sampling scheme to facilitate localizing the blooms. To account for tidal circulation, an area up to 100 km² within the study site should be overflowed by airplane providing composite maps, whereas drones help to identify bloom structures in proximity of the ship due to their limited spatial range. Environmental variables, plankton abundance and behaviour must be sampled as previously described; however, data must additionally be collected outside and within surface agglomerations to assess the behaviour of *N. scintillans* during bloom peak and end phase and the impact of dense *N. scintillans* agglomerations on water quality and food webs. Therefore, it is helpful to deploy a hydrographic drifter in the centre of the visible bloom structure to mark the bloom and ensure that the sampling within agglomerations is carried out in the same water mass. Furthermore, additional drifters deployed in the vicinity provide essential information about the frontal structures shaping *N. scintillans* surface slicks. During this bloom phase, satellite images supply information about bloom extent and duration to better quantify the impact of *N. scintillans* on the ecosystem. Once environmental conditions become unsuitable and *N. scintillans* cells stop reproducing, appear deteriorated and sink, the high-frequency sampling can cease. The different steps of this proposed sampling approach are summarized in Table 6.1. The sampling design can be adapted to fit the available budget and the focus of the research, either by simplifying or complementing it with additional methods. A basic sampling approach, that offers ample information while requiring only minimal equipment, is also presented in Table 6.1.

Table 6.1: Steps of the high resolution and basic proposed sampling framework for the targeted assessment of *N. scintillans* bloom dynamics and associated impacts; the corresponding timeline is sketched in Fig. 6.1.

Variable	Sensor	Sampling frequency and location		
		Long-term monitoring	Real-time data transfer, At station(s)	
			Phase 1	Phase 2
HIGH RESOLUTION SAMPLING				
Environmental drivers (temperature, salinity, nutrients)	Stationary CTD/ FerryBox	Real-time data transfer, At station(s)	Real-time data transfer, At station(s)	Real-time data transfer, At station(s)
	Towed CTD (attached to camera)	-	Weekly to daily, At and between station(s)	Weekly to daily, At and between station(s) within and outside surface agglomerations bloom structures
	FerryBox (on board)	-	Continuously, Study area	Continuously, Study area
	Water samples	Regular monitoring (Monthly to weekly), At station(s)	Weekly to daily, At station(s)	Weekly to daily, At station(s) within and outside surface agglomerations
	Drifter	-	-	Weekly to daily, At station(s) within surface agglomerations
Spatiotemporal <i>N. scintillans</i> occurrence	Satellite imagery	Regular monitoring (weekly to daily), Study area	-	Regular monitoring (weekly to daily), Study area
	Drones/airplanes	-	-	Hourly, Grid sampling of study area
Plankton abundance (incl. <i>N. scintillans</i>)	Stationary cabled UW camera(s)	Real-time data transfer, At station(s)	Real-time data transfer, At station(s)	Real-time data transfer, At station(s)
	Towed UW camera(s)	-	Weekly to daily, At and between station(s)	Weekly to daily, At and between station(s), within and outside surface agglomerations
<i>N. scintillans</i> behaviour (size, reproduction)	Stationary cabled UW camera(s)	Real-time data transfer, At station(s)	Real-time data transfer, At station(s)	Real-time data transfer, At station(s)
	Towed UW camera(s)	-	Weekly to daily, At and between station(s)	Weekly to daily, At and between station(s), within and outside surface agglomerations
BASIC SAMPLING				
Environmental drivers (temperature, salinity, nutrients)	Stationary CTD/ FerryBox	Real-time data transfer, At one station	Real-time data transfer, At one station	Real-time data transfer, At one station
Spatiotemporal <i>N. scintillans</i> occurrence	Satellite imagery	Regular monitoring (weekly to daily), Study area	-	Regular monitoring (weekly to daily), Study area
<i>N. scintillans</i> abundance and behaviour	Stationary cabled UW camera	Real-time data transfer, At one station	Real-time data transfer, At one station	Real-time data transfer, At one station

To enhance the sampling design, *in situ* measurements of bioluminescence could be included for example. A recent approach effectively used bioluminescence as an optical proxy for abundance in areas where *N. scintillans* is dominant (Xue *et al.*, 2020), and could hence be used in field monitoring surveys as an additional tool to differentiate *N. scintillans* from other phytoplankton species. To resolve spatially complex submesoscale oceanographic features shaping *N. scintillans* blooms, the novel Towed Instrument Array (TIA) can be added as it resolves the spatial structure of the water column at high resolution. It carries up to 20 instruments deployed at different depths and can be towed at high speed of up to 5 m s⁻¹ (Kock *et al.*, 2023). Sediment traps could be added to validate the information about feeding web density obtained with *in situ* cameras and, hence, widen our understanding of *N. scintillans*' contribution to carbon export. On the other hand, continuously measured cell sizes *in situ* can give precise information about the cellular carbon content of *N. scintillans* cells in different bloom phases (Menden-Deuer and Lessard, 2000). With underwater imaging, sinking *N. scintillans* colonies after intense blooms can be quantified. This could also substantially increase the understanding of the role of *N. scintillans* in the biological carbon pump.

6.2. Future expectations

The increasing trends in abundance, bloom duration and geographical expansion of *N. scintillans* in the North Sea and in other regions around the globe demonstrate the need to improve our understanding of this species. Particularly in the context of climate change with further increases in temperature and stratification, or anthropogenically induced increases in eutrophication, which have been predicted for the coming decades. In this thesis, it was demonstrated that these factors can positively influence *N. scintillans*. Hence, climate change might lead to further intensifications of this organism in the near future. This is alarming when considering the significant alterations of the coastal ecosystems associated to dense *N. scintillans* proliferations.

The impact *N. scintillans* exerts on diatoms is particularly concerning. Diatoms are a major source of productivity in the world's oceans as they account for up to 40% of the total primary production (Nelson *et al.*, 1995). Additionally, the siliceous frustules of diatoms increase their density leading to sinking rates of up to 100 m day⁻¹ (Kjørboe *et al.*, 1996). Therefore, diatoms have been identified as a key player in the biological carbon pump (Goldman, 1993), contributing up to 2150 Tmol C year⁻¹ of organic carbon production (Nelson *et al.*, 1995). Lastly, diatoms also heavily influence the global silica cycle, being responsible for most of the marine

biogenic silica production and contributing to nearly half of silicic acid removal from the euphotic zone (Assmy *et al.*, 2013). *Noctiluca scintillans* can graze down diatom blooms or even lead to their collapse (Saho Kitatsuji *et al.*, 2019). In consideration of the impact that *N. scintillans* can have on diatoms, it can be expected that in areas such as the North Sea, where abundances of *N. scintillans* increased in recent decades, important shifts in plankton community composition might occur. This in turn could alter the biological carbon pump and nutrient cycles. *Noctiluca scintillans* might also potentially contribute to the regional increase of toxic HABs. Harmful *Gymnodinium catenatum* for example, has a high affinity for ammonium (Yamamoto *et al.*, 2004) and could therefore benefit from the important ammonium release following the decay of *N. scintillans* blooms. *Noctiluca scintillans* positively influences jellyfishes, providing prey and increasing the water viscosity, thereby facilitating their food uptake (Fraser, 1969). Therefore, *N. scintillans* might have potentially contributed to the invasion and demographic explosions of jellyfishes reported in several regions around the globe since the early 2000s (Vandendriessche *et al.*, 2016). As mentioned in section 2.4.2., this can represent major economic impacts for tourism, but also for fisheries and aquaculture through the reduced ecosystem productivity as observed in the Black Sea (Oguz and Velikova, 2010). This highlights once more the need for continuous high-resolution *in situ* data. The continuous monitoring and imaging of cells interacting with their environment and with other plankton species would provide exceptional new insights into the ecological role of *N. scintillans* in coastal ecosystems and particularly into *N. scintillans*' impact on the plankton community. Eventually, this information could enhance predictions for HABs or jellyfish occurrences and limit economic damage.

With the further improvement of *in situ* imaging devices and the respective software algorithms, continuous observations of behaviour, food vacuole content, reproductive status, and cell health in *N. scintillans*' natural environment at near real-time can be expected in the future. At the Helgoland Underwater observatory for example, near-real time *in situ* image and environmental data are continuously collected (Fischer *et al.*, 2020). This type of data would provide parts of the missing information and greatly improve the understanding of *N. scintillans* bloom dynamics in the future. With the development of globally reproducible methodologies a better comparison among study sites would be ensured and could help understanding the differences in environmental preferences and bloom dynamics observed for this species around the globe.

The information obtained from satellite images, as well as the further development of the classification capacities of neural network-based algorithms such as the ONNS for Sentinel-3 OLCI (Hieronymi *et al.*, 2017), could bring the detection and monitoring of blooms from space a considerable step forward. Additionally, after obtaining *in situ* measurements of bio-optical

properties and gaining a better understanding of phytoplankton scattering properties, distinguishing phytoplankton groups based on hyperspectral data is possible (Bi *et al.*, 2023). Furthermore, novel methodologies and feature recognition allowing a systematic identification of *N. scintillans* were recently developed (Detoni *et al.*, 2023; Gernez *et al.*, 2023; Liu *et al.*, 2024). This could greatly improve the monitoring of this species in the coming years.

In consideration of the recent trends and associated impact of *N. scintillans* on coastal ecosystems, it is crucial to achieve realistic estimations of the spatiotemporal distribution of *N. scintillans* at global level in the future. Nevertheless, this can only be accomplished once regional high-resolution sampling campaigns, as proposed here, have been conducted, providing essential, yet currently unavailable insights into the bloom dynamics of *N. scintillans*. The proposed sampling scheme, particularly during the high frequency sampling, will provide detailed information about *N. scintillans* bloom timing, associated drivers, and impacts, as well as horizontal and vertical distribution of the cells. These efforts are necessary before proceeding with a global upscaling while using remote sensing data. The assessment of *N. scintillans* blooms under future climate change scenarios and further anthropogenic pressures will also significantly be improved.

7. Conclusions

Noctiluca scintillans affects food webs at different trophic levels, alters nutrient concentrations in the water, and thereby shapes the coastal ecosystems around the globe. Here, it was demonstrated that this important organism is increasing in several regions, and potentially at global level. The spatiotemporal trends of *N. scintillans* in the North Sea were analysed using two long-term time series of unique spatial (Continuous Plankton Recorder survey) and temporal (Helgoland Roads time series) resolution. This is the first analysis covering over 60 years of *N. scintillans* abundance data in combination with environmental variables in the North Sea. Results showed that since 1990, *N. scintillans* bloomed more often, longer and intensively around Helgoland. The occurrences of this dinoflagellate have geographically spread along the coast of the southern North Sea since the 1980s. Regional intensifications, where abundances doubled within a decade, occurred mainly in river estuaries. These increasing trends were mainly associated with changes in phytoplankton community composition, higher temperatures, and fluctuations in nutrient discharges. Spatiotemporal hotspots were identified in the North Sea, with *N. scintillans* most likely blooming in summer (from June to July) in coastal waters adjacent to the main estuaries of the Elbe and Rhine rivers.

The enhanced understanding of the spatiotemporal patterns of *N. scintillans* in the North Sea, allowed the planning and realization of three sampling campaigns in summer 2022 to enhance the knowledge about *N. scintillans* bloom dynamics and impact on coastal ecosystems. For the first time, an entire *N. scintillans* bloom from peak until decay was sampled with various novel imaging devices. This unique dataset provided new insights at unprecedented resolution into the ecological role of *N. scintillans*: the findings of this thesis showed a succession throughout the *N. scintillans* bloom period from diatoms over *N. scintillans* to dinoflagellates (*Prorocentrum sp.* and *Ceratium sp.*). *Noctiluca scintillans* heavily grazed on diatoms and thereby contributed to the drastic drop in diatom abundances. The *N. scintillans*-induced nutrient pulses (i.e. ammonium and phosphate) followed by increasing abundances of phosphate- and/or ammonium-affine dinoflagellates, suggested that *N. scintillans* also contributed to the successive dinoflagellate bloom formation. These findings demonstrated that the application of combined methodologies has the potential to greatly improve the understanding about *N. scintillans*' bloom dynamics, and its impact on water quality and coastal food webs.

This thesis permitted to identify the principal uncertainties associated with traditional sampling of *N. scintillans*, but also how to overcome these. With the proposed holistic sampling design developed here, it is possible to further increase the ecological understanding of this organism and ensure that occurrences of *N. scintillans* can be accurately predicted regionally and

potentially globally in the near future, thereby limiting potential ecological and economic damages.

References

- Agriculture Fisheries and Conservation department (2023) Hong Kong red tide information network.
- Aiyer, R. G. (1936) Mortality of fish of the Madras coast in June 1935. *Curr. Sci.*, **4**, 488–499.
- Ajani, P., Hallegraeff, G., and Pritchard, T. (2001) Historic overview of algal blooms in marine and estuarine waters of New South Wales, Australia. *Proc. Linn. Soc. New South Wales*, **123**, 1–22.
- Ajani, P., Lee, R., Pritchard, T., and Krogh, M. (2001) Phytoplankton dynamics at a long-term coastal station off Sydney, Australia. *J. Coast. Res.*, 60–73.
- Akin-oriola, G. A., Anetekhai, M. A., and Oriola, A. (2006) Algal blooms in Nigerian waters : an overview. *African J. Mar. Sci.*, **28**, 219–224.
- Akselman, R., Jurquiza, V., Costagliola, M. C., Fraga, S. G., Pichel, M., Hozbor, C., and Binsztein, N. (2010) *Vibrio cholerae* O1 found attached to the dinoflagellate *Noctiluca scintillans* in Argentine shelf waters. *Mar. Biodivers. Rec.*, **3**, e120.
- Al-Azri, A. R., Al-Hashmi, K. A., Al-Habsi, H., Al-Azri, N., and Al-Khusaibi, S. (2015) Abundance of harmful algal blooms in the coastal waters of Oman: 2006–2011. *Aquat. Ecosyst. Heal. Manag.*, **18**, 269–281.
- Albaina, A. and Irigoien, X. (2007) Fine scale zooplankton distribution in the Bay of Biscay in spring 2004. *J. Plankton Res.*, **29**, 851–870.
- Allen, E. W. (1937) A large catch of *Noctiluca*. *Science (80-)*, **86**, 197–198.
- Almeda, R., Connelly, T. L., and Buskey, E. J. (2014) Novel insight into the role of heterotrophic dinoflagellates in the fate of crude oil in the sea. *Sci. Rep.*, **4**, 1–9.
- Amorim, F. de L. L. de, Wiltshire, K. H., Lemke, P., Carstens, K., Peters, S., Rick, J., Gimenez, L., and Scharfe, M. (2023) Investigation of marine temperature changes across temporal and spatial Gradients: providing a fundament for studies on the effects of warming on marine ecosystem function and biodiversity. *Prog. Oceanogr.*, **216**, 103080.
- Anderson, C. R., Berdalet, E., Kudela, R. M., Cusack, C. K., Silke, J., O'Rourke, E., Dugan, D., McCammon, M., *et al.* (2019) Scaling up from regional case studies to a global harmful algal bloom observing system. *Front. Mar. Sci.*, **6**.
- Anderson, D. M., Glibert, P. M., and Burkholder, J. M. (2002) Harmful algal blooms and eutrophication: nutrient sources, composition, and consequences. *Estuaries*, **25**, 704–726.
- Anderson, D. M., Stock, C. A., Keafer, B. A., Bronzino Nelson, A., McGillicuddy, D. J., Keller, M., Thompson, B., Matrai, P. A., *et al.* (2005) *Alexandrium fundyense* cyst dynamics in the Gulf of Maine. *Deep. Res. Part II Top. Stud. Oceanogr.*, **52**, 2522–2542.
- Anderson, M. J. (2001) A new method for non-parametric multivariate analysis of variance. *Austral Ecol.*, **26**, 32–46.
- Ara, K., Nakamura, S., Takahashi, R., Shiimoto, A., and Hiromi, J. (2013) Seasonal variability of the red tide-forming heterotrophic dinoflagellate *Noctiluca scintillans* in the neritic area of Sagami Bay, Japan: its role in the nutrient-environment and aquatic ecosystem. *Plankt. Benthos Res.*, **8**, 9–30.
- Araújo, M. B. and Rahbek, C. (2006) How does climate change affect biodiversity? *Science (80-)*, **313**, 1396–1397.

- Ardyna, M. and Arrigo, K. R. (2020) Phytoplankton dynamics in a changing Arctic Ocean. *Nat. Clim. Chang.*, **10**, 892–903.
- Arrigo, K. R. (2005) Marine microorganisms and global nutrient cycles. *Nature*, **437**, 349–356.
- Arrigo, K. R., van Dijken, G., and Pabi, S. (2008) Impact of a shrinking Arctic ice cover on marine primary production. *Geophys. Res. Lett.*, **35**, 1–6.
- Artioli, Y., Blackford, J. C., Butenschön, M., Holt, J. T., Wakelin, S. L., Thomas, H., Borges, A. V., and Allen, J. I. (2012) The carbonate system in the North Sea: sensitivity and model validation. *J. Mar. Syst.*, **102–104**, 1–13.
- Arunpandi, N., Jyothibabu, R., Jagadeesan, L., Gireeshkumar, T. R., Karnan, C., and Naqvi, S. W. A. (2017) *Noctiluca* and copepods grazing on the phytoplankton community in a nutrient-enriched coastal environment along the southwest coast of India. *Environ. Monit. Assess.*, **189**, 1–20.
- Assmy, P., Smetacek, V., Montresor, M., Klaas, C., Henjes, J., Strass, V. H., Arrieta, J. M., Bathmann, U., *et al.* (2013) Thick-shelled, grazer-protected diatoms decouple ocean carbon and silicon cycles in the iron-limited Antarctic Circumpolar Current. *Proc. Natl. Acad. Sci. U. S. A.*, **110**, 20633–20638.
- Astoreca, R., Rousseau, V., Ruddick, K., Van Mol, B., Parent, J.-Y., and Lancelot, C. (2005) Optical properties of algal blooms in an eutrophicated coastal area and its relevance to remote sensing. *Remote Sens. Coast. Ocean. Environ.*, **5885**, 245–255.
- Aytan, U. and Şentürk, Y. (2018) Dynamics of *Noctiluca scintillans* (Macartney) Kofoid & Swezy and its contribution to mesozooplankton in the southeastern Black Sea. *Aquat. Sci. Eng.*, **33**, 84–89.
- Baek, S. H., Shimode, S., Han, M. S., and Kikuchi, T. (2008) Population development of the dinoflagellates *Ceratium furca* and *Ceratium fusus* during spring and early summer in Iwa Harbor, Sagami Bay, Japan. *Ocean Sci. J.*, **43**, 49–59.
- Baek, S. H., Shimode, S., Kim, H. cheol, Han, M. S., and Kikuchi, T. (2009) Strong bottom-up effects on phytoplankton community caused by a rainfall during spring and summer in Sagami Bay, Japan. *J. Mar. Syst.*, **75**, 253–264.
- Baek, S. H., Shin, H. H., Kim, D. S., Kim, Y. O., Bay, G., and Bay, J. (2011) Original articles : relationship between distributional characteristics of heterotrophic dinoflagellate *Noctiluca scintillans* and environmental factors in Gwangyang Bay and Jinhae Bay. *Korean J. Environ. Biol.*, **29**, 81–91.
- Balch, W. M. and Haxo, F. T. (1984) Spectral properties of *Noctiluca miliaris* Suriray, a heterotrophic dinoflagellate. *J. Plankton Res.*, **6**, 515–525.
- Balech, E. (1988) *Los dinoflagelados del Atlántico sudoccidental*. Ministerio. Madrid.
- Baliarsingh, S. K., Dwivedi, R. M., Lotliker, A. A., Sahu, K. C., Kumar, T. S., and Sheno, S. S. C. (2017) An optical remote sensing approach for ecological monitoring of red and green *Noctiluca scintillans*. *Environ. Monit. Assess.*, **189**, 1–10.
- Baliarsingh, S. K., Lotliker, A. A., Trainer, V. L., Wells, M. L., Parida, C., Sahu, B. K., Srichandan, S., Sahoo, S., *et al.* (2016) Environmental dynamics of red *Noctiluca scintillans* bloom in tropical coastal waters. *Mar. Pollut. Bull.*, **111**, 277–286.
- Baretta-Bekker, J. G., Baretta, J. W., Latuhihin, M. J., Desmit, X., and Prins, T. C. (2009) Description of the long-term (1991–2005) temporal and spatial distribution of phytoplankton carbon biomass in the Dutch North Sea. *J. Sea Res.*, **61**, 50–59.

- Barton, A. D., Irwin, A. J., Finkel, Z. V., and Stock, C. A. (2016) Anthropogenic climate change drives shift and shuffle in North Atlantic phytoplankton communities. *Proc. Natl. Acad. Sci. U. S. A.*, **113**, 2964–2969.
- Batistić, M., Garić, R., Jasprica, N., Ljubimir, S., and Mikuš, J. (2018) Bloom of the heterotrophic dinoflagellate *Noctiluca scintillans* (Macartney) Kofoid & Swezy, 1921 and tunicates *Salpa fusiformis* Cuvier, 1804 and *Salpa maxima* Forskål, 1775 in the open southern Adriatic in 2009. *J. Mar. Biol. Assoc. United Kingdom*, **99**, 1049–1058.
- Batten, S. D., Clark, R., Flinkman, J., Hays, G., John, E., John, A. W. G., Jonas, T., Lindley, J. A., *et al.* (2003) CPR sampling: the technical background, materials and methods, consistency and comparability. *Prog. Oceanogr.*, **57**, 193–215.
- Bax, N. J., Miloslavich, P., Muller-Karger, F. E., Allain, V., Appeltans, W., Batten, S. D., Benedetti-Cecchi, L., Buttigieg, P. L., *et al.* (2019) A response to scientific and societal needs for marine biological observations. *Front. Mar. Sci.*, **6**, 1–22.
- Benfield, M. C., Grosjean, P., Culverhouse, P. F., Irigoien, X., Sieracki, M. E., Lopez-Urrutia, A., and Gorsky, G. (2007) RAPID: research on automated plankton identification. *Oceanography*, **20**, 172–187.
- Bennett, G. (1860) *Gatherings of a naturalist in Australasia: being observations principally on the animal and vegetable productions of New South Wales, New Zealand, and some of the Austral Islands*. Voorst, J. Van (ed). Taylor & Francis, London.
- Berdalet, E., Fleming, L. E., Gowen, R., Davidson, K., Hess, P., Backer, L. C., Moore, S. K., Hoagland, P., *et al.* (2016) Marine harmful algal blooms, human health and wellbeing: Challenges and opportunities in the 21st century. *J. Mar. Biol. Assoc. United Kingdom*, **96**, 61–91.
- Bi, S., Hieronymi, M., and Röttgers, R. (2023) Bio-geo-optical modelling of natural waters. *Front. Mar. Sci.*, **10**, 1–25.
- Bindu, S., Dineshbabu, A. P., Saravanan, R., Bhat, G. S., and Lavanya, S. (2014) Occurrence of *Noctiluca scintillans* bloom off Mangalore in the Arabian Sea. *Indian J. Fish.*, **61**, 42–48.
- Black, K. D. (2001) *Environmental impacts of aquaculture (Vol. 5)*. Taylor & F. US.
- Bochinski, E., Bacha, G., Eiselein, V., Walles, T. J. W., Nejstgaard, J. C., and Sikora, T. (2019) Deep active learning for *in situ* plankton classification. *Lect. Notes Comput. Sci. (including Subser. Lect. Notes Artif. Intell. Lect. Notes Bioinformatics)*, **11188**, 5–15.
- Boni, I. (1983) Red tide off the coast of Emilia Romagna (northwestern Adriatic Sea) from 1975 to 1982. *Inform. Bot. Ital.*, **15**, 18–23.
- Bozec, Y., Thomas, H., Elkalay, K., and De Baar, H. J. W. (2005) The continental shelf pump for CO₂ in the North Sea - Evidence from summer observation. *Mar. Chem.*, **93**, 131–147.
- Brogueira, M. J. and Sampayo, M. A. M. (1983) On a *Noctiluca scintillans* (Macartney) Ehr. bloom off the south coast of Portugal. *Algarve Mar. Enviro. Qual. Cttee.*
- Brongersma-Sanders, M. (1945) The annual fish mortality near Walvis Bay (South West Africa), and its significance for paleontology. *Arch. Neer. Zool.*, **7**, 291–294.
- Brongersma-Sanders, M. (1948) The importance of upwelling water to vertebrate paleontology and oil geology. *Verh. der K. Nederlandsche Akad. van Wet. Afd. Natuurkd.*, **2**, 112.
- Browne, J. G. and Kingsford, M. J. (2005) A commensal relationship between the scyphozoan medusae *Catostylus mosaicus* and the copepod *Paramacrochiron maximum*. *Mar. Biol.*, **146**, 1157–1168.

- Brussaard, C. P., Riegman, R., Noordeloos, A. A., Cadée, G. C., Witte, H., Kop, A. J., Nieuwland, G., Van Duyl, F. C., *et al.* (1995) Effects of grazing, sedimentation and phytoplankton cell lysis on the structure of a coastal pelagic food web. *Mar. Ecol. Prog. Ser.*, **123**, 259–272.
- Buesseler, K. O., Lamborg, C. H., Boyd, P. W., Lam, P. J., Trull, T. W., Bidigare, R. R., Bishop, J. K. B., Casciotti, K. L., *et al.* (2007) Revisiting carbon flux through the ocean's twilight zone. *Science (80-.)*, **316**, 567–570.
- Buskey, E. J. (1995) Growth and bioluminescence of *Noctiluca scintillans* on varying algal diets. *J. Plankton Res.*, **17**, 29–40.
- Buskey, E. J., Strom, S., and Coulter, C. (1992) Bioluminescence of heterotrophic dinoflagellates from Texas coastal waters. *J. Exp. Mar. Bio. Ecol.*, **159**, 37–49.
- Bustillos-Guzmán, J. J., Band-Schmidt, C. J., López-Cortés, D. J., Hernández-Sandoval, F. E., Núñez-Vázquez, E., and Gárate-Lizárraga, I. (2013) Grazing of the dinoflagellate *Noctiluca scintillans* on the paralytic toxin-producing dinoflagellate *Gymnodinium catenatum*: does grazing eliminate cells during a bloom? *Ciencias Mar.*, **39**, 291–302.
- Cabal, J., González-Nuevo, G., and Nogueira, E. (2008) Mesozooplankton species distribution in the NW and N Iberian shelf during spring 2004: relationship with frontal structures. *J. Mar. Syst.*, **72**, 282–297.
- Canuti, E. (2023) Phytoplankton pigment in situ measurements uncertainty evaluation: an HPLC interlaboratory comparison with a European-scale dataset. *Front. Mar. Sci.*, **10**, 1–17.
- Cardoso, L. de S. (2012) Bloom of *Noctiluca scintillans* (Macartney) Kofoid & Swezy (Dinophyceae) in southern Brazil. *Brazilian J. Oceanogr.*, **60**, 265–268.
- Cassinari, E., Grillo, D., Princi, M., Specchi, M., Stravisi, F., and Valli, G. (1979) Osservazioni su *Noctiluca miliaris* (Suriray) del Golfo di Trieste. *Atti. Conv. Sc. Naz. P. F. Oceanogr. e fondi Mar.*, 1–8.
- Chang, F. H., Uddstrom, M. J., Pinkerton, M. H., and Richardson, K. M. (2008) Characterising the 2002 toxic *Karenia concordia* (Dinophyceae) outbreak and its development using satellite imagery on the north-eastern coast of New Zealand. *Harmful Algae*, **7**, 532–544.
- Chang, F. H., Zeldis, J., Gall, M., and Hall, J. (2003) Seasonal and spatial variation of phytoplankton assemblages, biomass and cell size from spring to summer across the north-eastern New Zealand continental shelf. *J. Plankton Res.*, **25**, 737–758.
- Changjiang, H., Sang, Q., Yuzao, Q., Xiaotao, L., and Qiang, O. (1997) The position and function of *Noctiluca scintillans* in its ecological community in Dapeng Bay, the South China Sea. *Oceanol. Limnol. Sin.*, **28**, 348–355.
- Changjiang, H., Yuzao, Q., Sang, Q., Songhui, L., and Tianjui, J. (1996) Seasonal and distribution character of *Noctiluca scintillans* in Dapeng Bay, the South China Sea. *Oceanol. Limnol. Sin.*, **27**, 493–498.
- Charernphol, S. (1957) Preliminary study of discolouration of sea water in the Gulf of Thailand. *Hydrogr. Dep.*, 1–8.
- Chassot, E., Bonhommeau, S., Dulvy, N. K., Mélin, F., Watson, R., Gascuel, D., and Le Pape, O. (2010) Global marine primary production constrains fisheries catches. *Ecol. Lett.*, **13**, 495–505.
- Chen, C., Zhu, J., Beardsley, R. C., and Franks, P. J. S. (2003) Physical-biological sources for dense algal blooms near the Changjiang River. *Geophys. Res. Lett.*, **30**, 1–4.

- Chen, Q. C., Wong, C. K., Tam, P. F., Lee, C. N. W., Yin, J. Q., Huang, L. M., and Tam, Y. H. (2003) Variations in the abundance and structure of the planktonic copepod community in the Pearl River Estuary, China. In Morton, B. (ed), *Perspectives on Marine Environment Change in Hong Kong and Southern China (1977-2001)*. Hong Kong, pp. 391–402.
- Chengxu, Z., Yulin, W., and Jingzhong, Z. (1994) Nutrient dynamics of *Noctiluca scintillans* (Macartney). *Oceanol. Limnol. Sin.*, **2**.
- Chiu, M. T. L. and Tse, T. K. W. (1978) Preliminary studies of the zooplankton distribution in the northern shelf of the South China Sea. Hong Kong: The Hong Kong Government.
- Colebrook, J. M. (1960) Continuous plankton records: methods of analysis, 1950–59. *Bull. Mar. Ecol.*, **5**, 51–64.
- Colombet, J., Fuster, M., Billard, H., and Sime-Ngando, T. (2020) Femtoplankton : what's new ? *Viruses*, **12**, 1–29.
- Cortés-Altamirano R, Manrique, F. A. and Luna-Soria, R. (1995) Occurrence of red tides in the eastern coast of the Gulf of California. *Rev. Latinoam. Microbiol.*, **37**, 337–342.
- Cowen, R. K. and Guigand, C. M. (2008) *In situ* ichthyoplankton imaging system (ISIIS): system design and preliminary results. *Limnol. Oceanogr. Methods*, **6**, 126–132.
- D’Silva, M. S., Anil, A. C., Naik, R. K., and D’Costa, P. M. (2012) Algal blooms: a perspective from the coasts of India. *Nat. Hazards*, **63**, 1225–1253.
- Daan, R. (1987) Impact of egg predation by *Noctiluca miliaris* on the summer development of copepod populations in the southern North Sea. *Mar. Ecol.*, **37**, 9–17.
- Dakin, W. J. and Colefax, A. N. (1940) The plankton of the Australian coastal waters off New South Wales. *Publ. Univ. Sydney*, **1**, 230.
- Daro, M., Breton, E., Antajan, E., Gasparini, S., and Rousseau, Véronique (2006) Do *Phaeocystis* colony blooms affect zooplankton in the Belgian Coastal Zone? In Rousseau, V., Lancelot, C., and Cox, D. (eds), *Current Status of Eutrophication in the Belgian Coastal Zone*. Presses Universitaires de Bruxelles, Brussels, pp. 61–72.
- Daskalov, G. M. (2002) Overfishing drives a trophic cascade in the Black Sea. *Mar. Ecol. Prog. Ser.*, **225**, 53–63.
- Davidson, K., Gowen, R. J., Harrison, P. J., Fleming, L. E., Hoagland, P., and Moschonas, G. (2014) Anthropogenic nutrients and harmful algae in coastal waters. *J. Environ. Manage.*, **146**, 206–216.
- Davies, C. (2023) National reference stations biogeochemical operations manual. *Integr. Mar. Obs. Syst.*, **4**, 1–58.
- Davies, C. H., Coughlan, A., Hallegraeff, G., Ajani, P., Armbrecht, L., Atkins, N., Bonham, P., Brett, S., et al. (2016) Data descriptor: a database of marine phytoplankton abundance, biomass and species composition in Australian waters. *Nat. Sci. Data*, **3**.
- Davis, C. S., Gallagher, S. M., Berman, M. S., Haury, L. R., and Strickler, J. R. (1992) The Video Plankton Recorder. 67–81.
- Decho, A. W. (1990) Microbial exopolymer secretions in ocean environments: their role(s) in food web and marine processes. *Oceanogr. Mar. Biol. - An Annu. Rev.*, **28**, 73–153.
- Dela-Cruz, J., Ajani, P., Lee, R., Pritchard, T., and Suthers, I. (2002) Temporal abundance patterns of the red tide dinoflagellate *Noctiluca scintillans* along the southeast coast of Australia.

Mar. Ecol. Prog. Ser., **236**, 75–88.

- Dela-Cruz, J., Middleton, J. H., and Suthers, I. M. (2003) Population growth and transport of the red tide dinoflagellate, *Noctiluca scintillans*, in the coastal waters off Sydney Australia, using cell diameter as a tracer. *Limnol. Oceanogr.*, **48**, 656–674.
- Dela-Cruz, J., Middleton, J. H., and Suthers, I. M. (2008) The influence of upwelling, coastal currents and water temperature on the distribution of the red tide dinoflagellate, *Noctiluca scintillans*, along the east coast of Australia. *Hydrobiologia*, **598**, 59–75.
- Detoni, A. M. S., Navarro, G., Garrido, J. L., Rodríguez, F., Hernández-Urcera, J., and Caballero, I. (2023) Mapping dinoflagellate blooms (*Noctiluca* and *Alexandrium*) in aquaculture production areas in the NW Iberian Peninsula with the Sentinel-2/3 satellites. *Sci. Total Environ.*, **868**, 161579.
- Devassy, V. P. (1989) Red tides discolouration and its impact on fisheries. *Red Tides, Biol. Environ. Sci. Toxicol.*
- Devassy, V. P., Bhattahiri, P. M. A., and Qasim, S. Z. (1979) Succession of grazing organisms following *Trichodesmium* phenomenon. *Indian J. Sci.*, **8**, 89–93.
- Dharani, G., Abdul Nazar, A. K., Kanagu, L., Venkateshwaran, P., Kumar, T. S., Ratnam, K., Venkatesan, R., and Ravindran, M. (2004) On the recurrence of *Noctiluca scintillans* bloom in Minnie Bay, Port Blair: impact on water quality and bioactivity of extracts. *Curr. Sci.*, **87**, 990–994.
- Dodgson, R. W. (1922) *Noctiluca* as an enemy of the oyster. *Nature*, **110**, 343–344.
- Dormann, C. F., Elith, J., Bacher, S., Buchmann, C., Carl, G., Carré, G., Marquéz, J. R. G., Gruber, B., *et al.* (2013) Collinearity: a review of methods to deal with it and a simulation study evaluating their performance. *Ecography (Cop.)*, **36**, 27–46.
- Douding, L., Zhidao, Z., Genhai, Z., and Yi, L. (1994) Distributive pattern of *Noctiluca scintillans* in the Zhejiang coastal water area. *Donghai Mar. Cent.*, **3**.
- Drinkwater, K., Belgrano, A., Borja, A., Conversi, A., Edwards, M., Greene, C. H., Ottersen, G., Pershing, A. J., *et al.* (2003) The response of marine ecosystems to climate variability associated with the North Atlantic Oscillation. In Hurrell, J., Kushnir, Y., Ottersen, G., and Visbeck, M. (eds), *The North Atlantic Oscillation: climate significance and environmental impact*. pp. 211–234.
- Drits, A. V, Nikishina, A. B., Sergeeva, V. M., and Solov'ev, K. A. (2013) Feeding, respiration, and excretion of the Black Sea *Noctiluca scintillans* Macartney in summer. *Oceanology*, **53**, 442–450.
- Dummermuth, A., Wiltshire, K. H., Kirstein, I., Brodte, E.-M., Wichels, A., Shama, L., Bergmann, A., Hofmann, C., *et al.* (2023) Marine Stations Helgoland and Sylt operated by the Alfred Wegener Institute Helmholtz Centre for Polar and Marine Research. *J. large-scale Res. Facil. JLSRF*, **8**.
- Dutkiewicz, S., Cermen, P., Jahn, O., Follows, M. J., Hickman, A. A., Taniguchi, D. A. A., and Ward, B. A. (2020) Dimensions of marine phytoplankton diversity. *Biogeosciences*, **17**, 609–634.
- Dwivedi, R., Baliarsingh, S. K., Lotliker, A. A., Kumar, T. S., and Sheno, S. S. C. (2016) An optical approach for synoptic monitoring of red *Noctiluca scintillans* bloom and its associates from space.
- Edward, J. K. P., Melkani, V. K., and Thangaraja, M, Wilhelmsson, D. (2009) A note on the algal bloom in Keezhakkarai coast of the Gulf of Mannar, southeastern India. *South Indian Coast.*

Mar. Bull., **1**, 14–15.

- Elbrächter, M. and Qi, Y. Z. (1998) Aspects of *Noctiluca* (Dinophyceae) population dynamics. In Anderson, D. M., Cembella, A. D., and Hallegraeff, G. M. (eds), *Physiological Ecology of Harmful Algal Blooms*. Springer, Berlin Heidelberg, pp. 315–335.
- Elith, J. and Leathwick, J. R. (2009) Species distribution models: ecological explanation and prediction across space and time. *Annu. Rev. Ecol. Evol. Syst.*, **40**, 677–697.
- Enomoto, Y. (1956) On the occurrence and food of *Noctiluca scintillans* (Macartney) in the waters adjacent to the west coast of Kyushu, with special reference to the possibility of damage caused to fish eggs by that plankton. *Bull. Japanese Soc. Sci. Fish.*, **22**, 82–88.
- Environmental Protection Department (2022) Marine Water Quality in Hong Kong in 2022.
- Erkan, F., Gucu, A. C., and Zagorodnyaya, J. (2000) The diel vertical distribution of zooplankton in the southeast Black Sea. *Turkish J. Zool.*, **24**, 417–427.
- Escalera, L., Pazos, Y., Morono, Á., and Reguera, B. (2007) *Noctiluca scintillans* may act as vector of toxigenic microalgae. *Harmful Algae*, **6**, 317–320.
- Fan, C. L., Glibert, P. M., and Burkholder, J. M. (2003) Characterization of the affinity for nitrogen, uptake kinetics, and environmental relationships for *Prorocentrum minimum* in natural blooms and laboratory cultures. *Harmful Algae*, **2**, 283–299.
- Fang, H. D., Zhu, A. J., Dong, Y. H., Xu, Z. Z., Ou, Q., Huang, Z. X., and Liu, J. Y. (2009) Study on the variation of zooplankton community in the Pearl River Estuary in 2005–2006. *J. Ocean. Taiwan Strait / Taiwan Haixia*, **28**, 30–37.
- Fei, H. (1952) The cause of red tides. *Sci. Art*, **22**, 1–3.
- Ferraz-Reyes, G., Ferraz-Reyes, E., and Vasques, E. (1979) Toxic dinoflagellate blooms in northeastern Venezuela during 1988. In Taylor, D. L. and Seliger, S. S. (eds), *Toxic Dinoflagellate Blooms*. Elsevier Publishing Co, Netherlands, pp. 191–194.
- Le Fèvre, J. and Grall, J. R. (1970) On the relationships of *Noctiluca* swarming off the western coast of Brittany with hydrological features and plankton characteristics of the environment. *J. Exp. Mar. Bio. Ecol.*, **4**, 287–306.
- Field, C. B., Behrenfeld, M. J., Randerson, J. T., and Falkowski, P. (1998) Primary production of the biosphere: Integrating terrestrial and oceanic components. *Science* (80-), **281**, 237–240.
- Figuroa-Torres, M. G. and Weiss-Martínez, I. (1999) Dinoflagelados (Dinophyceae) de la laguna de Tamiahua, Veracruz, México. *Rev. Biol. Trop.*, **47**, 43–46.
- Finlay, D., Schrapel, T., Morse, K., Miller, K., and Holz, M. (2015) Bioluminescence Australia. <https://www.facebook.com/groups/BioAustralia/>.
- Fischer, P., Brix, H., Baschek, B., Kraberg, A., Brand, M., Cisewski, B., Riethmüller, R., Breitbach, G., et al. (2020) Operating cabled underwater observatories in rough shelf-sea environments: a technological challenge. *Front. Mar. Sci.*, **7**, 1–20.
- Fock, H. O. and Greve, W. (2002) Analysis and interpretation of recurrent spatio-temporal patterns in zooplankton dynamics: a case study on *Noctiluca scintillans* (Dinophyceae) in the German Bight (North Sea). *Mar. Biol.*, **140**, 59–73.
- Fonda Umani, S., Beran, A., Parlato, S., Virgilio, D., Zollet, T., De Olazabal, A., Lazzarini, B., and Cabrini, M. (2004) *Noctiluca scintillans* Macartney in the northern Adriatic Sea: long-term dynamics, relationships with temperature and eutrophication, and role in the food web. *J.*

Plankton Res., **26**, 545–561.

- Fonda Umani, S., Princi, M., and Specchi, M. (1983) Note ecologiche su *Noctiluca miliaris* Suriray del Golfo di Trieste (Alto Adriatico). *Atti. Mus. Civ. Sci. Nat. Trieste*, **35**, 259–265.
- Foote, K. G. (2000) Optical methods. *ICES zooplankton methodology manual*. Academic Press, pp. 259–295.
- Fraga, S., Gallager, S. M., and Anderson, D. M. (1989) Chain-forming dinoflagellates: an adaptation to red tides. In Okaichi, T., Anderson, D. M., and Nemoto, T. (eds), *Red Tides: Biology, Environmental and Science and Toxicology*. Elsevier, New York, NY, pp. 281–284.
- Fraga, S. and Sanchez, S. (1997) A bloom of *Amphidinium sp.* in the ria de Vigo (NW of Spain). In Taylor, D. L. and Seliger, H. H. (eds), *Toxic Dinoflagellate Blooms*. Elsevier, New York.
- Frangópulos, M., Spyarakos, E., and Guisande, C. (2011) Ingestion and clearance rates of the red *Noctiluca scintillans* fed on the toxic dinoflagellate *Alexandrium minutum* (Halim). *Harmful Algae*, **10**, 304–309.
- Franks, P. J. S. (1997) Spatial patterns in dense algal blooms. *Limnol. Oceanogr.*, **42**, 1297–1305.
- Fraser, J. H. (1969) Experimental feeding of some medusae and chaetognatha. *J. Fish. Board Canada*, **26**, 1743–1762.
- Fraser, J. H. (1968) *Zooplankton sampling*. Tranter, D. J. (ed). Unesco, Paris.
- Friedland, K. D., Mouw, C. B., Asch, R. G., Ferreira, A. S. A., Henson, S., Hyde, K. J. W., Morse, R. E., Thomas, A. C., et al. (2018) Phenology and time series trends of the dominant seasonal phytoplankton bloom across global scales. *Glob. Ecol. Biogeogr.*, **27**, 551–569.
- Froján, M., Arbones, B., Zúñiga, D., Castro, C. G., and Figueiras, F. G. (2014) Microbial plankton community in the Ría de Vigo (NW Iberian upwelling system): impact of the culture of *Mytilus galloprovincialis*. *Mar. Ecol. Prog. Ser.*, **498**, 43–54.
- Fukuda, Y. and Endoh, H. (2006) New details from the complete life cycle of the red-tide dinoflagellate *Noctiluca scintillans* (Ehrenberg) Macartney. *Eur. J. Protistol.*, **42**, 209–219.
- Fukuda, Y. and Endoh, H. (2008) Phylogenetic analyses of the dinoflagellate *Noctiluca scintillans* based on β -tubulin and Hsp90 genes. *Eur. J. Protistol.*, **44**, 27–33.
- Fung, Y. C. and Trott, L. B. (1973) The occurrence of a *Noctiluca scintillans* (Macartney) induced red tide in Hong Kong. *Limnol. Oceanogr.*, **18**, 472–476.
- Furuya, K., Saito, H., Rujinard, S., Omura, T., Sopana, B., and Thaithaworn, L. (2006) Persistent whole-bay red tide of *Noctiluca scintillans* in Manila Bay, Philippines. *Coast. Mar. Sci.*, **30**, 74–79.
- Gallager, S. M. (2016) The Continuous Plankton Imaging and Classification Sensor (CPICS): a sensor for quantifying mesoplankton biodiversity and community structure. *Am. Geophys. Union*, 52A–57A.
- Gárate-Lizárraga, I. (1991) Analisis de una marea roja causada por *Noctiluca scintillans* (Macartney) Ehr. en Bahía Concepcion Baja California Sur en Frebrero de 1989. *Rev. Investig. Científica*, **2**, 35–43.
- Gárate-Lizárraga, I., Hernández-Orozco, M. L., Band-Schmidt, C., and Serrano-Casillas, G. (2001) Red tides along the coasts of Baja California Sur, México (1984 to 2001). *Oceánides*, 127–134.
- Garrido, J., Rodriguez, F., Campana, E., and Zapata, M. (2003) Rapid separation of chlorophylls a

- and *b* and their demetallated and dephytylated derivatives using a monolithic silica C18 column and a pyridine-containing mobile phase. *J. Chromatogr. A*, **994**, 85–92.
- Gaslikova, L., Grabemann, I., and Groll, N. (2013) Changes in North Sea storm surge conditions for four transient future climate realizations. 1501–1518.
- Genitsaris, S., Stefanidou, N., Moustaka-Gouni, M., Sommer, U., and Tsipas, G. (2020) Variability and community composition of marine unicellular eukaryote assemblages in a eutrophic mediterranean urban coastal area with marked plankton blooms and red tides. *Diversity*, **12**.
- Genitsaris, S., Stefanidou, N., Sommer, U., and Moustaka-Gouni, M. (2019) Phytoplankton blooms, red tides and mucilaginous aggregates in the urban Thessaloniki Bay, eastern Mediterranean. *Diversity*, **11**, 1–22.
- Gernez, P., Zoffoli, M. L., Lacour, T., Fariñas, T. H., Navarro, G., Caballero, I., and Harmel, T. (2023) The many shades of red tides: Sentinel-2 optical types of highly-concentrated harmful algal blooms. *Remote Sens. Environ.*, **287**, 113486.
- Gershwin, L., Walsh, F., and Holz, M. (2015) The definitive guide – How to find and photograph sea sparkle bioluminescence. <https://tasmaniangeographic.com>.
- Al Gheilani, H. M., Matsuoka, K., AlKindi, A. Y., Amer, S., and Waring, C. (2011) Fish kill incidents and harmful algal blooms in Omani waters. *J. Agric. Mar. Sci.*, **16**, 23.
- Giering, S. L. C., Cavan, E. L., Basedow, S. L., Briggs, N., Burd, A. B., Darroch, L. J., Guidi, L., Irisson, J. O., *et al.* (2020) Sinking organic particles in the ocean—flux estimates from in situ optical devices. *Front. Mar. Sci.*, **6**, 1–23.
- Gillbricht, M. (1983) Eine 'red tide' in der südlichen Nordsee und ihre Beziehungen zur Umwelt. *Helgol. Meeresunters*, **36**, 393–426.
- Glibert, P. M. (2017) Eutrophication, harmful algae and biodiversity — Challenging paradigms in a world of complex nutrient changes. *Mar. Pollut. Bull.*, **124**, 591–606.
- Gobler, C. J. (2020) Climate change and harmful algal blooms: insights and perspective. *Harmful Algae*, **91**, 101731.
- Gobler, C. J., Doherty, O. M., Hattenrath-Lehmann, T. K., Griffith, A. W., Kang, Y., and Litaker, R. W. (2017) Ocean warming since 1982 has expanded the niche of toxic algal blooms in the North Atlantic and North Pacific oceans. *Proc. Natl. Acad. Sci. U. S. A.*, **114**, 4975–4980.
- Goldman, J. C. (1993) Potential role of large oceanic diatoms in new primary production. *Deep. Res. Part I Oceanogr. Res. Pap.*, **40**, 159–168.
- Gomes, H. do R., Goes, J. I., Matondkar, S. G. P., Buskey, E. J., Basu, S., Parab, S., and Thoppil, P. (2014) Massive outbreaks of *Noctiluca scintillans* blooms in the Arabian Sea due to spread of hypoxia. *Nat. Commun.*, **5**, 1–8.
- Gómez-Aguirre, S. (1987) Dinoflagelados de la laguna de Tamiahua durante el periodo de Abril de 1984-Abril de 1986. *Reunión Nacional de la SOMPAAC*. Mazatlán, Sinaloa, México.
- Gómez-Aguirre, S. (1998) Red tide occurrences recorded in Mexico from 1980 to 1992. *An. del Inst. Biol. Ser. Zool.*, **69**, 13–22.
- Goncharov, I. (1857) Frigate Pallada. *Moskaw, Hydrojestsvennaya Lit.*, **2**, 508.
- González Taboada, F. and Anadón, R. (2014) Seasonality of North Atlantic phytoplankton from space: impact of environmental forcing on a changing phenology (1998-2012). *Glob. Chang.*

Biol., **20**, 698–712.

- Gouda, R. and Panigrahy, R. C. (1996) Ecology of phytoplankton in coastal waters off Gopalpur, east coast of India. *Indian J. Mar. Sci.*, **25**, 81–84.
- Grasshoff, K. (1976) *Methods of seawater analysis*. Verlag Chemie, Weinheim.
- Greve, W. and Lange, U. (1999) Plankton prognoses in the North Sea. *Dtsch. Hydrogr. Zeitschrift*, **51**, 155–160.
- Greve, W. and Reiners, F. (1988) Plankton time - space dynamics in German Bight - a systems approach. *Oecologia*, **77**, 487–496.
- Grindley, J. R. and Heydorn, A. E. F. (1970) Red water and associated phenomena in St. Lucia.
- Grindley, J. R. and Taylor, F. J. R. (1970) Factors affecting plankton blooms in False Bay. *Trans. R. Soc. South Africa*, **39**, 201–210.
- Grosjean, P., Picheral, M., Warembourg, C., and Gorsky, G. (2004) Enumeration, measurement, and identification of net zooplankton samples using the ZOOSCAN digital imaging system. *ICES J. Mar. Sci.*, **61**, 518–525.
- Groß, E., Di Pane, J., Boersma, M., Meunier, C. L., and Campbell, L. (2022) River discharge-related nutrient effects on North Sea coastal and offshore phytoplankton communities. *J. Plankton Res.*, **44**, 947–960.
- Guilang, J. X. H. J. W., Xiuqing, H., and Shonghui, L. (1992) Analysis of *Noctiluca scintillans* red tide occurred in red tide frequent area of Changjiang Estuary. *J. Jinan Univ.*, **3**.
- Guo, H., Liu, X., Ding, D., Guan, C., and Yi, X. (2014) The economic cost of red tides in China from 2008-2012. In Trainer, V. L. and Yoshida, T. (eds), *Proceedings of the Workshop on Economic Impacts of Harmful Algal Blooms on Fisheries and Aquaculture*. North Pacific Marine Science Organization (PICES) Scientific Report No. 47, Nanaimo, Canada, pp. 27–34.
- De Haas, H., Boer, W., and Van Weering, T. C. E. (1997) Recent sedimentation and organic carbon burial in a shelf sea: the North Sea. *Mar. Geol.*, **144**, 131–146.
- Hall, J. A., Safi, K., James, M. R., Zeldis, J., and Weatherhead, M. (2006) Microbial assemblage during the spring-summer transition on the northeast continental shelf of New Zealand. *New Zeal. J. Mar. Freshw. Res.*, **40**, 195–210.
- Hallegraeff, G. (1995) Algal blooms in Australian inshore and offshore waters. *J. Aust. Water Wastewater Assoc.*, **22**, 20–23.
- Hallegraeff, G., Hosja, W., Knuckey, R., and Wilkinson, C. (2008) Recent range expansion of the red-tide dinoflagellate *Noctiluca scintillans* in Australian coastal waters. *Harmful Algae News*, **38**, 10–11.
- Hallegraeff, G. M. (2010) Ocean climate change, phytoplankton community responses, and harmful algal blooms: a formidable predictive challenge. *J. Phycol.*, **46**, 220–235.
- Hallegraeff, G. M., Albinsson, M. E., Dowdney, J., Holmes, A. K., Mansour, M. P., and Seger, A. (2019) Prey preference, environmental tolerances and ichthyotoxicity by the red-tide dinoflagellate *Noctiluca scintillans* cultured from Tasmanian waters. *J. Plankton Res.*, **41**, 407–418.
- Hallegraeff, G. M., Davies, C., and Rochester, W. (2020) Range expansion of the red tide dinoflagellate *Noctiluca scintillans*. In Richardson, A. J., Eriksen, R., Moltmann, T., Hodgson-Johnston, I., and Wallis, J. R. (eds), *State and Trends of Australia's Ocean Report*. Hobart,

- Australia, pp. 361–365.
- Han, D. H., Hong, S. Y., and Ma, C. W. (1995) Distribution of zooplankton in Deukryang Bay, Korea. *J. Korean Fish. Soc.*, **28**, 517–532.
- Han, J., Li, G., Liu, H., Hu, H., and Zhang, X. (2013) Stimulation of bioluminescence in *Noctiluca sp.* using controlled temperature changes. *Luminescence*, **28**, 742–744.
- Hansen, H. P. and Koroleff, F. (1999) Determination of nutrients. In Grasshoff, K., Kremling, K., and Ehrhardt, M. (eds), *Methods of Seawater Analysis*. Weinheim, Germany, pp. 159–228.
- Hansson, L. A., Nicolle, A., Granéli, W., Hallgren, P., Kritzberg, E., Persson, A., Björk, J., Nilsson, P. A., *et al.* (2013) Food-chain length alters community responses to global change in aquatic systems. *Nat. Clim. Chang.*, **3**, 228–233.
- Hardy, A. C. (1955) A further example of the patchiness of plankton distribution. *Deep. Res.* **1**, **3**, 7–11.
- Harrison, P. J., Furuya, K., Glibert, P. M., Xu, J., Liu, H. B., Yin, K., Lee, J. H. W., Anderson, D. M., *et al.* (2011) Geographical distribution of red and green *Noctiluca scintillans*. *Chinese J. Oceanol. Limnol.*, **29**, 807–831.
- Harrison, P. J., Piontkovski, S., and Al-Hashmi, K. (2017) Understanding how physical-biological coupling influences harmful algal blooms, low oxygen and fish kills in the Sea of Oman and the western Arabian Sea. *Mar. Pollut. Bull.*, **114**, 25–34.
- Harrison, P. J., Xu, J., Yin, K., Liu, H. B., Lee, J. H. W., Anderson, D. M., Hodgkiss, I. J., and 1 (2010) Is There a Link Between N:P Ratios and Red Tides in Tolo Harbour? In Pagou, K. A. and Hallegraeff, G. M. (eds), *Proceedings of the 14th International Conference on Harmful Algae*. International Society for the Study of Harmful Algae and Intergovernmental Oceanographic Commission of UNESCO 2013, Hersonissos-Crete, Greece, pp. 90–92.
- Heil, C. A., Donuhue, M. J., and Dennison, W. C. (1998) Aspects of the winter phytoplankton community of Moreton Bay. In Tibbetts, J., Hall, N. J., and Dennison, W. C. (eds), *Moreton Bay and Catchment*. The University of Queensland, Brisbane, pp. 291–300.
- Heisler, J., Glibert, P. M., Burkholder, J. M., Anderson, D. M., Cochlan, W., Dennison, W. C., Dortch, Q., Gobler, C. J., *et al.* (2008) Eutrophication and harmful algal blooms: a scientific consensus. *Harmful Algae*, **8**, 3–13.
- Henschke, N., Bowden, D., Everett, J., Holmes, S., Kloser, R., Lee, R., and Suthers, I. (2013) Salp-falls in the Tasman Sea: a major food input to deep sea benthos. *Mar. Ecol. Prog. Ser.*, **491**, 165–175.
- Herren, C. M., Alldredge, A. L., and Case, J. F. (2004) Coastal bioluminescent marine snow: fine structure of bioluminescence distribution. *Cont. Shelf Res.*, **24**, 413–429.
- Hesse, K. J., Liu, Z. L., and Schaumann, K. (1989) Phytoplankton and fronts in the German Bight. *Top. Mar. Biol.*, **53**, 187–196.
- Heyen, H., Fock, H., and Greve, W. (1999) Detecting relationships between the interannual variability in ecological time series and climate using a multivariate statistical approach - A case study on Helgoland Roads zooplankton. *Clim. Res.*, **10**, 179–191.
- Hieronimi, M., Bi, S., Müller, D., Schütt, E. M., Behr, D., Brockmann, C., Lebreton, C., Steinmetz, F., *et al.* (2023) Ocean color atmospheric correction methods in view of usability for different optical water types. *Front. Mar. Sci.*, **10**, 1–23.
- Hieronimi, M., Müller, D., and Doerffer, R. (2017) The OLCI neural network swarm (ONNS): a

- bio-geo-optical algorithm for open ocean and coastal waters. *Front. Mar. Sci.*, **4**, 1–18.
- Hinder, S. L., Hays, G. C., Edwards, M., Roberts, E. C., Walne, A. W., and Gravenor, M. B. (2012) Changes in marine dinoflagellate and diatom abundance under climate change. *Nat. Clim. Chang.*, **2**, 271–275.
- Ho, K. C. (1994) Several fish kills in Hong Kong and the South China Sea by *Noctiluca scintillans* blooms. In Nontji, A. (ed), *Proceedings of the 3rd IOC-WESTPAC Scientific Symposium*. Bali, Indonesia, pp. 73–78.
- Hobson, L. A. and McQuoid, M. R. (2001) Pelagic diatom assemblages are good indicators of mixed water intrusions into Saanich Inlet, a stratified fjord in Vancouver Island. *Mar. Geol.*, **174**, 125–138.
- Hodgkiss, I. J. and Ho, K. C. (1997) Are changes in N:P ratios in coastal waters the key to increased red tide blooms? In Wong, Y. S. and Tam, N. F. Y. (eds), *Asia-Pacific Conference on Science and Management of Coastal Environment*. pp. 141–147.
- Hong, S. Y., Ma, C. W., and Kang, Y. S. (1994) Distribution of copepod indicator species and zooplankton communities in Pusan Harbor, Korea. *J. Korean Soc. Ocean.*, **29**, 132–144.
- Horstman, D. A. (1981) Reported red-water outbreaks and their effects on fauna of the west and south coasts of South Africa, 1959–1980. *Fish. Bull. S. Af.*, **15**, 71–88.
- Howard, J. (1996) Red tides rising. *Scripps Inst. Ocean. Explor.*, **2**, 2–9.
- Howarth, R. and Paerl, H. W. (2008) Coastal marine eutrophication: control of both nitrogen and phosphorus is necessary. *Proc. Natl. Acad. Sci.*, **105**, E103.
- Hsiao, S. H., Kâ, S., Fang, T. H., and Hwang, J. S. (2011) Zooplankton assemblages as indicators of seasonal changes in water masses in the boundary waters between the East China Sea and the Taiwan Strait. *Hydrobiologia*, **666**, 317–330.
- Huang, B., Ou, L., Hong, H., Luo, H., and Wang, D. (2005) Bioavailability of dissolved organic phosphorus compounds to typical harmful dinoflagellate *Prorocentrum donghaiense* Lu. *Mar. Pollut. Bull.*, **51**, 838–844.
- Huang, C. and Qi, Y. (1997) The abundance cycle and influence factors on red tide phenomena of *Noctiluca scintillans* (Dinophyceae) in Dapeng Bay, the South China Sea. *J. Plankton Res.*, **19**, 303–318.
- Hwang, H. J. and Choi, J. K. (1993) Seasonal characteristics of zooplankton community in the mid-eastern part of the Yellow Sea. *J. Oceanol. Soc. Korea*, **28**, 24–34.
- Ibebuchi, C. C. and Abu, I. O. (2023) Characterization of temperature regimes in Western Europe, as regards the summer 2022 Western European heat wave. *Clim. Dyn.*, **61**, 3707–3720.
- Imai, I., Yamaguchi, M., and Hori, Y. (2006) Eutrophication and occurrences of harmful algal blooms in the Seto Inland Sea, Japan. *Plankt. Benthos Res.*, **1**, 71–84.
- IPCC (2021) *Climate Change 2021 – The Physical Science Basis*. Cambridge University Press, Cambridge.
- Isinibilir, M., Hubareva, E., and Svetlichny, L. (2014) Interpopulation dynamics between *Acartia clausi* (Copepoda) and *Noctiluca scintillans* (Dinoflagellata) in the Bosphorus area of the Black and the Marmara Seas. *Ital. J. Zool.*, **81**, 451–456.
- Isinibilir, M., Kideys, A. E., Tarkan, A. N., and Yilmaz, I. N. (2008) Annual cycle of zooplankton abundance and species composition in Izmit Bay (the northeastern Marmara Sea). *Estuar.*

- Coast. Shelf Sci.*, **78**, 739–747.
- Isinibilir, M., Svetlichny, L., Hubareva, E., Yilmaz, I. N., Ustun, F., Belmonte, G., and Toklu-Alicli, B. (2011) Adaptability and vulnerability of zooplankton species in the adjacent regions of the Black and Marmara Seas. *J. Mar. Syst.*, **84**, 18–27.
- Jacques, G. and Sournia, A. (1978) Les eaux rouges dues au phytoplancton en Méditerranée. *Vie Milieu*, **28**, 175–187.
- Jakobsen, H. H. and Tang, K. W. (2002) Effects of protozoan grazing on colony formation in *Phaeocystis globosa* (Prymnesiophyceae) and the potential costs and benefits. *Aquat. Microb. Ecol.*, **27**, 261–273.
- Jang, M. C., Shin, K., Jang, P. G., and Lee, W. J. (2010) Relationship between environmental factors and short-term variations of mesozooplankton during summer in Jangmok Bay, South Coast of Korea. *Ocean Polar Res.*, **32**, 41–52.
- Jeffrey, S. and Carpenter, S. (1974) Seasonal succession of phytoplankton at a coastal station off Sydney. *Aust. J. Mar. Freshw. Res.*, **25**, 361–369.
- Jenkinson, I. R. (1986) Oceanographic implications of non-newtonian properties found in phytoplankton cultures. *Nature*, **323**, 435–437.
- Jensen, L. Ø., Mousing, E. A., and Richardson, K. (2017) Using species distribution modelling to predict future distributions of phytoplankton: case study using species important for the biological pump. *Mar. Ecol.*, **38**, 1–12.
- Jingzhong, Z., Liping, D., and Baoping, Q. (1985) Preliminary studies on eutrophication and red tide problems in Bohai Bay. *Hydrobiologia*, **127**, 27–30.
- Johns, D. G. (2020) CPR *Noctiluca* abundance records for North Atlantic - 1981 to 2018. The archive for marine species and habitats data (DASSH).
- Johnson, K. B. and Shanks, A. L. (2003) Low rates of predation on planktonic marine invertebrate larvae. *Mar. Ecol. Prog. Ser.*, **248**, 125–139.
- Kaiser, D., Voynova, Y. G., and Brix, H. (2023) Effects of the 2018 European heatwave and drought on coastal biogeochemistry in the German Bight. *Sci. Total Environ.*, **892**, 164316.
- Kamburska, Doncheva, and Stefanova (2003) On the recent changes of zooplankton community structure along the Bulgarian Black Sea coast: a post invasion effect of exotic ctenophores interactions. *Proc. First Int. Conf. Environ. Res. Assess.*, 69–85.
- Kang, J. (2020) Observation of items fed by *Noctiluca scintillans* around Dokdo in spring. *J. Korean Soc. Oceanogr.*, **25**, 160–172.
- Kang, J. H. (2010) Distributional characteristics and carrying capacity of the potentially risky species *Noctiluca scintillans* at international korean seaports. *Ocean Polar Res.*, **32**, 449–462.
- Kang, J. H., Kim, W. S., Chang, K. I. L., and Noh, J. H. (2004) Distribution of plankton related to the mesoscale physical structure within the surface mixed layer in the southwestern East Sea, Korea. *J. Plankton Res.*, **26**, 1515–1528.
- Kang, Y.-S., Park, J.-S., Lee, S.-S., Kim, H.-G., and Lee, P.-Y. (1996) Zooplankton community and distributions of copepods in relation to eutrophic evaluation in Chinhae Bay. *J. Korean Fish. Soc.*, **29**, 415–430.
- Kat, M. (1979) *Toxic Dinoflagellate Blooms*. Taylor, D. L. and Seliger, H. H. (eds). Elsevier, North-

Holland.

- Ki, J.-S. (2010) Nuclear 28S rDNA phylogeny supports the basal placement of *Noctiluca scintillans* (Dinophyceae; Noctilucales) in dinoflagellates. *Eur. J. Protistol.*, **46**, 111–120.
- Kim, S.-W. and Lee, J. H. (1994) Seasonal distribution of zooplankton communities in Incheon Dock, an artificially closed marine embayment facing the Yellow Sea, Western Korea. *J. Korean Soc. Oceanogr.*, **29**, 376–382.
- Kimor, B. (1979) Predation by *Noctiluca miliaris* Souriray on *Acartia tonsa* Dana eggs in the inshore waters of southern California. *Limnol. Oceanogr.*, **24**, 568–572.
- Kjørboe, T. (2003) High turnover rates of copepod fecal pellets due to *Noctiluca scintillans* grazing. *Mar. Ecol. Prog. Ser.*, **258**, 181–188.
- Kjørboe, T., Hansen, J. L. S., Alldredge, A. L., Jackson, G. A., Passow, U., Dam, H. G., Drapeau, D. T., Waite, A., *et al.* (1996) Sedimentation of phytoplankton during a diatom bloom: rates and mechanisms. *J. Mar. Res.*, **54**, 1123–1148.
- Kjørboe, T., Tiselius, P., Mitchell-Innes, B., Hansen, J. L. S., Visser, A. W., and Mari, X. (1998) Intensive aggregate formation with low vertical flux during an upwelling-induced diatom bloom. *Limnol. Oceanogr.*, **43**, 104–116.
- Kjørboe, T. and Titelman, J. (1998) Feeding, prey selection and prey encounter mechanisms in the heterotrophic dinoflagellate *Noctiluca scintillans*. *J. Plankton Res.*, **20**, 1615–1636.
- Kirchner, M., Sahling, G., Uhlig, G., Gunkel, W., and Klings, K. W. (1996) Does the red tide-forming dinoflagellate *Noctiluca scintillans* feed on bacteria? *Sarsia*, **81**, 45–55.
- Kirchner, M., Wichels, A., Seibold, A., Sahling, G., and Schütt, C. (2001) New and potentially toxic isolates from *Noctiluca scintillans* (Dinoflagellata). In Hallegraeff, G. (ed), *Proceedings on Harmful Algae. Ninth International Conference on Harmful Algae Blooms, Tasmania 2000*. pp. 379–382.
- Kitatsuji, S., Shikata, T., Sakamoto, S., Nakayama, N., Nagai, K., Onitsuka, G., and Tada, K. (2019) Detection of harmful algae grazed by *Noctiluca scintillans* by lamp method. *J. Fish. Technol.*, **12**, 23–29.
- Kitatsuji, S., Sato, Y., Yamaguchi, H., Asahi, T., Ichimi, K., Onitsuka, G., and Tada, K. (2019) Does *Noctiluca scintillans* end the diatom bloom in coastal water? *J. Exp. Mar. Bio. Ecol.*, **510**, 10–14.
- Kock, T., Baschek, B., Wobbe, F., Heineke, M., Riethmueller, R., Deschner, S. C., Seidel, G., and Calil, P. H. R. (2023) An advanced towed CTD chain for physical-biological high resolution *in situ* upper ocean measurements. *Front. Mar. Sci.*, **10**, 1–21.
- Kopuz, U., Feyzioglu, A. M., and Valente, A. (2014) An unusual red-tide event of *Noctiluca scintillans* (Macartney) in the southeastern Black Sea. *Turkish J. Fish. Aquat. Sci.*, **14**, 261–268.
- Kraberg, A., Baumann, M., and Dürselen, C. D. (2010) *Coastal phytoplankton: photo guide for Northern European seas*. Wiltshire, K. H. and Boersma, M. (eds). Pfeil, München.
- Kuroda, I. and Saga, S. (1978) The distribution and ecology of *Noctiluca scintillans* in Ohsaka Bay. *Bull Japan Soc. Fish. Ocean.*, **32**, 56–67.
- Kuroda, K. (1990) *Noctiluca scintillans* (Macartney) Ehrenberg. In Fukuyo, Y., Takano, H., Chihara, M., and Matsuyoka, K. (eds), *Red tide organisms in Japan —An Illustrated Taxonomic Guide*. Uchida Rokakuho, Tokyo, pp. 78–79.

- Kutser, T. (2004) Quantitative detection of chlorophyll in cyanobacterial blooms by satellite remote sensing. *Limnol. Oceanogr.*, **49**, 2179–2189.
- Lam, C. W. Y. and Ho, K. C. (1989) Red tides in Tolo Harbor, Hong Kong. In Okaichi, T., Anderson, D. M., and Nemoto, T. (eds), *Red tides: Biology, Environmental Science and Toxicology*. Elsevier, New York, pp. 49–52.
- Landry, M. R. and Calbet, A. (2004) Microzooplankton production in the oceans. *ICES J. Mar. Sci.*, **61**, 501–507.
- Lebrato, M., Pitt, K. A., Sweetman, A. K., Jones, D. O. B., Cartes, J. E., Oschlies, A., Condon, R. H., Molinero, J. C., *et al.* (2012) Jelly-falls historic and recent observations: a review to drive future research directions. *Hydrobiologia*, **690**, 227–245.
- Lee, C. N. W. and Chen, Q. C. (2001) A historical and biogeographical analysis of the marine planktonic copepod community in Hong Kong: a record of change. In Morton, B. (ed), *Perspectives on Marine Environment Change in Hong Kong and Southern China (1977-2001)*. Hong Kong University Press, Hong Kong, pp. 433–457.
- Lee, C. R., Kang, H. K., and Noh, J. H. (2009) Temporal and spatial variation of zooplankton community structure post construction of Saemangeum dyke. *Ocean Polar Res.*, **31**, 327–338.
- Lee, J. H. (1985) Phytoplankton red tide blooms in the Jinhae Bay, southern coast of Korea. *Bull. Mar. Sci.*, **37**, 770.
- Lee, Jung Keun and Hirayama, K. (1992) Effects of salinity, food level and temperature on the population growth of *Noctiluca scintillans* (Macartney). *Bull. Fac. Fish. Nagasaki Univ.*, **71**, 163.
- Lee, J. K. and Hirayama, K. (1992) The food removal rate by *Noctiluca scintillans* feeding on *Tetraselmis tetrathelle* and *Gymnodinium nagasakiense*. *Bull. Fac. Fish. Nagasaki Univ.*, **71**, 169–175.
- van Leeuwen, S., Tett, P., Mills, D., and Van Der Molen, J. (2015) Stratified and nonstratified areas in the North Sea: long-term variability and biological and policy implications. *J. Geophys. Res. Ocean.*, **120**, 4670–4685.
- Lessard, E. J. (1991) The trophic role of heterotrophic dinoflagellates in diverse marine environments. *Mar. Microb. Food Webs*, **5**, 49–58.
- Leterme, S. C., Seuront, L., and Edwards, M. (2006) Differential contribution of diatoms and dinoflagellates to phytoplankton biomass in the NE Atlantic Ocean and the North Sea. *Mar. Ecol. Prog. Ser.*, **312**, 57–65.
- Lewandowska, A. M., Boyce, D. G., Hofmann, M., Matthiessen, B., Sommer, U., and Worm, B. (2014) Effects of sea surface warming on marine plankton. *Ecol. Lett.*, **17**, 614–623.
- Lewitus, A. J., Horner, R. A., Caron, D. A., Garcia-mendoza, E., Hickey, B. M., Hunter, M., Huppert, D. D., Kudela, R. M., *et al.* (2012) Harmful algal blooms along the North American west coast region : History , trends , causes , and impacts. *Harmful Algae*, **19**, 133–159.
- Liang, Z., Xinming, T., Lin, L., and Wenliang, J. (2005) Temporal association rule mining based on t-apriori algorithm and its typical application. *Proc. Int. Symp. Spat. Model. Spat. Reason. Anal. Data Min. Data Fusion*, 1–6.
- Liao, Y. Y., Xie, Y., Xie, W. Y., Liang, J. A., and Ling, Y. T. . (2012) Harmfull algal blooms of *Noctiluca scintillans* resulted from wastewater of aquaculture in the waters around the Naozhou Island, Zhanjiang, China. *J. Trop. Org.*, **3**, 276–280.

- Lin, F. A., Guan, C. J., and Lu, X. W. (2010) Effects of red tide events monitoring, existence questions and suggestions in coastal areas in recent years in China. *Mar. Environ. Sci.*, **29**, 148–152.
- Lin, Y. S. (1989) The dominant red tide organisms in the Zhujiang Estuary, China.
- Liu, H., Li, K., Huang, H., Song, X., Yin, J., and Huang, L. (2013) Seasonal community structure of mesozooplankton in the Daya Bay, South China Sea. *J. Ocean Univ. China*, **12**, 452–458.
- Liu, R., Cui, B., Dong, W., Fang, X., Xiao, Y., Zhao, X., Cui, T., Ma, Y., *et al.* (2024) A refined deep-learning-based algorithm for harmful-algal-bloom remote-sensing recognition using *Noctiluca scintillans* algal bloom as an example. *J. Hazard. Mater.*, **467**, 1–9.
- Liu, X. J. and Wong, C. K. (2006) Seasonal and spatial dynamics of *Noctiluca scintillans* in a semi-enclosed bay in the northeastern part of Hong Kong. *Bot. Mar.*, **49**, 145–150.
- Löder, M. G. J., Kraberg, A. C., Aberle, N., Peters, S., and Wiltshire, K. H. (2012) Dinoflagellates and ciliates at Helgoland Roads, North Sea. *Helgol. Mar. Res.*, **66**, 11–23.
- Lombard, F., Boss, E., Waite, A. M., Uitz, J., Stemmann, L., Sosik, H. M., Schulz, J., Romagnan, J. B., *et al.* (2019) Globally consistent quantitative observations of planktonic ecosystems. *Front. Mar. Sci.*, **6**.
- Lu, S. and Hodgkiss, I. J. (2004) Harmful algal bloom causative collected from Hong Kong waters. *Hydrobiologia*, **512**, 231–238.
- Lucas, I. A. N. (1982) Observations on *Noctiluca scintillans* Macartney (Ehrenb.) (Dinophyceae) with notes on an intracellular bacterium. *J. Plankton Res.*, **4**, 401–409.
- Lutz, R. A. and Incze, L. S. (1979) The impact of toxic dinoflagellate blooms on the North American shellfish industry. In Taylor, D. L. and Seliger, H. H. (eds), *Developments in Marine Biology*. Elsevier, New York, pp. 476–483.
- Maclean, J. L. (1989) Indo-Pacific red tides, 1985-1988. *Mar. Pollut. Bull.*, **20**, 304–310.
- Malej, A. (2001) Are irregular plankton phenomena getting more frequent in the northern Adriatic Sea? In Briand, F. (ed), *CIESM Workshop Series, Gelatinous zooplankton outbreaks: Theory and practice*. Commission Internationale pour l'Exploration Scientifique de la mer Méditerranée, Naples, Italy, p. 112.
- Malej, A. (1983a) *Noctiluca miliaris* Suriray red tide in the Gulf of Trieste. *Thalass. Jugosl.*, **19**, 261–269.
- Malej, A. (1982) Unusual occurrence of *Pelagia noctiluca* in the Adriatic. *Acta Adriat.*, **23**, 97–102.
- Malej, A. (1983b) Vertical distribution of *Noctiluca miliaris* Suriray in the Gulf of Trieste during spring 1982. *Rapp. Comm. int. Mer Médit.*, **28**, 117–119.
- Margalef, R. (1973) Fitoplancton marino de la región de afloramiento del NW de África. 65–94.
- Marshall, H. G. (1976) Phytoplankton distribution along the eastern coast of the USA. I. Phytoplankton composition. *Mar. Biol.*, **38**, 81–89.
- Marshall, H. G., Lacouture, R. V., Buchanan, C., and Johnson, J. M. (2006) Phytoplankton assemblages associated with water quality and salinity regions in Chesapeake Bay, USA. *Estuar. Coast. Shelf Sci.*, **69**, 10–18.
- Marshall, J. A. (2004) Algal bloom impacts on Australian finfish aquaculture. *Austasia Aquac.*, 54–57.

- Martinez, E., Antoine, D., D'Ortenzio, F., and De Boyer Montégut, C. (2011) Phytoplankton spring and fall blooms in the North Atlantic in the 1980s and 2000s. *J. Geophys. Res. Ocean.*, **116**, 1–11.
- Matus-Hernández, M. Á., Martínez-Rincón, R. O., Aviña-Hernández, R. J., and Hernández-Saavedra, N. Y. (2019) Landsat-derived environmental factors to describe habitat preferences and spatiotemporal distribution of phytoplankton. *Ecol. Modell.*, **408**, 108759.
- Mc Ginn, M. P. (1971) Axenic cultivation of *Noctiluca scintillans*.
- McLeod, D. J., Hallegraeff, G. M., Hosie, G. W., and Richardson, A. J. (2012) Climate-driven range expansion of the red-tide dinoflagellate *Noctiluca scintillans* into the Southern Ocean. *J. Plankton Res.*, **34**, 332–337.
- Van Meerssche, E. and Pinckney, J. L. (2019) Nutrient Loading Impacts on Estuarine Phytoplankton Size and Community Composition: Community-Based Indicators of Eutrophication. *Estuaries and Coasts*, **42**, 504–512.
- Menden-Deuer, S. and Lessard, E. J. (2000) Carbon to volume relationships for dinoflagellates, diatoms, and other protist plankton. *Limnol. Oceanogr.*, **45**, 569–579.
- Mendez, S. M. (1993) Uruguayan red tide monitoring programme: preliminary results (1990–1991).
- Métivier, C. and Soyer-Gobillard, M. O. (1988) Organization of cytoskeleton during the tentacle contraction and cytostome movement in the dinoflagellate *Noctiluca scintillans* McCartney. *Cell Tissue Res.*, **251**, 359–370.
- Michaelis, R., Hass, H. C., Mielck, F., Papenmeier, S., Sander, L., Gutow, L., and Wiltshire, K. H. (2019) Epibenthic assemblages of hard-substrate habitats in the German Bight (south-eastern North Sea) described using drift videos. *Cont. Shelf Res.*, **175**, 30–41.
- Mikaelyan, A. S., Malej, A., Shiganova, T. A., Turk, V., Sivkovitch, A. E., Musaeva, E. I., Kogovšek, T., and Lukashova, T. A. (2014) Populations of the red tide forming dinoflagellate *Noctiluca scintillans* (Macartney): a comparison between the Black Sea and the northern Adriatic Sea. *Harmful Algae*, **33**, 29–40.
- Miloslavich, P., Bax, N. J., Simmons, S. E., Klein, E., Appeltans, W., Aburto-Oropeza, O., Andersen Garcia, M., Batten, S. D., *et al.* (2018) Essential ocean variables for global sustained observations of biodiversity and ecosystem changes. *Glob. Chang. Biol.*, **24**, 2416–2433.
- Miloslavich, P., Pearlman, J., and Kudela, R. (2018) Sustainable Observations of Plankton, the Sea's Food Foundation. *Eos (Washington. DC)*.
- Miyaguchi, H., Fujiki, T., Kikuchi, T., Kuwahara, V. S., and Toda, T. (2006) Relationship between the bloom of *Noctiluca scintillans* and environmental factors in the coastal waters of Sagami Bay, Japan. *J. Plankton Res.*, **28**, 313–324.
- Miyaguchi, H., Kurosawa, N., and Toda, T. (2008) Real-time polymerase chain reaction assays for rapid detection and quantification of *Noctiluca scintillans* zoospore. *Mar. Biotechnol.*, **10**, 133–140.
- Mohamed, K., Kripa, V., Jugnu, R., Radhakrishnan, P., Alloyicious, P., Jenni, B., Joseph, M., and Velayudhan, T. (2007) Mortality of farmed pearl oyster *Pinctada fucata* (Gould, 1850) due to the blooming of *Noctiluca scintillans* and *Cochlodinium sp.* at Kollam Bay, Kerala. *J. Mar. Biol. Assoc. India*, **49**, 213–218.
- Mohanty, A. K., Satpathy, K. K., Sahu, G., Sasmal, S. K., Sahu, B. K., and Panigrahy, R. C. (2007) Red tide of *Noctiluca scintillans* and its impact on the coastal water quality of the near-shore

- waters, off the Rushikulya River, Bay of Bengal. *Curr. Sci.*, **93**, 616–618.
- Van Mol, B., Ruddick, K., Astoreca, R., Park, Y., and Nechad, B. (2007) Optical detection of a *Noctiluca scintillans* bloom. *EARSeL eProceedings* 6. pp. 130–137.
- Monier, A., Comte, J., Babin, M., Forest, A., Matsuoka, A., and Lovejoy, C. (2015) Oceanographic structure drives the assembly processes of microbial eukaryotic communities. *ISME J.*, **9**, 990–1002.
- Montani, S., Pithakpol, S., and Tada, K. (1998) Nutrient regeneration in coastal seas by *Noctiluca scintillans*, a red tide-causing dinoflagellate. *J. Mar. Biotechnol.*, **6**, 224–228.
- Moore, S. K., Trainer, V. L., Mantua, N. J., Parker, M. S., Laws, E. A., Backer, L. C., and Fleming, L. E. (2008) Impacts of climate variability and future climate change on harmful algal blooms and human health. *Environ. Heal. A Glob. Access Sci. Source*, **7**, 1–12.
- Moreno, H. D., Köring, M., Di Pane, J., Tremblay, N., Wiltshire, K. H., Boersma, M., and Meunier, C. L. (2022) An integrated multiple driver mesocosm experiment reveals the effect of global change on planktonic food web structure. *Commun. Biol.*, **5**, 1–9.
- Morton, B. and Twentyman, P. R. (1971) The occurrence and toxicity of a red tide caused by *Noctiluca scintillans* (Macartney) Ehrenb., in the coastal waters of Hong Kong. *Environ. Res.*, **4**, 544–557.
- Murray, S. and Suthers, I. (1999) Population ecology of *Noctiluca scintillans* Macartney, a red-tide-forming dinoflagellate. *Mar. Freshw. Res.*, **50**, 243–252.
- Nakamura, Y. (1998a) Biomass, feeding and production of *Noctiluca scintillans* in the Seto Inland Sea, Japan. *J. Plankton Res.*, **20**, 2213–2222.
- Nakamura, Y. (1998b) Growth and grazing of a large heterotrophic dinoflagellate, *Noctiluca scintillans*, in laboratory cultures. *J. Plankton Res.*, **20**, 1711–1720.
- Naqvi, S. W. A., George, M. D., Narvekar, P. V., Jayakumar, D. A., Shailaja, M. S., Sardesai, S., Sarma, V., Shenoy, D. M., *et al.* (1998) Severe fish mortality associated with 'red tide' observed in the sea off Cochin. *Curr. Sci.*, **75**, 543.
- Nawata, T. and Sibaoka, T. (1976) Ionic composition and pH of the vacuolar sap in marine dinoflagellate noctiluca. *Plant Cell Physiol.*, **17**, 265–272.
- Nayar, S., Gupta, T. R. C., and Prabhu, H. V. (2001) Bloom of *Noctiluca scintillans* Macartney in the Arabian Sea off Mangalore, southwest India. *Asian Fish. Sci.*, **14**, 77–82.
- Nelder, A. J. A., Wedderburn, R. W. M., Journal, S., Statistical, R., and Series, S. (1972) Generalized linear models. *J. R. Stat. Soc. Ser. A*, **135**, 370–384.
- Nelson, D. M., Tréguer, P., Brzezinski, M. A., Leynaert, A., and Quéguiner, B. (1995) Production and dissolution of biogenic silica in the ocean: revised global estimates, comparison with regional data and relationship to biogenic sedimentation. *Global Biogeochem. Cycles*, **9**, 359–372.
- Nicol, J. A. C. (1958) Observations on luminescence in *Noctiluca*. *J. Mar. Biol. Assoc. United Kingdom*, 535–549.
- Nikishina, A. B., Drits, A. V., Vasilyeva, Y. V., Timonin, A. G., Solovyev, K. A., Ratkova, T. N., and Sergeeva, V. M. (2011) Role of the *Noctiluca scintillans* population in the trophic dynamics of the Black Sea plankton over the spring period. *Oceanology*, **51**, 1029–1039.
- Nikolaidis, G., Koukaras, K., Aligizaki, K., Heracleous, A., Kalopesa, E., Moschandreu, K., Tsolaki,

- E., and Mantoudis, A. (2005) Harmful microalgal episodes in Greek coastal waters. *J. Biol. Res.*, **3**, 77–85.
- Núñez-Vázquez, E. J., Gárate-Lizarraga, I., Band-Schmidt, C. J., Cordero-Tapia, A., Lopez-Cortes, D. J., Sandoval, F. E. H., Heredia-Tapia, A., and Bustillos-Guzman, J. J. (2011) Impact of harmful algal blooms on wild and cultured animals in the Gulf of California. *J. Environ. Biol.*, **32**, 413–423.
- Odebrecht, C. and Abreu, P. C. (1995) Raphidophycean in southern Brazil. *IOC/UNESCO Harmful Algal News*, **12**, 4.
- Ogawa, Y. and Nakahara, T. (1979a) Interrelationships between pelagic fishes and plankton in the coastal fishing ground of the southwestern Japan Sea. *Mar. Ecol. Prog. Ser.*, **1**, 115–122.
- Ogawa, Y. and Nakahara, T. (1979b) Interrelationships between pelagic fishes and plankton in the coastal fishing grounds of the southwestern Japan Sea. *Mar. Ecol. Prog. Ser.*, **1**, 115–122.
- Oguz, T. and Velikova, V. (2010) Abrupt transition of the northwestern Black Sea shelf ecosystem from a eutrophic to an alternative pristine state. *Mar. Ecol. Prog. Ser.*, **405**, 231–242.
- Okaichi, T. and Nishio, S. (1976) Identification of ammonia as the toxic principle of red tide of *Noctiluca miliaris*. *Bull. Plank. Soc. Jpn.*, **23**, 25–30.
- Oke, P. R. and Middleton, J. H. (2001) Nutrient enrichment off Port Stephens: the role of the East Australian Current. *Cont. Shelf Res.*, **21**, 587–606.
- Oliver, E. C. J., Donat, M. G., Burrows, M. T., Moore, P. J., Smale, D. A., Alexander, L. V., Benthuyzen, J. A., Feng, M., *et al.* (2018) Longer and more frequent marine heatwaves over the past century. *Nat. Commun.*, **9**, 1–12.
- Ollevier, A., Mortelmans, J., Aubert, A., Deneudt, K., and Vandegehuchte, M. B. (2021) *Noctiluca scintillans*: dynamics, size measurements and relationships with small soft-bodied plankton in the Belgian part of the North Sea. *Front. Mar. Sci.*, **8**, 1–14.
- Ollevier, A., Mortelmans, J., Deneudt, K., and Vandegehuchte, M. (2020) Population dynamics of *Noctiluca scintillans* in the Belgian part of the North Sea and its relation with small gelatinous plankton. In Mees, J. and Seys, J. (eds), *Book of abstracts - Vliz Marine Science Day*. Vlaams Instituut voor de Zee – Flanders Marine Institute (VLIZ), Oostende, Belgium, p. 32.
- Olson, R. J. and Sosik, H. M. (2007) A submersible imaging-in-flow instrument to analyze nano- and microplankton: Imaging FlowCytobot. *Limnol. Oceanogr. Methods*, **5**, 195–203.
- Omori, M. and Hamner, W. M. (1982) Patchy distribution of zooplankton: behavior, population assessment and sampling problems. *Mar. Biol.*, **72**, 193–200.
- Orellana-Cepeda, E., Morales-Zamorano, L. A., and Castro-Castro, N. (1993) A conceptual model of coastal red tides off Baja California. *Vlith Conf. Int. Toxic Mar. Phytoplankton*. Nantes, France, p. 152.
- Orlova, T. Y., Konovalova, G. V., Stonik, I. V., Selina, M. S., Morozova, T. V., and Shevchenko, O. G. (2002) Harmful algal blooms on the eastern coast of Russia.
- Ortner, P. B., Hill, L. C., and Edgerton, H. E. (1981) *In-situ* silhouette photography of Gulf Stream zooplankton. *Deep Sea Res. Part A. Oceanogr. Res. Pap.*, **28**, 1569–1576.
- Ostroumov, A. (1924) *Noctiluca miliaris* in Simbiosis mit grünen Algen. *Zool. Anz. Bd.*, **58**.
- Ou, L., Lundgren, V., Lu, S., and Granéli, E. (2014) The effect of riverine dissolved organic matter and other nitrogen forms on the growth and physiology of the dinoflagellate *Prorocentrum*

- minimum (Pavillard) Schiller. *J. Sea Res.*, **85**, 499–507.
- Özdemir, G. P. and Ak, O. (2015) The qualitative and quantitative distribution of the zooplankton in the southeastern Black Sea (Trabzon coast). *J. Black Sea / Mediterr. Environ.*, **18**, 279–298.
- Özdemir, N. Sen, Caf, F., Feyzioglu, A. M., and Yildiz, I. (2017) Biochemical content (fatty acids, sterols, lipophilic vitamins, total protein, MDA, GSH, GSSG) of *Noctiluca scintillans* in the Southeastern Black Sea. *Turkish J. Fish. Aquat. Sci.*, **17**, 301–311.
- Padmakumar, K. B., Cicily, L., and Sudhakar, M. (2016) Extensive outbreaks of heterotrophic dinoflagellate *Noctiluca scintillans* blooms along coastal waters of the southeastern Arabian Sea. *Harmful Algae News*, **52**, 11–12.
- Padmakumar, K. B., SreeRenjima, G., Fanimol, C. L., Menon, N. R., and Sanjeevan, V. N. (2010) Preponderance of heterotrophic *Noctiluca scintillans* during a multi- species diatom bloom along the southwest coast ... *Int. J. Ocean. Oceanogr.*, **4**, 55–63.
- Padmakumar, K. B., Thomas, L. C., Vijayan, A., and Sudhakar, M. (2016) “Crab Jubilee” subsequent to red tide of *Noctiluca scintillans* along the central Kerala coast (SW coast of India). *Indian J. Geo-Marine Sci.*, **45**, 1549–1551.
- Pan, Y., Wang, L., Zhang, W., Liu, G., and Lin, S. (2016) Genetic analysis of *Noctiluca scintillans* populations indicates low latitudinal differentiation in China but high China-America differences. *J. Exp. Mar. Bio. Ecol.*, **477**, 31–39.
- Di Pane, J., Wiltshire, K. H., McLean, M., Boersma, M., and Meunier, C. L. (2022) Environmentally induced functional shifts in phytoplankton and their potential consequences for ecosystem functioning. *Glob. Chang. Biol.*, **28**, 2804–2819.
- Pearson, K. F. R. S. (1920) Notes on the history of correlation. *Soc. Biometricians Math. Stat.*, **13**, 25–45.
- Peter, S., Agnes, F., Sreeparvathy, P., Pillai, D., and Kumar, B. M. (2016) *Noctiluca scintillans* (Macartney) Kofoid and Swezy bloom and its impact on the coastal water quality off Alappuzha, Arabian Sea. *Fish. Technol.*, **53**, 82–85.
- Petersen, W., Reinke, S., Breitbach, G., Petschatnikov, M., Wehde, H., and Thomas, H. (2018) FerryBox data in the North Sea from 2002 to 2005. *Earth Syst. Sci. Data*, **10**, 1729–1734.
- Petersen, W., Schroeder, F., and Bockelmann, F. D. (2011) FerryBox - Application of continuous water quality observations along transects in the North Sea. *Ocean Dyn.*, **61**, 1541–1554.
- Picheral, M., Catalano, C., Brousseau, D., Claustre, H., Coppola, L., Leymarie, E., Coindat, J., Dias, F., et al. (2022) The Underwater Vision Profiler 6: an imaging sensor of particle size spectra and plankton, for autonomous and cabled platforms. *Limnol. Oceanogr. Methods*, **20**, 115–129.
- Piontkovski, S. A., Serikova, I. M., Evstigneev, V. P., Prusova, I. Y., Zagorodnaya, Y. A., Al Hashmi, K. A., and Alabri, N. M. (2021) Seasonal blooms of the dinoflagellate algae *Noctiluca scintillans*: regional and global scale aspects. *Reg. Stud. Mar. Sci.*, **44**, 1–11.
- Pitt, K. A., Kingsford, M. J., Rissik, D., and Koop, K. (2007) Jellyfish modify the response of planktonic assemblages to nutrient pulses. *Mar. Ecol. Prog. Ser.*, **351**, 1–13.
- Pollina, T., Larson, A. G., Lombard, F., Li, H., Le Guen, D., Colin, S., de Vargas, C., and Prakash, M. (2022) PlanktoScope: affordable modular quantitative imaging platform for citizen oceanography. *Front. Mar. Sci.*, **9**, 1–15.

- Porumb, F. (1992a) Evolution du zooplancton des eaux du plateau continental roumain de la Mer Noire au cours de trois decennies. *Rapp. Comm. int. Mer Médit.*, **33**, 266.
- Porumb, F. (1989) On the development of *Noctiluca scintillans* (Macartney) Kofoid and Swezy under the eutrophication of the Romanian Black Sea waters. *Cercet. Mar.*, **22**, 247–262.
- Porumb, F. (1992b) On the development of *Noctiluca scintillans* under eutrophication of Romanian Black Sea waters. *Mar. Coast. Eutrophication*, 907–920.
- Prasad, R. (1953) Swarming of *Noctiluca* in the Palk Bay and its effect on the ‘Choodai’ fishery, with a note on the possible use of *Noctiluca* as an indicator species. *Proceedings of the Indian Academy of Sciences-Section B (Vol. 38, No. 1)*. Springer India, pp. 40–47.
- Prasad, R. R. (1958) A note on the occurrence and feeding habits of *Noctiluca* and their effects on the plankton community and fisheries. *Proc. Indian Acad. Sci. B*, **47**, 331–337.
- Qi, L., Hu, C., Liu, J., Ma, R., Zhang, Y., and Zhang, S. (2022) *Noctiluca* blooms in the East China Sea bounded by ocean fronts. *Harmful Algae*, **112**, 1–8.
- Qi, L., Tsai, S. F., Chen, Y., Le, C., and Hu, C. (2019) In search of red *Noctiluca scintillans* blooms in the East China Sea. *Geophys. Res. Lett.*, **46**, 5997–6004.
- Qi, Y., Chen, J., Wang, Z., Xu, N., Wang, Y., Shen, P., and Hodgkiss, I. J. (2004) Some observations on harmful algal bloom (HAB) events along the coast of Guangdong, southern China in 1998. *Hydrobiologia*, **512**, 209–214.
- Qi, Y., Zhang, Z., and Hong, Y. (1993) Occurrence of red tides on the coasts of China. In Smayda, T. J. and Shimizu, Y. (eds), *Toxic Phytoplankton Blooms in the Sea*. Elsevier Science Publishers, pp. 17–21.
- Quante, M. and Colijn, F. (2016) *North Sea region climate assessment (NOSCCA)*.
- Quayle, D. B. (1969) Paralytic shellfish poisoning in British Columbia. *Fish. Res. Bd. Can. Bull.*, **168**.
- Quevedo, M., Gonzalez-Quiros, R., and Anadon, R. (1999) Evidence of heavy predation by *Noctiluca scintillans* on *Acartia clausi* (Copepoda) eggs off the central Cantabrian coast (NW Spain). *Oceanol. Acta*, **22**, 127–131.
- R Core Team (2023) R: A language and environment for statistical computing.
- Rainville, L. and Pinkel, R. (2001) Wirewalker: an autonomous wave-powered vertical profiler. *J. Atmos. Ocean. Technol.*, **18**, 1048–1051.
- Ramyani, T. (2023) 11 sparkling places that appear to be from another world but are actually on Earth. <https://traveltriangle.com>.
- Rao, D. S., Mathew, K. J., Gopinathan, C. P., Regunathan, A., and Murty, A. V. S. (1980) Mud banks and coastal erosion in relation to fisheries. *Mar. Fish. Inf. Serv. Tech. Ext. Ser.*, **19**, 1–10.
- Reid, P. C., Fischer, A. C., Lewis-Brown, E., Meredith, M. P., Sparrow, M., Andersson, A. J., Antia, A., Bates, N. R., *et al.* (2009) Impacts of the oceans on climate change. In Sims, D. W. (ed), *Advances in Marine Biology*. Academic Press, Burlington, pp. 1–150.
- Remy, M., Hillebrand, H., and Flöder, S. (2017) Stability of marine phytoplankton communities facing stress related to global change: interactive effects of heat waves and turbidity. *J. Exp. Mar. Bio. Ecol.*, **497**, 219–229.
- Rewrie, L. C. V., Voynova, Y. G., van Beusekom, J. E. E., Sanders, T., Körtzinger, A., Brix, H., Ollesch, G., and Baschek, B. (2023) Significant shifts in inorganic carbon and ecosystem state in a

- temperate estuary (1985–2018). *Limnol. Oceanogr.*, **68**, 1920–1935.
- Richardson, A. J. (2008) In hot water: zooplankton and climate change. *ICES J. Mar. Sci.*, **65**, 279–295.
- Richardson, A. J., John, E. H., Irigoien, X., Harris, R. P., and Hays, G. C. (2004) How well does the Continuous Plankton Recorder (CPR) sample zooplankton? A comparison with the Longhurst Hardy Plankton Recorder (LHPR) in the northeast Atlantic. *Deep. Res. Part I Oceanogr. Res. Pap.*, **51**, 1283–1294.
- Richardson, A. J., Walne, A. W., John, A. W. G., Jonas, T. D., Lindley, J. A., Sims, D. W., Stevens, D., and Witt, M. (2006) Using continuous plankton recorder data. *Prog. Oceanogr.*, **68**, 27–74.
- Righetti, D., Vogt, M., Gruber, N., Psomas, A., and Zimmermann, N. E. (2019) Global pattern of phytoplankton diversity driven by temperature and environmental variability. *Sci. Adv.*, **5**, 1–10.
- Rizzo, P. J. (2003) Those amazing dinoflagellate chromosomes. *Cell Res.*, **13**, 215–217.
- Rodríguez, A. R., Ochoa, J. L., and Uribe-Alcocer, M. (2005) Grazing of heterotrophic dinoflagellate *Noctiluca scintillans* (Macartney) Kofoid on *Gymnodinium catenatum* Graham. *Rev. Latinoam. Microbiol.*, **47**, 6–10.
- Roy, S., Llewellyn, C. A., Egeland, E. S., and Johnsen, G. (2011) *Phytoplankton pigments: characterization, chemotaxonomy and application in oceanography*. Cambridge.
- Ruddick, K. G., Ovidio, F., and Rijkeboer, M. (2000) Atmospheric correction of SeaWiFS imagery for turbid coastal and inland waters. *Appl. Opt.*, **39**, 897–912.
- Ruiz-Villarreal, M., Sourisseau, M., Anderson, P., Cusack, C., Neira, P., Silke, J., Rodriguez, F., Ben-Gigirey, B., *et al.* (2022) Novel methodologies for providing *in situ* data to HAB early warning systems in the European Atlantic Area: the PRIMROSE experience. *Front. Mar. Sci.*, **9**, 791329.
- Sahayak, S., Jyothibabu, R., Jayalakshmi, K. J., Habeebrehman, H., Sabu, P., Prabhakaran, M. P., Jasmine, P., Shaiju, P., *et al.* (2005) Red tide of *Noctiluca miliaris* off south of Thiruvananthapuram subsequent to the ‘stench event’ at the southern Kerala coast. *Curr. Sci.*, **89**, 1472–1473.
- Saifullah, S. M. and Chaghtai, F. (1990) Incidence of *Noctiluca scintillans* (Macartney) Ehrenb., blooms along Pakistan shelf. *Pakistan J. Bot.*, **22**, 94–99.
- Sakamoto, Y., Ishiguro, M., and Kitagawa, G. (1986) *Akaike information criterion statistics*. Reidel, D. (ed). Netherlands.
- Salamanca, J. M. (2001) Las medusas invaden las aguas del Mar Menor. *Mar*, **394**, 68.
- Sallée, J. B., Pellichero, V., Akhoudas, C., Pauthenet, E., Vignes, L., Schmidtke, S., Garabato, A. N., Sutherland, P., *et al.* (2021) Summertime increases in upper-ocean stratification and mixed-layer depth. *Nature*, **591**, 592–598.
- Sang, C. H. Q. (1991) The feeding and vegetative reproduction diurnal rhythms of *Noctiluca scintillans*. *J. Jinan Univ.*, **3**.
- Sang, Q. and Dayong, L. (1994) Unequal cell division of *Noctiluca scintillans*. *Oceanol. Limnol. Sin.*, **2**.
- Sathish, T., Thomas, L. C., and Padmakumar, K. B. (2021) Vegetative and sexual reproduction of bloom-forming dinoflagellate *Noctiluca scintillans* (Ehrenberg) Macartney from tropical

- Cochin Estuary (southwest coast of India): in situ and laboratory studies. *Thalass. An Int. J. Mar. Sci.*, **37**, 31–37.
- Sato, M. S. and Hayashi, H. (1998) A decrease in temperature triggers a luminescent response in *Noctiluca scintillans*. *J. Plankton Res.*, **20**, 1259–1266.
- Sato, N. E., Hernández, D., and Viñas, M. D. (2010) Hábitos alimentarios de *Noctiluca scintillans* en aguas costeras de la provincia de Buenos Aires, Argentina. *Lat. Am. J. Aquat. Res.*, **38**, 403–412.
- Sautour, B., Artigas, L. F., Delmas, D., Herbland, A., and Laborde, P. (2000) Grazing impact of micro- and mesozooplankton during a spring situation in coastal waters off the Gironde estuary. *J. Plankton Res.*, **22**, 531–552.
- Schanz, T., Ove Möller, K., Rühl, S., and Greenberg, D. S. (2023) Robust detection of marine life with label-free image feature learning and probability calibration. *Mach. Learn. Sci. Technol.*, **4**.
- Schaumann, K., Gerdes, D., and Hesse, K. J. (1988) Hydrographic and biological characteristics of a *Noctiluca scintillans* red tide in the German Bight, 1984. *Meeresforsch.*, **32**, 77–91.
- Schlüter, M. H., Merico, A., Wiltshire, K. H., Greve, W., and Von Storch, H. (2008) A statistical analysis of climate variability and ecosystem response in the German Bight. *Ocean Dyn.*, **58**, 169–186.
- Schnepf, E. and Drebes, G. (1993) Anisogamy in the dinoflagellate *Noctiluca*? *Helgoländer Meeresuntersuchungen*, **47**, 265–273.
- Schoemann, V., De Baar, H. J. W., De Jong, J. T. M., and Lancelot, C. (1998) Effects of phytoplankton blooms on the cycling of manganese and iron in coastal waters. *Limnol. Oceanogr.*, **43**, 1427–1441.
- Seibold, A., Wichels, A., and Schütt, C. (2001) Diversity of endocytic bacteria in the dinoflagellate *Noctiluca scintillans*. *Aquat. Microb. Ecol.*, **25**, 229–235.
- Sekiguchi, H. and Kato, T. (1976) Influence of *Noctiluca*'s predation on the *Acartia* population in Ise Bay, central Japan. *J. Oceanogr. Soc. Japan*, **32**, 195–198.
- Sellner, K. G. and Fonda Umani, S. (1999) Dinoflagellate blooms and mucilage production. In Malone, T., Malej, A., Harding, L. W., Smolaka, N., and Turner, R. E. (eds), *Ecosystem at the Land–Sea Margin: Drainage Basin to Coastal Sea*. pp. 173–206.
- Shaju, S. S., Akula, R. R., and Jabir, T. (2018) Characterization of light absorption coefficient of red *Noctiluca scintillans* bloom in the southeastern Arabian Sea. *Oceanologia*, **60**, 419–425.
- Shanks, A. and Walters, K. (1996) Feeding by a heterotrophic dinoflagellate (*Noctiluca scintillans*) in marine snow. *Limnol. Oceanogr.*, **41**, 177–181.
- Shunmugapandi, R., Gedam, S. S., and Inamdar, A. B. (2019) Long-time-scale investigation on episodic events of *Noctiluca scintillans* bloom in the North-west Arabian Sea. *AGU Fall Meeting Abstracts*. pp. OS21C-1752.
- Siegel, D. A., Buesseler, K. O., Doney, S. C., Sailley, S. F., Behrenfeld, M. J., and Boyd, P. W. (2014) Global assessment of ocean carbon export by combining satellite observations and food-web models. *Global Biogeochem. Cycles*, 181–196.
- Siegismund, F. and Schrum, C. (2001) Decadal changes in the wind forcing over the North Sea. *Clim. Res.*, **18**, 39–45.

- Sieracki, C. K., Sieracki, M. E., and Yentsch, C. S. (1998) An imaging-in-flow system for automated analysis of marine microplankton. *Mar. Ecol. Prog. Ser.*, **168**, 285–296.
- Smayda, T. J. (1997) Bloom dynamics: physiology, behavior, trophic effects. *Limnology Oceanogr.*, **42**, 1132–1136.
- Smayda, T. J. (2006) Harmful algal bloom communities in Scottish coastal waters: relationship to fish farming and regional comparisons: a review. Edinburgh, United Kingdom.
- Smayda, T. J. and Reynolds, C. S. (2003) Strategies of marine dinoflagellate survival and some rules of assembly. *J. Sea Res.*, **49**, 95–106.
- Smith, C. R., Leo, F. C. De, Bernardino, A. F., Sweetman, A. K., and Martinez-Arbizu, P. (2008) Abyssal food limitation, ecosystem structure and climate change. *Trends Ecol. Evol.*, **23**, 518–528.
- Smith, K., Sherman, A., Huffard, C., McGill, P., Henthorn, R., Von Thun, S., Ruhl, H., Kahru, M., *et al.* (2014) Large salp bloom export from the upper ocean and benthic community response in the abyssal northeast Pacific: day to week resolution. *Limnol. Oceanogr.*, **59**, 745–757.
- Song, J., Bi, H., Cai, Z., Cheng, X., He, Y., Benfield, M. C., and Fan, C. (2020) Early warning of *Noctiluca scintillans* blooms using *in situ* plankton imaging system: an example from Dapeng Bay, P. R. China. *Ecol. Indic.*, **112**, 106123.
- Song, N. Q., Wang, N., Lu, Y., and Zhang, J. R. (2016) Temporal and spatial characteristics of harmful algal blooms in the Bohai Sea during 1952-2014. *Cont. Shelf Res.*, **122**, 77–84.
- Sournia, A. (1995) Red tide and toxic marine phytoplankton of the world ocean: and inquiry into biodiversity. *Harmful marine algal blooms*. Proceedings of the 6th International Conference on Toxic Marine Phytoplankton, Nantes, France, pp. 103–112.
- Spector, D. L. (1984) Dinoflagellate nuclei. *Dinoflagellates*, **1**, pp. 107–147.
- Spillane, T. (2016) Diatom frustules as a mechanical defense against predation by heterotrophic dinoflagellates.
- Stauffer, B. A., Gellene, A. G., Rico, D., Sur, C., and Caron, D. A. (2017) Grazing of the heterotrophic dinoflagellate *Noctiluca scintillans* on dinoflagellate and raphidophyte prey. *Aquat. Microb. Ecol.*, **80**, 193–207.
- Steuer, A. (1903) Beobachtungen über das Plankton des Golfes vom Triest im Jahre 1902. *Zool. Anz. Bd.*, **27**, 369.
- Strom, S. L. (2001) Light-aided digestion, grazing and growth in herbivorous protists. *Aquat. Microb. Ecol.*, **23**, 253–261.
- Su, M. M., Wall, G., Wu, B., Xu, H., Fu, X., and Deng, Y. (2021) Tourism place making through the bioluminescent “Blue Tears” of Pingtan Islands, China. *Mar. Policy*, **133**, 104744.
- Sulkin, S., Lehto, J., Strom, S., and Hutchinson, D. (1998) Nutritional role of protists in the diet of first stage larvae of the Dungeness crab *Cancer magister*. *Mar. Ecol. Prog. Ser.*, **169**, 237–242.
- Sun, D., Zhao, D. Z., Wen, S. Y., Xing, X. G., and Wang, L. (2010) Fuzzy analysis on relationship between *Noctiluca scintillans* blooms and environmental factors. *Mar. Environ. Sci.*, **29**, 70–75.
- Sun, J.-Y., Song, Y., Ma, Z.-P., Zhang, H.-J., Yang, Z.-D., Cai, Z.-H., and Zhou, J. (2017) Fungal community dynamics during a marine dinoflagellate (*Noctiluca scintillans*) bloom. *Mar.*

Environ. Res., **131**, 183–194.

- Suzuki, T., Yamamoto, K., and Narasaki, T. (2014) Predation pressure of *Noctiluca scintillans* on diatoms and thecate dinoflagellates off the western coast of Kyushu, Japan. *Plankt. Benthos Res.*, **8**, 186–190.
- Tada, K., Asahi, T., Kitatsuji, S., Nomura, M., Yamaguchi, H., and Ichimi, K. (2020) Low-active high-density *Noctiluca scintillans* cells in surface seawater. *Oceanologia*, **62**, 402–407.
- Tada, K., Pithakpol, S., and Montani, S. (2004) Seasonal variation in the abundance of *Noctiluca scintillans* in the Seto Inland Sea, Japan. *Plankt. Biol. Ecol.*, **51**, 7–14.
- Tada, K., Pithakpol, S., Yano, R., and Montani, S. (2000) Carbon and nitrogen content of *Noctiluca scintillans* in the Seto Inland Sea, Japan. *J. Plankton Res.*, **22**, 1203–1211.
- Takayama, H. (1977) Culture of *Noctiluca scintillans* (Macartney). *Bull. Plankt. Soc. Japan*, 159–162.
- Tang, D. L., Di, B. P., Wei, G., Ni, I. H., Im, S. O., and Wang, S. F. (2006) Spatial, seasonal and species variations of harmful algal blooms in the South Yellow Sea and East China Sea. *Hydrobiologia*, **568**, 245–253.
- Tangen, K. (1979) *Dinoflagellate blooms in Norwegian waters Toxic Dinoflagellate Blooms*. Taylor, D. L. and Seliger, H. H. (eds). Elsevier, North-Holland, New York.
- Tarkan, A. N., Isinibilir, M. I., and Tarkan, A. S. (2005) Seasonal variations of the zooplankton composition and abundance in the Istanbul Strait. *Asian Netw. Sci. Inf.*
- Thangaraja, M., Al-Aisry, A., and Al-Kharusi, L. (2007) Harmful algal blooms and their impacts in the middle and outer ROPME sea area. *Int. J. Ocean. Oceanogr.*, **2**, 85–98.
- Thomas, L. C., Nandan, S. B., and Padmakumar, K. B. (2020) Understanding the dietary relationship between extensive *Noctiluca* bloom outbreaks and Jellyfish swarms along the eastern Arabian Sea (West coast of India). *Indian J. Geo-Marine Sci.*, **49**, 1389–1394.
- Thompson, P. A., Bonham, P. I., and Swadling, K. M. (2008) Phytoplankton blooms in the Huon Estuary, Tasmania: top-down or bottom-up control? *J. Plankton Res.*, **30**, 735–753.
- Thrisiamma, J., Shaiju, P., Laluraj, C. M., Balachandran, K. K., Nair, M., George, R., Nair, K. K. C., Sahayak, S., *et al.* (2008) Nutrient environment of red tide-infested waters off south-west coast of India. *Environ. Monit. Assess.*, **143**, 355–361.
- Tian, D. (2017) Population dynamic of *Noctiluca scintillans* and its grazing properties in Jiaozhou Bay.
- Tibbs, J. F. (1967) On some planktonic protozoa taken from the track of drift station. *Arctic*, **20**, 247–254.
- Tiselius, P. and Kiørboe, T. (1998) Colonization of diatom aggregates by dinoflagellate *Noctiluca scintillans*. *Limnol. Oceanogr.*, **43**, 154–159.
- Torrey, H. B. (1902) An unusual occurrence of *Dinoflagellata* on the California coast. *Am. Nat.*, **36**, 187–192.
- Tsai, S. F., Wu, L. Y., Chou, W. C., and Chiang, K. P. (2018) The dynamics of a dominant dinoflagellate, *Noctiluca scintillans*, in the subtropical coastal waters of the Matsu archipelago. *Mar. Pollut. Bull.*, **127**, 553–558.
- Tseng, L. C., Kumar, R., Chen, Q. C., and Hwang, J. S. (2011) Summer distribution of *Noctiluca scintillans* and mesozooplankton in the western and southern East China Sea prior to the

- Three Gorges Dam operation. *Hydrobiologia*, **666**, 239–256.
- Tseng, L. C., Kumar, R., Dahms, H. U., Chen, C. Te, Chen, Q. C., and Hwang, J. S. (2008) Epipelagic mesozooplankton succession and community structure over a marine outfall area in the northeastern South China Sea. *J. Environ. Biol.*, **29**, 275–280.
- Turkoglu, M. (2013) Red tides of the dinoflagellate *Noctiluca scintillans* associated with eutrophication in the Sea of Marmara (the Dardanelles, Turkey). *Oceanologia*, **55**, 709–732.
- Turner, J. T. (2014) Planktonic marine copepods and harmful algae. *Harmful Algae*, **32**, 81–93.
- Ueno, M. (1938) Stratification of *Noctiluca* in a Brackish Water Lake of Hokkaido, Japan. *Proc. Imp. Acad.*, **14**, 231–232.
- Uhlig, G. and Sahling, G. (1985) Blooming and red tide phenomenon in *Noctiluca scintillans*. *Bull. Mar. Sci.*, **37**, 779–780.
- Uhlig, G. and Sahling, G. (1990) Long-term studies on *Noctiluca scintillans* in the German Bight population dynamics and red tide phenomena 1968-1988. *Netherlands J. Sea Res.*, **25**, 101–112.
- Uhlig, G. and Sahling, G. (1995) *Noctiluca scintillans*: zeitliche Verteilung bei Helgoland und räumliche Verbreitung in der Deutschen Bucht (Langzeitreihen 1970-1993). *Berichte der Biol. Anstalt Helgol.*, **9**, 1–127.
- Uhlig, G., Sahling, G., and Hanslik, M. (1995) Zur Populationsdynamik von *Noctiluca scintillans* in der südlichen Deutschen Bucht 1988-1992. *Berichte der Biol. Anstalt Helgol.*, **10**, 1–32.
- Ustün, F., Bat, L., Sahin, F., Satilmis, H. H., Özdemir, Z. B., and Kideys, A. E. (2007) Annual cycle of zooplankton off Sinop, the southern Black Sea, in 2003-2004. *Rapp. Comm. int. Mer Médit.*, **38**, 628.
- Valiadi, M., de Rond, T., Amorim, A., Gittins, J. R., Gubili, C., Moore, B. S., Iglesias-Rodriguez, M. D., and Latz, M. I. (2019) Molecular and biochemical basis for the loss of bioluminescence in the dinoflagellate *Noctiluca scintillans* along the west coast of the U.S.A. *Limnol. Oceanogr.*, **64**, 2709–2724.
- Vandendriessche, S., Vansteenbrugge, L., Derweduwen, J., Maelfait, H., and Hostens, K. (2016) Jellyfish jelly press and jelly perception. *J. Coast. Conserv.*, **20**, 117–125.
- Vasas, V., Lancelot, C., Rousseau, V., and Jordán, F. (2007) Eutrophication and overfishing in temperate nearshore pelagic food webs: a network perspective. *Mar. Ecol. Prog. Ser.*, **336**, 1–14.
- Vaswani, A. R. and Möller, K. O. (2022) New framework for analysis of aquatic ecosystems. 1–5.
- Venugopal, P., Haridas, P., Madhupratap, M., and Rao, T. S. S. (1979) Incidence of red water along south Kerala coast. *Indian J. Mar. Sci.*, **8**, 94–97.
- Vijayalakshmy, K. C., Abhijith, M., Megha, M. K., Hatha, A. A. M., and Saramma, A. V. (2018) Incidence of heterotrophic red *Noctiluca scintillans* bloom along Chavakkad, southwest coast of India. *Indian J. Geo-Marine Sci.*, **47**, 1648–1651.
- Voynova, Y. G., Brix, H., Petersen, W., Weigelt-Krenz, S., and Scharfe, M. (2017) Extreme flood impact on estuarine and coastal biogeochemistry: the 2013 Elbe flood. *Biogeosciences*, **14**, 541–557.
- Walker, C. F., Harvey, M. J., Bury, S. J., and Chang, F. H. (2000) Biological and physical controls on dissolved dimethylsulfide over the north-eastern continental shelf of New Zealand. *J. Sea*

Res., **43**, 253–264.

- Wan, A. and Zhang, G. (2012) Annual occurrence of moon jellyfish *Aurelia sp.* in the Jiaozhou Bay and its impacts on zooplankton community. *Oceanol. Limnol. Sin.*, **43**, 494–501.
- Wang, H. and Liu, M. (2020) Stationary distribution of a stochastic hybrid phytoplankton–zooplankton model with toxin-producing phytoplankton. *Appl. Math. Lett.*, **101**, 106077.
- Wang, K., Lin, H., Peng, C., Sun, L., Gao, Y., and Chen, B. (2023) Long-term changes in *Noctiluca scintillans* blooms along the Chinese coast from 1933 to 2020. *Glob. Chang. Biol.*, **29**, 5099–5113.
- Wang, S. F., Tang, D. L., He, F. L., Fukuyo, Y., and Azanza, R. V. (2008) Occurrences of harmful algal blooms (HABs) associated with ocean environments in the South China Sea. *Hydrobiologia*, **596**, 79–93.
- Wang, W., Sun, S., Sun, X., Zhang, F., Zhang, G., and Zhu, M. (2018) Seasonal phenology of the heterotrophic dinoflagellate *Noctiluca scintillans* (Macartney) in Jiaozhou Bay and adjacent coastal Yellow Sea, China. *J. Oceanol. Limnol.*, **36**, 1280–1293.
- Wang, Z., Zhao, J., Zhang, Y., and Cao, Y. (2009) Phytoplankton community structure and environmental parameters in aquaculture areas of Daya Bay, South China Sea. *J. Environ. Sci.*, **21**, 1268–1275.
- Warner, A. J. and Hays, G. C. (1994) Sampling by the continuous plankton recorder survey. *Prog. Oceanogr.*, **34**, 237–256.
- Wells, M. L., Karlson, B., Wulff, A., Kudela, R., Trick, C., Asnaghi, V., Berdalet, E., Cochlan, W., *et al.* (2020) Future HAB science: Directions and challenges in a changing climate. *Harmful Algae*, **91**.
- Wells, M. L., Trainer, V. L., Smayda, T. J., Karlson, B. S. O., Trick, C. G., Kudela, R. M., Ishikawa, A., Bernard, S., *et al.* (2015) Harmful algal blooms and climate change : learning from the past and present to forecast the future. *Harmful Algae*, **49**, 68–93.
- Weston, K., Greenwood, N., Fernand, L., Pearce, D. J., and Sivyer, D. B. (2008) Environmental controls on phytoplankton community composition in the Thames plume, U.K. *J. Sea Res.*, **60**, 246–254.
- Wiebe, P. H. and Benfield, M. C. (2003) From the Hensen net toward four-dimensional biological oceanography. *Prog. Oceanogr.*, **56**, 7–136.
- Wiltshire, K. H., Kraberg, A., Bartsch, I., Boersma, M., Franke, H. D., Freund, J., Gebühr, C., Gerdts, G., *et al.* (2010) Helgoland Roads, North Sea: 45 years of change. *Estuaries and Coasts*, **33**, 295–310.
- Wiltshire, K. H., Malzahn, A. M., Wirtz, K., Greve, W., Janisch, S., Mangelsdorf, P., Manly, B. F. J., and Boersma, M. (2008) Resilience of North Sea phytoplankton spring bloom dynamics: an analysis of long-term data at Helgoland Roads. *Limnol. Oceanogr.*, **53**, 1294–1302.
- Wiltshire, K. H. and Manly, B. F. J. (2004) The warming trend at Helgoland Roads, North Sea: phytoplankton response. *Helgol. Mar. Res.*, **58**, 269–273.
- Wong, C. K., Chan, A. L. C., and Chen, Q. C. (1993) Planktonic copepods of Tolo harbour, Hong Kong. *Crustaceana*, **64**, 76–84.
- Wong, J. C. Y., Raven, J. A., Aldunate, M., Silva, S., Gaitán-Espitia, J. D., Vargas, C. A., Ulloa, O., and von Dassow, P. (2023) Do phytoplankton require oxygen to survive? A hypothesis and model synthesis from oxygen minimum zones. *Limnol. Oceanogr.*, **68**, 1417–1437.

- Wong, P. S. (1989) The occurrence and distribution of red tides in Hong Kong: applications in red tide management. In Okaichi, T., Anderson, D. M., and Nemoto, T. (eds), *Red Tides: Biology, Environmental Science, and Toxicology*. Elsevier, Netherlands, pp. 125–128.
- Wood, E. J. E. (1964) Studies in microbial ecology of the Australian region. *Nov. Hedwigia*, **8**.
- Wood, S. (2017) Generalized additive models: an introduction with R, 2 edition.
- Wood, S. N. (2008) Fast stable direct fitting and smoothness selection for generalized additive models. *J. R. Stat. Soc. Ser. B Stat. Methodol.*, **70**, 495–518.
- Vander Woude, A., Ruberg, S., Johengen, T., Miller, R., and Stuart, D. (2019) Spatial and temporal scales of variability of cyanobacteria harmful algal blooms from NOAA GLERL airborne hyperspectral imagery. *J. Great Lakes Res.*, **45**, 536–546.
- Wu, R. Z., Lin, D., and Ma, Y. (2007) Survey and adapted hydro-meteorological conditions of *Noctiluca scintillans* red tides in South China Sea. *J. Oceanogr. Taiwan Strait*, **26**, 590.
- Xi, H., Hieronymi, M., Krasemann, H., and Röttgers, R. (2017) Phytoplankton group identification using simulated and *in situ* hyperspectral remote sensing reflectance. *Front. Mar. Sci.*, **4**, 1–13.
- Xi, H., Hieronymi, M., Röttgers, R., Krasemann, H., and Qiu, Z. (2015) Hyperspectral differentiation of phytoplankton taxonomic groups: a comparison between using remote sensing reflectance and absorption spectra. *Remote Sens.*, **7**, 14781–14805.
- Xi, Y. J., Zhao, Z. L., Sun, G. Q., Zhao, C. L., Wu, Y., Yan, L., Yang, C. C., Wang, Z. Z., *et al.* (2015) Analysis of grey incidence between density of *Noctiluca scintillans* and factors. 1141–1145.
- Xia, X., Ki Leung, S., Cheung, S., Zhang, S., and Liu, H. (2020) Rare bacteria in seawater are dominant in the bacterial assemblage associated with the bloom-forming dinoflagellate *Noctiluca scintillans*. *Sci. Total Environ.*, **711**, 1–13.
- Xiang, C., Tan, Y., Zhang, H., Liu, J., Ke, Z., and Li, G. (2019) The key to dinoflagellate (*Noctiluca scintillans*) blooming and outcompeting diatoms in winter off Pakistan, northern Arabian Sea. *Sci. Total Environ.*, **694**, 1–9.
- Xiao, W., Liu, X., Irwin, A. J., Laws, E. A., Wang, L., Chen, B., Zeng, Y., and Huang, B. (2018) Warming and eutrophication combine to restructure diatoms and dinoflagellates. *Water Res.*, **128**, 206–216.
- Xiaodong, L., Weijing, L., Fan, J., Ziqin, C., Yang, C., Ziyang, W., Tan, Y., Jing, L., *et al.* (2023) The dinoflagellate *Noctiluca scintillans* in China: a review of its distribution and role in harmful algal blooms. *Mar. Pollut. Bull.*, **194**, 115415.
- Xu, Z. (2009) The inter-annual variations in *Noctiluca scintillans* abundance and eutrophication in Changjiang estuary. *Oceanol. Limnol. Sin. Yang Yu Hu Chao*, **40**, 793–798.
- Xue, C., Chen, S., and Zhang, T. (2020) Optical proxy for the abundance of red *Noctiluca scintillans* from bioluminescence flash kinetics in the Yellow Sea and Bohai Sea. *Opt. Express*, **28**, 25618–25632.
- Yamamoto, T., Oh, S. J., and Kataoka, Y. (2004) Growth and uptake kinetics for nitrate, ammonium and phosphate by the toxic dinoflagellate *Gymnodinium catenatum* isolated from Hiroshima Bay, Japan. *Fish. Sci.*, **70**, 108–115.
- Yamamoto, T., Okai, M., Takeshita, K., and Hashimoto, T. (1997) Characteristics of meteorological conditions in the years of intensive red tide occurrence in Mikawa Bay, Japan. *Bull Japan Soc. Fish. Ocean.*, **61**, 114–122.

- Yan, T., Zhou, M.-J., and Zou, J.-Z. (2002) A national report on harmful algal blooms in China. Sidney, B.C., Canada.
- Yan, W., Zang, S., Sun, P., and Seitzinger, S. P. (2003) How do nitrogen inputs to the Changjiang basin impact the Changjiang River nitrate: a temporal analysis for 1968-1997. *Global Biogeochem. Cycles*, **17**, 1–9.
- Yilmaz, I. N., Okuş, E., and Yükses, A. (2005) Evidences for influence of a heterotrophic dinoflagellate (*Noctiluca scintillans*) on zooplankton community structure in a highly stratified basin. *Estuar. Coast. Shelf Sci.*, **64**, 475–485.
- Yin, C., Zhang, Q., Zou, T., Zhang, C., Cui, J., and Sun, J. (2013) Analysis for *Noctiluca scintillans* red tide in Bohai Bay. *Trans. Oceanol. Limnol.*
- Yin, K. (2003) Influence of monsoons and oceanographic processes on red tides in Hong Kong waters. *Mar. Ecol. Prog. Ser.*, **262**, 27–41.
- Yoo, J. K., Youn, S. H., and Choi, J. K. (2006) Temporal fluctuations and ecological characteristics of *Noctiluca scintillans* (Dinophyceae) in the coastal waters of Icheon, Korea. *Korean J. Environ. Biol.*, **24**, 372–379.
- Yu-Zao, H. W. J. Q. and Xuan-Hong, Q. (1992) The identification of a mechanism model on the population dynamics of *Noctiluca scintillans* in the Dapeng Bay in the South China Sea. *Acta Ecol. Sin.*, **3**.
- Yuanshao, L. and Wenqing, C. (1994) An ecological investigation of a *Noctiluca scintillans* around Fujian Islets. *J. Xiamen Univ. (Natural Sci.)*, **S1**.
- Yulin, W., Chengxu, Z., and Yongshan, Z. (1994) Laboratory culture of *Noctiluca scintillans* (Macartney). *Oceanol. Limnol. Sin.*, **2**.
- Zevenboom, W., Rademaker, M., and Colijn, F. (1991) Exceptional algal blooms in Dutch North Sea waters. *Water Sci. Technol.*, **24**, 251–260.
- Zhang, S., Chan, K. Y. K., Shen, Z., Cheung, S., Landry, M. R., and Liu, H. (2016) A cryptic marine ciliate feeds on progametes of *Noctiluca scintillans*. *Protist*, **168**, 1–11.
- Zhang, S., Harrison, P. J., Song, S., Chen, M., Kung, H. S., Lau, W. K., Guo, C., Wu, C. J., *et al.* (2017) Population dynamics of *Noctiluca scintillans* during a bloom in a semi-enclosed bay in Hong Kong. *Mar. Pollut. Bull.*, **121**, 238–248.
- Zhang, S., Li, C., Cheung, S., Sun, M., Song, S., Guo, W., Guo, C., Wu, G., *et al.* (2020) Snapshot of peptidomics of the red tide forming species *Noctiluca scintillans*. *Front. Mar. Sci.*, **7**, 1–11.
- Zhang, S., Liu, H., Chen, B., and Wu, C. J. (2015) Effects of diet nutritional quality on the growth and grazing of *Noctiluca scintillans*. *Mar. Ecol. Prog. Ser.*, **527**, 73–85.
- Zhang, S., Liu, H., Glibert, P. M., Guo, C., and Ke, Y. (2017) Effects of prey of different nutrient quality on elemental nutrient budgets in *Noctiluca scintillans*. *Sci. Rep.*, **7**, 1–12.
- Zhang, S., Liu, H., Guo, C., and Harrison, P. J. (2016) Differential feeding and growth of *Noctiluca scintillans* on monospecific and mixed diets. *Mar. Ecol. Prog. Ser.*, **549**, 27–40.
- Zhang, S., Liu, H., Ke, Y., and Li, B. (2017) Effect of the silica content of diatoms on protozoan grazing. *Front. Mar. Sci.*, **4**.
- Zhang, S., Xia, X., Ke, Y., Song, S., Shen, Z., Cheung, S., and Liu, H. (2021) Population dynamics and interactions of *Noctiluca scintillans* and *Mesodinium rubrum* during their successive blooms in a subtropical coastal water. *Sci. Total Environ.*, **755**, 142349.

- Zhang, T. W., Zhu, L. Y., Xu, P. P., Zhou, H., and Qi, B. J. (2009) Seasonal variation and distribution characteristics of *Noctiluca scintillans* in Jiaozhou Bay. *Period. Ocean Univ. China*, **39**, 89–93.
- Zhang, W., Zhijun, D., Zhang, C., Sun, X., Hou, C., Liu, Y., Wang, L., Ma, Y., *et al.* (2020) Effects of physical-biogeochemical coupling processes on the *Noctiluca scintillans* and *Mesodinium* red tides in October 2019 in the Yantai nearshore, China. *Mar. Pollut. Bull.*, **160**, 111609.
- Zhang, X., Yu, K., Li, M., Jiang, H., Gao, W., Zhao, J., and Li, K. (2024) Diatom-dinoflagellate succession in the Bohai Sea: the role of N/P ratios and dissolved organic nitrogen components. *Water Res.*, **251**, 121150.
- Zhang, Y., Song, S., Chen, T., Sun, X., and Li, C. (2022) Population dynamics and reproduction of the heterotrophic dinoflagellate *Noctiluca scintillans* in Jiaozhou Bay, China. *Mar. Ecol. Prog. Ser.*, **693**, 55–68.
- Zhou, C. and Yan, X. (2002) New observations on the meiotic process in the marine dinoflagellate *Noctiluca scintillans* (Noctilucales, dinophyceae). *Chinese J. Oceanol. Limnol.*, **20**, 67–73.
- Zingmark, R. G. (1970) Sexual reproduction in the dinoflagellate *Noctiluca miliaris* Suriray. *J. Phycol.*, **6**, 122–126.
- Zingone, A. and Enevoldsen, H. O. (2000) The diversity of harmful algal blooms: a challenge for science and management. *Ocean Coast. Manag.*, **43**, 725–748.
- Zondervan, I., Zeebe, R., Rost, B., and Riebesell, U. (2001) Decreasing marine biogenic calcification: a negative feedback on rising atmospheric pCO₂. *Global Biogeochem. Cycles*, **15**, 507–516.

Appendixes

Appendix 1: List of literature mentioning *N. scintillans* blooms.

Reference	Location	Continent	Number of recorded blooms	Period
(Aiyer, 1936)	Madras Coast	Asia	1	1935
(P Ajani <i>et al.</i> , 2001)	Tasman Sea	Oceania	54	1982-1999
(Akin-oriola <i>et al.</i> , 2006)	Nigerian coast	Africa	1	1995
(Albaina and Irigoien, 2007)	Bay of Biscay	Europe	1	2004
(Al Gheilani <i>et al.</i> , 2011)	Oman Sea	Asia	2	1988, 2005
(Allen, 1937)	Isla Ángel de la Guardia	America	1	1937
(Ara <i>et al.</i> , 2013)	West Pacific	Asia	11	2002-2006
(Arunpandi <i>et al.</i> , 2017)	South Arabian Sea	Asia	3	2013-2014
(Astoreca <i>et al.</i> , 2005)	North Sea	Europe	1	2005
(Aytan and Şentürk, 2018)	Southeast Black Sea	Europe	2	2015-2016
(Baek <i>et al.</i> , 2008)	Sagami Bay	Asia	3	2003
(Baek <i>et al.</i> , 2011)	Sea of Japan	Asia	4	2010
(Balch and Haxo, 1984)	East Pacific	America	2	1969, 1982
(Balech, 1988)	Quequén	America	3	1917, 1980
(Baliarsingh <i>et al.</i> , 2016)	Bay of Bengal	Asia	4	1935, 1998, 2004, 2014
(Baliarsingh <i>et al.</i> , 2017)	Northwest Bay of Bengal	Asia	1	2003
(Batistić <i>et al.</i> , 2018)	Adriatic	Europe	2	2009
(Bennett, 1860)	Tasman Sea	Oceania	1	1860
(Bindu <i>et al.</i> , 2014)	Mangalore	Asia	2	2011
(Boni, 1983)	Emiliana Romana	Europe	1	1978
(Brogueira and Sampayo, 1983)	Algarve	Europe	1	1980s
(Brongersma-Sanders, 1945)	Walvis Bay	Africa	1	1940s
(Brongersma-Sanders, 1948)	Peruvian coast	America	1	1940s
(Browne and Kingsford, 2005)	New South Wales	Oceania	2	1999-2000
(Brussaard <i>et al.</i> , 1995)	North Sea	Europe	2	1992
(Cabal <i>et al.</i> , 2008)	East Atlantic	Europe	1	2004
(Cardoso, 2012)	Southwest Atlantic	America	2	2005, 2008
(Cassinari <i>et al.</i> , 1979)	Adriatic	Europe	1	1977
(Chang <i>et al.</i> , 2003)	Hauraki gulf	Oceania	4	1996-1997
(Chang <i>et al.</i> , 2008)	Hauraki gulf	Oceania	4	2002, 2007
(Changjiang <i>et al.</i> , 1996)	South China Sea	Asia	3	1990-1992
(Charernphol, 1957)	Shizuoka	Asia	1	1899
(C. Chen <i>et al.</i> , 2003)	Yangtze River Estuary	Asia	1	2000
(Cortés-Altamirano R, Manrique and Luna-Soria, 1995)	Gulf of California	America	2	1994

(Daan, 1987)	North Sea	Europe	2	1984-1985
(Dela-Cruz <i>et al.</i> , 2002)	Tasman Sea	Oceania	4	1997-1998
(Dela-Cruz <i>et al.</i> , 2008)	Tasman Sea	Oceania	2	1998-1999
(Detoni <i>et al.</i> , 2023)	Ria de Vigo	Europe	2	2017-2018
	Pontevedra		3	2020-2021
	Vigo		3	2020-2021
	Arousa		1	2021
	Ceuta		1	2022
(Devassy <i>et al.</i> , 1979)	Gulf of Goa	Asia	1	1977
(Devassy, 1989)	Gulf of Goa	Asia	2	1973, 1977
(Drits <i>et al.</i> , 2013)	Black Sea	Europe	1	2011
(Dwivedi <i>et al.</i> , 2016)	Bay of Bengal	Asia	1	2014
(Edward <i>et al.</i> , 2009)	Gulf of Mannar	Asia	1	2008
(Enomoto, 1956)	West coast of Kyushu	Asia	1	1950
(Erkan <i>et al.</i> , 2000)	Black Sea	Europe	1	1996
(Escalera <i>et al.</i> , 2007)	East Atlantic	Europe	1	2003
(Fang <i>et al.</i> , 2009)	Pearl River estuary	Asia	2	2005-2006
(Fei, 1952)	Shanghai	Asia	2	1933, 1952
(Ferraz-Reyes <i>et al.</i> , 1979)	Gulf of Caraico	America	1	1977
(Figueroa-Torres and Weiss-Martínez, 1999)	Laguna de Tamiahua	America	4	1996-1997
(Fock and Greve, 2002)	North Sea	Europe	4	1979, 1984
(Fonda Umani <i>et al.</i> , 1983)	Adriatic	Europe	1	1980
(Fonda Umani <i>et al.</i> , 2004)	Adriatic	Europe	17	1988-2003
(Fraga and Sanchez, 1997)	Atlantic	Europe	1	1979
(Franks, 1997)	La Jolla	America	1	1995
(Froján <i>et al.</i> , 2014)	Ria de Vigo	Europe	2	2007-2008
(Fukuda and Endoh, 2006)	West Pacific	Asia	1	2004
(Fukuda and Endoh, 2008)	Sea of Japan	Asia	1	2006
(Fung and Trott, 1973)	South China Sea	Asia	4	1970-1972
(Gárate-Lizárraga, 1991)	Bahia Concepcion	America	1	1989
(Gárate-Lizárraga <i>et al.</i> , 2001)	Gulf of California	America	2	1984, 2001
(Genitsaris <i>et al.</i> , 2020)	East Mediterranean	Europe	3	2017
(Gernez <i>et al.</i> , 2023)	Gran Canaria	Europe	1	2016
(Gillbricht, 1983)	North Sea	Europe	1	1975
(Gómez-Aguirre, 1987)	Laguna de Tamiahua	America	3	1984-1986
(Gómez-Aguirre, 1998)	Gulf of Mexico	America	3	1981, 1986, 1991
(Goncharov, 1857)	Possyet Bay	Asia	1	1850s
(Greve and Reiners, 1988)	North Sea	Europe	7	1975-1981
(Grindley and Heydorn, 1970)	St Lucia	Africa	3	1969
(Grindley and Taylor, 1970)	False Bay	Africa	3	1963
(Guilang <i>et al.</i> , 1992)	Changjiang Estuary	Asia	1	2005
(Hall <i>et al.</i> , 2006)	Hauraki gulf	Oceania	1	1996

(Hallegraeff <i>et al.</i> , 2008)	Tasman Sea	Oceania	6	1994, 2008, 2010
(Hallegraeff <i>et al.</i> , 2019)	Tasman Sea	Oceania	5	1993-2012
(Hallegraeff <i>et al.</i> , 2020)	Tasman Sea	Oceania	5	2013-2017
(Han <i>et al.</i> , 1995)	Deukryang Bay	Asia	3	1993
(Harrison <i>et al.</i> , 2011)	NA	Global	26	1965-2004
(Heil <i>et al.</i> , 1998)	Moreton Bay	Oceania	3	1996-1997
(Herren <i>et al.</i> , 2004)	Northeast Pacific	America	1	1998
(Hesse <i>et al.</i> , 1989)	North Sea	Europe	1	1984
(Heyen <i>et al.</i> , 1999)	North Sea	Europe	18	1974-1994
(Hobson and McQuoid, 2001)	Northeast Pacific	America	2	1997
(Hong <i>et al.</i> , 1994)	Pusan harbor	Asia	2	1990-1991
(Horstman, 1981)	South African coast	Africa	1	1981
(Howard, 1996)	Californian coast	America	1	1995
(Hsiao <i>et al.</i> , 2011)	East China Sea	Asia	2	2005
(Huang and Qi, 1997)	South China Sea	Asia	8	1990-1992
(Hwang and Choi, 1993)	Yellow Sea	Asia	2	1987-1988
(Imai <i>et al.</i> , 2006)	Seto Inland Sea	Asia	27	1973-2005
(Isinibilir <i>et al.</i> , 2014)	Black Sea	Europe	2	2006-2007
(Isinibilir <i>et al.</i> , 2008)	Northeast Marmara Sea	Europe	2	2001-2002
(Isinibilir <i>et al.</i> , 2011)	Black Sea	Europe	2	2005, 2007
(Jacques and Sournia, 1978)	Mediterranean Sea	Europe	4	1971-1972
(Jang <i>et al.</i> , 2010)	East China Sea	Asia	3	2003
(Jeffrey and Carpenter, 1974)	Sydney	Oceania	1	1970s
(Jingzhong <i>et al.</i> , 1985)	Bohai Sea	Asia	4	1978-1981
(Johnson and Shanks, 2003)	West Sound	America	3	1996
(Kang <i>et al.</i> , 1996)	Chinhae Bay	Asia	8	1993
(Kang <i>et al.</i> , 2004)	Ulleung Basin	Asia	3	2000-2001
(Kang, 2010)	Sea of Japan	Asia	2	2008-2009
(Kang, 2020)	Sea of Japan	Asia	6	2009-2017
(Kamburska <i>et al.</i> , 2003)	Bulgarian Black Sea	Europe	2	1999-2000
(Kat, 1979)	South North Sea	Europe	1	1979
(Ki, 2010)	South China Sea	Asia	1	2006
(Kim and Lee, 1994)	Kyeonggi Bay	Asia	1	1990
(Kimor, 1979)	East Pacific	America	4	1970-1977
(Kiørboe, 2003)	West Atlantic	America	2	2002
(Kiørboe and Titelman, 1998)	Baltic Sea	Europe	1	1996
(Kiørboe <i>et al.</i> , 1998)	St Helena Bay	Africa	1	1995
(Kirchner <i>et al.</i> , 1996)	North Sea	Europe	17	1970-1993
(Saho Kitatsuji <i>et al.</i> , 2019)	Seto Inland Sea	Asia	1	2015
(Kopuz <i>et al.</i> , 2014)	Southeast Black Sea	Europe	1	2011
(Kuroda, 1990)	Seto Inland Sea	Asia	2	1980
(Kuroda and Saga, 1978)	Osaka Bay	Asia	1	1970s

(Lam and Ho, 1989)	Tolo Harbour	Asia	11	1976-1986
(Le Fèvre and Grall, 1970)	Brittany	Europe	1	1967
(Lee, 1985)	Jinhae Bay	Asia	5	1979-1983
(Lee <i>et al.</i> , 2009)	Seamangeum dyke	Asia	2	2007-2008
(Liang <i>et al.</i> , 2005)	South China Sea	Asia	2	1991
(Lin, 1989)	Zhujiang estuary	Asia	2	1980
(Lin <i>et al.</i> , 2010)	Bohai Sea	Asia	1	2002
(Liu and Wong, 2006)	South China Sea	Asia	4	2002-2005
(Löder <i>et al.</i> , 2012)	North Sea	Europe	3	2007-2009
(Lu and Hodgkiss, 2004)	South China Sea	Asia	2	1997-1998
(Lutz and Incze, 1979)	Alaska	America	1	1970s
(Maclean, 1989)	Jakarta Bay	Asia	1	1976
(Malej, 1983a)	Gulf of Trieste	Europe	1	1980
(Malej, 1983b)	Gulf of Trieste	Europe	1	1982
(Malej, 2001)	Adriatic Sea	Europe	6	1971-1995
(Margalef, 1973)	Northwestern Africa	Africa	2	1972
(Marshall, 1976)	Eastern US coast	America	2	1964-1974
(Marshall <i>et al.</i> , 2006)	Chesapeake Bay	America	1	1984-2002
(McLeod <i>et al.</i> , 2012)	Southern Ocean	Oceania	1	2010
(Mendez, 1993)	Montevideo	America	1	1990
(Mikaelyan <i>et al.</i> , 2014)	Adriatic Sea/Black Sea	Europe	11	2004-2012
(Miyaguchi <i>et al.</i> , 2006)	Sagami Bay	Asia	7	1997-2003
(Miyaguchi <i>et al.</i> , 2008)	Sagami Bay	Asia	2	2005-2006
(Mohamed <i>et al.</i> , 2007)	Indian Ocean	Asia	2	2003
(Mohanty <i>et al.</i> , 2007)	Gulf of Bengal	Asia	1	2005
(Morton and Twentyman, 1971)	South China Sea	Asia	1	1971
(Murray and Suthers, 1999)	Tasman Sea	Oceania	2	1996-1997
(Nakamura, 1998b)	Seto Inland Sea	Asia	9	1984-1992
(Nakamura, 1998a)	Seto Inland Sea	Asia	2	1997
(Naqvi <i>et al.</i> , 1998)	Kerala	Asia	1	1998
(Nayar <i>et al.</i> , 2001)	Mangalore	Asia	1	1998
(Nicol, 1958)	English Channel	Europe	3	1956-1957
(Nikishina <i>et al.</i> , 2011)	Northeast Black Sea	Europe	2	2008, 2010
(Nikolaidis <i>et al.</i> , 2005)	Mediterranean	Europe	10	2000-2004
(Odebrecht and Abreu, 1995)	Patos Lagoon	America	1	1995
(Ogawa and Nakahara, 1979a)	Southwest Japan Sea	Asia	3	1970
(Oguz and Velikova, 2010)	Black Sea	Europe	7	1975-2003
(Okaichi and Nishio, 1976)	Sea of Japan	Asia	2	1972, 1975
(Oke and Middleton, 2001)	Tasman Sea	Oceania	1	1997
(Ollevier <i>et al.</i> , 2021)	Belgian North Sea	Europe	4	2017-2018
(Omori and Hamner, 1982)	Philippine Sea	Oceania	2	1978
(Orellana-Cepeda <i>et al.</i> , 1993)	Sonora	America	1	1993

(Orlova <i>et al.</i> , 2002)	Kuril Islands	Asia	1	1948
	Peter the Great Bay		6	1980-1995
	Patrokl Bay		2	1926, 1990
(Ostroumov, 1924)	Patrokl Bay	Asia	2	2009, 2017
(Özdemir and Ak, 2015)	Black Sea	Europe	3	2008
(Özdemir <i>et al.</i> , 2017)	Black Sea	Europe	3	2012-2013
(Padmakumar <i>et al.</i> , 2010)	Kochi	Asia	1	2008
(Padmakumar, Thomas, <i>et al.</i> , 2016)	South Arabian Sea	Asia	1	2013
(Padmakumar, Cicily, <i>et al.</i> , 2016)	Arabian Sea	Asia	2	2015
(Pan <i>et al.</i> , 2016)	South China Sea/Gulf of Mexico	Asia/America	5	2004, 2011-2013
(Peter <i>et al.</i> , 2016)	South Arabian Sea	Asia	1	2015
(Pitt <i>et al.</i> , 2007)	Tasman Sea	Oceania	1	2001
(Porumb, 1992b)	West Black Sea	Europe	25	1959-1989
(Prasad, 1958)	Gulf of Mannar	Asia	1	1949
(Prasad, 1953)	Palk Bay	Asia	4	1952
(Qi <i>et al.</i> , 1993)	Yangtze River estuary	Asia	2	1982, 1988
(Qi <i>et al.</i> , 2004)	South China Sea	Asia	1	1998
(Qi <i>et al.</i> , 2019)	East China Sea	Asia	51	2000-2017
(Qi <i>et al.</i> , 2022)	East China Sea	Asia	13	2018-2020
(Quayle, 1969)	British Columbia	America	2	1942, 1965
(Quevedo <i>et al.</i> , 1999)	East Atlantic	Europe	1	1995
(Rao <i>et al.</i> , 1980)	Alapuzzha	Asia	3	1983
(Rodríguez <i>et al.</i> , 2005)	Gulf of California	America	1	2000
(Sahayak <i>et al.</i> , 2005)	Arabian Sea	Asia	1	2004
(Saifullah and Chaghtai, 1990)	Pakistan coast	Asia	1	1980
(Sang and Dayong, 1994)	South China Sea	Asia	1	1993
(Sato <i>et al.</i> , 2010)	Southwest Atlantic	America	6	2000-2001
(Sautour <i>et al.</i> , 2000)	East Atlantic	Europe	1	1995
(Schaumann <i>et al.</i> , 1988)	North Sea	Europe	2	1984
(Schoemann <i>et al.</i> , 1998)	North Sea	Europe	3	1993-1994
(Schnepf and Drebes, 1993)	North Sea	Europe	1	1992
(Seibold <i>et al.</i> , 2001)	Helgoland Roads	Europe	3	1997
(Sekiguchi and Kato, 1976)	Sea of Japan	Asia	2	1974
(Shaju <i>et al.</i> , 2018)	Southeast Arabian Sea	Asia	2	2016
(Shanks and Walters, 1996)	San Juan Island	America	1	1992
(Song <i>et al.</i> , 2020)	South China Sea	Asia	2	2016
(Steuer, 1903)	Adriatic Sea	Europe	1	1902
(Sun <i>et al.</i> , 2010)	Yellow Sea	Asia	1	2006
(Sun <i>et al.</i> , 2017)	Yellow Sea	Asia	1	2016
(Suzuki <i>et al.</i> , 2014)	Sea of Japan	Asia	4	2009
(Tada <i>et al.</i> , 2000)	Seto Inland Sea	Asia	2	1995, 1998
(Tada <i>et al.</i> , 2020)	Seto Inland Sea	Asia	1	2018

(Tada <i>et al.</i> , 2004)	Seto Inland Sea	Asia	9	1992-1997
(Tang <i>et al.</i> , 2006)	South China Sea	Asia	25	1980-2004
(Tangen, 1979)	Norwegian west coast	Europe	1	1979
(Tarkan <i>et al.</i> , 2005)	Istanbul strait	Europe	1	2000
(Thangaraja <i>et al.</i> , 2007)	Oman Sea	Asia	24	1976-1997
(Thomas <i>et al.</i> , 2020)	East Arabian Sea	Asia	8	2010-2017
(Thompson <i>et al.</i> , 2008)	Huon estuary	Oceania	3	2002-2005
(Thrisiamma <i>et al.</i> , 2008)t	Southwest Indian coast	Asia	1	2004
(Tian, 2017)	Yellow Sea	Asia	2	2015
(Tibbs, 1967)	Point Barrow	America	1	1960
(Tiselius and Kjørboe, 1998)	Southeast Atlantic	Africa	1	1995
(Torrey, 1902)	San Diego	America	1	1901
(Tsai <i>et al.</i> , 2018)	East China Sea	Asia	2	2016
(Tseng <i>et al.</i> , 2011)	East China Sea	Asia	1	2001
(Tseng <i>et al.</i> , 2008)	East China Sea	Asia	3	2002
(Turkoglu, 2013)	Sea of Marmara	Europe	5	2001-2003
(Ueno, 1938)	Northeastern Hokkaido	Asia	1	1936
(Uhlig and Sahling, 1990)	North Sea	Europe	17	1979-1988
(Uhlig and Sahling, 1985)	North Sea	Europe	4	1982-1991
(Uhlig <i>et al.</i> , 1995)	North Sea	Europe	5	1984-1988
(Ustün <i>et al.</i> , 2007)	South Black Sea	Europe	1	2004
(Van Mol <i>et al.</i> , 2007)	North Sea	Europe	1	2005
(Venugopal <i>et al.</i> , 1979)	Quilon, Kerala	Asia	1	1976
(Vijayalakshmy <i>et al.</i> , 2018)	South Arabian Sea	Asia	1	2016
(Walker <i>et al.</i> , 2000)	Northeastern New Zealand	Oceania	1	1996
(Wan and Zhang, 2012)	Yellow Sea	Asia	1	2009
(Wang <i>et al.</i> , 2008)	South China Sea	Asia	22	1980-1998
(Wang <i>et al.</i> , 2018)	Yellow Sea	Asia	16	2004-2013
(Weston <i>et al.</i> , 2008)	English Channel	Europe	1	2001
(Wong, 1989)	Hong Kong	Asia	2	1975, 1986
(Wood, 1964)	Moreton Bay	Oceania	1	1951
(Y. J. Xi <i>et al.</i> , 2015)	Bohai Sea	Asia	1	1914
(Xia <i>et al.</i> , 2020)	South China Sea	Asia	5	2016-2018
(Xu, 2009)	Yellow Sea	Asia	2	1959, 2002
(Xue <i>et al.</i> , 2020)	Yellow Sea/Bohai Sea	Asia	2	2018
(Yamamoto <i>et al.</i> , 1997)	Mikawa Bay	Asia	12	1979-1990
(Yan <i>et al.</i> , 2002)	North Pacific	America	4	1980-1993
(Yan <i>et al.</i> , 2003)	Bohai Sea		1	Jul-99
	Changjiang estuary	Asia	2	1988-1989
	Gouqi Sea		1	1987
	Sansha Sea		1	1981
(Yilmaz <i>et al.</i> , 2005)	Sea of Marmara	Europe	4	2001-2002
(Yin, 2003)	South China Sea	Asia	16	1983-1998
(Yoo <i>et al.</i> , 2006)	Yellow Sea	Asia	5	1999-2000

(Yuanshao and Wenqing, 1994)	South China Sea	Asia	1	1990
(Yu-Zao and Xuan-Hong, 1992)	South China Sea	Asia	1	1990
(Zevenboom <i>et al.</i> , 1991)	North Sea	Europe	11	1979-1989
(Zhang, Liu, <i>et al.</i> , 2016)	South China Sea	Asia	1	2011
(Zhang, Chan, <i>et al.</i> , 2016)	South China Sea	Asia	2	2014
(Zhang, Harrison, <i>et al.</i> , 2017)	South China Sea	Asia	1	2013
(W. Zhang <i>et al.</i> , 2020)	Northern Yellow Sea	Asia	1	2019
(Zhang <i>et al.</i> , 2021)	South China Sea	Asia	1	2014
(Zhang <i>et al.</i> , 2022)	Jiaozhou Bay	Asia	5	2019
(Zhou and Yan, 2002)	Yellow Sea	Asia	1	1995

Appendix 2: Drivers associated with *N. scintillans* in literature. Indications “High” or “Low” were used when no values were provided. Fields without values or indications, imply that the driver has been mentioned as important in the corresponding publication, but without further precisions.

Continent	Drivers	Maximal number (cellsL ⁻¹)	cell	Reference
America	Calm/stratified conditions	1300000		(Rodríguez <i>et al.</i> , 2005)
	Light intensity			
	High	1300000		(Rodríguez <i>et al.</i> , 2005)
	High	NA		(Hobson and McQuoid, 2001)
	Low	NA		(Sulkin <i>et al.</i> , 1998)
	Precipitation			
	High	NA		(Mc Ginn, 1971)
	Prey availability			
	High	144000		(Cardoso, 2012)
	Salinity			
	23	NA		(Pan <i>et al.</i> , 2016)
	34-35	NA		(Almeda <i>et al.</i> , 2014)
	34.5-35.4	157000-182000		(Gárate-Lizárraga, 1991)
	SST			
	12°C	NA		(Sulkin <i>et al.</i> , 1998)
	14.5-16.8°C	9-13		(Kimor, 1979)
	14.8-20.2°C	NA		(Hobson and McQuoid, 2001)
	16-17.5°C	157000-182000		(Gárate-Lizárraga, 1991)
	18°C	144000		(Cardoso, 2012)
	18°C	NA		(Balch and Haxo, 1984)
	19.3°C	1300000		(Rodríguez <i>et al.</i> , 2005)
	20°C	NA		(Almeda <i>et al.</i> , 2014)
	20°C	NA		(Buskey, 1995)
20°C	NA		(Buskey <i>et al.</i> , 1992)	
23°C	NA		(Pan <i>et al.</i> , 2016)	
Wind				
1.4 m s ⁻¹	1300000		(Rodríguez <i>et al.</i> , 2005)	
	NA		(Bustillos-Guzmán <i>et al.</i> , 2013)	
Asia	Calm/stratified conditions	NA		(Changjiang <i>et al.</i> , 1997)
		100		(Nakamura, 1998a)
		900000		(Sahayak <i>et al.</i> , 2005)
	Nutrient concentration			
	High	25		(Ara <i>et al.</i> , 2013)

High	NA	(Douding <i>et al.</i> , 1994)
High	2800000	(Fung and Trott, 1973)
High	NA	(Liao <i>et al.</i> , 2012)
High	238000	(Mohanty <i>et al.</i> , 2007)
High	100	(Nakamura <i>et al.</i> 1998a)
High	100	(Nakamura, 1998b)
High	250000	(Padmakumar, Thomas, <i>et al.</i> , 2016)
High	NA	(Peter <i>et al.</i> , 2016)
High	NA	(Qi <i>et al.</i> , 2019)
High	750000	(Vijayalakshmy <i>et al.</i> , 2018)
High	48.58	(Xu, 2009)
High	NA	(Yu-Zao and Xuan-Hong, 1992)
High	26100	(Zhang <i>et al.</i> , 2021)
Light intensity		
High	NA	(Qi <i>et al.</i> , 2019)
Low	189.29	(Song <i>et al.</i> , 2020)
pH		
6.87-8.33	NA	(Liao <i>et al.</i> , 2012)
6.87-8.42	NA	(Wang <i>et al.</i> , 2023)
8.02	NA	(Peter <i>et al.</i> , 2016)
8.4	750000	(Vijayalakshmy <i>et al.</i> , 2018)
High	189.29	(Song <i>et al.</i> , 2020)
Precipitation		
Low	238000	(Mohanty <i>et al.</i> , 2007)
Low	2300000	(Baek <i>et al.</i> , 2009)
Low	610	(Miyaguchi <i>et al.</i> , 2006)
Prey availability		
High	330000	(Baliarsingh <i>et al.</i> , 2016)
High	340000	(Dwivedi <i>et al.</i> , 2016)
High	NA	(Gouda and Panigrahy, 1996)
High	62900 (cells tow ⁻¹)	(Saho Kitatsuji <i>et al.</i> , 2019)
High	NA	(J. K. Lee and Hirayama, 1992)
High	100	(Nakamura, 1998b)
High	NA	(Qi <i>et al.</i> , 2019)
High	0.5-10	(Sekiguchi and Kato, 1976)
High	473000	(Shaju <i>et al.</i> , 2018)
High	NA	(Thomas <i>et al.</i> , 2020)
High	1610	(Tsai <i>et al.</i> , 2018)
High	NA	(Yin <i>et al.</i> , 2013)
High	3-1976	(Zhang, Harrison, <i>et al.</i> , 2017)
High	26100	(Zhang <i>et al.</i> , 2021)
High	91400-2460000	(W. Zhang <i>et al.</i> , 2020)
Salinity		
17-31	1610	(Tsai <i>et al.</i> , 2018)
18.6-33	NA	(Wang <i>et al.</i> , 2023)
22	NA	(Jung Keun Lee and Hirayama, 1992)
27	2800000	(Fung and Trott, 1973)
27-32	NA	(Liao <i>et al.</i> , 2012)
27.75-33.87	238000	(Mohanty <i>et al.</i> , 2007)
>30	2300000	(Baek <i>et al.</i> , 2009)
30.4-31.7	62900 (cells tow ⁻¹)	(Saho Kitatsuji <i>et al.</i> , 2019)
30.57-30.83	280000	(Huang and Qi, 1997)
31.5-32.5	26100	(Zhang, Chan, <i>et al.</i> , 2016)
31.64-33.05	26100	(Zhang <i>et al.</i> , 2021)
33.53	NA	(Peter <i>et al.</i> , 2016)
33.9-34.2	0.09	(Hsiao <i>et al.</i> , 2011)
34.9-35.3	610	(Miyaguchi <i>et al.</i> , 2006)
40	750000	(Vijayalakshmy <i>et al.</i> , 2018)

	High	189.29	(Song <i>et al.</i> , 2020)
	High	900000	(Sahayak <i>et al.</i> , 2005)
	SST		
	10.2-30°C	NA	(Wang <i>et al.</i> , 2023)
	11°C	NA	(Nakamura, 1998b)
	15-27°C	1142	(Baek <i>et al.</i> , 2011)
	15.2-17.8°C	610	(Miyaguchi <i>et al.</i> , 2006)
	16-25°C	NA	(Changjiang <i>et al.</i> , 1997)
	16-26°C	26100	(Zhang, Chan, <i>et al.</i> , 2016)
	16-27°C	1610	(Tsai <i>et al.</i> , 2018)
	16.6-20.6°C	NA	(Liang <i>et al.</i> , 2005)
	16.7-25.8°C	1800	(Ara <i>et al.</i> , 2013)
	17-20°C	NA	(Yu-Zao and Xuan-Hong, 1992)
	17-24°C	3-1976	(Zhang, Harrison, <i>et al.</i> , 2017)
	17.42-25.02°C	26100	(Zhang <i>et al.</i> , 2021)
	17.53°C	48.58	(Xu, 2009)
	19°C	2800000	(Fung and Trott, 1973)
	19°C	NA	(Liao <i>et al.</i> , 2012)
	< 20°C	2300000	(Baek <i>et al.</i> , 2009)
	20°C	NA	(Zhou and Yan, 2002)
	20.6-21.3°C	280000	(Huang and Qi, 1997)
	< 21°C	28.10	(Zhang <i>et al.</i> , 2009)
	21°C	4050	(Tada <i>et al.</i> , 2004)
	22.3-27.2°C	62900 (cells tow ⁻¹)	(Saho Kitatsuji <i>et al.</i> , 2019)
	23°C	NA	(Jung Keun Lee and Hirayama, 1992)
	23.1-25.8°C	100	(Nakamura, 1998a)
	26.7-30.6°C	238000	(Mohanty <i>et al.</i> , 2007)
	27°C	750000	(Vijayalakshmy <i>et al.</i> , 2018)
	27.2°C	0.85	(Hsiao <i>et al.</i> , 2011)
	27.9°C	NA	(Peter <i>et al.</i> , 2016)
	28.35°C	340000	(Dwivedi <i>et al.</i> , 2016)
	28-30°C	NA	(Qi <i>et al.</i> , 2019)
	29°C	NA	(Arunpandi <i>et al.</i> , 2017)
	Low	900000	(Sahayak <i>et al.</i> , 2005)
	High	189.29	(Song <i>et al.</i> , 2020)
	Wind		
	Low	26100	(Zhang <i>et al.</i> , 2021)
	Moderate	900000	(Sahayak <i>et al.</i> , 2005)
	Direction	610	(Miyaguchi <i>et al.</i> , 2006)
Europe	Calm/stratified conditions	89-323	(Cabal <i>et al.</i> , 2008)
		3250000	(Genitsaris <i>et al.</i> , 2019)
		22000	(Hesse <i>et al.</i> , 1989)
		1138000	(Quevedo <i>et al.</i> , 1999)
		220000	(Turkoglu, 2013)
		NA	(Van Mol <i>et al.</i> , 2007)
		100000	(Zevenboom <i>et al.</i> , 1991)
	Nutrient concentration		
	High	0.4	(Batistić <i>et al.</i> , 2018)
	High	NA	(Boni, 1983)
	High	3250000	(Genitsaris <i>et al.</i> , 2019)
	High	550000	(Isinibilir <i>et al.</i> , 2014)
	High	NA	(Oguz and Velikova, 2010)
	High	1534	(Porumb, 1992a)
	High	NA	(Sellner and Fonda Umani, 1999)
	High	220000	(Turkoglu, 2013)
	High	217	(Yilmaz <i>et al.</i> , 2005)
	Light intensity		

	Moderate	31	(Uhlig and Sahling, 1990)
	High	100000	(Zevenboom <i>et al.</i> , 1991)
	pH		
	8.2	NA	(Schoemann <i>et al.</i> , 1998)
	Precipitation		
	Low	6810000	(Kopuz <i>et al.</i> , 2014)
	Prey availability		
	High	89-323	(Cabal <i>et al.</i> , 2008)
	High	0.4	(Batistić <i>et al.</i> , 2018)
	High	3250000	(Genitsaris <i>et al.</i> , 2019)
	High	NA	(Greve and Reiners, 1988)
	High	6810000	(Kopuz <i>et al.</i> , 2014)
	High	NA	(Oguz and Velikova, 2010)
	High	425	(Porumb, 1992b)
	High	1138000	(Quevedo <i>et al.</i> , 1999)
	High	220000	(Turkoglu, 2013)
	High	NA	(Uhlig and Sahling, 1990)
	High	NA	(Van Mol <i>et al.</i> , 2007)
	Salinity		
	10	NA	(Uhlig and Sahling, 1995)
	15.04-16.08	6810000	(Kopuz <i>et al.</i> , 2014)
	21-25	NA	(Uhlig and Sahling, 1985)
	35.2	240000	(Le Fèvre and Grall, 1970)
	< 35.5	89-323	(Cabal <i>et al.</i> , 2008)
	37.79-38.42	0.4	(Batistić <i>et al.</i> , 2018)
	38.6	3250000	(Genitsaris <i>et al.</i> , 2019)
	38.8	NA	(Genitsaris <i>et al.</i> , 2020)
		NA	(Greve and Lange, 1999)
	SST		
	> 5-6°C	31	(Uhlig and Sahling, 1990)
	7.3-20°C	2 -142.48	(Fonda Umani <i>et al.</i> , 2004)
	9-25°C	0.1-70	(Mikaelyan <i>et al.</i> , 2014)
	10.4-11.7°C	220000	(Turkoglu, 2013)
	11.8-13.4°C	6810000	(Kopuz <i>et al.</i> , 2014)
	< 12.5°C	1138000	(Quevedo <i>et al.</i> , 1999)
	14°C	89-323	(Cabal <i>et al.</i> , 2008)
	14-25°C	3250000	(Genitsaris <i>et al.</i> , 2019)
	15.65°C	2400000	(Le Fèvre and Grall, 1970)
	22-24°C	0.4	(Batistić <i>et al.</i> , 2018)
	Low	NA	(Uhlig and Sahling, 1985)
	High	NA	(Oguz and Velikova, 2010)
	High	NA	(Heyen <i>et al.</i> , 1999)
	High	425	(Porumb, 1992b)
	High	NA	(Van Mol <i>et al.</i> , 2007)
		100000	(Zevenboom <i>et al.</i> , 1991)
		NA	(Greve and Lange, 1999)
		NA	(Ollevier <i>et al.</i> , 2020)
		NA	(Schlüter <i>et al.</i> , 2008)
	Wind		
	Low	6810000	(Kopuz <i>et al.</i> , 2014)
	Low	0.1-70	(Mikaelyan <i>et al.</i> , 2014)
	Windless	500	(Porumb, 1989)
	< 10.7 m s ⁻¹	100000	(Zevenboom <i>et al.</i> , 1991)
		15000	(Schaumann <i>et al.</i> , 1988)
Oceania	Calm/stratified conditions	80.3	(Dela-Cruz <i>et al.</i> , 2002)
	Nutrient concentration		
	High	NA	(P Ajani <i>et al.</i> , 2001)

High	80.3	(Dela-Cruz <i>et al.</i> , 2002)
High	28.1	(Dela-Cruz <i>et al.</i> , 2008)
High	220000	(Murray and Suthers, 1999)
Precipitation		
High	NA	(P Ajani <i>et al.</i> , 2001)
Prey availability		
High	80.3	(Dela-Cruz <i>et al.</i> , 2002)
High	28.1	(Dela-Cruz <i>et al.</i> , 2008)
High	NA	(Hallegraeff <i>et al.</i> , 2019)
High	220000	(Murray and Suthers, 1999)
Salinity		
20-35	NA	(Hallegraeff <i>et al.</i> , 2019)
28-36.5	220000	(Murray and Suthers, 1999)
SST		
10-12°C	NA	(Hallegraeff <i>et al.</i> , 2008)
10-23°C	NA	(Hallegraeff <i>et al.</i> , 2019)
13.5°C	0.24	(McLeod <i>et al.</i> , 2012)
14.2-24.2°C	220000	(Murray and Suthers, 1999)
< 25°C	28.1	(Dela-Cruz <i>et al.</i> , 2008)

Appendix 3: Summary of sampling campaigns and monitoring program carried out around China over time, “-“ indicates unknown information.

Location	Date	Frequency	Reference
Bohai Sea	1952-2014	-	(Song <i>et al.</i> , 2016)
Hong Kong	1954-1959	-	(Lee and Chen, 2001)
Hong Kong	1968-1969	2 cruises	(Chiu and Tse, 1978)
Tolo harbour, Hong Kong	1969-1971	Weekly	(Fung and Trott, 1973)
South China Sea	1980-2004	-	(Wu <i>et al.</i> , 2007)
Hong Kong	1983-ongoing	-	(Agriculture Fisheries and Conservation department, 2023)
Yellow Sea	1986-1998	-	(Q. C. Chen <i>et al.</i> , 2003)
Hong Kong	1986-ongoing	Monthly	(Environmental Protection Department, 2022)
Tolo Harbour, Hong Kong	1987-1991	Monthly	(Wong <i>et al.</i> , 1993)
Dapeng Bay, South China Sea	1990	Every 2 weeks	(Yu-Zao and Xuan-Hong, 1992)
Hong Kong	1990-1992	Every 3 days	(Huang and Qi, 1997)
Dapeng Bay, Hong Kong	1990-1992	Seasonally	(Changjiang <i>et al.</i> , 1996)
Junk Bay, Hong Kong	1997-1998	3 times/month	(Lu and Hodgkiss, 2004)
Pearl River Estuary, Hong Kong	1998-2000	Seasonal	(Q. C. Chen <i>et al.</i> , 2003)
South China Sea	2002	3 cruises	(Tseng <i>et al.</i> , 2008)
Hong Kong	2003-2005	Monthly	(Liu and Wong, 2006)
Jiaozhou Bay	2004-2013	Seasonally	(Wang <i>et al.</i> , 2018)
East China Sea	2005	2 cruises	(Hsiao <i>et al.</i> , 2011)
Daya Bay, South China Sea	2005-2006	Monthly	(Wang <i>et al.</i> , 2009)
Daya Bay, South China Sea	2006	2 cruises	(Liu <i>et al.</i> , 2013)
Port Shelter, Hong Kong	2012-2013	Min. 2 times/month	(Zhang, Harrison, <i>et al.</i> , 2017)
East China Sea	2000-2017	-	(Qi <i>et al.</i> , 2019)
Dapeng Bay, Hong Kong	2016	Daily	(Song <i>et al.</i> , 2020)
East China Sea	2018-2020	-	(Qi <i>et al.</i> , 2022)
Yellow Sea	2019	Daily	(W. Zhang <i>et al.</i> , 2020)

Appendix 4: Listed negative impacts on **(A.)** trophic ecology and **(B.)** on water quality, and **(C.)** positive impacts associated with *N. scintillans* in literature.

A.

Impact category	Observed negative impacts	Reference	Max. abundance (cellsL ⁻¹)
Aquaculture	Reduced Aquacultural yields	(Mohamed <i>et al.</i> , 2007)	98000
		(Hallegraeff <i>et al.</i> , 2019)	>1000000
		(Ho, 1994)	NA
		(Marshall, 2004)	NA
		(Yan <i>et al.</i> , 2002)	NA
Fisheries	Impacted fish populations	(Ogawa and Nakahara, 1979b)	2.70
		(Padmakumar, Thomas, <i>et al.</i> , 2016)	310000
		(Quevedo <i>et al.</i> , 1999)	1138000
		(Sekiguchi and Kato, 1976)	33
		(Shaju <i>et al.</i> , 2018)	473000
		(D'Silva <i>et al.</i> , 2012)	NA
		(Hallegraeff <i>et al.</i> , 2019)	NA
		(Lu and Hodgkiss, 2004)	NA
		(Thangaraja <i>et al.</i> , 2007)	NA
		(Vasas <i>et al.</i> , 2007)	NA
Food chains	Impacted food-chains	(Fock and Greve, 2002)	48000
		(Padmakumar, Thomas, <i>et al.</i> , 2016)	310000
		(Hallegraeff <i>et al.</i> , 2019)	NA
		(Oguz and Velikova, 2010)	NA
Jellification	High abundance of jellyfishes, salps or ctenophores	(Padmakumar, Thomas, <i>et al.</i> , 2016)	310000
		(Piontkovski <i>et al.</i> , 2021)	10000000
		(Turkoglu, 2013)	220000
		(Malej, 1982)	NA
		(Thomas <i>et al.</i> , 2020)	NA
Plankton diversity	Unusually low diversity in the plankton community	(Kopuz <i>et al.</i> , 2014)	6810000
		(Padmakumar, Thomas, <i>et al.</i> , 2016)	310000
		(Yilmaz <i>et al.</i> , 2005)	217
		(Changjiang <i>et al.</i> , 1997)	NA
		(Shunmugapandi <i>et al.</i> , 2019)	NA
		(Tian, 2017)	NA
		(Tsai <i>et al.</i> , 2018)	1610
Phytoplankton	Impacted Diatom populations	(Zhang <i>et al.</i> , 2021)	26100
		(Daro <i>et al.</i> , 2006)	NA
		(Saho Kitatsuji <i>et al.</i> , 2019)	NA
		(Tian, 2017)	NA
	Impacted phytoplankton populations	(Kopuz <i>et al.</i> , 2014)	6810000
		(Nikishina <i>et al.</i> , 2011)	298905
		(Shaju <i>et al.</i> , 2018)	473000

		(Sekiguchi and Kato, 1976)	33
		(Tada <i>et al.</i> , 2004)	4050
		(P Ajani <i>et al.</i> , 2001)	NA
		(Balch and Haxo, 1984)	NA
		(Jakobsen and Tang, 2002)	NA
		(Tian, 2017)	NA
Zooplankton	Competition with Copepods	(Arunpandi <i>et al.</i> , 2017)	1600
		(Isinibilir <i>et al.</i> , 2014)	550000
		(Le Fèvre and Grall, 1970)	2400000
		(McLeod <i>et al.</i> , 2012)	0.24
		(Tada <i>et al.</i> , 2004)	4050
	Competition with zooplankton	(Fonda Umani <i>et al.</i> , 2004)	NA
		(Ollevier <i>et al.</i> , 2020)	NA
	Impacted Copepod populations	(Hsiao <i>et al.</i> , 2011)	0.85
		(Isinibilir <i>et al.</i> , 2014)	550000
		(Kimor, 1979)	132
		(Nikishina <i>et al.</i> , 2011)	298905
		(Schaumann <i>et al.</i> , 1988)	15000
		(Sekiguchi and Kato, 1976)	33
		(Yoo <i>et al.</i> , 2006)	80
		(Daro <i>et al.</i> , 2006)	NA
	Impacted mollusc larvae	(Johnson and Shanks, 2003)	NA
	Impacted nauplii recruitment	(Quevedo <i>et al.</i> , 1999)	1138000
	Impacted zooplankton populations	(Jang <i>et al.</i> , 2010)	987
		(Özdemir and Ak, 2015)	3.75
		(Ustün <i>et al.</i> , 2007)	172000
(Sato <i>et al.</i> , 2010)		NA	
(Vasas <i>et al.</i> , 2007)		NA	
B.			
Food availability	Reduced food availability for other species	(Omori and Hamner, 1982)	NA
		(Shaju <i>et al.</i> , 2018)	473000
Hypoxia/Anoxia	Reduced O ₂ availability	(Al-Azri <i>et al.</i> , 2015)	93
		(Huang and Qi, 1997)	8900
		(Padmakumar, Thomas, <i>et al.</i> , 2016)	250000
		(Zevenboom <i>et al.</i> , 1991)	100000
		(D'Silva <i>et al.</i> , 2012)	NA
		(Hallegraeff <i>et al.</i> , 2019)	NA
		(Schoemann <i>et al.</i> , 1998)	NA
		(Shunmugapandi <i>et al.</i> , 2019)	NA
		(Zingone and Enevoldsen, 2000)	NA
NH₄	High ammonium concentrations	(P Ajani <i>et al.</i> , 2001)	NA
		(Dela-Cruz <i>et al.</i> , 2002)	80.3
		(Genitsaris <i>et al.</i> , 2019)	3250000

		(Hallegraeff <i>et al.</i> , 2019)	2000000
		(Núñez-Vázquez <i>et al.</i> , 2011)	NA
		(Okaichi and Nishio, 1976)	NA
		(Smayda, 1997)	NA
Nutrients	Reduced nutrient availability	(Guilang <i>et al.</i> , 1992)	3.49
		(S. Zhang <i>et al.</i> , 2020)	1976
Toxin release	<i>N. scintillans</i> -associated toxins	(Escalera <i>et al.</i> , 2007)	NA
		(Wang and Liu, 2020)	NA
Vector	Transfer of viruses, pathogens or toxins	(Akselman <i>et al.</i> , 2010)	NA
		(Kirchner <i>et al.</i> , 2001)	NA
		(Xia <i>et al.</i> , 2020)	NA
Water consistency	Gelatinous waters	(Harrison <i>et al.</i> , 2011)	100000
		(Hesse <i>et al.</i> , 1989)	22000
		(Schaumann <i>et al.</i> , 1988)	15000
		(Jenkinson, 1986)	NA
C.			
Bioremediation	Termination of HABs	(Drits <i>et al.</i> , 2013)	1120000
		(Genitsaris <i>et al.</i> , 2019)	3250000
		(Frangópulos <i>et al.</i> , 2011)	NA
	High nutrient concentrations	(Ara <i>et al.</i> , 2013)	1800
		(Baek <i>et al.</i> , 2009)	2300000
		(Schaumann <i>et al.</i> , 1988)	15000
		(S. Zhang <i>et al.</i> , 2020)	1976
		(Zhang, Liu, Glibert, <i>et al.</i> , 2017)	NA
		(Ara <i>et al.</i> , 2013)	1800
		(Baek <i>et al.</i> , 2008)	2300000
Nutrients	Nutrient regeneration	(Drits <i>et al.</i> , 2013)	1120000
		(Genitsaris <i>et al.</i> , 2019)	NA
		(Montani <i>et al.</i> , 1998)	NA
		(Schaumann <i>et al.</i> , 1988)	15000
		(Schoemann <i>et al.</i> , 1998)	NA
		(Vasas <i>et al.</i> , 2007)	NA
		(Zhang, Liu, Glibert, <i>et al.</i> , 2017)	NA
Phytoplankton	Increased phytoplankton abundances	(Drits <i>et al.</i> , 2013)	1120000
		(Schaumann <i>et al.</i> , 1988)	15000
		(Uhlrig and Sahling, 1995)	NA
Zooplankton	Increased ciliate biomass	(Zhang, Chan, <i>et al.</i> , 2016)	140000
	Increased zooplankton abundance/diversity	(Isinibilir <i>et al.</i> , 2008)	126
Other	Oil removal	(Almeda <i>et al.</i> , 2014)	NA

Appendix 5: Prey associated with *N. scintillans* in literature.

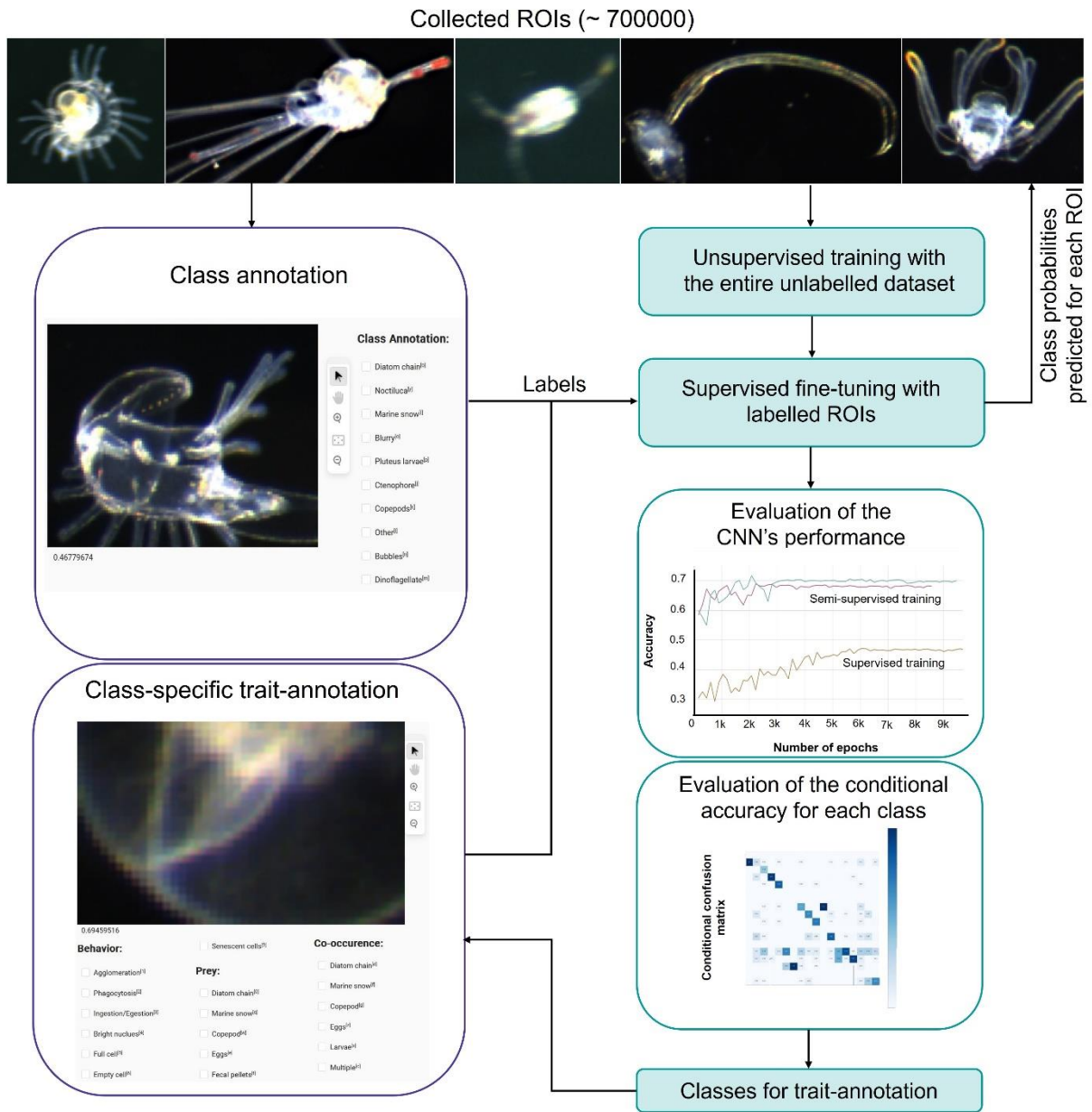
	Prey	References
Laboratory	Bacteria	(Lucas, 1982)
	Chlorophytes	(Mc Ginn, 1971; Nawata and Sibaoka, 1976; Takayama, 1977; J. K. Lee and Hirayama, 1992; Schnepf and Drebes, 1993; Chengxu <i>et al.</i> , 1994; Yulin <i>et al.</i> , 1994; Sato and Hayashi, 1998; Zhou and Yan, 2002; Fukuda and Endoh, 2006; Han <i>et al.</i> , 2013; Zhang <i>et al.</i> , 2015; Zhang, Liu, <i>et al.</i> , 2016; Pan <i>et al.</i> , 2016; Valiadi <i>et al.</i> , 2019)
	Coccolithophores	(Drits <i>et al.</i> , 2013)
	Copepod eggs	(Drits <i>et al.</i> , 2013)
	Diatoms	(Métivier and Soyer-Gobillard, 1988; J. K. Lee and Hirayama, 1992; Buskey, 1995; Kiørboe and Titelman, 1998; Montani <i>et al.</i> , 1998; Sato and Hayashi, 1998; Tada <i>et al.</i> , 2000, 2004; Drits <i>et al.</i> , 2013; Suzuki <i>et al.</i> , 2014; Zhang <i>et al.</i> , 2015; Zhang, Liu, <i>et al.</i> , 2016; Zhang, Liu, Ke, <i>et al.</i> , 2017; Shaju <i>et al.</i> , 2018; Hallegraeff <i>et al.</i> , 2019; Xia <i>et al.</i> , 2020)
	Dinoflagellates	(Balch and Haxo, 1984; J. K. Lee and Hirayama, 1992; Nakamura, 1998b, 1998a; Sulkin <i>et al.</i> , 1998; Escalera <i>et al.</i> , 2007; Bustillos-Guzmán <i>et al.</i> , 2013; Drits <i>et al.</i> , 2013; Almeda <i>et al.</i> , 2014; Zhang <i>et al.</i> , 2015; Valiadi <i>et al.</i> , 2019; S. Kitatsuji <i>et al.</i> , 2019)
	Marine Snow/Detritus	(Sang, 1991; Kiørboe, 2003; Herren <i>et al.</i> , 2004; Tada <i>et al.</i> , 2004)
	Prymnesiophytes	(Jakobsen and Tang, 2002)
	Rapidophytes	(Takayama, 1977; Nakamura, 1998b; S. Kitatsuji <i>et al.</i> , 2019)
	Zooplankton	(Brussaard <i>et al.</i> , 1995; Tada <i>et al.</i> , 2004)
	Zooplankton larvae	(Johnson and Shanks, 2003)
Field	Chaetognathes	(Enomoto, 1956)
	Coccolithophores	(Nikishina <i>et al.</i> , 2011)
	Copepod eggs	(Sekiguchi and Kato, 1976; Kimor, 1979; Daan, 1987; Quevedo <i>et al.</i> , 1999; Fock and Greve, 2002; Daro <i>et al.</i> , 2006; Yoo <i>et al.</i> , 2006; Cabal <i>et al.</i> , 2008; Sato <i>et al.</i> , 2010; Hsiao <i>et al.</i> , 2011; Nikishina <i>et al.</i> , 2011; Isinibilir <i>et al.</i> , 2014; Mikaelyan <i>et al.</i> , 2014; Zhang, Harrison, <i>et al.</i> , 2017)
	Copepods (adults, larvae)	(Nikishina <i>et al.</i> , 2011)
	Crustacean eggs	(Changjiang <i>et al.</i> , 1997)
	Diatoms	(Porumb, 1992a; Gouda and Panigrahy, 1996; Kiørboe and Titelman, 1998; P. Ajani <i>et al.</i> , 2001; Tada <i>et al.</i> , 2004; Daro <i>et al.</i> , 2006; Liu and Wong, 2006; Miyaguchi <i>et al.</i> , 2006; Baek <i>et al.</i> , 2009; Harrison <i>et al.</i> , 2010; Sato <i>et al.</i> , 2010; McLeod <i>et al.</i> , 2012; Ara <i>et al.</i> , 2013; Turkoglu, 2013; Kopuz <i>et al.</i> , 2014; Suzuki <i>et al.</i> , 2014; Baliarsingh <i>et al.</i> , 2016; Zhang, Harrison, <i>et al.</i> , 2017; Batistić <i>et al.</i> , 2018; Shaju <i>et al.</i> , 2018; Genitsaris <i>et al.</i> , 2019; Hallegraeff <i>et al.</i> , 2019; Saho Kitatsuji <i>et al.</i> , 2019; Zhang <i>et al.</i> , 2021)
	Dinoflagellates	(Nakamura, 1998b; Rodríguez <i>et al.</i> , 2005; Nikishina <i>et al.</i> , 2011; Qi <i>et al.</i> , 2019; S. Kitatsuji <i>et al.</i> , 2019)
	Fish eggs	(Changjiang <i>et al.</i> , 1997)
	Marine Snow/Detritus	(Shanks and Walters, 1996; Kiørboe, 2003; Tada <i>et al.</i> , 2004; Nikishina <i>et al.</i> , 2011; Kang, 2020)
	Prymnesiophytes	(Daro <i>et al.</i> , 2006; Weston <i>et al.</i> , 2008)
	Zooplankton larvae	(Changjiang <i>et al.</i> , 1997; Tada <i>et al.</i> , 2004; Nikishina <i>et al.</i> , 2011; Cardoso, 2012; Liu <i>et al.</i> , 2013)

Appendix 6: Output of stepwise selection of GAMs for the bloom, pre-bloom, and post-bloom phases for the Helgoland Roads time series. * indicates the best-fitting model. AIC: Akaike's Information Criterion. Variables in italic correspond to the three most influential variables.

Family	Variable	Deviance explained (%)	Adjusted R ²	AIC
BLOOM PHASE				
Gaussian				
<i>Non-transformed</i>	Full	8.33	0.08	163312.7
<i>Log-transformed</i>	Full	36.11	0.36	43340.9
Poisson*				
<i>Non-transformed</i>	Full	55.54 *	0.16	1470186
	-Precipitation	55.41	0.16	1474437
	-DIN	55.10	0.15	1484550
	-SSS	54.59	0.15	1501233
	-Solar radiation	53.71	0.14	1530035
	-Year	52.62	0.13	1565609
	-SST	49.89	0.12	1654836
	-Wind speed	45.99	0.09	1782298
	-Months	< 0.00	0.00	3286872
<i>Log-transformed</i>	Full	47.88	0.47	27101.0
Non-binomial				
<i>Non-transformed</i>	Full	30.46	0.09	42549.7
<i>Log-transformed</i>	Full	40.32	0.38	22066.7
PRE-BLOOM PHASE				
Gaussian				
<i>Non-transformed</i>	Full	13.63	0.12	7188.49
<i>Log-transformed</i>	Full	14.75	0.13	2643.60
Poisson*				
<i>Non-transformed</i>	Full	15.05*	0.12	70966.52
	-Wind speed	14.64	0.12	71293.11
	-Precipitation	13.96	0.12	71840.99
	-Solar radiation	13.05	0.12	72562.86
	-DIN	10.90	0.10	74294.15
	-SSS	6.12	0.04	78145.46
	-SST	< 0.00	0	83081.19
<i>Log-transformed</i>	Full	12.24	0.13	2787.82
Non-binomial				
<i>Non-transformed</i>	Full	6.94	0.04	5484.41
<i>Log-transformed</i>	Full	10.82	0.11	2569.63
POST-BLOOM PHASE				
Gaussian				
<i>Non-transformed</i>	Full	11.26	0.10	7432.34
<i>Log-transformed</i>	Full	10.90	0.09	2795.25
Poisson*				
<i>Non-transformed</i>	Full	14.47*	0.10	74167.56
	-Precipitation	14.26	0.10	74339.96
	-Wind speed	13.64	0.10	74858.45
	-SSS	12.43	0.09	75873.32
	-DIN	10.45	0.08	77529.95
	-Solar radiation	6.20	0.04	81107.16

	-SST	< 0.00	0	86330.05
Log-transformed	Full	9.56	0.09	2925.73
Non-binomial				
Non-transformed	Full	5.93	0.04	4948.96
Log-transformed	Full	6.49	0.08	2471.05

Appendix 7: Flowchart of the data analysis pipeline for the classification of *in situ* plankton images collected during the three cruises in summer 2022 near Helgoland, Germany (adapted from Vaswani and Möller, 2022).



Appendix 8: Output of stepwise selection of GAMs for the Continuous Plankton Recorder survey. * indicates the best-fitting model. Variables in italic correspond to the three most influential variables.

Family	Variable	Deviance explained (%)	Adjusted R ²	AIC
Gaussian	Full	4.9	0.05	71608.64
Poisson	Full	28.2	0.10	INF
Non-binomial*	Full	29.5	0.05	7569.35
	-Decade	29.5*	0.05	7563.79
	-SSS	29.3	0.05	7569.26
	-SST	29.0	0.05	7567.84
	-Season	24.3	0.02	7642.36
	-MLD	24.0	0.02	7750.09
	- <i>x(Lon, Lat)</i>	< 0.00	0	8059.76

Appendix 9: Summary of the yearly mean abundances of *N. scintillans* and standard errors at Helgoland Roads between 1962 and 2020.

Year	Winter		Spring		Summer		Autumn	
	Mean	Std. error						
1962	0	0	0	0	378.38	91.54	6.32	5.34
1963	0	0	0	0	62.11	29.86	1.18	1.18
1964	0	0	0	0	55	23.61	0	0
1965	0	0	0	0	0	0	3.24	2.39
1966	0.57	0.57	0	0	119.47	26.64	1.62	0.91
1967	0.54	0.54	33.13	10.76	186.84	35.77	1.67	0.93
1968	0	0	8.57	3.21	138.42	64.29	0	0
1969	0	0	0	0	119.68	27.38	5.71	2.19
1970	0	0	6.53	3.57	290.46	47.09	0.83	0.83
1971	0	0	0	0	56.41	19.97	0	0
1972	0	0	0	0	139.49	32.39	9.14	8.05
1973	1.6	1.6	44.71	10.78	307	81.45	1.25	1.25
1974	6.06	3.94	7.37	2.96	249.73	59.17	1.08	1.08
1975	1.90	1.33	0	0	318.13	69.07	0	0
1976	0	0	0	0	341.25	110.54	0	0
1977	0	0	1.94	1.94	161.23	66.97	0	0
1978	0	0	1.43	1.43	373.94	302.53	0	0
1979	6.94	6.94	0	0	420.85	986.55	0	0
1980	1.85	1.36	0	0	171.54	38.29	0	0
1981	0.68	0.68	0.68	0.68	222.89	61.64	0	0
1982	2.86	1.39	0	0	128	38.24	0	0
1983	0	0	0	0	155.23	40.50	0	0
1984	2.07	1.17	1.85		544.77	345.65	1.33	0.93
1985	1.45	1.02	0	0	154.22	26.70	3.15	1.61
1986	2.07	1.53	0	0	92.26	23.28	1.90	1.08
1987	0	0	4.21	1.92	287.10	43.87	3.23	1.67
1988	0	0	73.90	20.67	513.65	129.26	0	0
1989	20	14.02	17.45	7.89	281.11	53.42	0	0
1990	0	0	64.67	12.58	235.56	108.29	1.27	1.27
1991	0	0	0	0	147.69	31.63	0	0
1992	0	0	56	22.98	265.23	55.10	0.67	0.67
1993	0	0	0	0	229.54	40.88	0	0
1994	3.51	2.51	4.91	3.76	110.77	26.73	0	0
1995	0	0	0	0	137.23	25.82	0	0
1996	0	0	0	0	47.38	13.01	1.38	1.38

1997	0	0	21.38	15.93	202.46	53.14	0	0
1998	0.74	0.74	15.71	7.26	42	24.93	0	0
1999	0	0	7.21	4.13	78.18	31.07	0.63	0.63
2000	1.40	0.98	0	0	318.73	90.84	0	0
2001	0.70	0.70	1.97	1.46	65.23	11.59	2	0.91
2002	0.36	0.36	1.69	0.88	125.54	21.68	3.44	2.02
2003	2.30	1.06	1.33	0.65	224.44	49.62	7.81	1.58
2004	3.67	1.21	3.23	1.67	86.06	16.54	1.61	0.95
2005	0.34	0.34	4.52	1.81	335.45	50.77	2.86	1.10
2006	0.70	0.49	3.45	2.26	346.46	65	2.95	1.03
2007	2.86	1.19	1.31	0.92	69.38	14.04	1.69	0.88
2008	1.33	0.65	4.92	1.91	104.76	19	2.86	1
2009	1.38	0.67	6.33	2.15	110.63	24.47	9.49	2.83
2010	1.40	0.85	2.33	1.43	233.64	33.58	11.23	7.08
2011	2.14	0.83	17.05	4.88	147.62	41.47	4.07	1.16
2012	4.41	1.46	13	4.70	190	35.98	6	1.53
2013	3.02	0.99	0	0	294.52	68.63	29.31	17.48
2014	1.05	0.60	4	1.63	196.21	56.17	13.46	2.94
2015	0.38	0.38	1.38	0.83	189.85	49.86	1.64	0.85
2016	3.45	1.31	4.07	1.43	56.06	7.92	1.33	1.05
2017	2.07	1.45	1.64	0.71	2225.85	118.71	1.67	0.86
2018	0.36	0.36	2.14	0.83	291.82	70.83	6.32	1.75
2019	3.33	1.02	4.29	1.42	326.23	127.94	9.31	2.42
2020	4.67	1.53	13.33	4.02	247.58	72.16	25.31	21.23

Declaration

I hereby declare that this dissertation is my own original work, prepared independently and without unauthorized assistance, apart from the guidance provided by my supervisor. This dissertation has not been submitted, either in whole or in part, to any other institution as part of any examination or degree process. This is my first and only doctoral submission. I affirm that this work adheres to the rules of good scientific practice as outlined by the German Research Foundation. Lastly, I hereby declare that I have not been deprived of any academic degree and that I have provided all the information in this dissertation to the best of my knowledge and belief.

Geesthacht, 19.09.24



Katharina Kordubel

Erklärung des Eigenanteils an den erfolgten Publikationen

Publikation 1: Kordubel, K., Baschek, B., Hieronymi, M., Voynova, Y.G., Möller, K.O., 2024. Improving the sampling of red *Noctiluca scintillans* to understand its impact on coastal ecosystem dynamics. J. Plankton Res. 00, 1–21. <https://doi.org/10.1093/plankt/fbae010>

Die Kandidatin hat einen sehr großen Eigenanteil an allen Aspekten der Veröffentlichung. Die Literatur Recherche auf welcher diese Arbeit basiert wurde vollständig von der Kandidatin durchgeführt. Genauso wurden Konzeptionierung und Manuskripterstellung von der Kandidatin übernommen. Die Betreuer (K.O. Möller und B. Baschek) haben bei der Konzeptionierung und Redaktion deutliche, aber nicht dominante Anteile. Die Beiträge der Ko-AutorInnen (M. Hieronymi und Y.G. Voynova) betreffen vor allem inhaltliche und redaktionelle Überprüfungen und Verbesserungen.

Publikation 2: Kordubel, K., Martínez Rincón, R.O., Baschek, B., Boersma, M., Hieronymi, M., Johns, D.G., Kirstein, I.V., Voynova, Y.G., Möller, K.O., 2024. Long-term changes in spatiotemporal distribution of *Noctiluca scintillans* in the southern North Sea. Harmful Algae. <https://doi.org/10.1016/j.hal.2024.102699>

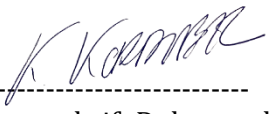
Die Kandidatin hat einen sehr großen Eigenanteil an allen Aspekten der Publikation. Dies umfasst die Konzeptionierung, die formale Datenanalyse, Durchführung der Arbeit sowie die Erstellung des Manuskripts. Der Ko-Autor (R.O. Martínez Rincón) hat neben der redaktionellen Überprüfung auch wesentlich, jedoch nicht dominierend, zu der Datenanalyse beigetragen. Die Betreuer (K.O. Möller und B. Baschek) haben zu der Konzeptionierung und Redaktion beigetragen. Die Ko-AutorInnen (M. Boersma, D.G. Johns und I.V. Kirstein) haben neben inhaltlichen and redaktionelle Überprüfungen auch zu der Erhebung der Daten beigetragen. Die Ko-AutorInnen (M. Hieronymi und Y.G. Voynova) haben vor allem inhaltliche und redaktionelle Überprüfungen und Verbesserungen kontribuiert.

Publikation 3: Kordubel, K., Vaswani, A. R., Baschek, B., Hinners, J., Voynova, Y.G., Möller, K.O. (in Vorbereitung). The role of *Noctiluca scintillans* in the phytoplankton community composition of the southern North Sea.

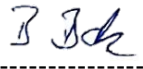
Die Kandidatin hat einen sehr großen Eigenanteil an allen Aspekten der Veröffentlichung. Dies beinhaltet die Organisation und Durchführung der Seereisen, Datenerhebung, Konzeptionierung,

formale Datenanalyse, Durchführung der Arbeit sowie die Erstellung des Manuskripts. Die Betreuer (K.O. Möller und B. Baschek) haben bei der Konzeptionierung und Redaktion deutliche, aber nicht dominante Anteile. Die Ko-Autorinnen A. R. Vaswani und J. Hinners, haben zu der Datenerhebung und Bilddatenanalyse wesentlich, jedoch nicht dominierend, beigetragen. Der Beitrag der Ko-Autorin Y.G. Voynova betrifft vor allem inhaltliche und redaktionelle Überprüfungen und Verbesserungen.

Die vorliegende Einschätzung über die erbrachte Eigenleistung wurde mit den am Artikel beteiligten Ko-AutorenInnen einvernehmlich abgestimmt.

19.09.24 

Datum, Unterschrift DoktorandIn

19.09.24 

Datum, Unterschrift BetreuerIn